SIMPLIFIED METHOD FOR ESTIMATING FUTURE SCOUR DEPTH AT EXISTING BRIDGES

A Dissertation

by

ANAND V GOVINDASAMY

Submitted to the Office of Graduate Studies of
Texas A&M University
in partial fulfillment of the requirements for the degree of

DOCTOR OF PHILOSOPHY

May 2009

Major Subject: Civil Engineering

SIMPLIFIED METHOD FOR ESTIMATING FUTURE SCOUR DEPTH AT EXISTING BRIDGES

A Dissertation

by

ANAND V GOVINDASAMY

Submitted to the Office of Graduate Studies of
Texas A&M University
in partial fulfillment of the requirements for the degree of

DOCTOR OF PHILOSOPHY

Approved by:

Chair of Committee,	Jean-Louis Briaud
Committee Members,	Hamn-Ching Chen
	Francisco Olivera
	Christopher C. Mathewson
Head of Department,	David V. Rosowsky

May 2009

Major Subject: Civil Engineering

ABSTRACT

Simplified Method for Estimating Future Scour Depth at Existing Bridges. (May 2009)

Anand V Govindasamy

B.Eng., Universiti Sains Malaysia, Pulau Pinang, Malaysia;

M.Eng., Asian Institute of Technology, Bangkok, Thailand

Chair of Advisory Committee: Dr. Jean-Louis Briaud

Bridge scour is the term which describes the erosion of soil surrounding a bridge foundation due to water. Bridge scour can cause the reduction of the load carrying capacity of bridge foundations, excessive foundation settlements, and damage to bridge abutments. Bridges with foundations that are unstable for calculated and/or observed scour conditions are termed scour critical bridges.

Approximately 25,000 bridges in the United States are classified as scour critical and about 600 of them are in Texas. This designation comes in part from the use of over-conservative methods that predict excessive scour depths in erosion resistant materials. Other methods have been developed to eliminate this over-conservatism but are uneconomical because they require site-specific erosion testing.

The major contribution of this dissertation is a new method to assess a bridge for scour and erosion classification charts which categorizes the erodibility of geomaterials according to conventional engineering properties. The new method is a three level Bridge Scour Assessment (BSA) procedure which is relatively simple and economical. It does not require site-specific erosion testing and eliminates the over-conservatism in

current methods. The first level, BSA 1, uses charts that extrapolate the maximum scour depth recorded during the life of the bridge to obtain the scour depth corresponding to a specified future flood event. The second level, BSA 2, determines the maximum scour depth and is carried out if BSA 1 does not conclude with a specific plan of action for the bridge. The third level, BSA 3, determines the time dependent scour depth and is carried out if BSA 2 does not conclude with a specific plan of action. The scour vulnerability depends on the comparison between the predicted and allowable scour depths.

The 11 case histories used to validate the new method showed good agreement between predicted values and field measurements. BSA 1 was then applied to 16 bridges. In this process, 6 out of 10 bridges classified as scour critical by current methods were found to be stable. These results show that the new method allows for more realistic evaluation of bridges for scour while not requiring site-specific erosion testing.

DEDICATION

Dedicated to my parents

ACKNOWLEDGEMENTS

I would like to express my gratitude to the chair of my dissertation committee, Dr. Jean-Louis Briaud, for his guidance, insight and unconditional support. I have learned a lot from Dr. Briaud. One of the first things he thought me was accountability. I remember him saying while reviewing the slides of my first research presentation, "If it is on one of your slides, make sure it's right and that there is no one else who knows more about it!" From our numerous discussions, I learned to approach problems methodically, beginning by understanding the big picture, applying the fundamentals and then finding a solution. Dr. Briaud is a wonderful mentor, both as professor and person. And I truly enjoy his great sense of humor.

I would like to thank the members of my dissertation committee: Drs. Francisco Olivera, Hamn-Ching Chen and Christopher Mathewson for their valuable guidance and knowledge. These professors introduced diversity into our research group by bringing together the fields of hydrology, hydraulics and engineering geology. I also thank Dr. Paolo Gardoni for all his guidance and support.

Dekay Kim has been my research partner for the last two years on the Texas Department of Transportation project which funded my doctoral studies. He provided the hydrologic and hydraulic data I needed as input into my models. Dekay, a wizard at computer programming, has on several occasions provided valuable advice on the codes I was developing for my research. I really appreciate all his help and support.

I would like to thank Radhakrishna Pillai for all his support, help and encouragement. I have been very fortunate to have Pillai's support during the many

challenges I faced as a doctoral student. Pillai was there for me on so many occasions. In particular, I thank him for his help with my laboratory experiments, dissertation writing, defense presentation, and also the countless engaging technical discussions we've had.

My friends Anjana Talapatra, Ali Nejat and Valliyappan David have been very supportive during my Ph.D. Anjana provided support in many ways, especially with the dissertation during the final weeks leading to my defense. She has been a very good friend. Ali has been my officemate for the past year. I was fortunate to have Ali around to discuss ideas as they occurred to me. I truly appreciate that he always took the time to understand my work and give me the general perspective of a civil engineer. David was especially helpful in my preparations for the final defense.

I would like to thank Pritha Ghosh, Saradhi Koneru, Tushara Raghavan, and Veni Kunasegaran for all the good food as well as preparations for my final defense. Abilasha Katariya and Guruprakash Thirumalaisamy helped with some editing of figures and tables.

Members of my extended family have been very supportive over the years. Specifically, I would like to thank Sanda Chemah and Prema Chemah for all their love and care.

I would like to thank Alo and her parents for all the love and encouragement. Alo has supported me in many ways throughout my Ph.D. I appreciate the support Bala has given me, right from the time we were in Singapore.

It has truly been a blessing growing up with my siblings. Chechi and Yettan, I can't thank you enough for all you have done for me. You both have played an integral

part in my studies and career. AIT would not have happened without you, and to me that is where it all began. Chaandni and Tej Anand, I think of you almost every day. You have made me laugh on many difficult days!

Mugdha came into my life on the second week of my doctoral studies. Mugdha, you have given me a new reason in life and for this, I thank you.

I would like to thank my parents for their love and the million other things they have done for me. Appa, I still remember you saying when we were deciding on AIT, "You can't put a price on education and you should go ahead - no hesitation on my part." You can't imagine how grateful I am you said that. Amma, you always believed in me. Your encouragement and love has been a vital element in my life. Both of you always put our education above everything else, and it is for this and the way you love your children that I dedicate this dissertation to you.

TABLE OF CONTENTS

Page

Page

Page

Page

LIST OF FIGURES

Page

Page

Page

Page

LIST OF TABLES

Page

1. INTRODUCTION

1.1. BRIDGE SCOUR

Bridge scour is the term used to describe the loss of geomaterials (soils, rocks and intermediate geomaterials) caused by water flowing around bridge supports. There are two major categories of scour which are general scour and local scour.

General scour refers to the aggradation or degradation of geomaterials in the riverbed that is not related to the local obstacles present at a bridge. Aggradation is the gradual and general accumulation of sediments at the bottom of the river and degradation is the gradual and general removal of sediments from the riverbed (Briaud et al. 2004).

Local scour is the term that refers to the erosion of geomaterials around flow obstacles posed by the presence of the bridge. Figure 1-1 gives a general illustration of how river flow is affected by a bridge. There are three types of local scour: pier scour, abutment scour and contraction scour. Pier scour is the removal of geomaterials around the foundation of a pier. Abutment scour is the removal of geomaterials around an abutment at the junction between a bridge and an embankment. Contraction scour

---

This dissertation follows the style of the *Journal of Geotechnical and Geoenvironmental Engineering.*

is the removal of geomaterials from the bottom of the river due to the narrowing of the river channel created by the approach embankments and piers of a bridge (Briaud et al. 2004). Figure 1-2 illustrates the three components of local scour.

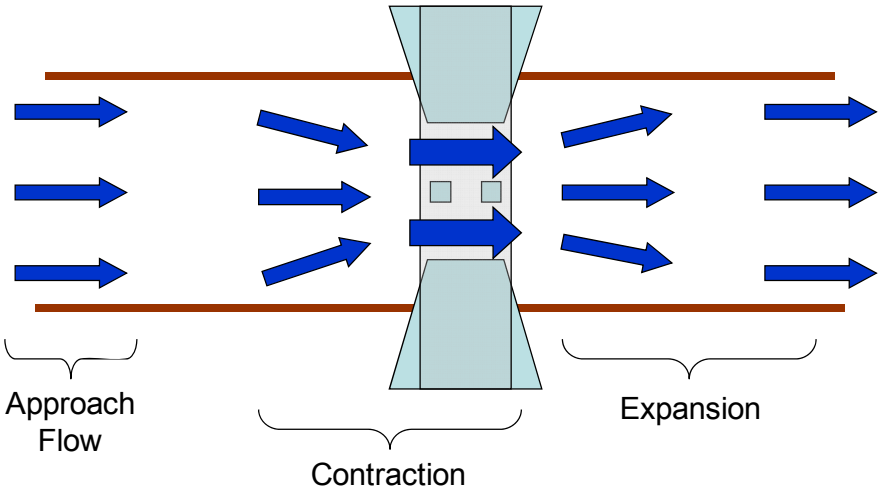

Figure 1-1. General illustration of how a bridge affects river flow.

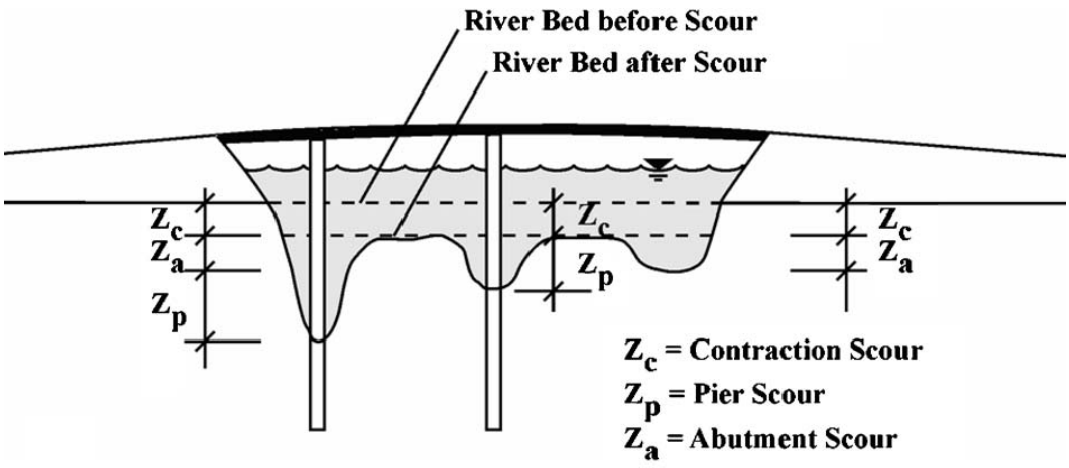

Figure 1-2. The three components of scour (after Briaud et al. 2005).

1.2. GEOMATERIALS: A DEFINITION

Geomaterials can be classified into three categories: soils, rocks and intermediate geomaterials such as cobbles and boulders. Briaud (2008) defines soil as an earth element which can be classified by the Unified Soil Classification System (USCS). The classification tests for soils are the grain size analysis (sieve analysis and hydrometer analysis) and the Atterberg Limits. The grain size analysis leads to the determination of the mean grain size D_{50} of a material which is the grain size corresponding to 50% of the soil weight passing a sieve with an opening size that is equal to D_{50}. The first major division in soils is the classification between coarse-grained soils and fine grained-soils. Soils that have a D_{50} greater than 0.075 mm are the coarse-grained soils. Conversely, soils with a D_{50} smaller that 0.075 mm are the fine-grained soils. Coarse-grained soils

include gravels and sands and are identified by their grain size. Fine-grained soils include silts and clays and are identified on the basis of Atterberg Limits (Briaud et al. 2004). Briaud (2008) defines rock as an earth element which has a joint spacing of more than 0.1 m and an unconfined compressive strength of the intact rock core of more than 500 kPa. Intermediate geomaterials are materials whose behavior is intermediate between soils and rocks, such as cobbles, boulder and riprap.

1.3. ERODIBILITY OF GEOMATERIALS

The erodibility of soil or rock is defined as the relationship between the erosion rate, $\dot{Z}$ and the velocity of water, V at the soil / rock - water interface. This definition however is not very satisfactory because the velocity varies in direction and intensity in the flow field (Briaud 2008). To be exact, the velocity of water is zero at the soil/rock interface. A more adequate definition is the relationship between erosion rate $\dot{Z}$ and shear stress at the soil/rock interface. However, the velocity is often used as it is easier to gauge an erosion problem from a velocity standpoint.

One of the most important material parameters in soil erosion is the threshold of erosion (Briaud 2008). Below the threshold value, erosion does not take place. Once the applied hydraulic stress (or more simply the velocity) exceeds the threshold value, erosion is initiated until the equilibrium scour depth is obtained. The threshold values for erosion in terms of shear stress is the critical shear stress τ_c and in terms of velocity is the critical velocity V_c. Important parameters that assist in describing the erosion function include the threshold value, the initial rate of scour and the equilibrium scour

depth. The erosion rate in clays and rocks can be many times smaller than the erosion rate in sands.

1.4. THE PROBLEM ADDRESSED

This research deals with the development of a bridge scour assessment procedure that is relatively simple, economical and does not require site-specific erosion testing. Previously, the Texas Department of Transportation (TxDOT) in a project with Texas A&M University developed the Erosion Function Apparatus (EFA) to measure the erosion function of soils and rocks. In conjunction with that research project, a method to determine the scour rate in cohesive soils at bridge piers was developed. This method is termed the SRICOS-EFA Method for bridge piers. SRICOS stands for Scour Rate in Cohesive Soils. This method predicts the scour depth as a function of time when a cylindrical pier in layered soil is subjected to a long term deep-water flow velocity hydrograph. Subsequently, Texas A&M University in collaboration with the National Cooperative Highway Research Program (NCHRP) developed the SRICOS-EFA Method for bridge contractions. This method predicts the scour depth as a function of time when a bridge contraction in layered soil is subjected to a long term deep-water flow velocity hydrograph. For each of these two methods, two levels of complexity were developed by the Texas A&M University scour research group. The first level is termed the Extended SRICOS method which requires the testing of soil samples, the use of a velocity hydrograph, and a computer program. The second level is termed the Simple SRICOS-EFA Method which also requires the testing of soil samples, but does not

require a computer program and instead can be done at the back of an envelope (Briaud et al. 2004). In this research, the Simple SRICOS-EFA Method was employed in simulations that led to a more simple and economical method for bridge scour assessment that did not require site-specific erosion testing.

1.5. WHY THIS PROBLEM WAS ADDRESSED

The reason for solving this problem is that there are approximately 600 bridges in Texas that have been classified as scour critical, but many of them are so because of the use of over-conservative scour calculation methods that predict excessive scour depths under a design flood event. The locations of the scour critical bridges are shown in Figure 1-3. Current available methods of bridge scour evaluation rely upon three categories of assessment methods. The first category, termed Level 1 analysis is a preliminary scour evaluation procedure that is based on field observations and is primarily qualitative in nature, but could also rely on simplified scour depth – hydraulic parameter relationships that are mainly based on flume tests in sand. This category does not utilize actual measured scour data. The second and third categories, termed Level 2 and Level 3 analysis involve more detailed calculations of maximum scour depth based on flume tests on sand. The difference between the second and third categories is that a Level 2 analysis consists of hydraulic modeling and the computation of the estimated depth of maximum potential scour resulting from a design flood event whereas a Level 3 analysis consists of a fluvial computer model simulation or a laboratory model study of a site to assess complex conditions which are beyond the scope of the Level 2 analysis

procedures. The first method does not provide realistic results in many cases because of its reliance on a more qualitative form of assessment. The second and third methods are often conservative in the case of clays, which are known to erode at a much slower rate than sand.

In order to overcome the over-conservative nature of these methods, Briaud et al. (1999, 2005) at Texas A&M University developed the SRICOS-EFA Method to calculate scour depths due to pier and contraction scour that are capable of accounting for time-dependent scour in clays. However, these methods require site specific erosion testing. Carrying out soil sampling at the 600 scour critical bridges and subsequently testing them would represent a huge cost and is therefore uneconomical in addressing the bridge scour problem in Texas.

Therefore, for geomaterials that erode at much slower rates than sands, for example clays and some rocks, a more realistic method that is relatively low cost and economical is required to replace the calculation methods based on sand. In order to overcome the qualitative nature of current initial evaluation procedures, a method that utilizes actual scour measurements and compares them with the foundations load carrying capacity is also required.

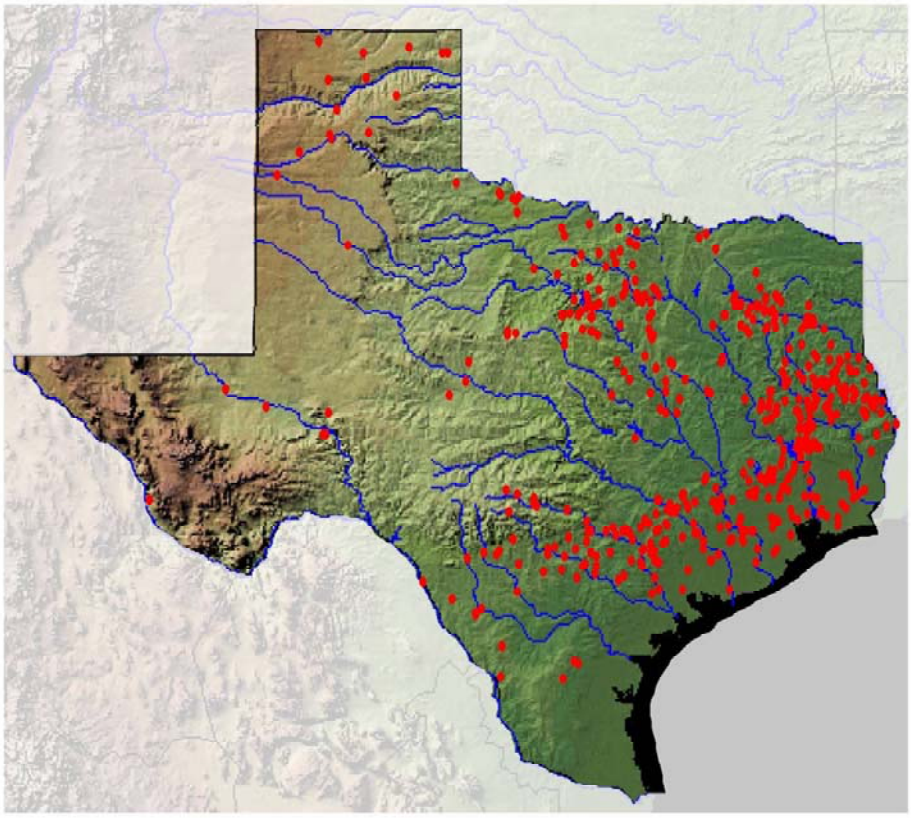

Figure 1-3. The location of scour critical bridges in Texas.

1.6. APPROACH SELECTED TO SOLVE THE PROBLEM

The approach selected to solve the problem of assessing a bridge more realistically for scour was based on a combination of a review of existing knowledge, EFA tests, study of case histories, computer simulation, fundamental principles in method development, and verification of the method against available data. The review of existing knowledge avoided duplication of effort and helped establish a solid foundation. The EFA tests

provided a database of erodibility properties according to soil type which led to the development of erosion categories. These categories were plotted on a chart and help eliminate the need for site-specific erosion testing at the preliminary design level and with a conservative approach. The case histories gave an idea of the data that bridge inspectors have and use. It was also a good overview of bridges in Texas. The computer simulations were also used to simulate a very large number of combinations of bridge scour parameters which enabled the development of bridge scour assessment charts, termed Z-Future Charts. Verification was based on comparison between case histories that were subjected to the proposed assessment procedure and actual field measurements.

1.7. VALIDATION OF THE PROPOSED ASSESSMENT METHOD

Several full case histories were selected for the validation of the proposed bridge scour assessment procedure. The required information was soil data, flow data, age of the bridge, foundation type and dimensions, and scour depths. There were 11 cases that were considered adequate and suitable, and were used in the validation process.

The bridge records for the case histories had limited bridge scour measurements. In fact, there were no bridge scour measurements taken before the year 1991. Since most of the bridges were reasonably old (up to approximately 80 years old), they had experienced the largest flow velocity prior to the first bridge scour measurement. This resulted in all the cases having a V_{fut}/V_{mo} ratio equal to or less than unity for the BSA 1 validation. Results of the BSA 1 validation showed good agreement between predicted

and measured values. However, this validation is only for V_{fut}/V_{mo} ratios equal to or less than unity. The results of the validation of BSA 2 also showed good agreement between the BSA 2 method and the SRICOS-EFA Method. The validation of BSA 3 indicated that BSA 3 tends to overestimate the scour depth when compared to field measurements. This could be due to the fact that the selection of erosion categories on the basis of soil type is very conservative (by design). However, BSA 3 does improve on the over-estimation of scour depth by 2 ft to 4 ft when compared to maximum scour depths.

1.8. APPLICATION TO SCOUR CRITICAL BRIDGES

BSA 1 was validated using 16 bridges in the State of Texas. Out of the 16 bridges, 6 bridges that were classified as scour critical by TxDOT were found to be stable by BSA 1. Of the 16, 3 bridges could not be evaluated due insufficient information or unsuitable field conditions. The remaining 7 bridges had outcomes similar to the TxDOT designation. Out of the 7 bridges that had similar outcomes for both BSA 1 and the TxDOT designation, 3 were stable and 4 were scour critical. So, 6 of the 10 bridges that were originally scour critical and had sufficient information were found to be stable after BSA 1 according to the stability criterion.

2. BACKGROUND

2.1. INTRODUCTION

Current available methods of bridge scour evaluation rely upon three categories of assessment methods. The first category, termed Level 1 analysis is a preliminary scour evaluation procedure that is based on field observations and is primarily qualitative in nature, but could also rely on simplified scour depth – hydraulic parameter relationships that are mainly based on flume tests in sand. This category does not utilize actual measured scour data. The second and third categories, termed Level 2 and Level 3 analysis involve more detailed calculations of maximum scour depth based on flume tests on sand. The difference between the second and third categories is that a Level 2 analysis consists of hydraulic modeling and the computation of the estimated depth of maximum potential scour resulting from a design flood event whereas a Level 3 analysis consists of a fluvial computer model simulation or a laboratory model study of a site to assess complex conditions which are beyond the scope of the Level 2 analysis procedures. The first method does not provide realistic results in many cases due to its reliance on a more qualitative form of assessment. The second and third methods are often conservative in the case of clays, which are known to erode at a much slower rate than sand. Briaud et al. (1999, 2005) at Texas A&M University developed models to calculate scour depths due to pier and contraction scour that are capable of accounting for time-dependent scour in clays. These methods, collectively called the SRICOS

method (Briaud et al. 1999, 2005) require site specific erosion testing (Govindasamy et al. 2008).

Preliminary scour evaluation procedures have been developed by or for several state Departments of Transportation (DOTs). For example, the Montana DOT, in collaboration with the United States Geological Survey (USGS), developed a rapid scour evaluation process that relies upon calculated scour depth – measured hydraulic parameter relationships (Holnbeck and Parrett 1997). A similar method has also been adopted by the Missouri DOT (Huizinga and Rydlund 2004). The Tennessee DOT uses an initial evaluation process that utilizes a qualitative index based on field observations to describe the potential problems resulting from scour (Simon et al., 1989). Similar qualitative methods have been adopted by the California, Idaho and Texas DOTs and the Colorado Highway Department for their initial assessment of bridges for scour. Johnson (2005) developed a preliminary assessment procedure that individually rates 13 stream channel stability indicators, which are then summed to provide an overall score that places a bridge in one of four categories: excellent, good, fair and poor (Govindasamy et al. 2008).

Current practice for more detailed scour evaluation is heavily influenced by two United States Federal Highway Administration (FHWA) hydraulic engineering circulars (HEC) called HEC-18 and HEC-20 (Richardson and Davis 2001; Lagasse et al. 1995). These methods are known to be overly conservative in the case of clays and some types of rock due to the fact that they are based on flume tests in sand and do not account for time-dependent scour (Govindasamy et al. 2008).

2.2. CURRENT ASSESSMENT METHODS IN PRACTICE

2.2.1. FHWA Guidelines for Evaluating Scour at Bridges

On October 28, 1991 the United States Federal Highway Administration (FHWA) issued Technical Advisory T 5140.23 entitled "Evaluating Scour at Bridges", which requires that a plan of action (POA) be developed for each existing bridge in the nation found to be scour critical. Jones and Ortiz (2002) define a scour critical bridge as one with foundation elements that are determined to be unstable for the calculated and/or observed stream stability or scour conditions. To monitor the conditions of bridges throughout the nation, FHWA maintains a database called the National Bridge Inventory (NBI) (Jones and Ortiz 2002). In the NBI database, FHWA codes bridges in terms of scour and stream stability according Technical Advisory T5140.23 (1991), which categorizes the evaluation of these issues according to the following items:

1. Item 61 for Channel and Channel Protection
2. Item 113 for Scour Critical Bridges

For Item 61, the bridge being evaluated is rated from numbers 0 to 9 or the letters "N". For Item 113, the bridge being evaluated is rated from numbers 0 to 9 or letters "T", "U" or "N". The smaller the numeric rating the more serious scour or channel stability problem. For example, in Item 113, a ranking of "0" would indicate that a bridge is scour critical, has failed and is closed to traffic. A ranking of "9" would indicate that the bridge foundations are on dry land, well above flood water elevation. The letter ranking "T" indicates that the bridge is over tidal waters and is considered low

risk even though it has not been evaluated for scour. The ranking "U" indicates that the bridge is supported by unknown foundations. A bridge with unknown foundations should have a plan of action until its risk to scour can be determined. The ranking "N" indicates that the bridge is not over a waterway (Richardson and Davis 2001). A detailed description of the codes used can be found in Appendix J of the FHWA HEC-18 circular (Richardson and Davis 2001). Table 2-1 shows the codes in FHWA Item 113.

2.2.2. Bridge Scour Evaluation Practice in Texas

Launched in 1991, the Texas Department of Transportation (TxDOT) bridge scour evaluation and mitigation program consists of the use of a bridge inventory database, scour inspection procedures, and several levels of screening processes (Haas et al. 1999). The TxDOT bridge inventory database is called the Bridge Inventory, Inspection and Appraisal Program (BRINSAP) database and is devised to meet the inventory system requirements of Section 650.311(a) of the National Bridge Inspection Standards (NBIS) (Federal Highway Administration, 2004). In the BRINSAP database, Item 113 provides the scour rating while Item 113.1 provides a scour vulnerability assessment for each bridge. The TxDOT's inspection procedures comprise initial inspections, routine inspections and special inspections. Under certain circumstances, damage inspections and in-depth inspections are also conducted. Bridges that have a low vulnerability to scour are excluded from extensive hydraulic analyses to reduce costs. These mechanisms are used by TxDOT to meet NBIS regulations and establish procedures to ensure the safety of bridges. Additionally, these mechanisms provide data which indicate the risk of

scour-related damage for each bridge, which would then enable the prioritization of bridge sites to receive scour countermeasures.

Table 2-1. Codes in FHWA Item 113 (after Richardson and Davis 2001).

Codes	Description
N	Bridge not over waterway.
U	Unknown foundation that has not been evaluated for scour. Until risk is determined, POA should be developed.
T	Bridge is over tidal waters that have not been evaluated for scour, but considered low risk. Bridge will be monitored with regular inspection cycle until evaluation is performed.(Unknown foundations in tidal waters should be coded U)
9	Bridge foundations on dry land well above flood water elevations.
8	Bridge foundations determined to be stable for the assessed or calculated scour condition. Scour is determined to be above top of footing by assessment, calculation or installation of properly designed countermeasures.
7	Countermeasures have been installed to mitigate an existing problem with scour and to reduce the risk of bridge failure during flood event.
6	Scour calculations/evaluation has not been made. (Use only to describe case where bridge has not yet been evaluated for scour potential)
5	Bridge foundations determined to be stable for assessed or calculated scour condition. Scour is determined to be within the limits of footings or piles by assessment, calculations or installation of properly designed countermeasures.
4	Bridge foundations determined to be stable for assessed or calculated scour conditions; field review indicates action is required to protect exposed foundations.
3	Bridge is scour critical; bridge foundations determined to be unstable for assessed or calculated scour conditions: scour within limits of footings or piles; scour below spread-footing base or pile tips
2	Bridge is scour critical; field review indicates that extensive scour has occurred at bridge foundations, which are determined to be unstable by: a comparison of calculated scour and observed scour during the bridge inspection; an engineering evaluation of the observed scour reported by the bridge inspector.
1	Bridge is scour critical; field review indicates that failure of piers/abutments is imminent. Bridge is closed to traffic. Failure is imminent based on : a comparison of calculated and observed scour during the bridge inspection; an engineering evaluation of the observed scour condition reported by the bridge inspector.
0	Bridge is scour critical. Bridge has failed and is closed to traffic.

2.2.2.1. The BRINSAP Database

TxDOT has a state level equivalent of NBI called the BRINSAP database. The BRINSAP database comprises 135 fields for each bridge record and gives a comprehensive account of the physical and functional characteristics of each bridge. The database categorizes bridges into two major groups of structures, which are the on-system and off-system bridges. On-system bridges generally are structures which belong to the state highway department or other state or federal agencies, which are responsible for their maintenance. Off-system structures in general belong to local municipalities. The state of Texas comprises 25 districts which are divided into 254 counties (Haas et al. 1999). The majority of scour problems occur in East Texas where annual rainfall is higher and soil conditions are more susceptible to erosion. The BRINSAP database includes entries for the district and county where each structure is located. TxDOTs twenty-five districts are shown in Table 2-2 and Figure 2-1.

Table 2-2. TxDOT district identification (after Haas et al. 1999).

District	No.	District	No.
Paris	1	Austin	14
Ft. Worth	2	San Antonio	15
Wichita Falls	3	Corpus Christi	16
Amarillo	4	Bryan	17
Lubbock	5	Dallas	18
Odessa	6	Atlanta	19
San Angelo	7	Beaumont	20
Abilene	8	Pharr	21
Waco	9	Laredo	22
Tyler	10	Brownwood	23
Lufkin	11	El Paso	24
Houston	12	Childress	25
Yoakum	13		

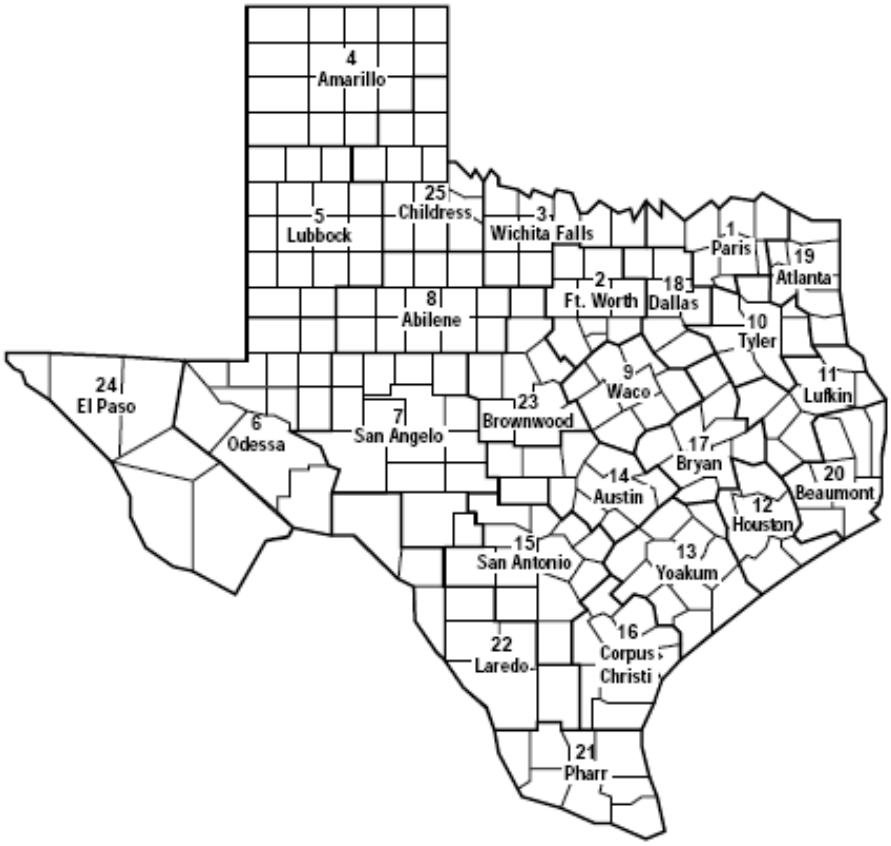

Figure 2-1. Map showing the twenty-five districts of Texas (after Haas et al. 1999).

2.2.2.2. Initial Screening Method for Scour Evaluation (SVEAR)

The FHWA Technical Advisory T 5140.23 requirement for plans of actions for scour critical bridges prompted TxDOT to develop an initial scour screening process aimed at detecting bridges that may require further scour evaluation. The proposed initial screening process comprised a cursory geomorphic survey of bridges over waterways.

The evaluation of the bridges is performed by carrying out a field survey of the hydraulic and physical characteristics of the bridge site. The results of the survey were then used to complete the Scour Vulnerability Examination and Ranking Format (SVEAR) shown in Figure 2-2, which would lead to a scour susceptibility ranking of the bridges (Haas, et al. 1999). The objective of the program was to identify the bridges with scour problems and the extent of the associated problem and subsequently provide a means of prioritizing bridges to receive further evaluation. The SVEAR process categorizes bridges into those having known scour problems, being highly susceptible to scour, having medium susceptibility to scour, or having low risk. The prioritization procedure for the bridges relies on the outcome of the SVEAR process and data in the BRINSAP database (Olona 1992).

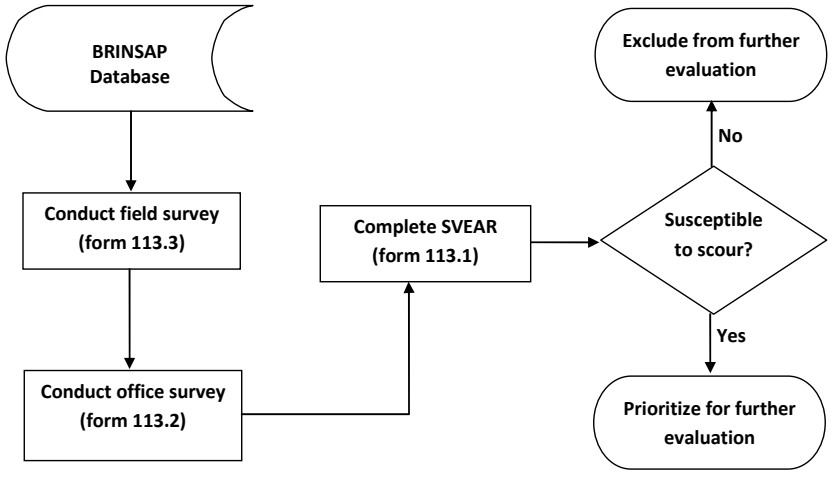

Figure 2-2. The SVEAR screening process flowchart (after Haas, et al., 1999).

Because the initial screening process (SVEAR) yielded a large number of bridges that were designated as vulnerable to scour, there was a need to refine the evaluation process to better assess and understand the bridges. To achieve this, TxDOT developed the Texas Secondary Evaluation and Analysis for Scour, known as TSEAS (Haas et al. 1999). TSEAS consists of two distinct parts. The first part is a question and answer process termed Secondary Screening and is rather similar to the initial screening process. The Secondary Screening process is aimed at determining risk factors and differentiating between stream stability and bridge scour factors. The second part is termed Concise Analysis (or Detailed Analysis) and is a simplified bridge scour analysis procedure which is performed, depending on the outcome of the Secondary Screening.

2.2.2.3. Secondary Screening

The secondary screening is a procedure that contains 11 questions that need to be answered by the bridge inspector. The issues covered in the questions are as follows (Texas Department of Transportation 1993):

1. The presence of non-erodible rock or cohesive materials with SPT-N values greater than 100 blows per foot as the foundation material
2. The presence of existing scour countermeasures
3. The presence of sand as the foundation material
4. Evidence of general channel degradation, local bridge scour or, both
5. The impact of stream migration
6. Historical scour damage at the bridge
7. The effects of mining or mining related operations on the bridge site

8. The impact of skewed bents on scour at the bridge site
9. The impact of dams and other control structures on the bridge site
10. The presence of spread footings that are not supported by piles or embedded in rock
11. The impact of debris

The response to some of the issues mentioned above may require a field visit if documentation established during the initial screening process was insufficient (Texas Department of Transportation 1993). Figure 2-3 shows the secondary screening flowchart, where BS refers to bridge scour problems and SS refers stream stability problems. In the figure, the definitions of Item 113 and Item 113.1 and the associated numeric code has been explained in the preceding section.

2.2.2.4. Concise and Detailed Analysis

Depending on the outcome of the secondary screening process, concise or detailed analysis may be required under certain scour and stream stability conditions (Figure 2-3). These analyses involve bridge scour calculations which require suitable hydraulic parameters but are otherwise straight-forward. Detailed Analysis typically includes acquisition of several stream cross sections and field data, hydrologic parameters, standard-step backwater analysis and data manipulation to extract variables to be applied in the appropriate scour equations. For the Concise Analysis, the hydraulic data retrieval is simplified by considering variables that either have been determined in the design phase of the structure (and blue prints) or can be estimated based on historic and/or

nominal additional field data. If neither of these techniques yields reasonable hydraulic parameters for a Concise Analysis, a Detailed Analysis is recommended (Texas Department of Transportation 1993).

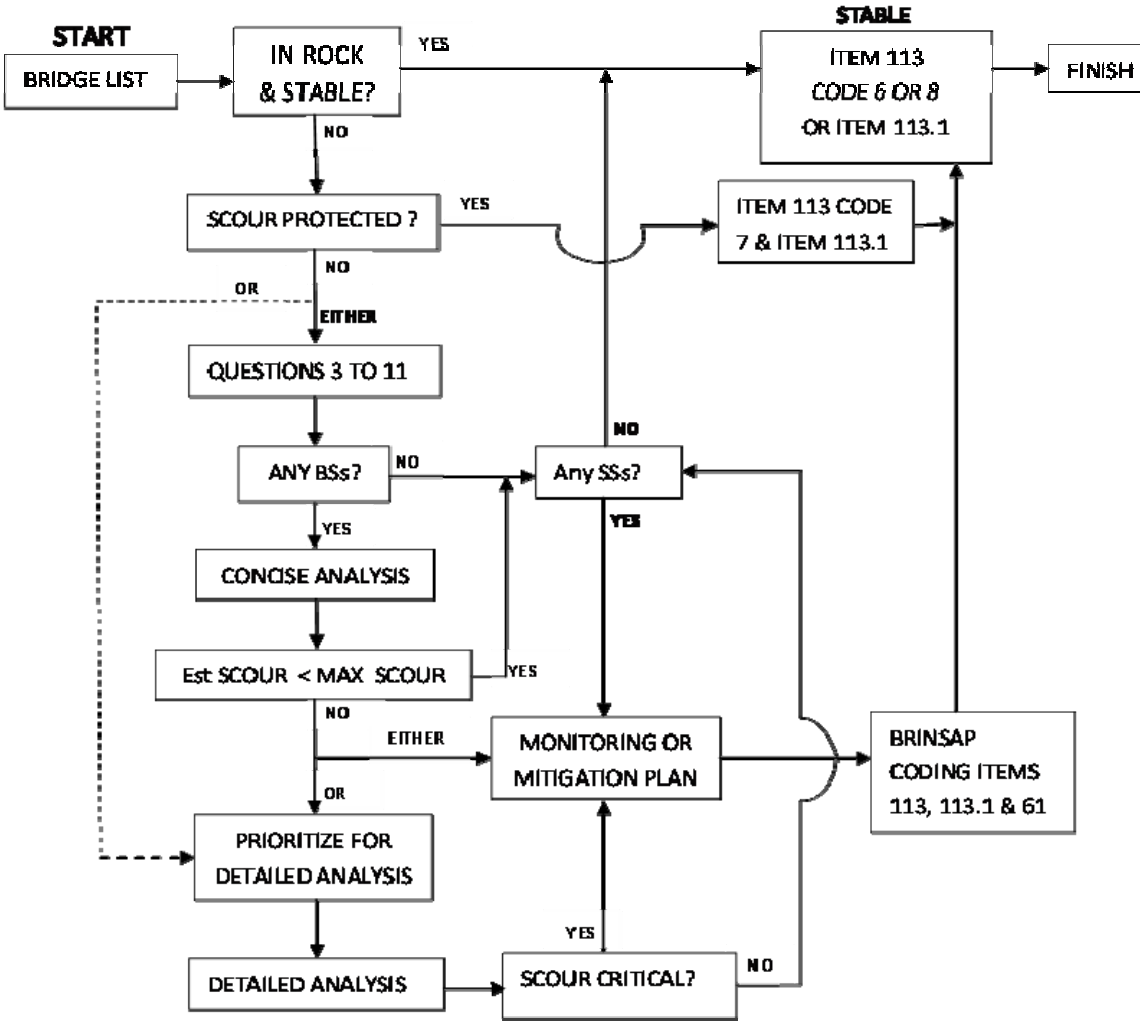

Figure 2-3. Secondary screening flowchart (after Texas Department of Transportation 1993).

The following is an outline of the steps required for the Detailed and Concise Analyses as presented in TSEAS (Texas Department of Transportation 1993):

1. Determination of hydraulic variables such as natural channel and through-bridge velocities, wetted perimeter and Manning's n values.
2. Determination of maximum allowable scour based on estimated foundation bearing capacity and lateral stability.
3. Estimation of maximum pier scour.
4. Determination of potential pier scour.
5. Determination of maximum allowable flow contraction ratio.
6. Determination of channel geometry contraction ratio.
7. Estimation of actual flow contraction ratio.
8. Comparison of allowable scour depths with estimated scour depths.
9. Recommendations for BRINSAP coding and/or further handling.

2.2.3. Tennessee Level 1 Assessment

The Tennessee Level 1 Assesment (United States Geological Survey 1993) procedure which is an initial bridge scour assessment technique is designed to provide a qualitative index indicating the potential for problems due to localized scour and general stream instability. In this procedure, a bridge inspector makes basic scour or stream stability related measurements or visually estimates them. These and other qualitative measurements are recorded in a form. These data provide information on the general stability of the stream reach in which the bridge is located. The data include observations of land use in the watershed, bed and bank material, bank slope, bank vegetation,

meander and point bar locations, debris production, channel constriction and observable bank-erosion processes. Additionally, the data include more detailed information on the structural components of the bridge that could influence local scour such as the number of piers in the main channel, skew angle of the piers with respect to flow, the skew angle and placement of abutments, observable localized scour at piers and abutments and debris accumulation at the bridge. Two indices, i.e. the potential scour index and observed scour index are produced by the Tennessee Level 1 analysis. As a follow up to the Level 1 Analysis, the Tennessee DOT employs a Level 2 Analysis which adopts the HEC-18 (Richardson and Davis 2001) methods to estimate maximum scour depth.

2.2.3.1. Potential Scour Index

The potential scour index is used to identify and rank bridges with significant potential scour problems. The potential scour index is computed by summing a collection of variables that have been assigned a ranking and is used to indicate problems for local scour and channel instability. Sites with a potential scour index greater than 20 have substantial potential for scour problems. The potential scour index comprises the following variables (United States Geological Survey 1993):

1. Erodibilty of bed material
2. Bed protection & bank protection
3. Stage of channel evolution
4. Percent of channel constriction
5. Number of piers in channel

6. Percent horizontal and vertical blockage
7. Bank erosion
8. Meander impact point from bridge
9. Pier skew
10. Mass wasting at pier
11. High flow angle of approach

While the rankings of the above variables are not weighted for relative importance, certain variables can be weighted higher than others if deemed appropriate by local transportation departments.

2.2.3.2. Observed Scour Index

The observed scour index is used to identify bridges with immediate scour problems. It can also provide additional insight into the potential for scour at a site. The observed scour index only considers local scour problems and does not account for general stream stability problems. The observed scour index is computed using the following variables (United States Geological Survey 1993):

1. Signs of pier scour.
2. Exposure of abutment piling.
3. Failed rip-rap at the bridge.
4. Movement of bed rip-rap.
5. Presence of blow holes.
6. Mass wasting at pier.

2.2.3.3. Relationship between Potential Scour Index and Observed Scour Index

Because they are not comparable values, the potential scour index and observed scour index should not be compared directly. There is neither a theoretical relationship nor a correlation implied between the two indices. The observed scour index only captures scour observable by the inspector and may not necessarily affect the bridge's structural stability. For example, exposed piling at several bridge piers can produce a high observed scour index even though very little localized scour or general channel degradation has occurred. The observed scour index should supplement the potential scour index to identify bridges requiring a more detailed analysis.

2.2.4. The Idaho Plan of Action for Scour Critical Bridges

The Idaho Plan of Action is a prioritizing mechanism for Idaho's scour critical bridges and bridges with unknown foundation. The method used to prioritize these bridges is based on the lifetime risk, which by definition is the lifetime cost of failure multiplied by the lifetime probability of failure and for scour critical bridges, the estimated probability of failure (Ayres and Associates 2004). Ayres and Associates (2004) go on to state that the lifetime risk is the expected cost of scour-related bridge failure, which is obtained by combining the cost of failure with the probability of failure. The values of probability of failure and failure cost are based on the expanded HYRISK method which is detailed in Pearson et al. (2000). As a simple illustration, a bridge with a high failure cost due to heavy traffic volume may still have a lifetime risk that is relatively low due to a low

probability of failure. The application of the IDAHO POA to scour critical bridges is shown in Table 2-3.

Table 2-3. Application of priority rankings to scour critical bridges (after Ayres Associates 2004).

Category	Scour Vulnerability	Number of Bridges	Lifetime Risk (L_r)	Annual Probability of Failure (P_f)
A	Vital	37	L_r > \$5,000,000 (lifetime cut-off value set in consultation with Idaho DOT Scour Committee)	-
B	Extreme	12	L_r < \$5,000,000	$P_f \geq 10\%$
C	Severe	109	L_r < \$5000,000	$P_f < 10\%$ (for bridges founded on spread footings)
D	Moderate	37	-	$P_f < 1\%$ (for bridges on driven pile foundation)

2.2.5. USGS Method for Rapid Estimation of Scour Based on Limited Site Data

In 1997, Holnbeck and Parrett developed a method for the rapid estimation of scour at highway bridges for the United States Geological Survey (USGS). This procedure was initially developed for the state of Montana for the purpose of aiding the Montana Department of Transportion in meeting the national bridge scour program requirements. The method was developed based on the following requirements:

1. Requirement of only limited site data
2. Provides estimates of scour depth that would be reasonably comparable to estimates from more detailed methods, for example the Level 2 scour analysis.
3. Provides estimates at each site in a few hours or less

Holnbeck and Parrett (1997) developed this method from Level 2 scour analyses performed by USGS in 10 states, namely Montana, Colorado, Indiana, Iowa, Mississippi, Missouri, New Mexico, South Carolina, Texas and Vermont. The components of bridge scour that were considered in both the Level 2 analysis and the proposed rapid estimation method are contraction scour and local scour at piers and abutments. Based on the Level 2 analysis, they presented the components of scour as a function of more easily estimated parameters during a bridge inspection. The contraction scour was expressed as a function of discharge at the contracted section, approach water depth, and D_{50}. The pier scour was expressed as a function of flow attack angle, Froude number, and pier width. Abutment scour was expressed as a function of abutment shape and flow depth at abutment. The reader is referred to Holnbeck and Parrett (1997) for a

detailed description of these relationships. The outcome of the rapid method was compared with its corresponding Level 2 analysis for several bridge sites and is shown in Figure 2-4, Figure 2-5 and Figure 2-6.

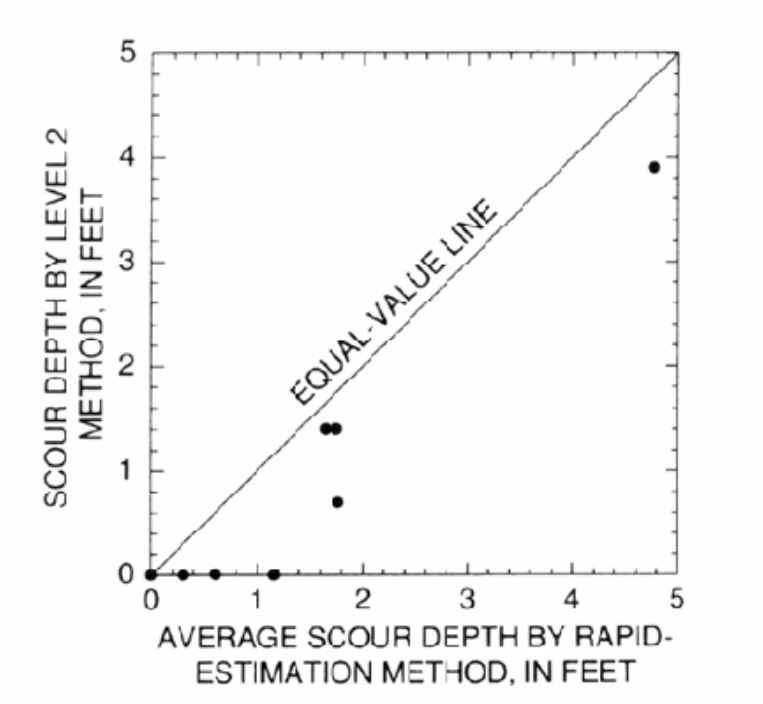

Figure 2-4. Comparision of contraction scour depth by the rapid estimation method and by Level 2 method (after Holnbeck and Parrett 1997).

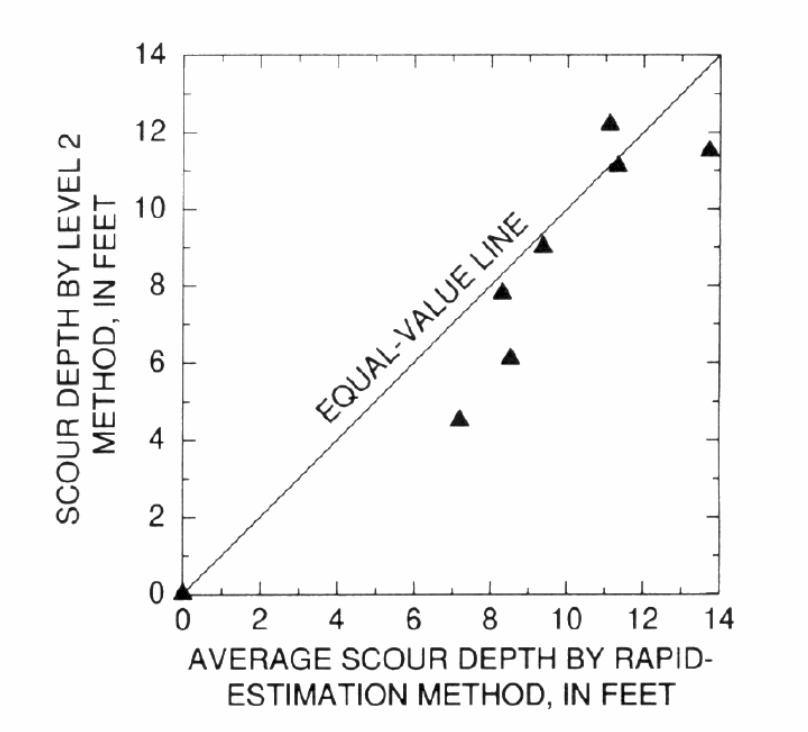

Figure 2-5. Comparision of pier scour depth by the rapid estimation method and by Level 2 method (after Holnbeck and Parrett 1997).

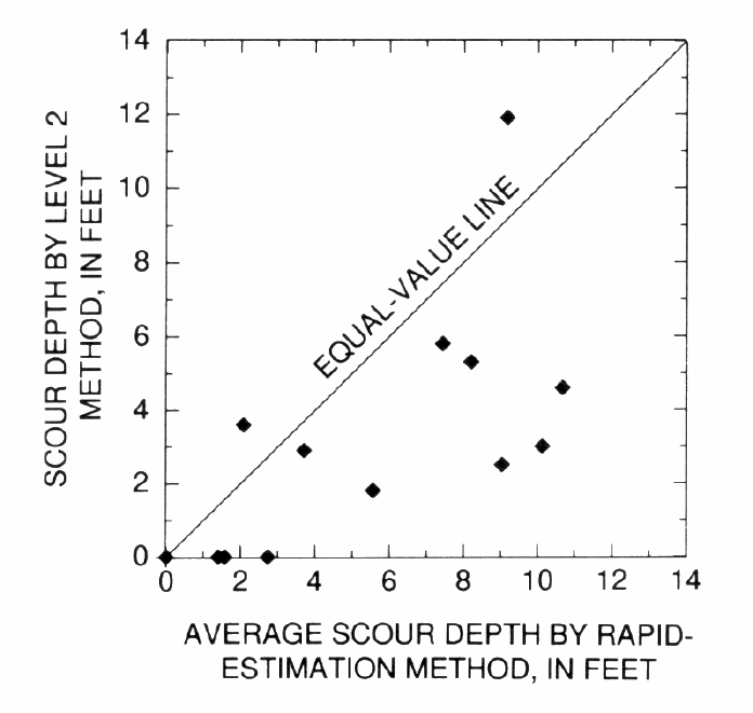

Figure 2-6. Comparision of abutment scour depth by the rapid estimation method and by Level 2 method (after Holnbeck and Parrett 1997).

2.2.6. Other Bridge Scour Assessment Procedures

Several state DOT and government agencies have developed techniques for assessing scour at bridges. For example, the Colorado Highway Department (1990) developed a scour vulnerability assessment procedure based on the geology, hydraulics, river conditions and foundations of bridges which enable scour prioritizing in scour susceptibility categories. This procedure incorporates three flowcharts (shown in Figure 2-7, Figure 2-8, and Figure 2-9) which are for general scour and stream stability issues, abutment scour and pier scour. The numerical values included in the flowchart were selected to emphasize the relative effect of each parameter on the potential to produce scour. Note that the values of each parameter are such that the most scour vulnerable bridge will have the largest value. As evident from the flow chart, this procedure is highly qualitative.

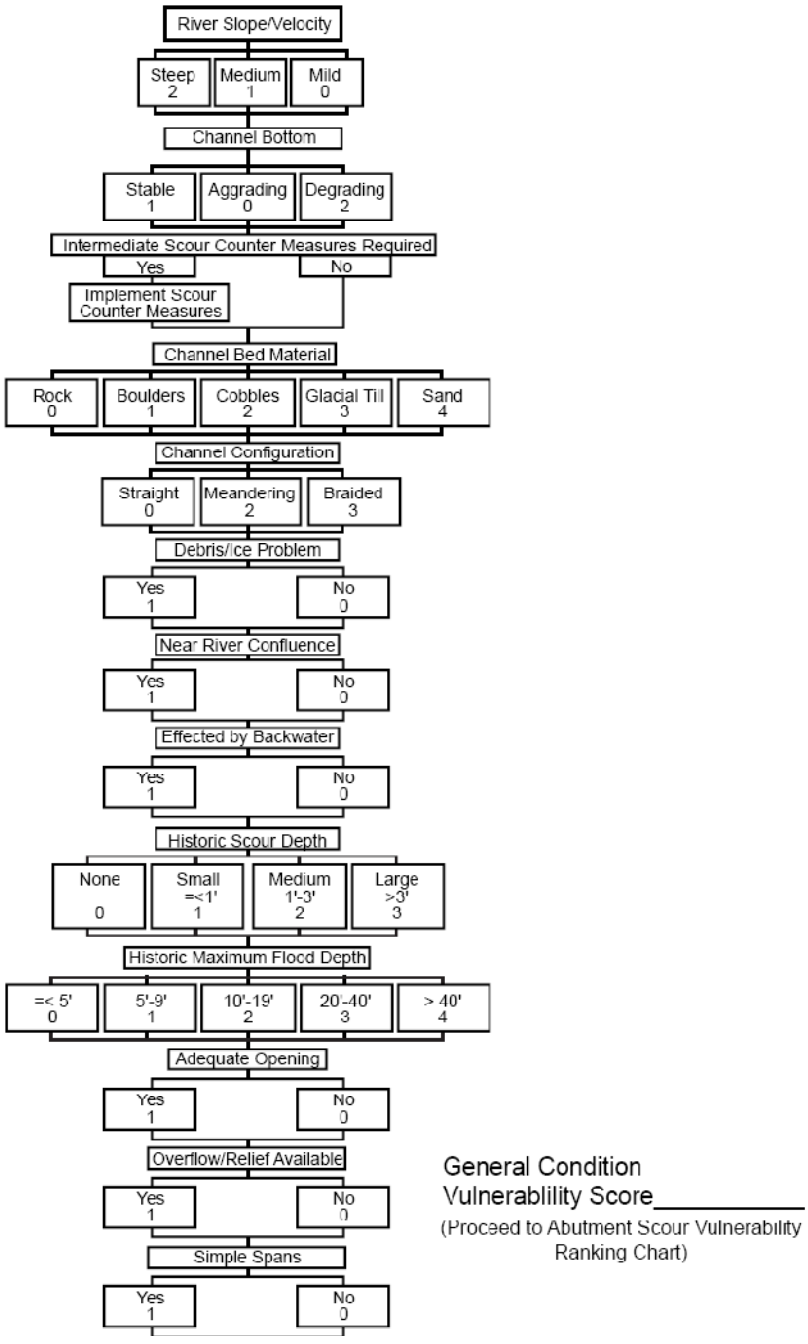

Figure 2-7. General conditions scour vulnerability ranking flowchart (after Colorado Highway Department 1990).

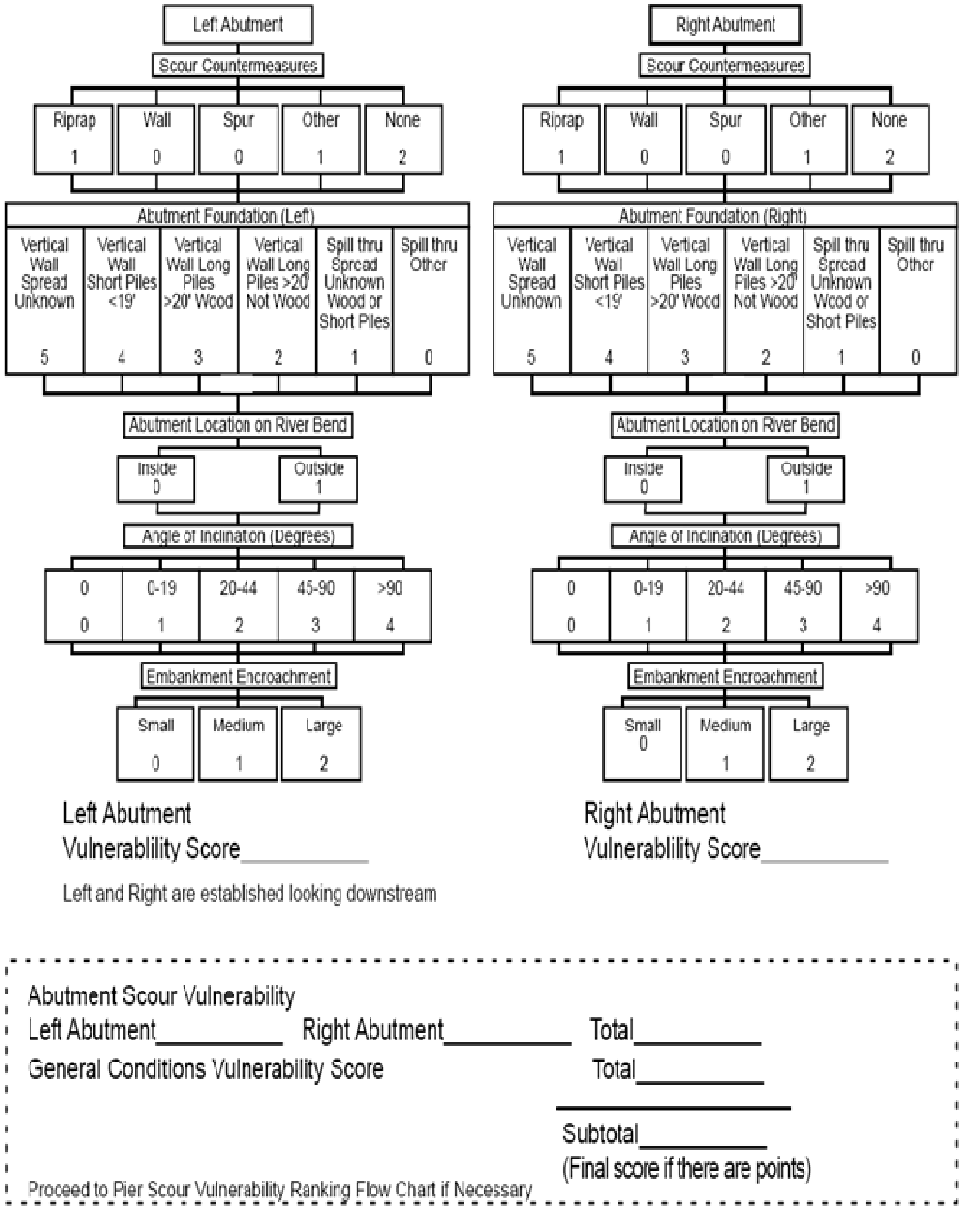

Figure 2-8. Abutment scour vulnerability ranking flowchart (after Colorado Highway Department 1990).

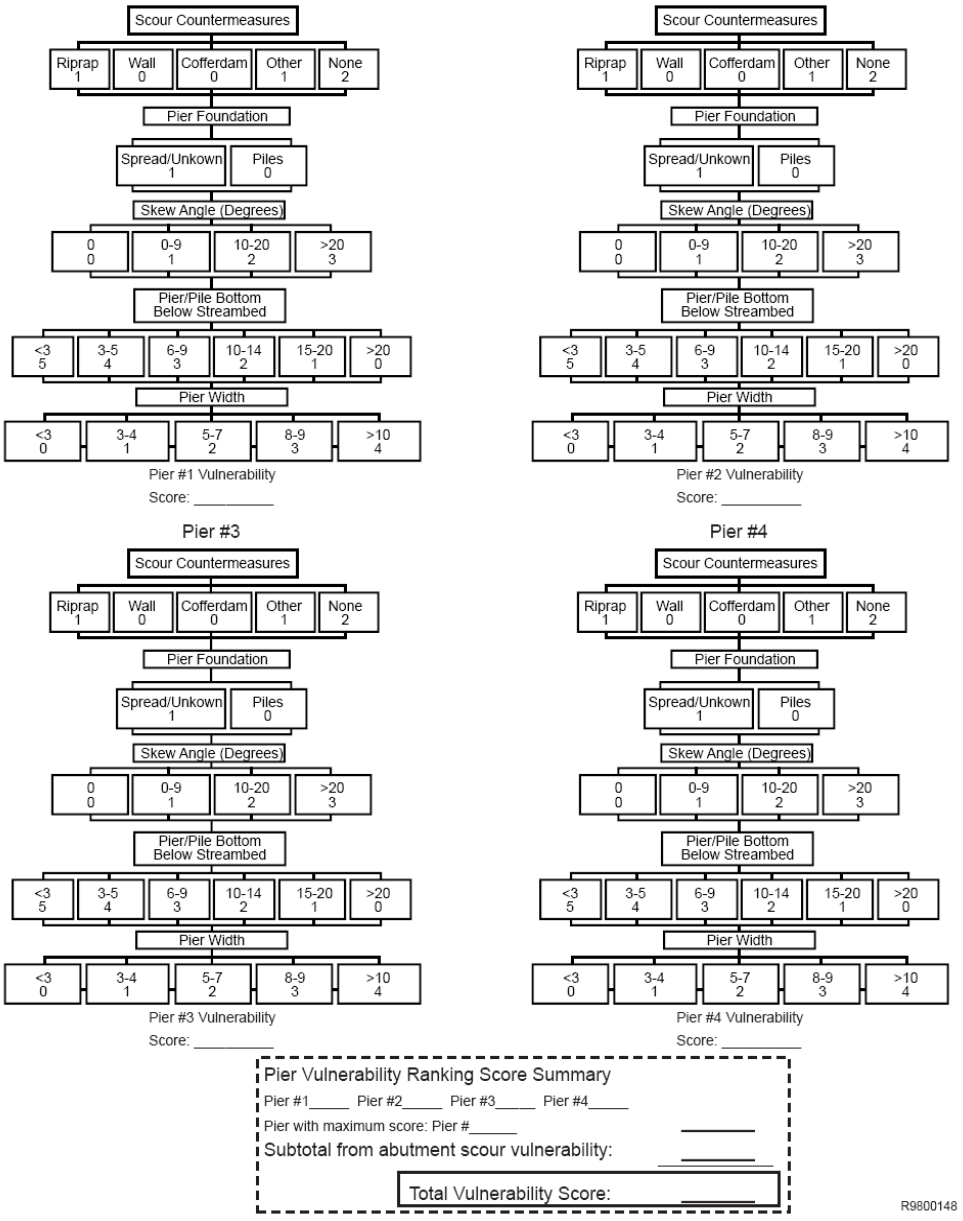

Figure 2-9. Pier scour vulnerability ranking flowchart (after Colorado Highway Department 1990).

Kattell and Eriksson (1998) developed a bridge scour evaluation procedure for the United States Department of Agriculture Forest Service, which covered a screening process, scour analysis and countermeasures. This procedure has four steps as indicated below:

- Step 1: Office screening and management priority analysis
- Step 2: Field review, scour vulnerability analysis, and prioritizing
- Step 3: Detailed scour evaluation.
- Step 4: Plan of action.

Steps 1 and 2 are similar to the more qualitative assessment procedures as described in the preceding sections. In fact, the method proposed by Kattell and Eriksson (1998) utilizes the Colorado Highway Department flowcharts and also recommends the USGS Rapid Estimation procedure. Step 3 in the method follows the guidelines in HEC-18 (Richardson and Davis 2001).

Palmer et al. (1999) at the University of Washington developed an expert system for evaluation of scour and stream stability. Their method, termed Cataloging and Expert Evaluation of Scour Risk and River Stability at Bridge Sites (CAESAR) is a field deployable decision support system that helps bridge inspectors identify probable scour risks and assess the bridge sites economically (Harmsen et al. 2001).

Harmsen et al. (2001) go on to state that the purpose of the expert system is as follows:

1. Determine the scour risk of a bridge based on site observations and history.
2. Catalog, store and retrieve information pertaining to the bridge site conditions.

The CAESAR expert system is based on user input information such as the presence of bank countermeasures and associated damage, evidence of localized erosion, accumulation of debris, and bed cross-section profile. The system relies on a rule base that determines if measures to mitigate scour damage are required. It uses knowledge and expertise obtained from existing literature including HEC-18 (Richardson and Davis, 2001) and HEC-20 (Lagasse et al. 1995), and from experienced professionals in the field of bridge inspection, river hydraulics, and geomorphology to draw conclusions about the site based upon bridge construction information and characteristics, and inspection records (Harmsen et al. 2001). This knowledge base was developed mainly through surveys and extensive interviews with experts (Adams et al. 1995). The key feature of the CAESAR expert system is the logic that is employed to reach a conclusion describing the scour risk of the bridge. As mentioned above, existing literature and the views of scour experts were used to develop this logic, which has been encoded in a Bayesian network to account for the lack of confidence in the qualitative input of the bridge inspector. The reader is referred to Harmsen et al. (2001) and Palmer et. al. (1997) for detailed descriptions of the logic and Bayesian network in the CAESAR expert system.

Other states, such as Missouri (Huizinga and Rydlund 2004) and California (California Department of Trabsportation 2007) have adopted similar scour assessment procedures. These methods are either similar to the more qualitative forms of assessments described in the preceding sections and/or use detailed maximum scour depth calculations based on HEC-18 (Richardson and Davis 2001). The Massachusetts Highway Department used a bridge inspection data collection, storage and distribution system called the Integrated Bridge Inspection Information System (IBIIS) which however was not developed for the purpose of scour risk determination (Harmsen et al. 2001; Leung 1996).

2.2.7. Limitations of Current Assessment Methods

The current methods of bridge scour assessment have several limitations. The procedures that fall within the category of a Level 1 analysis are qualitative in nature and are very dependent on the inspector that is carrying out the inspection. Additionally, these methods including those assigning a scour index to bridges do not actually assess the current scour condition and probable future state of the bridge against the capacity of the bridge foundations. This could be dangerous as a qualitative inspection may not identify the bridge foundation in terms of its safety factor against failure. For procedures falling within the category of a Level 2 and level 3 Analysis, the most evident limitation is the use of the HEC-18 (Richardson and Davis, 2001) method for the determination of maximum scour depth in clays and some rocks. The sole use of the maximum scour depth tends to be overly conservative and lead to the designation of actually stable

bridges as scour critical bridges. The method proposed by Briaud et al. (1999, 2005) which will be discussed in the next section overcomes this shortcoming by introducing a time-dependent scour depth. This method however requires site-specific erosion testing.

2.3. THE SRICOS-EFA METHOD

2.3.1. The SRICOS-EFA Method for Bridge Piers

Briaud et al. (1999) developed a method to predict the scour depth versus time curve around a cylindrical pier founded in clay. This method, termed the SRICOS-EFA method for bridge piers is employed in development and application of BSA 2 and BSA 3. The procedure involves obtaining soil samples at the bridge site and testing it in the Erosion Function Apparatus (EFA) to obtain the erosion function (Briaud et al. 2001a). Further analysis is carried out based on the erosion function to determine the scour depth versus time curve around the bridge pier. This procedure is described as follows (Briaud et al. 1999):

1. Obtain samples at the bridge site, as close as possible to the pier and within the estimated maximum scour depth, $Z_{max,p}$.

2. Test the samples in the EFA to obtain the erosion function, i.e the scour rate, $\dot{Z}$ versus the applied hydraulic shear stress, τ. In addition to this, the EFA test also provides the scour rate $\dot{Z}$ versus velocity V curve.

3. Predict the maximum shear stress, τ_{max} which will be induced around the pier by the flowing water, prior to the initiation of scour at the pier. The maximum pier scour depth is the maximum scour that can take place at the pier under the given flow condition and is independent of time and is given by

$$\tau_{max,p} = 0.094\rho V_{appr}^{\ 2}\left(\frac{1}{\log R_e} - \frac{1}{10}\right) \qquad (2.1)$$

where the Reynolds Number, R_e is defined as $V_{appr}D/\upsilon$, V_{appr} is the mean upstream approach velocity, D is the pier diameter, and υ is the kinematic viscosity of water (10^{-6} m^2/s at 20º C). Equation (2.1) is obtained from numerical simulations and is detailed in Wei et al. (1997).

4. Use the measured $\dot{Z}$ versus time, τ (or V) curve to obtain the initial scour rate, $\dot{Z}_i$ corresponding to τ_{max}. This is illustrated in Figure 2-10

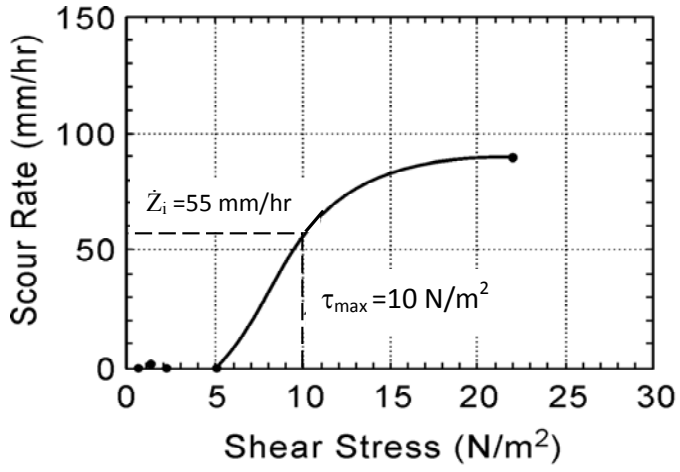

Figure 2-10. Initial erosion rate.

5. Predict the maximum depth of pier scour, $Z_{max,p}$ using the following equation:

$$Z_{max,p}(mm) = 0.18R_e^{\ 0.635} \qquad (2.2)$$

Equation (2.2) is obtained from a series of flume tests in clay and is described in detail in Gudavalli et al. (1997).

6. Use $\dot{Z}_i$ and $Z_{max,p}$ to develop the hyperbolic function describing the scour depth Z versus time, t curve. The hyperbolic function is shown in Equation (2.3) below:

$$Z_{fin,\,p} = \frac{t}{\frac{1}{\dot{Z}} + \frac{t}{Z_{max,\,p}}} \qquad (2.3)$$

where $Z_{fin,p}$ is the pier scour depth corresponding to a given time t and is termed the final pier scour depth.

2.3.2. The SRICOS-EFA Method for Bridge Contractions

Briaud et al. (2005) developed a method to predict the scour depth versus time curve in a contracted channel when water flows at a constant velocity. This method, termed the SRICOS-EFA method for bridge contractions is employed in BSA 2 and BSA 3. Similar to the SRICOS-EFA method for bridge piers, this procedure also involves obtaining soil samples at the bridge site and testing them in the Erosion Function Apparatus (EFA) to obtain the erosion function (Briaud et al. 2001a). Further analysis is carried out based on the erosion function to determine the scour depth versus time curve in the contracted channel. This procedure is described as follows (Briaud et al. 1999):

1. Obtain samples at the contracted bridge section within the estimated maximum scour depth, $Z_{max,c}$.
2. Test the samples in the EFA to obtain the erosion function, i.e the scour rate, $\dot{Z}$ versus the applied hydraulic shear stress, τ. In addition to this, the EFA test also provides the scour rate $\dot{Z}$ versus velocity V curve.
3. Calculate the maximum contraction scour depth, $Z_{max,c}$ for a given velocity using the following equation:

$$Z_{max,\,c} = 1.90 H_1 \left(1.38 \frac{B_1}{B_2} F - F_c \right) \qquad (2.4)$$

where H_1 is the upstream water depth, B_1 is the uncontracted channel width, B_2 is the contracted channel width (Figure 2-11), F is the Froude Number which is defined as $V_{appr}/(gH_1)^{0.5}$, F_c is the critical Froude Number and is defined as $V_c/(gH_1)^{0.5}$, V_{appr} is mean approach velocity, V_c is the critical velocity of the soil and g is the acceleration due to gravity.

4. Calculate the maximum shear stress, $\tau_{max,c}$ which will be induced at the contracted section by the flowing water, prior to the initiation of contraction scour. The maximum contraction scour depth is the maximum scour that can take place at the contracted section under the given flow condition and is independent of time and is given by:

$$\tau_{max,c} = k_R \; k_\theta \; k_H \; k_L \; \gamma_w \; n^2 \; V_{appr}^2 \; R_h^{-0.33} \qquad (2.5)$$

where k_R = contraction ratio factor

$$= 0.62+0.38\left(\frac{B_1}{B_2}\right)^{1.75}$$

k_θ = transition angle factor

$$= 1+0.9\left(\frac{\theta_1}{90}\right)^{1.5}$$

k_L = contraction length factor

$$= \begin{cases} 1 & \text{, for } \left(\dfrac{L}{B_1\text{-}B_2}\right) \geq 0.35 \\ 0.77 + 1.36\left(\dfrac{L}{B_1\text{-}B_2}\right) - 2\left(\dfrac{L}{B_1\text{-}B_2}\right)^2 & \text{, for } \left(\dfrac{L}{B_1\text{-}B_2}\right) < 0.35 \end{cases}$$

k_H = water depth factor = 1

R_h = hydraulic radius

$$= \frac{A}{P}$$

where A is the flow area and P the wetted perimeter in the uncontracted zone

γ_w = unit weight of water

5. Use the measured $\dot{Z}$ versus time, τ (or V) curve to obtain the initial scour rate, $\dot{Z}_i$ corresponding to $\tau_{max,c}$. This is illustrated in Figure 2-10.

6. Use $\dot{Z}_i$ and $Z_{max,p}$ to develop the hyperbolic function describing the scour depth Z versus time, t curve. The hyperbolic function is shown in Equation (2.6) below:

$$Z_{fin,\,c} = \frac{t}{\frac{1}{\dot{Z}} + \frac{t}{Z_{max,\,c}}} \tag{2.6}$$

where $Z_{fin,c}$ is the contraction scour depth corresponding to a given time t and is termed the final contraction scour depth.

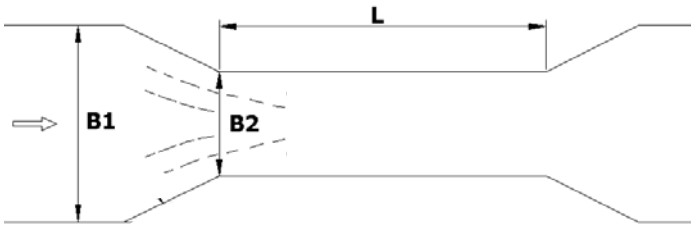

Figure 2-11. Contracted and uncontracted widths of a channel (after Briaud et al. 2005).

2.3.3. The SRICOS-EFA Method for Bridge Abutments

The SRICOS-EFA Method for bridge abutments is being finalized at Texas A&M University under a recently concluded National Cooperative Highway Research Program (NCHRP) research project (Briaud et al. 2009).

2.3.4. Concept of Equivalent Time

2.3.4.1. Equivalent Time for Bridge Piers

The concept of equivalent time (t_e) was first developed for pier scour by Briaud et al. (2001) who defined it as the time required for the maximum velocity in the hydrograph, V_{max} to create the same scour depth as the one created by the complete hydrograph. The equivalent time concept was needed to enable a simple back of the envelope calculation of time dependent scour depth, rather than carrying out more complex hydrograph based scour analysis. The steps in the development of equivalent time for bridge piers are as follows (after Briaud et al., 2004):

1. The equivalent time for bridge piers, $t_{e,p}$ was developed based on 55 case histories that were generated from 8 bridge sites.

2. Soil samples were collected at each bridge site in Shelby tubes and tested in the EFA to obtain the erosion function, $\dot{Z}$ versus τ.

3. The hydrograph from the nearest gage station was obtained and the SRICOS program (Briaud et. al. 1999, 2005) was used to calculate the scour depth.

4. The scour depth using the SRICOS program was entered into Equation (2.6)with the corresponding $\dot{Z}_i$ and Z_{max} values in order to obtain $t_{e,p}$. The value for $\dot{Z}_i$ was obtained from the average $\dot{Z}$ versus τ curve within the final scour depth by reading the $\dot{Z}$ value corresponding to τ_{max}, which was obtained from Equation (2.1). In Equation (2.1) the pier diameter, B and the maximum velocity appearing in the hydrograph, V_{max}, over the period of interest was used. The value for Z_{max} was obtained from Equation (2.2), using the same values for pier diameter and velocity that was used in Equation (2.1).

5. The single hydrograph at a bridge site was further broken down into smaller units that themselves were considered hydrographs. This process was done for all the 8 bridge sites investigated. This process generated 55 cases.

6. The equivalent time obtained from the steps described above was then correlated to the duration of the hydrograph (t_{hyd}), the maximum hydrograph velocity (V_{max}), and the initial erosion rate ($\dot{Z}_i$). A multiple regression was performed on the data.

The multiple regression mentioned in Step 6 above lead to an expression for the equivalent time for bridge piers (Equation (2.7)).

$$t_{e,p}(\text{hrs}) = 73\left[t_{hyd}(\text{years})\right]^{0.126}\left[V_{max}(\text{m/s})\right]^{1.706}\left[\dot{Z}_i(\text{mm/hr})\right]^{-0.20} \quad (2.7)$$

Equation (2.7) had a regression coefficient of 0.77. A comparison between the pier scour depth using the complete hydrograph input (termed Extended-SRICOS) and the pier scour depth obtained from the equivalent time method (Simple-SRICOS) was compared and is presented in Figure 2-12.

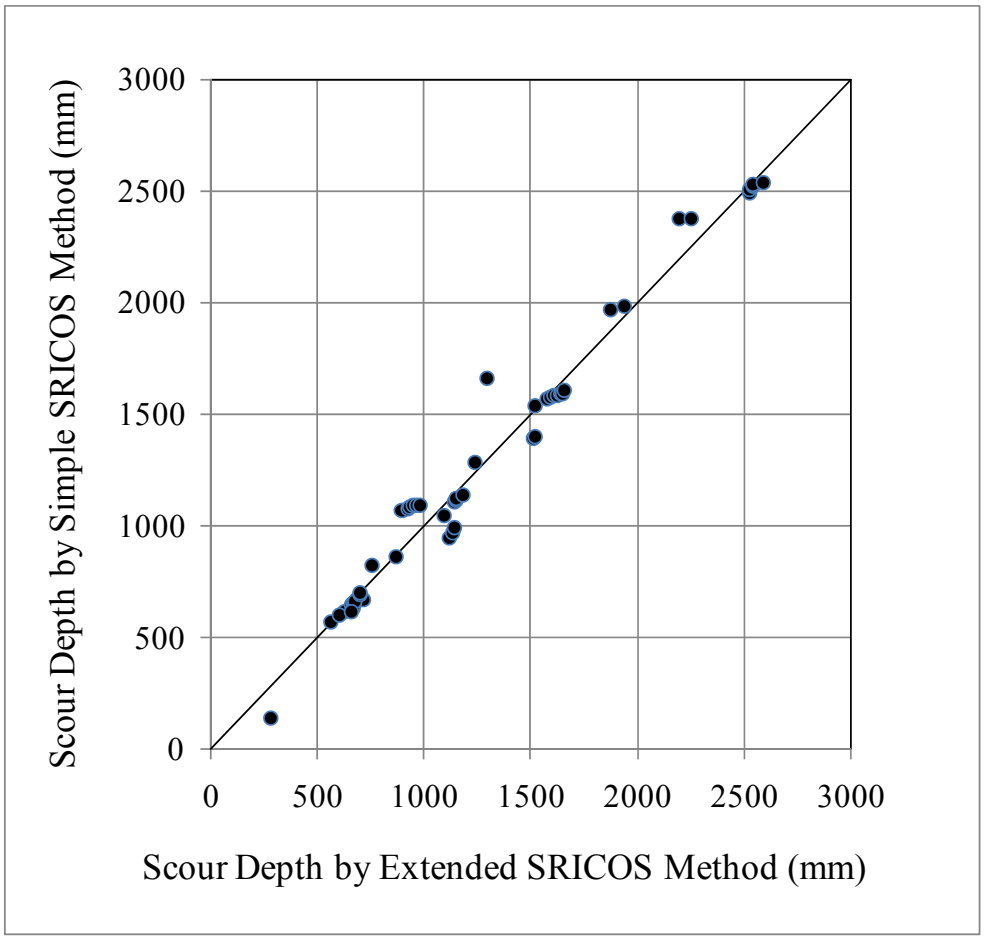

Figure 2-12. Comparison of pier scour depth using Extended-SRICOS and Simple-SRICOS Methods (after Briaud et al. 2001).

The equivalent time as presented in Equation (2.7) can be used to calculate the pier scour depth at the end of a given hydrograph just by applying the maximum velocity, initial scour rate, and hydrograph duration.

2.3.4.2. Equivalent Time for Bridge Contractions

The equivalent time for contraction scour, $t_{e,c}$ was developed by Wang (2004). It was developed using a similar method as the one used for the development of equivalent time for bridge piers. Wang (2004) used 6 bridge sites which generated 28 cases by segmenting the hydrographs for the 6 bridges, in addition to using the complete hydrograph. The initial rate of scour ($\dot{Z}_i$) was determined from the erosion function at a shear stress corresponding to τ_{max} obtained from Equation (2.5). Multiple regression was performed on the data and the following equation was obtained:

$$t_{e,c}(\text{hrs}) = 644.32\left[t_{hyd}(\text{years})\right]^{0.4242}\left[V_{max}(\text{m/s})\right]^{1.648}\left[\dot{Z}_i(\text{mm/hr})\right]^{-0.605} \quad (2.8)$$

The regression coefficient for Equation (2.8) was 0.965. A comparison between the contraction scour depth using the complete hydrograph input (termed SRICOS-EFA) and the contraction scour depth obtained from the equivalent time method (Simple SRICOS-EFA) was compared and is presented in Figure 2-13.

The equivalent time as presented in Equation (2.8) can be used to calculate the contraction scour depth at the end of a given hydrograph just by applying the maximum velocity and initial scour rate and hydrograph duration.

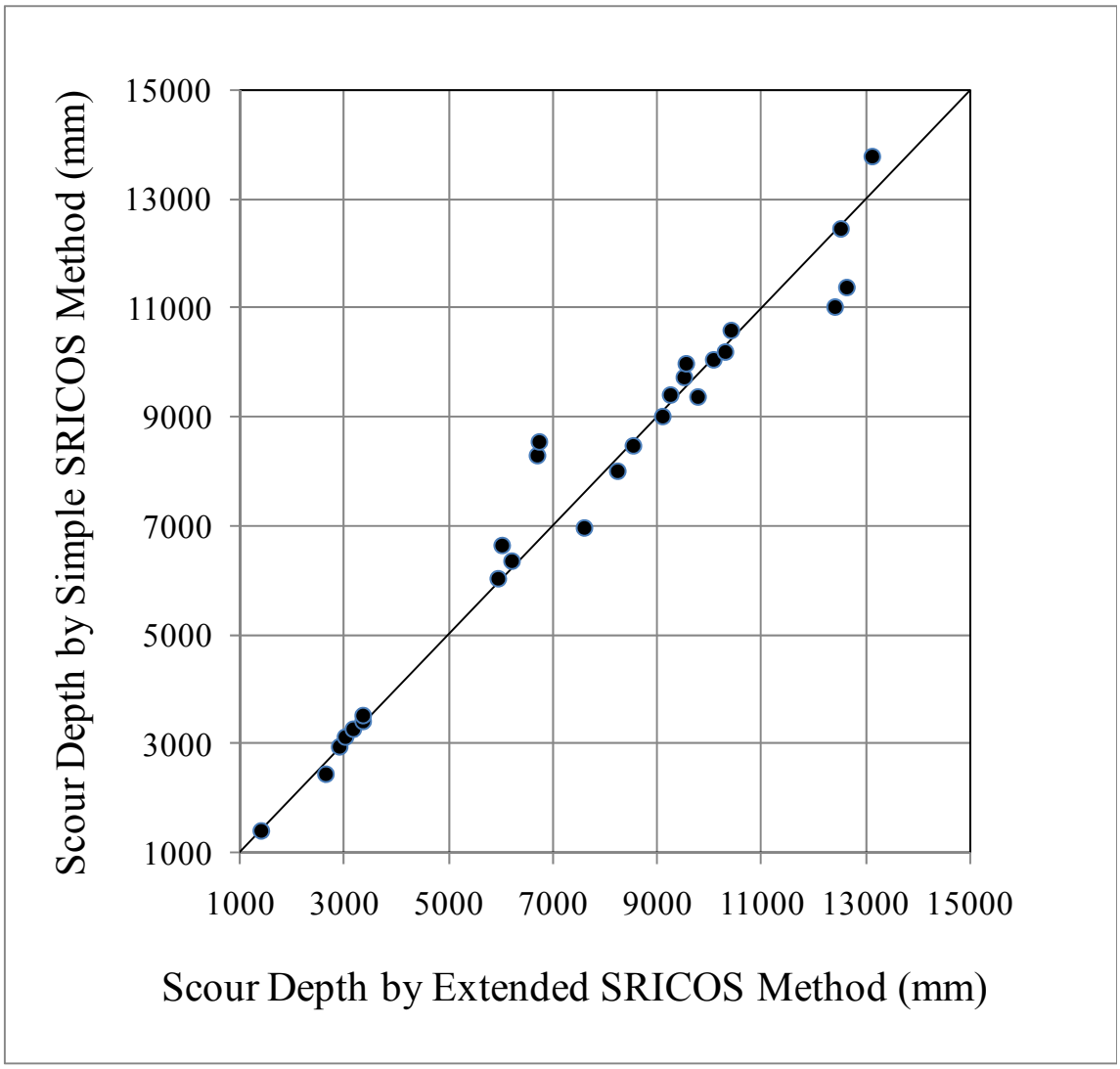

Figure 2-13. Comparison of contraction scour depth using SRICOS-EFA and Simple SRICOS-EFA Methods (after Wang 2004).

2.4. THE HEC-18 ABUTMENT SCOUR EQUATIONS

Two types of abutment scour equations are employed in BSA 2 to compute the maximum abutment scour depth, $Z_{max,a}$. These equations are Froehlich's live-bed abutment scour equation (Froehlich 1989a, 1989b) and the HIRE live-bed abutment scour equation (Richardson and Davis 2001). Richardson and Davis (2001) recommend these equations for both live-bed and clear-water abutment scour conditions.

2.4.1. Froehlich's Live-Bed Abutment Scour Equation

The Froehlich's equation was developed based on a compilation of measurements from several laboratory studies of local scour at bridge abutments. A total of 170 live bed measurements compiled for maximum depth of local scour at model bridge abutments were assembled and analyzed (Froehlich 1989b, Richardson and Davis 2001). The equation proposed by Froehlich (1989b) is as follows:

$$Z_{max,a}/y_a = 2.27\, K_1 K_2 (L'/y_a)^{0.43}\, F^{0.61} \qquad (2.9)$$

where L' is the length of active flow obstructed by the embankment, y_a is the average depth of flow on the floodplain and is defined as A_e/L, A_e is the flow area of the approach cross section obstructed by the embankment, L is the length of embankment projected normal to the flow (Figure 2-14) and F is the Froude number of approach flow upstream of the abutment. K_1 is the abutment shape coefficient (Figure 2-15 and Table 2-4) and K_2 is the coefficient for angle of embankment to flow and is defined as $(\theta/90)^{0.13}$ (Figure 2-14).

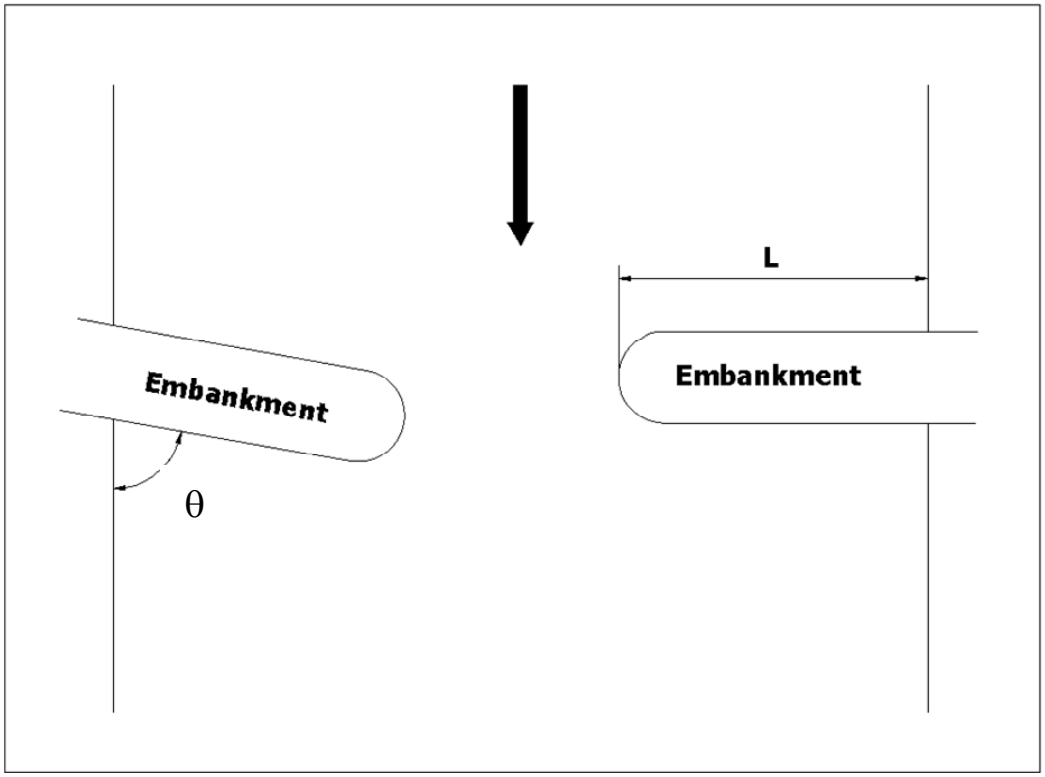

Figure 2-14. Some abutment scour parameters.

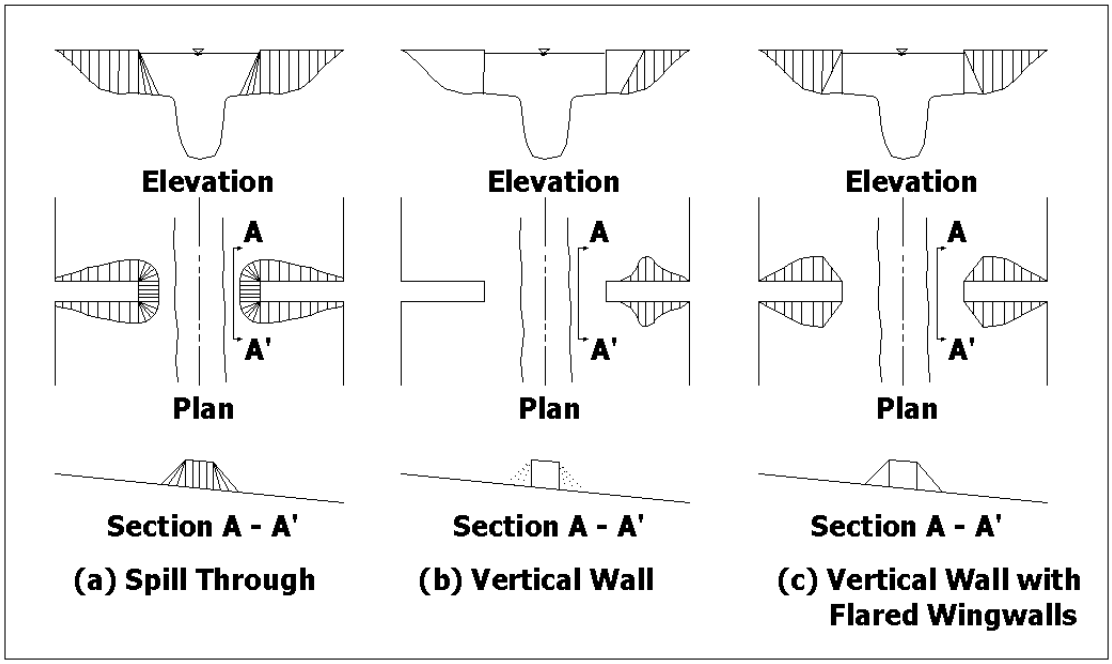

Figure 2-15. Abutment shapes (after Richardson and Davis 2001).

Table 2-4. Abutment shape coefficients (after Richardson and Davis 2001).

Abutment Shape Coefficients	
Description	K_1
Vertical-wall abutment	1.00
Vertical-wall abutment w/wing walls	0.82
Spill-through abutment	0.55

2.4.2. The HIRE Live-Bed Abutment Scour Equation

The HIRE equation is a modified equation of an equation based on field scour data at the end of spurs in the Mississippi River obtained by United States Army Corps of Engineers (USACE) (Richardson et al. 2001). The HIRE equation is applicable when the ratio of the projected abutment length, L to the flow depth, y_1 is greater than 25. The HIRE equation is given by Richardson and Davis (2001) as follows:

$$Z_{max,\,a}(\mathrm{m}) = 4y_1 Fr^{0.33} K_1 K_2 / 0.55 \qquad (2.10)$$

where y_1 is the depth of flow at the abutment on the overbank or in the main channel, F is the Froude Number based on the velocity and depth adjacent to and upstream of the abutment, K_1 is the abutment shape coefficient (Figure 2-15 and Table 2-4) and K_2 is the coefficient for skew angle of abutment flow as calculated for Froehlich's equation (Figure 2-14).

3. ERODIBILITY CHARTS

3.1. INTRODUCTION

The erodibility of soil or rock is defined as the relationship between the erosion rate, $\dot{Z}$ and the velocity of water, V at the soil / rock - water interface. This definition however is not very satisfactory because the velocity varies in direction and intensity in the flow field (Briaud 2008). To be exact, the velocity of water is zero at the soil/rock interface. A more adequate definition is the relationship between erosion rate $\dot{Z}$ and shear stress at the soil/rock interface and is given by

$$\dot{Z} = f(\tau) \tag{3.1}$$

However, the velocity is often used because it is easier to gauge an erosion problem from a velocity standpoint. In this report, the methods to obtain scour depth are primarily based on velocity. These methods were developed by previous researchers and presented in terms of velocity (Briaud et al. 1999, 2005; Richardson and Davis, 2001; Froehlich 1989b).

Briaud (2008) describes erodible materials according to three material categories, i.e. soil, rock and intermediate geomaterials. Here soil is defined as an earth element which can be classified by the Unified Soil Classification System (USCS) and rock is defined as an earth element which has a joint spacing of more than 0.1 m and an unconfined compressive strength of the intact rock core of more than 500 kPa.

Intermediate geomaterials are materials whose behavior is intermediate between soils and rocks, such as cobbles, boulder and riprap. The erosion of rock occurs through two main processes, i.e. rock substance erosion and rock mass erosion. Briaud (2008) defines rock substance erosion as the erosion of rock material itself and rock mass erosion as the removal of blocks from the jointed rock mass. In the case of rock mass erosion, the eroded material can be identified with the parent material.

3.2. FACTORS INFLUENCING EROSION RESISTANCE

The erodibility of geomaterials can vary significantly according to their properties as well as the properties of the water flowing over the soil. The soil properties influencing erodibility are listed in Table 3-1.

Table 3-1. Some soil properties influencing erodibility (after Briaud 2008).

Soil water content	Soil dispersion ratio
Soil unit weight	Soil cation exchange capacity
Soil plasticity index	Soil sodium absorption rate
Soil undrained shear strength	Soil pH
Soil void ratio	Soil temperature
Soil swell	Water temperature
Soil mean grain size	Water salinity
Soil percent passing #200 sieve	Water pH
Soil clay minerals	

As mentioned above, erodibility is a function and therefore attempts at correlating conventional soil properties such as plasticity index, undrained shear strength, percent passing #200 sieve, water content, and unit weight with the erosion

resistance can only be made for elements of the erosion function such as the critical shear stress (and critical velocity) and the initial slope of the erosion function. Such correlations were attempted by Cao et al. (2002) and presented here in Figure 3-1 and Figure 3-2.

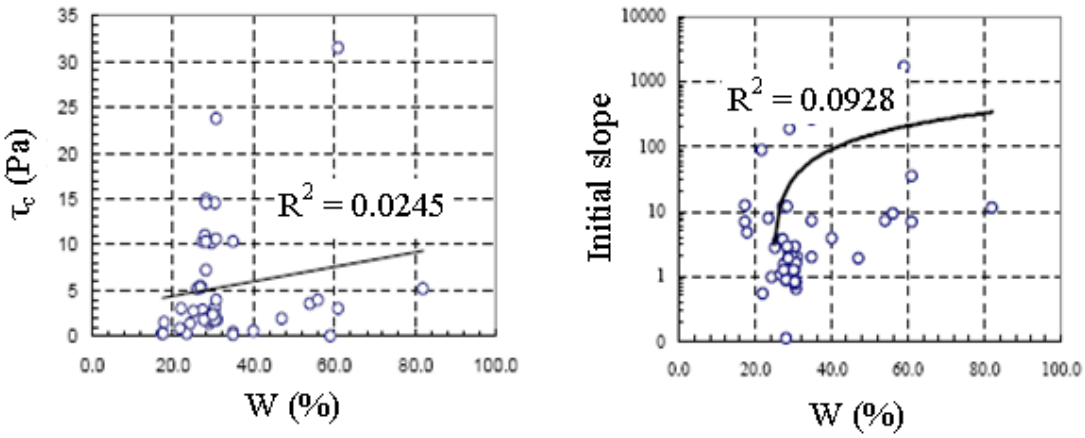

Figure 3-1. Failed attempts at correlating the critical shear stress and initial slope with water content (Cao et al. 2002).

Because attempts at obtaining a reasonable correlation between erosion resistance and soil properties failed, it is most preferable to measure the erosion function directly in an apparatus such as the Erosion Function Apparatus (Briaud et al. 2001a). The Erosion Function Apparatus (EFA) is a test apparatus that measures the erosion function of a soil, which is the relationship between the soil erosion rate and the applied hydraulic shear stress or velocity. However, direct measurements require soil sampling at the bridge site and can create substantial costs in a bridge scour assessment. Therefore, several charts collectively termed the Erodibility Charts were developed for

the purpose of this report. The erodibility charts comprise the Erosion Function Charts and the Erosion Threshold Charts. These charts will be introduced and detailed in the following subsections of this section.

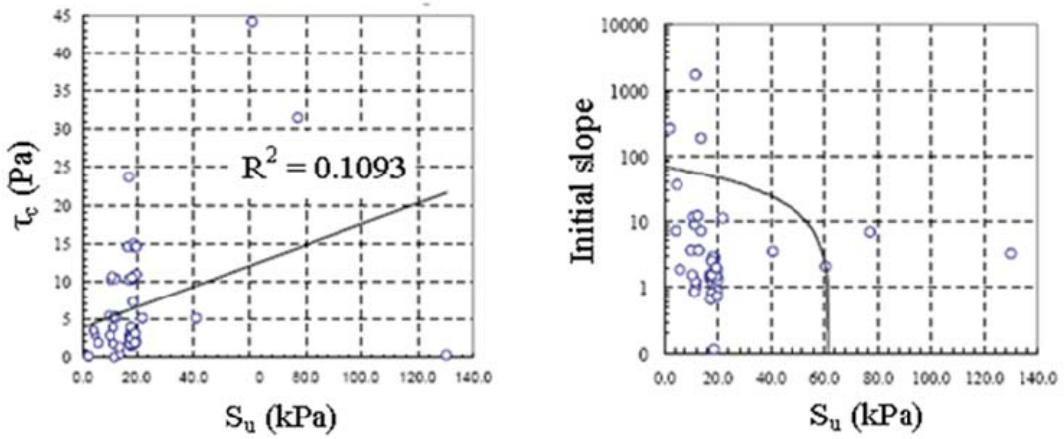

Figure 3-2. Failed attempts at correlating the critical shear stress and initial slope with undrained shear strength (Cao et al. 2002).

3.3. CRITICAL SHEAR STRESS – CRITICAL VELOCITY RELATIONSHIP

The critical shear stress (τ_c) – critical velocity (V_c) relationship was investigated to provide a useful means of interchanging known values of either one of these values with the other. A database comprising 81 EFA tests was used to investigate this relationship. τ_c values were plotted against V_c values and presented in Figure 3-3. This resulted in a very reasonable relationship with an R^2 value of 0.96. For simplicity, the relationship between these two parameters is proposed as

$$\tau_c = 5(V_c)^2 \quad (3.2)$$

While τ_c depends mostly on the soil properties, V_c depends also on the water depth in an open channel. The above equation comes from tests in the EFA which creates a pipe flow. In this case, the water depth is not involved. Calculations using the US Army Corps of Engineers EM 1601 Equation show that ignoring the water depth in calculating the critical velocity may create a ± 20% error for common values of water depth (1 m to 25 m).

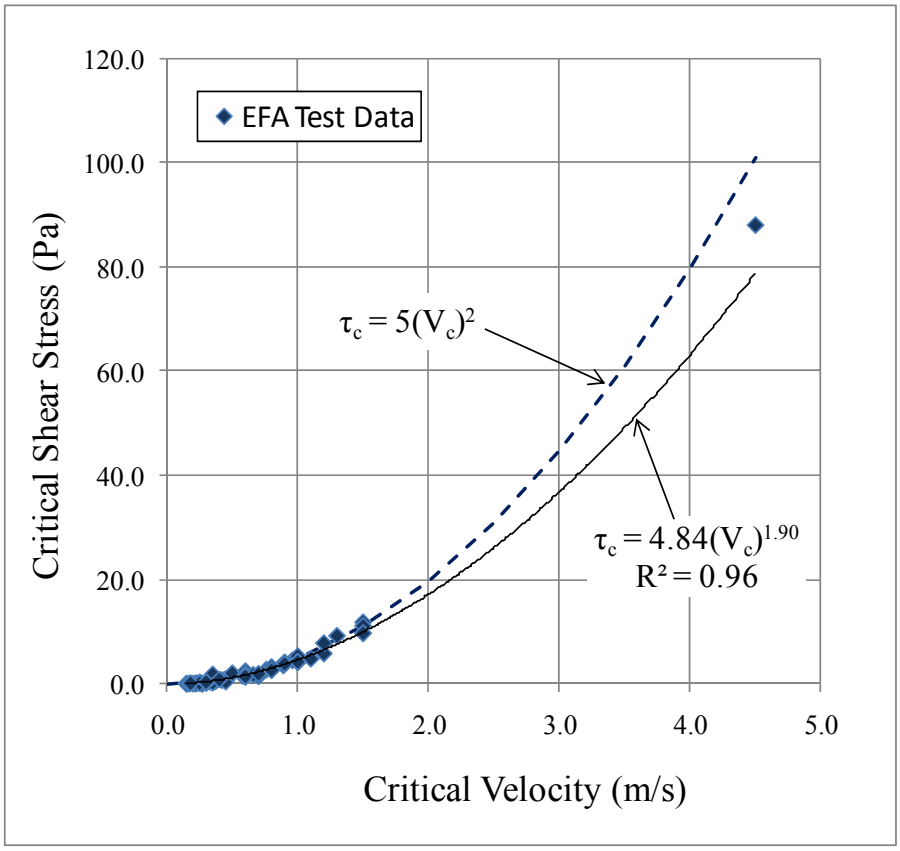

Figure 3-3. Critical shear stress – critical velocity relationship.

3.4. THE EROSION FUNCTION CHARTS

3.4.1. Overview

The Erosion Function charts are charts that show erosion categories demarcated on the $\dot{Z} - \tau$ and $\dot{Z} - V$ charts (Figure 3-4 and Figure 3-5). The erosion categories are shown in Table 3-2. These charts were developed on the basis of EFA tests and the experience of the authors. The Erosion Function Charts essentially eliminate the need for site specific erosion testing for preliminary investigation (Govindasamy et al. 2008). Based on the material category in question, the user can use the boundaries of these erosion categories to determine the critical velocity, τ_c or critical velocity V_c of the material. The definition of τ_c is the hydraulic shear stress corresponding to an erosion rate of 0.1 mm/hour and the definition of V_c is the water velocity corresponding to an erosion rate of 0.1 mm/hour. The user can also use these boundaries or the space between them to arbitrarily determine the erosion function of a geomaterial based on engineering judgment. Table 3-2 also shows the values of τ_c and V_c according to erosion categories.

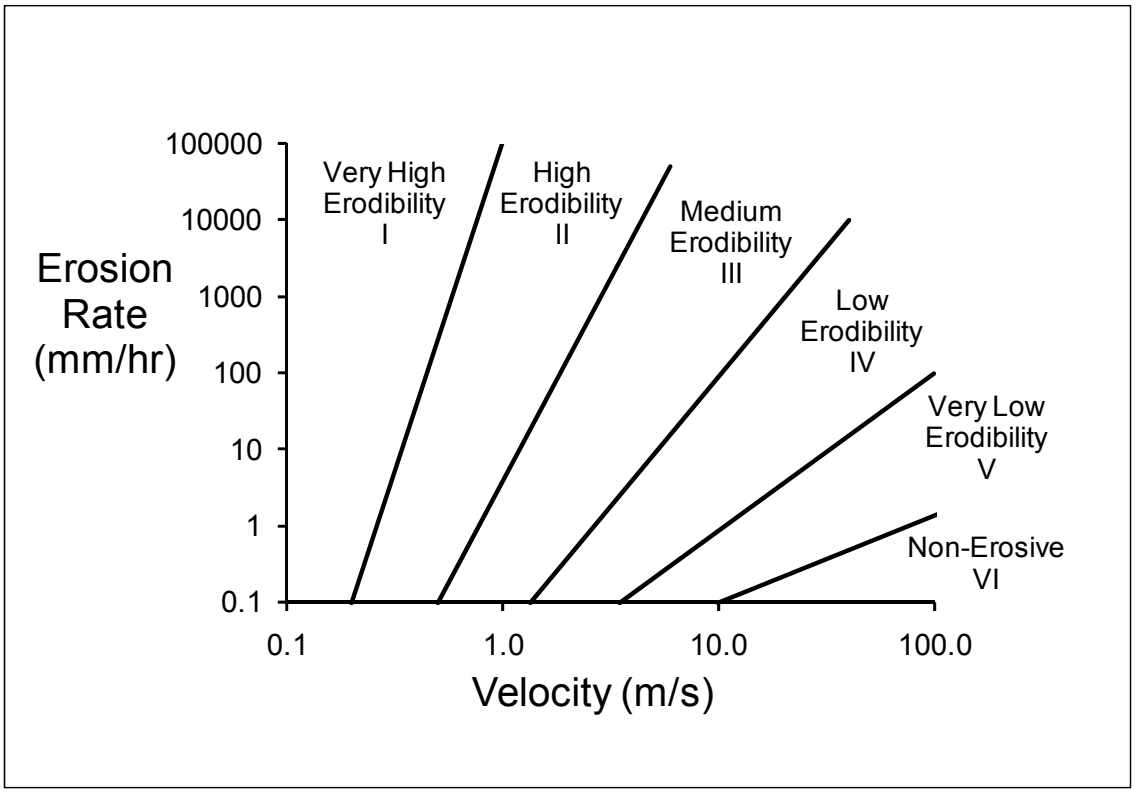

Figure 3-4. Erosion categories based on velocity.

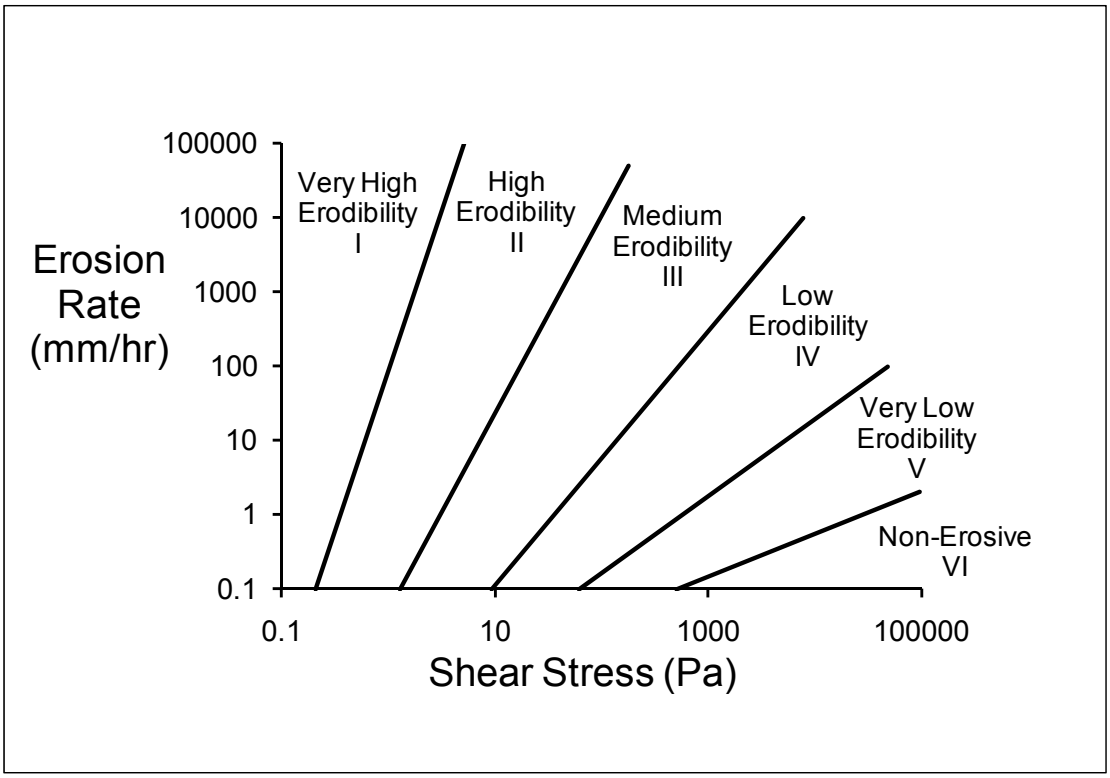

Figure 3-5. Erosion categories based on shear stress.

Table 3-2. Erosion categories in the erosion function charts.

Erosion Category	Description	Critical Shear Stress, τ_c (Pa)	Critical Velocity, V_c (m/s)
I	Very high erobility geomaterials	0.1	0.1
II	High erodibility geomaterials	0.2	0.2
III	Medium erodibility geomaterials	1.3	0.5
IV	Low erodibility geomaterials	9.3	1.35
V	Very low erodibility geomaterials	62.0	3.5
VI	Non-erosive materials	500	10

3.4.2. Relationship between Selected Geomaterials and the Erosion Function Charts

This report incorporates 81 erosion function tests that were carried out at Texas A&M University and the Texas Department of Transportation (TxDOT) laboratories. A summary table of these samples with EFA data and routine soil properties (e.g. index properties, unit weight, undrained shear strength, percent passing #200 sieve, mean grain size) is presented in Appendix D. These samples were classified using the Unified Soil Classification System (USCS). From the 81 samples, the following soil categories were obtained:

1. Low plasticity clay (CL)
2. High plasticity clay (CH)
3. Low plasticity silts (ML)
4. High plasticity silts (MH)
5. Soil intermediate between low plasticity clay and low plasticity silt (CL-ML)
6. Clayey sand (SC)
7. Soil intermediate between silty sand and clayey sand (SM-SC)
8. Poorly graded sands (SP)
9. Fine gravel

These samples were grouped according to their USCS categories and plotted separately on the Erosion Function Charts (Figure 3-6 through Figure 3-14). This was done to provide a suitable erosion function of a particular material type based on USGS

classification on the Erosion Function Charts. It should be noted that the materials do not generally fall distinctly into a single category. The materials generally seem to plot approximately across two categories. In four of these figures, the mean ($\mu_{\dot{z}}$) of the erosion rate as a function of velocity range are shown. The mean and coefficient of variation of the material critical velocity (μ_{Vc} and COV_{Vc}) are indicated in the top right corner of these figures. The remaining five figures do not have this information because of insufficient test data for the corresponding material type. For the CL materials, one data set, i.e. for the San Jacinto Layer 2 sample was ingnored in the calculation of the mean and COV as this was considered to be an outlier. For the CH materials, three data sets, i.e. for the samples B3-(30-32), EFA-38, and B3-(48-50) were not considered in the calculation of the mean and COV as these were considered to be outliers.

Care should be exercised while selecting the erosion function for a material being investigated. As explained earlier in this section, there are many factors that impact erodibility. In cases when these are unknown, it is recommended that the user exercise some caution when selecting the erosion category by selecting conservative values.

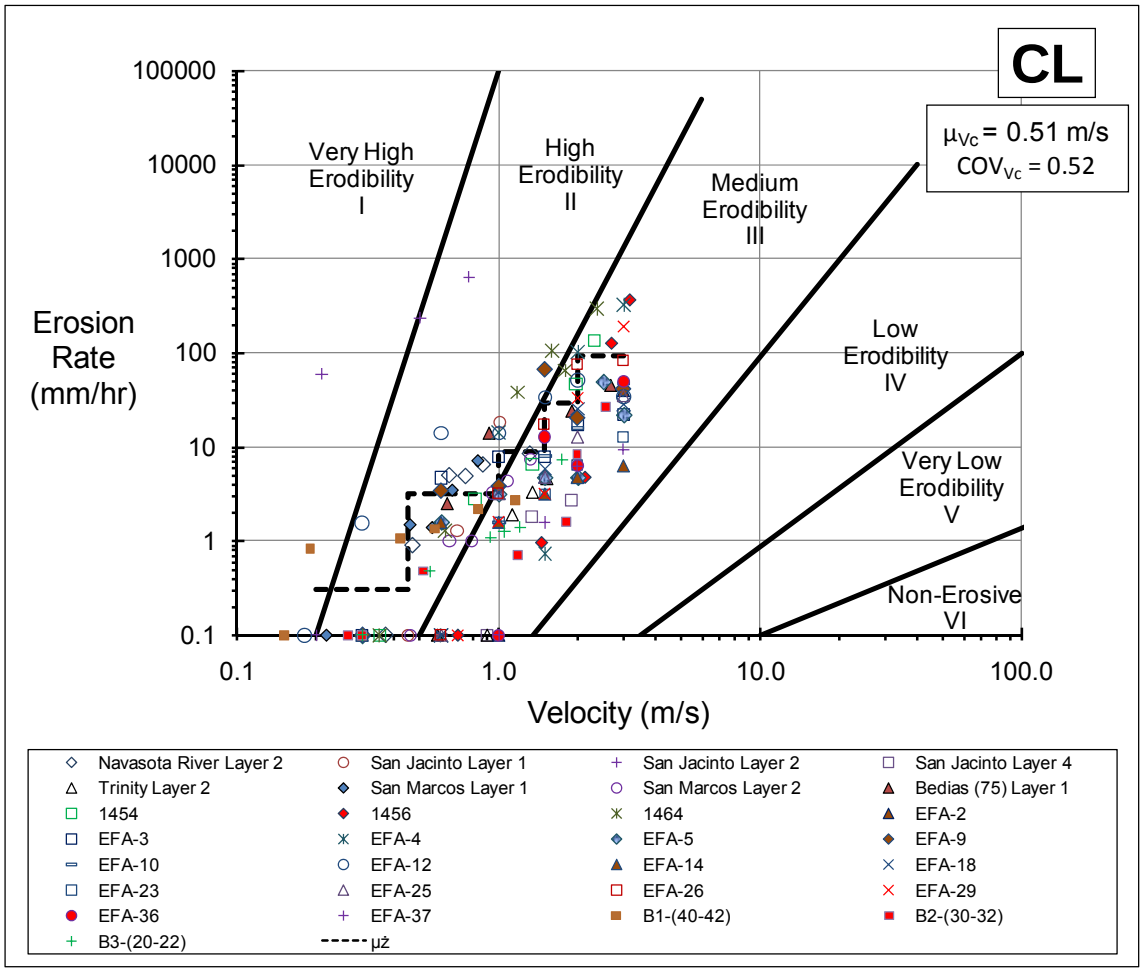

Figure 3-6. EFA test data on low plasticity clays plotted on the Erosion Function Chart.

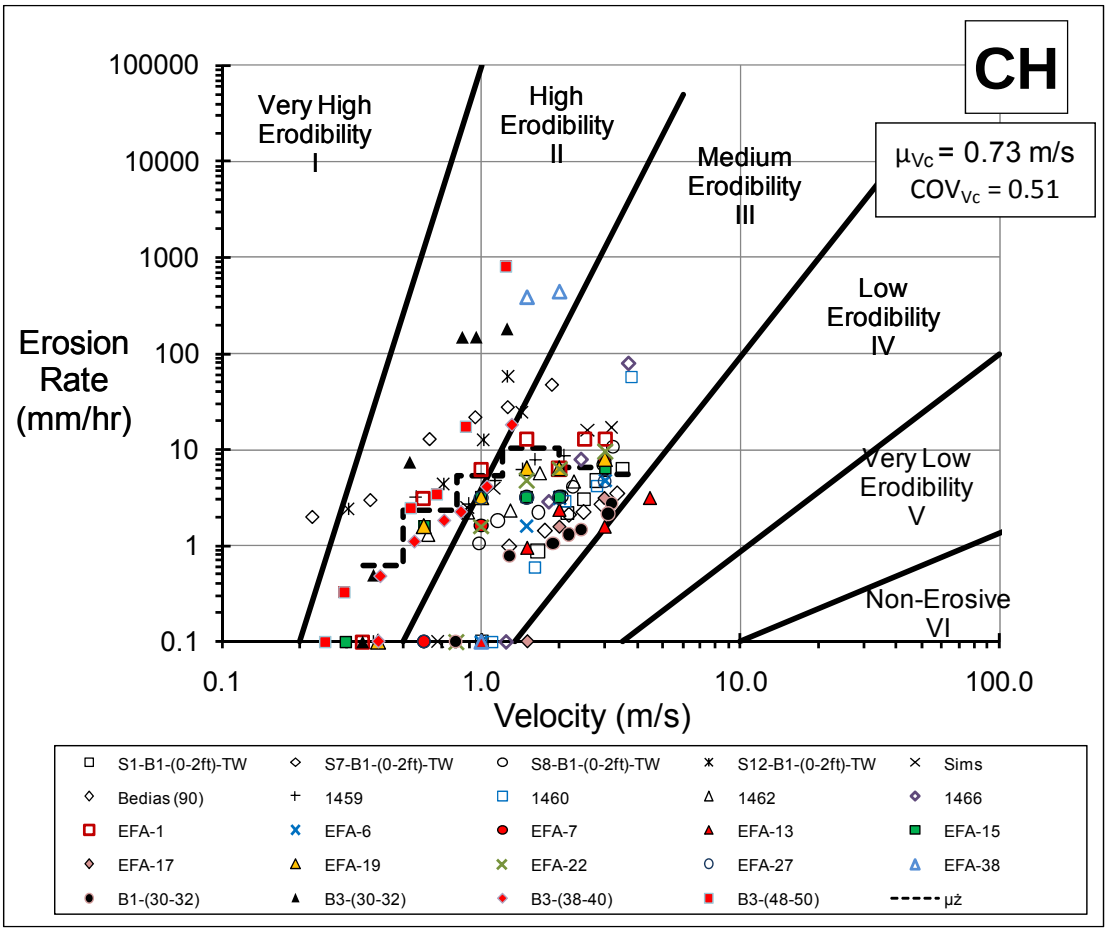

Figure 3-7. EFA test data on high plasticity clays plotted on the Erosion Function Chart.

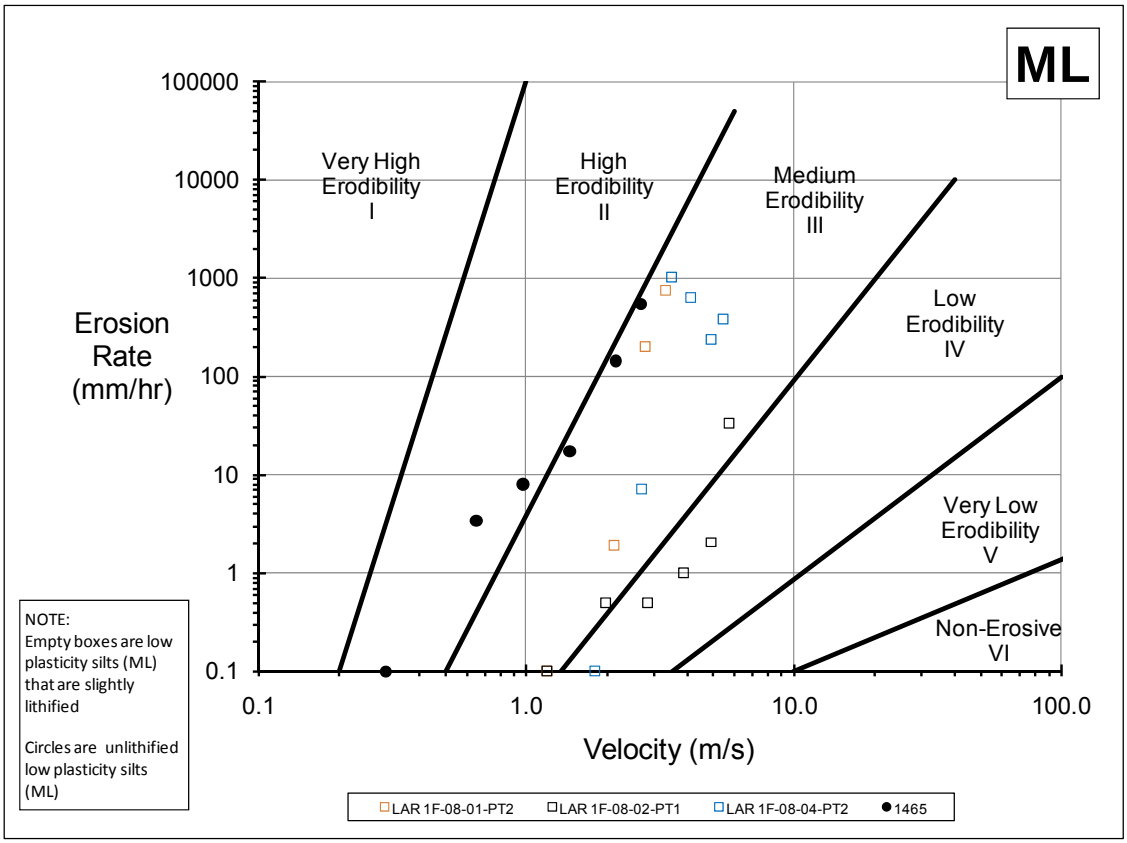

Figure 3-8. EFA test data on low plasticity silts plotted on the Erosion Function Chart.

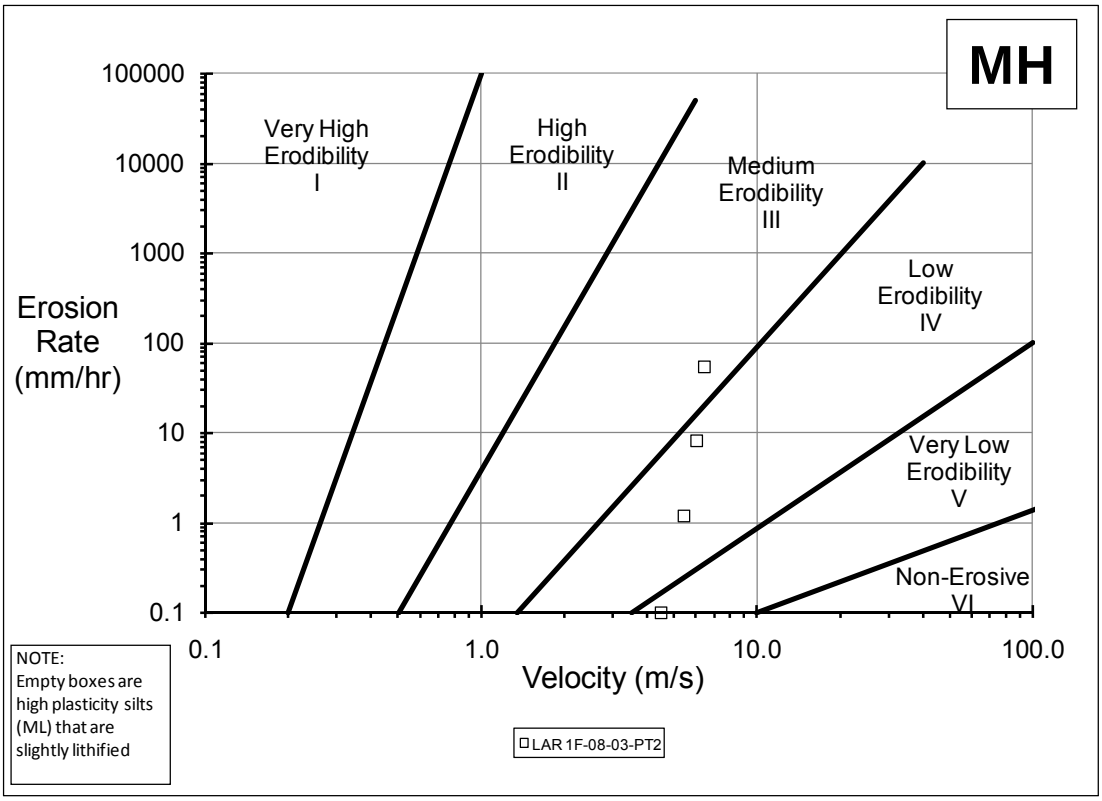

Figure 3-9. EFA test data on high plasticity silt plotted on the Erosion Function Chart.

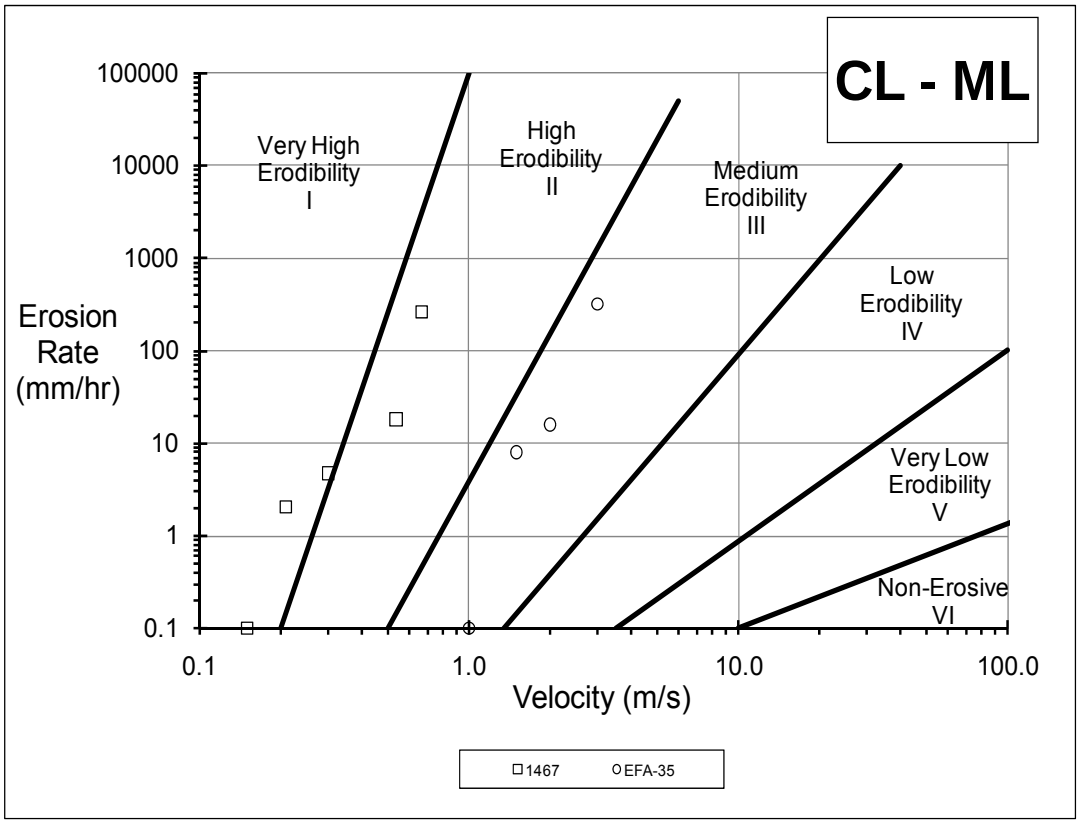

Figure 3-10. EFA test data on samples intermediate between low plasticity clay and low plasticity silt plotted on the Erosion Function Chart.

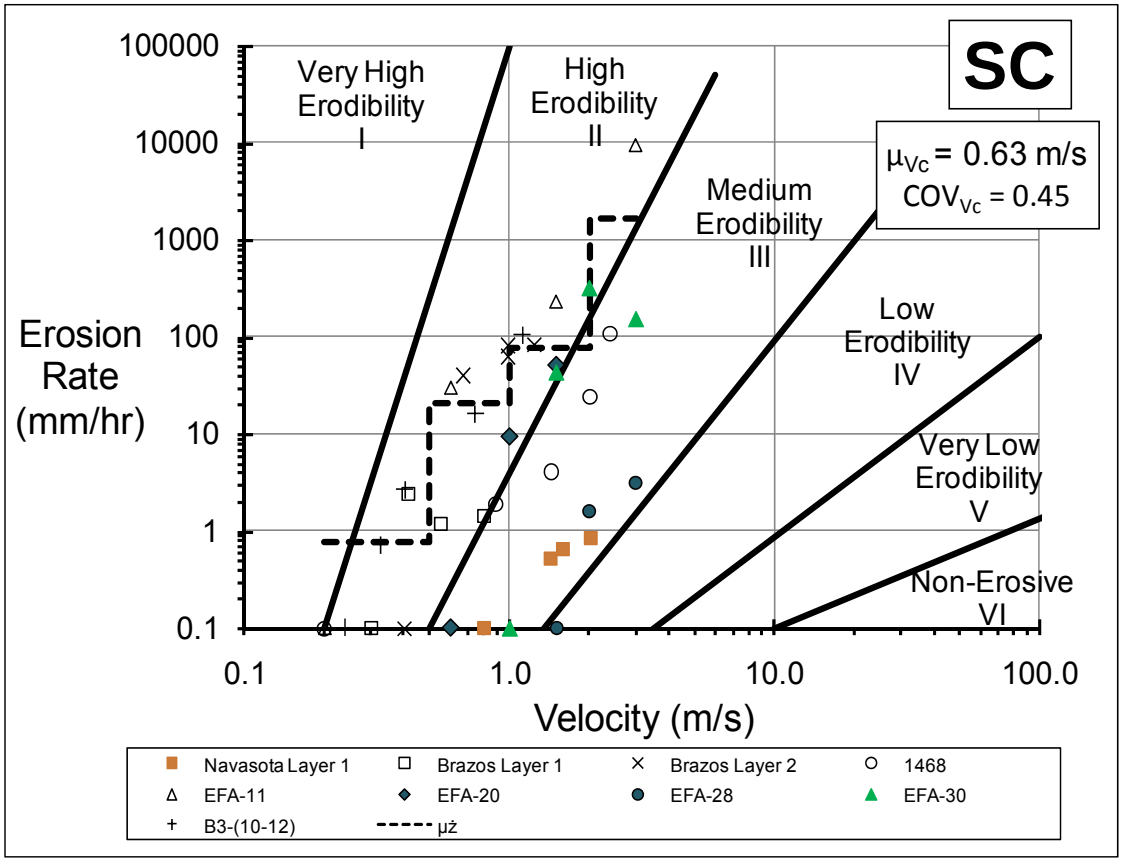

Figure 3-11. EFA test data on clayey sands plotted on the Erosion Function Chart.

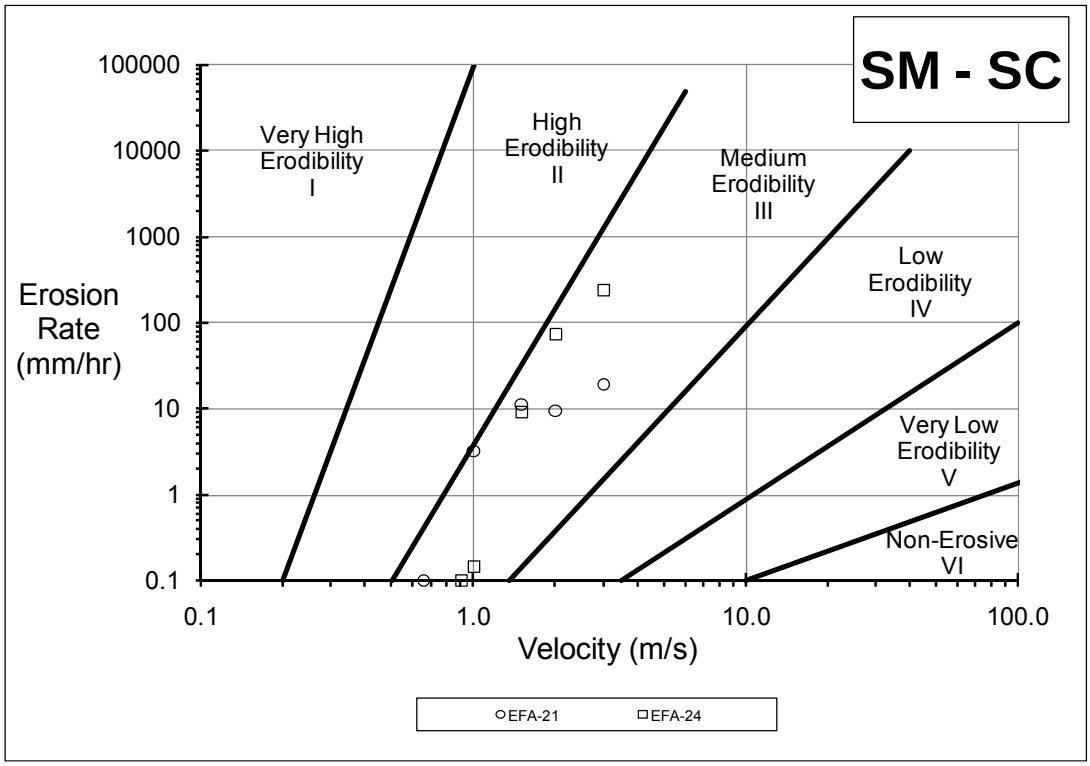

Figure 3-12. EFA test data on samples intermediate between silty sand and clayey sand plotted on the Erosion Function Chart.

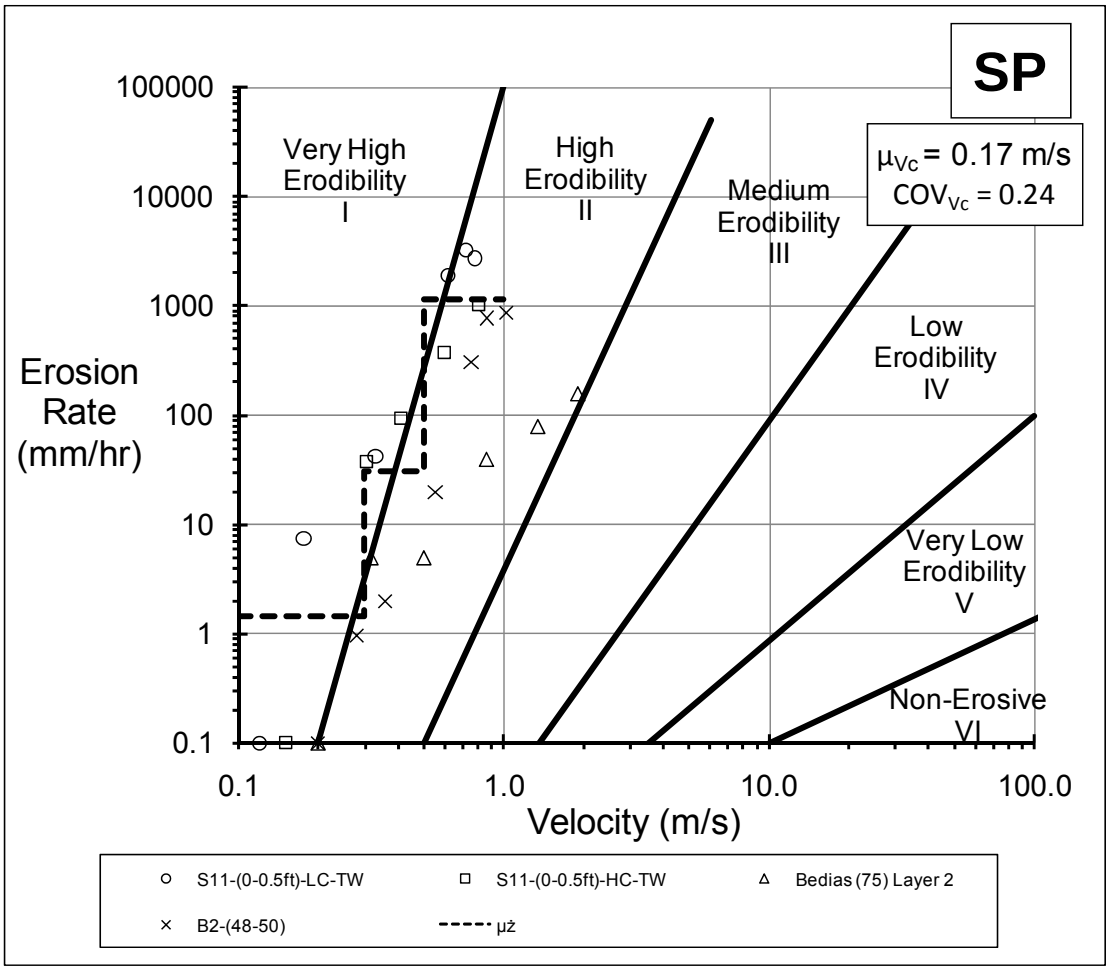

Figure 3-13. EFA test data on poorly graded sands plotted on the Erosion Function Chart.

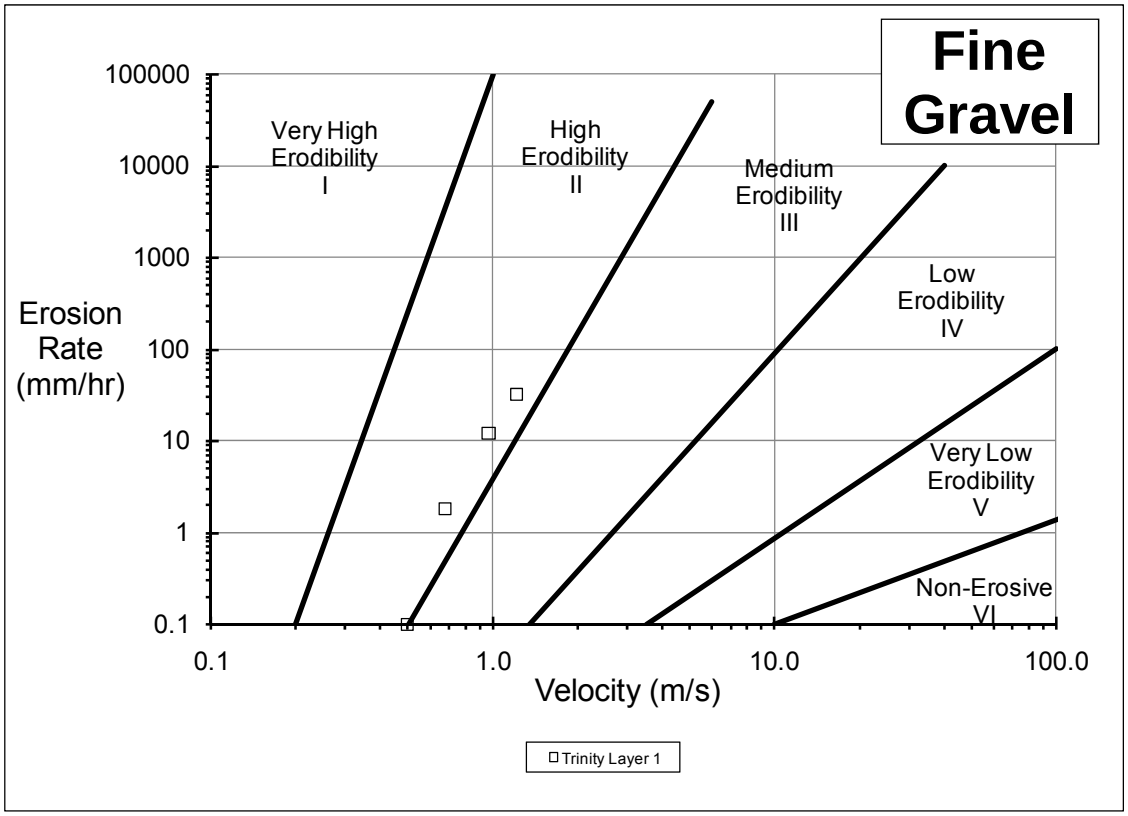

Figure 3-14. EFA test data on gravel plotted on the Erosion Function Chart.

Figure 3-15 through Figure 3-17 show the approximate zones for CL, CH, SM, SC, SM-SC and SP materials. These zones are based on the EFA test data that were presented in Figure 3-6, Figure 3-7, Figure 3-10, Figure 3-11, Figure 3-12 and Figure 3-13. The rest of the materials were not zoned on the erosion function charts due to lack of test data.

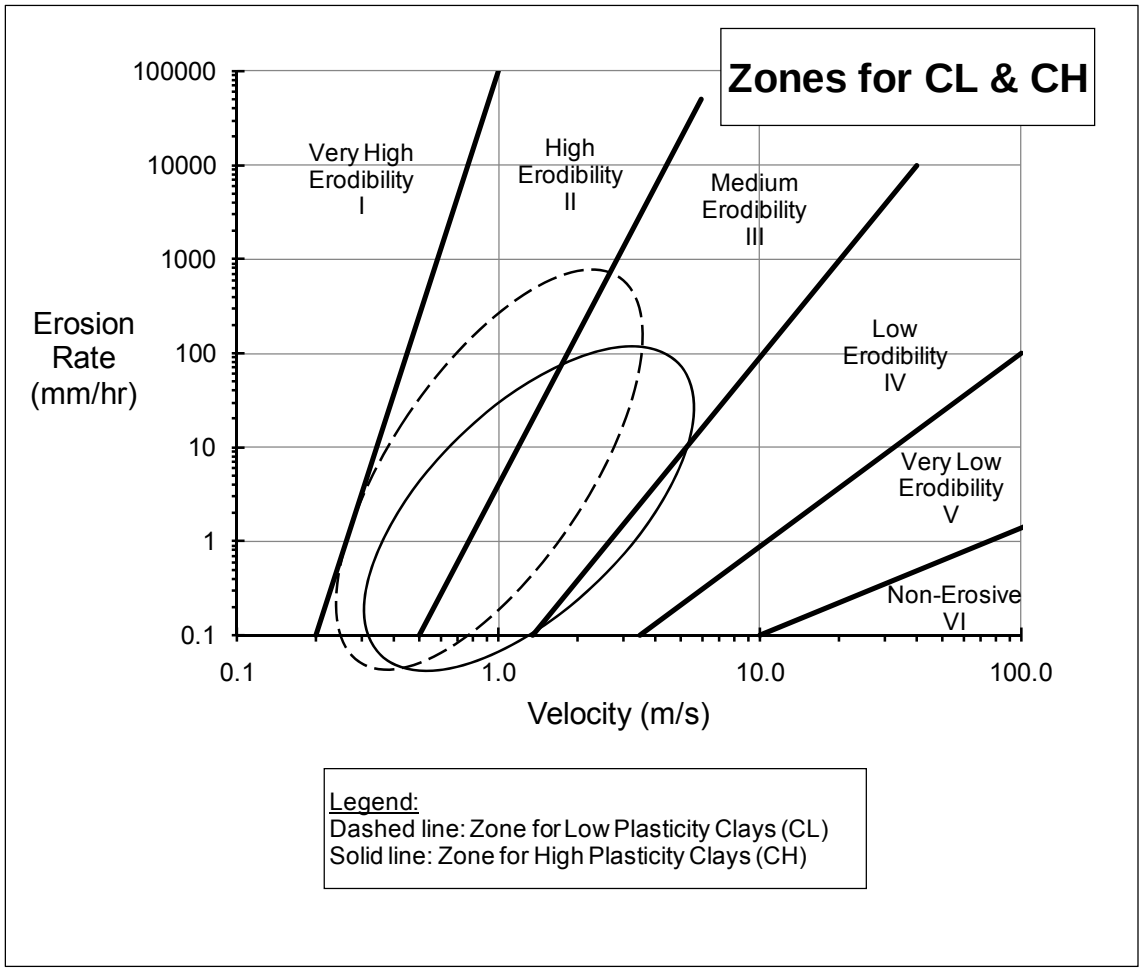

Figure 3-15. Zones for low plasticity and high plasticity clays.

\

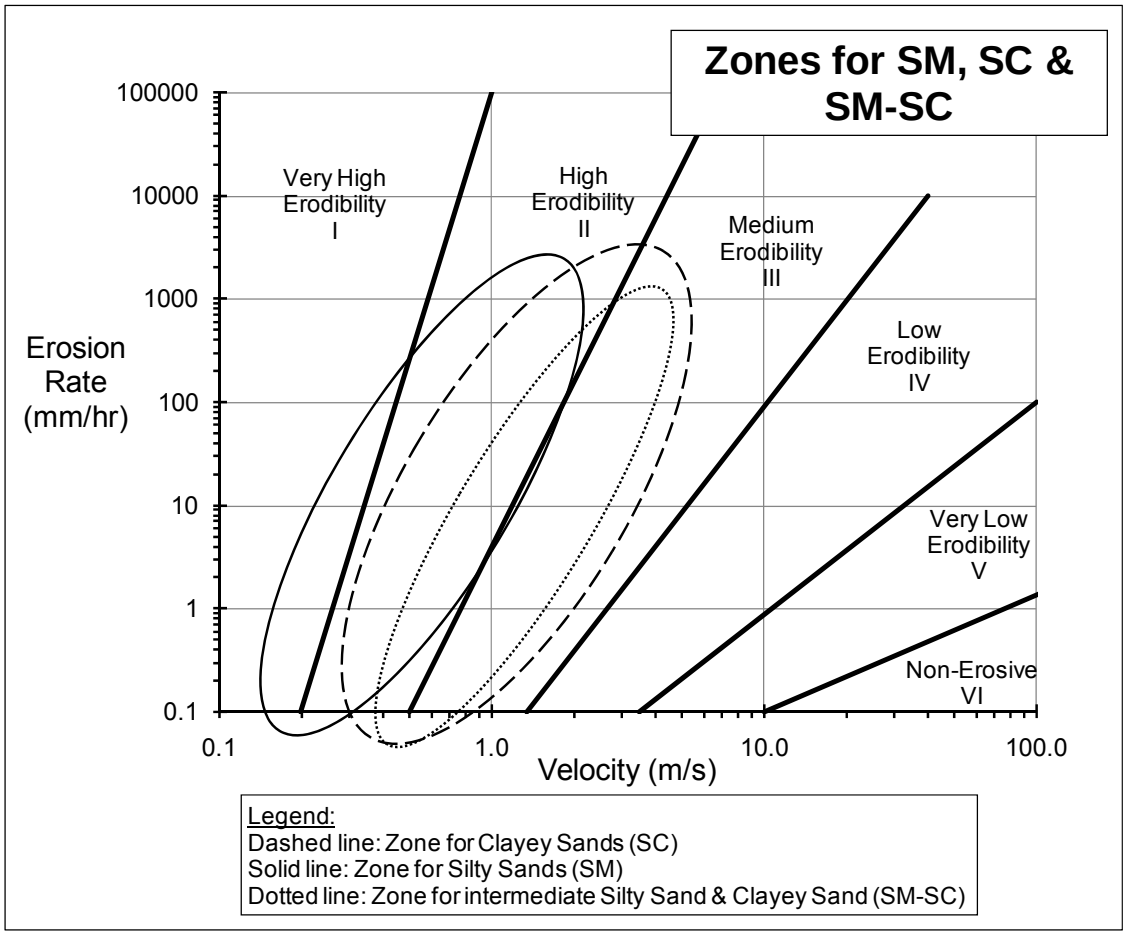

Figure 3-16. Zones for clayey sands, silty sands and intermediate silty sands and silty clays.

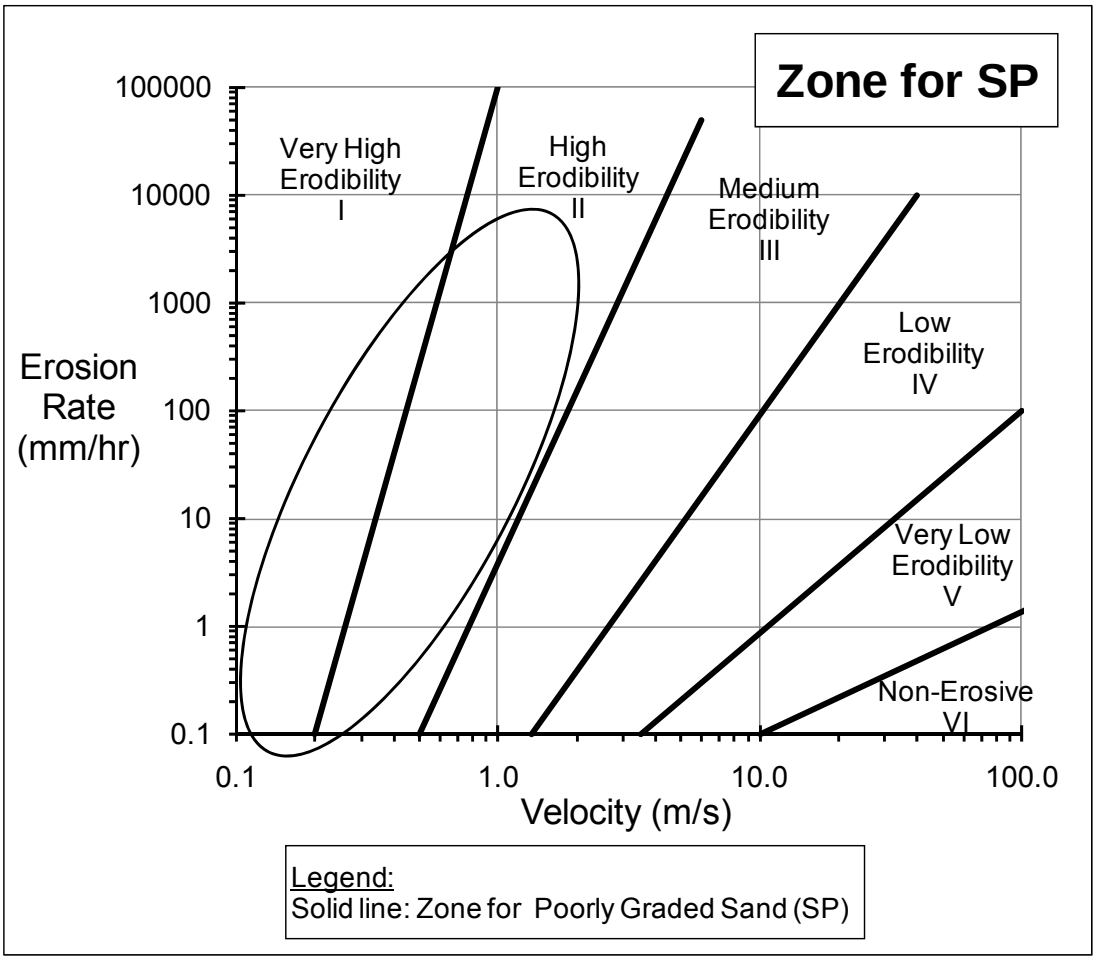

Figure 3-17. Zone for poorly graded sand.

3.5. THE EROSION THRESHOLD CHARTS

3.5.1. Overview

Briaud (2008) suggests that the threshold of erosion is one of the most important soil parameters in erosion. Below the threshold value, erosion does not take place. Once the applied hydraulic stress exceeds the threshold value, erosion is initiated until the

equilibrium scour depth is achieved. As mentioned in Section 2, the threshold values for erosion in terms of shear stress is the critical shear stress τ_c and in terms of velocity is the critical velocity V_c. Because of their importance, the threshold values were investigated and charts were developed to aid engineers in estimating them. Essentially, these are charts that show the relationship between the erosion threshold values and the particle size of the geomaterial. Collectively, these charts are termed the Erosion Threshold Charts, presented in terms of τ_c and V_c.

3.5.2. The Use of a Riprap Design Equation for Scour in Fractured Rock

In order to include fractured rock in Erosion Threshold Charts, a study was done by employing a riprap design equation to estimate the threshold velocity that would cause a block of riprap with a certain size (particle diameter) to erode. The design equation employed was the U.S. Army Corps of Engineers EM 1601 riprap design equation (U.S. Army Corps of Engineers 1995). The EM 1601 equation is as follows:

$$\frac{d_{30}}{y} = 0.30\left[\frac{V}{\sqrt{(S_g\text{-}1)gy}}\right]^{2.5} \tag{3.3}$$

where d_{30} is the particle diameter corresponding to 30% passing by weight, V is the mean depth velocity of flow, y is the water depth, g is the acceleration of gravity, and S_g is the particle specific gravity.

In order to perform this study, Equation (3.3) was rearranged as follows:

$$V = \left[\frac{3.33 d_{30}}{y}\right]^{0.4} \sqrt{(S_g - 1) g y} \qquad (3.4)$$

Subsequently, the velocity corresponding to a specified range for both of particle size, d_{30} and water depth, y was computed for a fixed $S_g = 2.65$. The range of particle diameter was between 100 to 10000 mm. The range of water depth was between 1 to 25 m. This resulted in 300 combinations of these parameters. The results of these simulations will be shown when the erosion threshold charts are present below.

3.5.3. The Erosion Threshold – Mean Grain Size Chart

The erosion threshold – mean grain size charts are shown in Figure 3-18, Figure 3-19, and Figure 3-20. Figure 3-18 presents the erosion threshold in terms of velocity and Figure 3-19 shows the data points from the simulation of the riprap design equation. Figure 3-20 presents the erosion threshold in terms of shear stress. This chart was essentially developed using EFA test results as well as data in the literature to relate the critical velocity of the geomaterial to its mean grain size. As can be observed in the charts, the critical value and the grain size displays a "V" shape. It can be seen that the most erodible materials are the fine sands. The charts also point out that particle size controls the erosion threshold in coarse grained soils and does not provide a correlation with the threshold value for fine grained soils. It should be noted that the curve proposed by Shields (1936) has been presented on the charts as well. It is also worth to note that

Hjulstrum (1935) proposed a similar curve for both fine grained and coarse grained soils but his method turned out to be too simple (after Briaud 2008).

The range of threshold velocities V_c obtained using the riprap design (Equation (3.4)) is shown in Figure 3-19. Note that for fractured rock, the particle diameter is assumed to be the rock fracture spacing which seems to be a reasonable assumption because one can expect a piece of fractured rock with a certain fracture spacing to have similar critical erosion properties as a piece of riprap with a diameter that is equal to the fracture spacing.

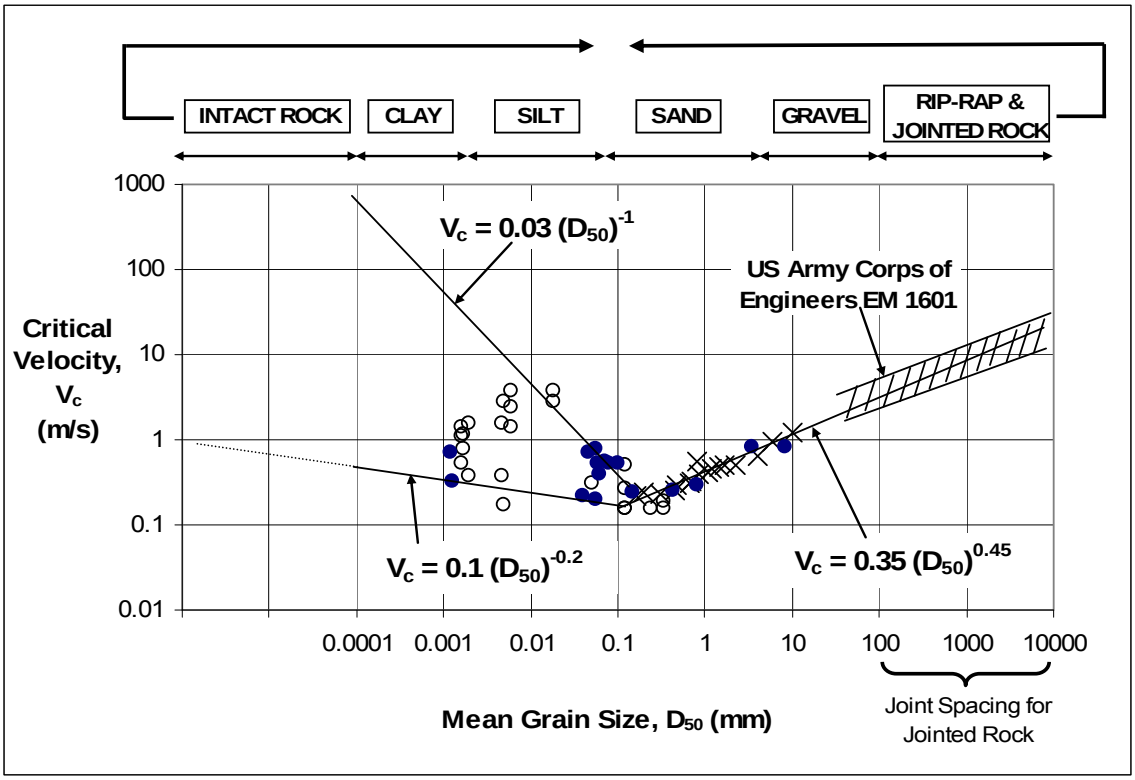

Legend:

- ● TAMU Data as reported by Briaud, J.-L. et. al. (2001). "Erosion Function Apparatus for Scour Rate Predictions." *J. Geotech. and Geoenvir. Engrg.,* ASCE, 127(2), 105-113.
- ○ TAMU Data as reported by Briaud, J.-L. (2006). "Erosion Tests on New Orleans Levee Samples." *Texas A&M University Internal Report.*
- x Data from Shields, Casey, US.WES, Gilbert, White as reported by Vanoni, V.A., ed. (1975). "Sedimentation Engineering." *ASCE manuals and reports on engineering practice,* ASCE, New York.

Figure 3-18. Critical velocity as a function of mean grain size.

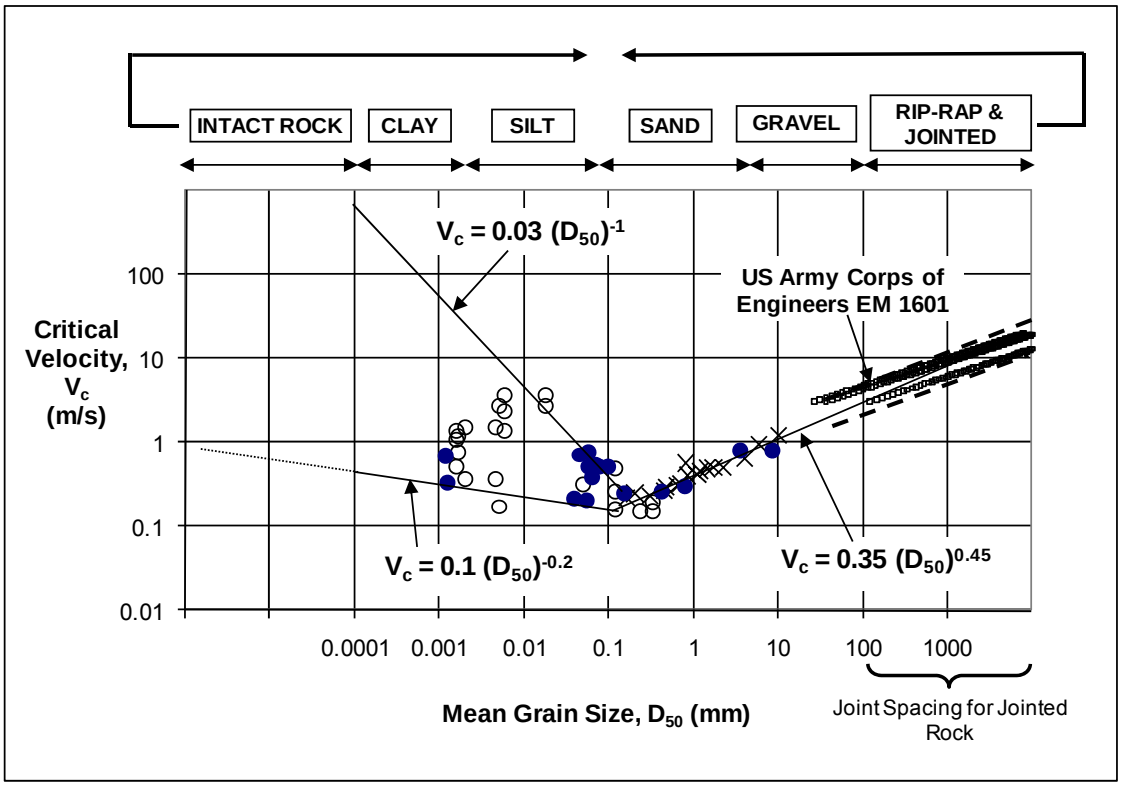

Legend:

- TAMU Data as reported by Briaud, J.-L. et. al. (2001). "Erosion Function Apparatus for Scour Rate Predictions." *J. Geotech. and Geoenvir. Engrg.,* ASCE, 127(2), 105-113.
- TAMU Data as reported by Briaud, J.-L. (2006). "Erosion Tests on New Orleans Levee Samples." *Texas A&M University Internal Report.*
- Data from Shields, Casey, US.WES, Gilbert, White as reported by Vanoni, V.A., ed. (1975). "Sedimentation Engineering." *ASCE manuals and reports on engineering practice,* ASCE, New York.
- Data points from simulation using U.S. Army Corps of Engineers EM 1601 Riprap Design Equation (U.S. Army Corps of Engineers 1995).

Figure 3-19. Critical velocity as a function of mean grain size including data points from simulation using U.S. Army Corps of Engineers EM 1601 Riprap Design Equation.

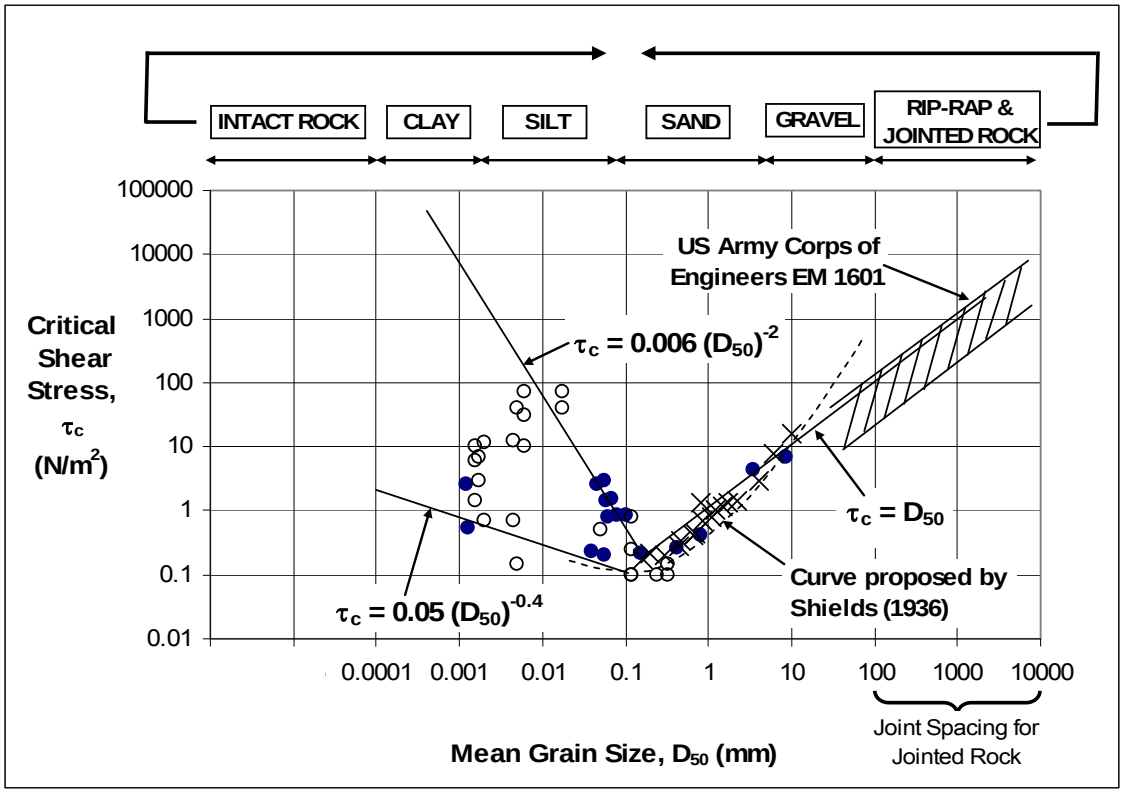

Legend:

- ● TAMU Data as reported by Briaud, J.-L. et. al. (2001). "Erosion Function Apparatus for Scour Rate Predictions." *J. Geotech. and Geoenvir. Engrg.,* ASCE, 127(2), 105-113.
- ○ TAMU Data as reported by Briaud, J.-L. (2006). "Erosion Tests on New Orleans Levee Samples." *Texas A&M University Internal Report.*
- x Data from Shields, Casey, US.WES, Gilbert, White as reported by Vanoni, V.A., ed. (1975). "Sedimentation Engineering." *ASCE manuals and reports on engineering practice,* ASCE, New York.

Figure 3-20. Critical shear stress as a function of mean grain size.

4. BRIDGE SCOUR ASSESSMENT 1

4.1. INTRODUCTION

Bridge Scour Assessment 1 (BSA 1) is a bridge scour assessment procedure that makes use of existing data collected either from bridge records maintained by the authorities or by site visit (Govindasamy et al. 2008). Figure 4-1 and Figure 4-2 show the BSA 1 flowcharts.

The main idea behind the BSA 1 procedure is that the scour depth corresponding to a specified future flood event is obtained through extrapolation charts that relate the scour depth ratio (Z_{fut}/Z_{mo}) to the velocity ratio (V_{fut}/V_{mo}). Here, Z_{fut} is the scour depth corresponding to a specified future flood, Z_{mo} is the maximum observed scour at the bridge, V_{fut} is the velocity corresponding to the specified future flood, and V_{mo} is the maximum velocity observed at the bridge until the time Z_{mo} is measured. The extrapolation charts, termed the Z-Future Charts are presented in Figure 4-3 through Figure 4-7. The vulnerability of the bridge associated with scour depends on the comparison between Z_{fut} and the allowable scour depth of the foundation, Z_{thresh}. There are two flowcharts for BSA 1; the first one is an assessment procedure for a bridge site that is underlain by a uniform deposit or when the scour depth being investigated is not expected to exceed the top layer in a non-uniform deposit. This assessment procedure is termed BSA 1 (Uniform Deposit) and is shown in Figure 4-1. The second flowchart is called BSA 1 (Multilayer Analysis) and is used for layered deposits when the scour

depth being investigated extends beyond the top layer. The BSA 1 (Multilayer Analysis) flowchart is shown in Figure 4-2. Both analyses are explained in detail in this Section.

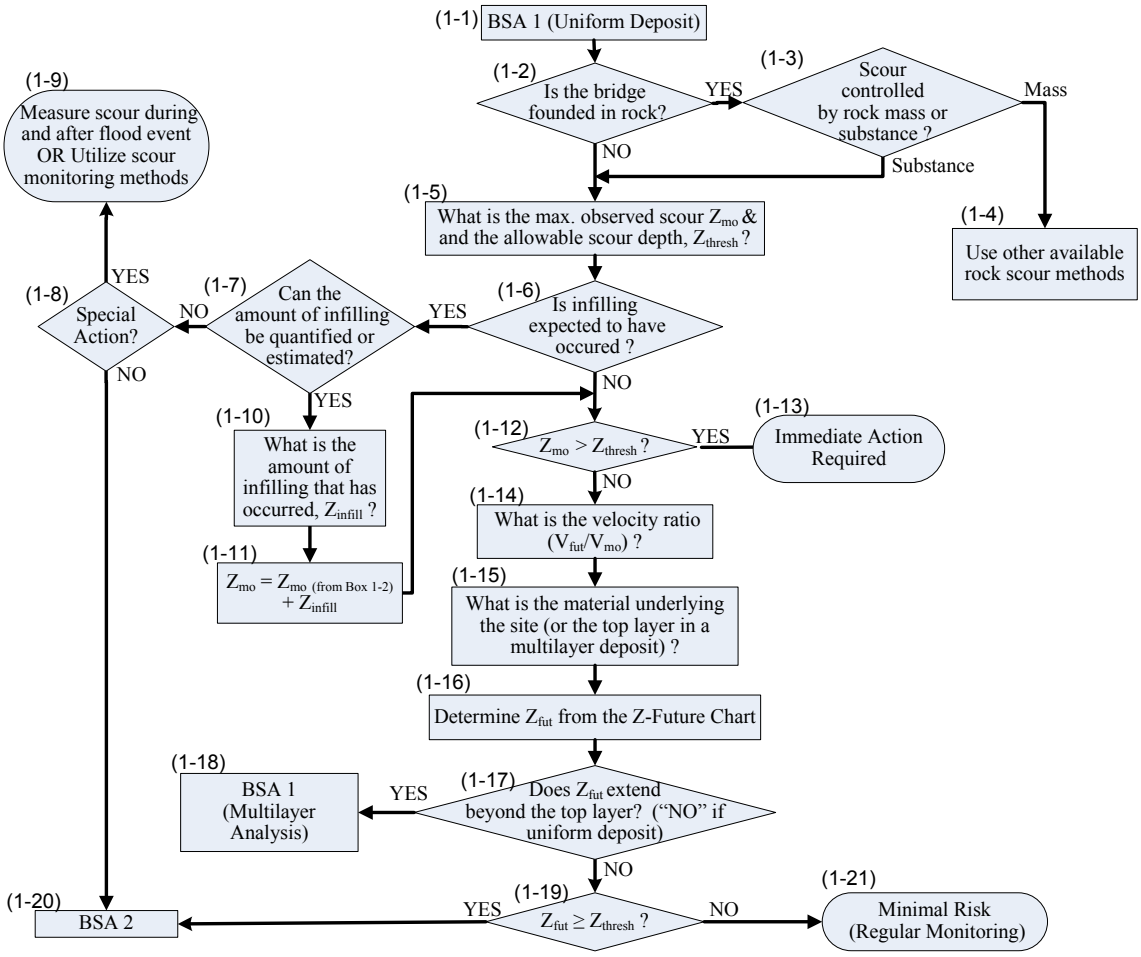

Figure 4-1. BSA 1 (Uniform Deposit) flowchart.

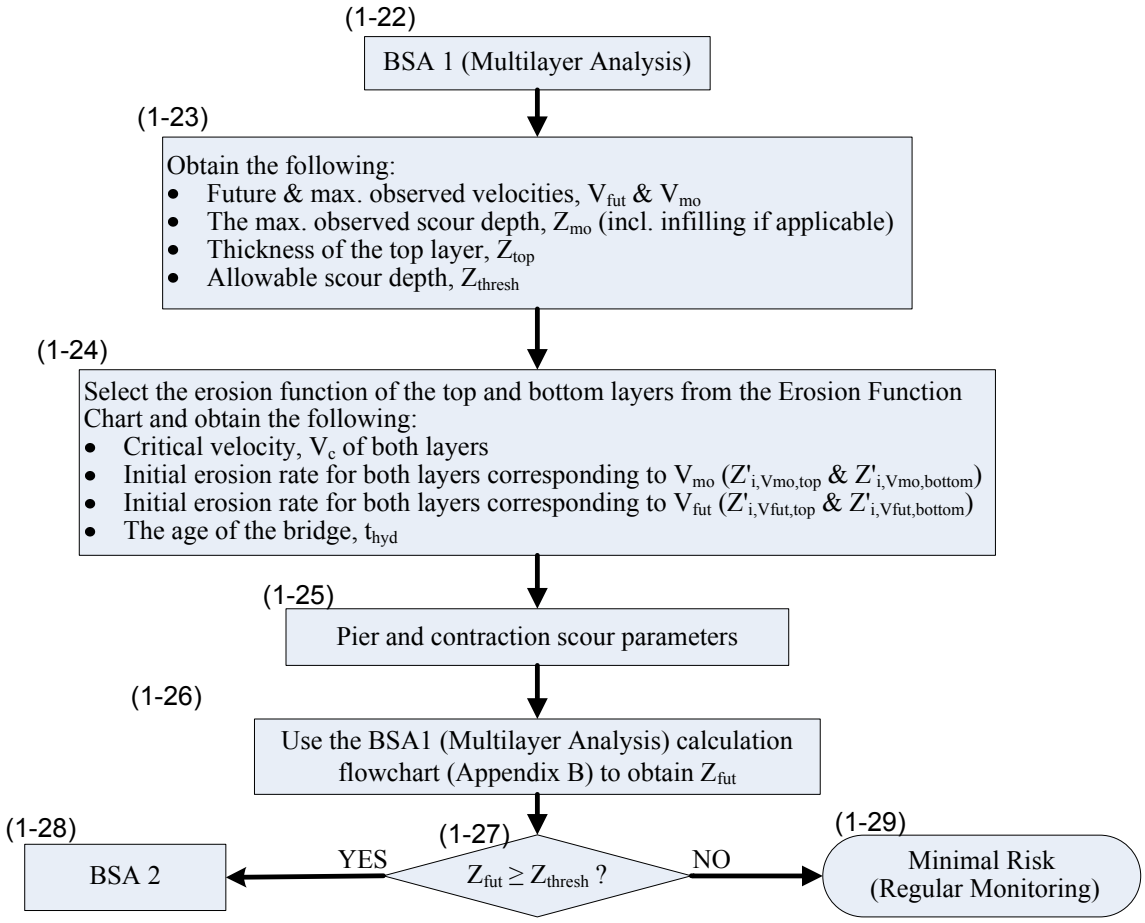

Figure 4-2. BSA 1 (Multilayer Analysis) flowchart.

4.2. THE Z-FUTURE CHARTS

The Z-Future Charts (Figure 4-3 through Figure 4-7) are essentially extrapolation charts that determine the scour depth Z_{fut} corresponding to a specified future flood event based on the following information:

1. The maximum observed scour depth at the bridge site, termed Z_{mo}.

2. The maximum flow velocity experienced by the bridge from the time it was built to when Z_{mo} is recorded, termed $V_{mo.}$

3. The velocity of the future flood being considered, termed $V_{fut.}$

4. The age of the bridge at the time Z_{mo} was recorded, termed t_{hyd}.

5. The pier scour parameter: pier size

6. The contraction scour parameters: water depth, soil critical velocity, contraction ratio

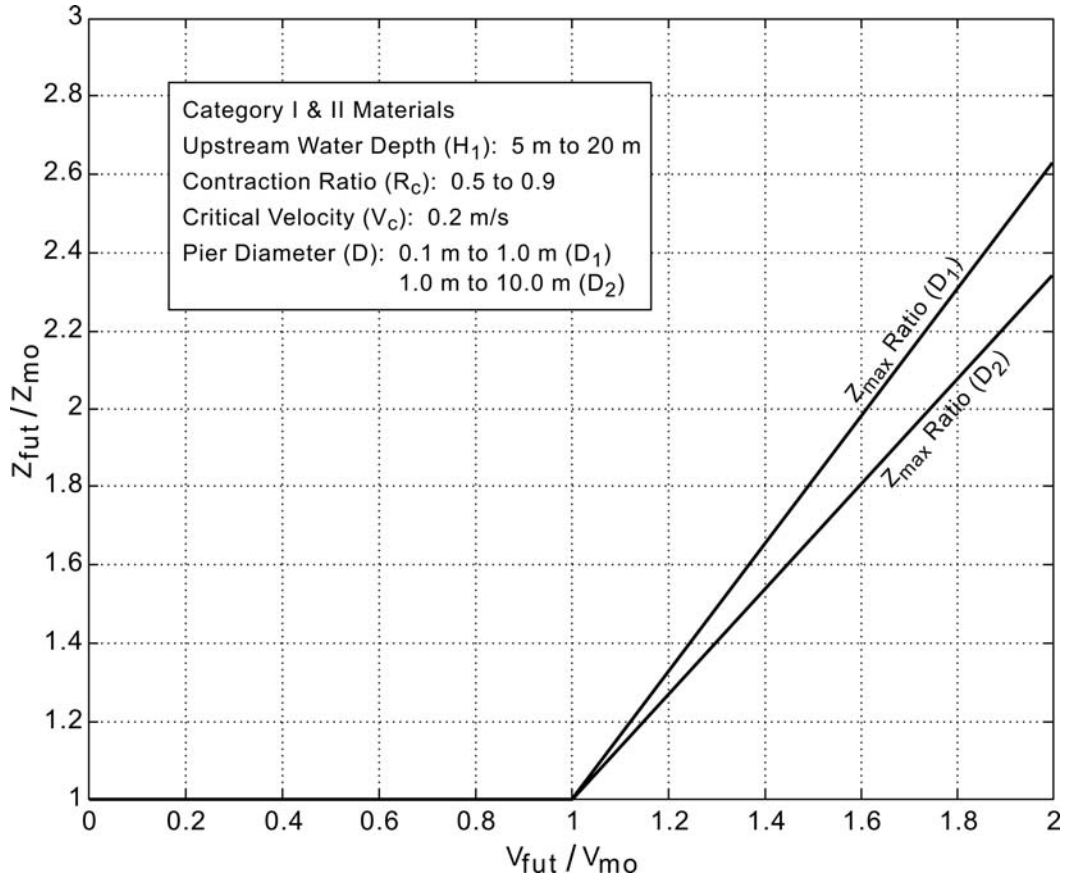

Figure 4-3. Z-Future Chart for Category I & II materials.

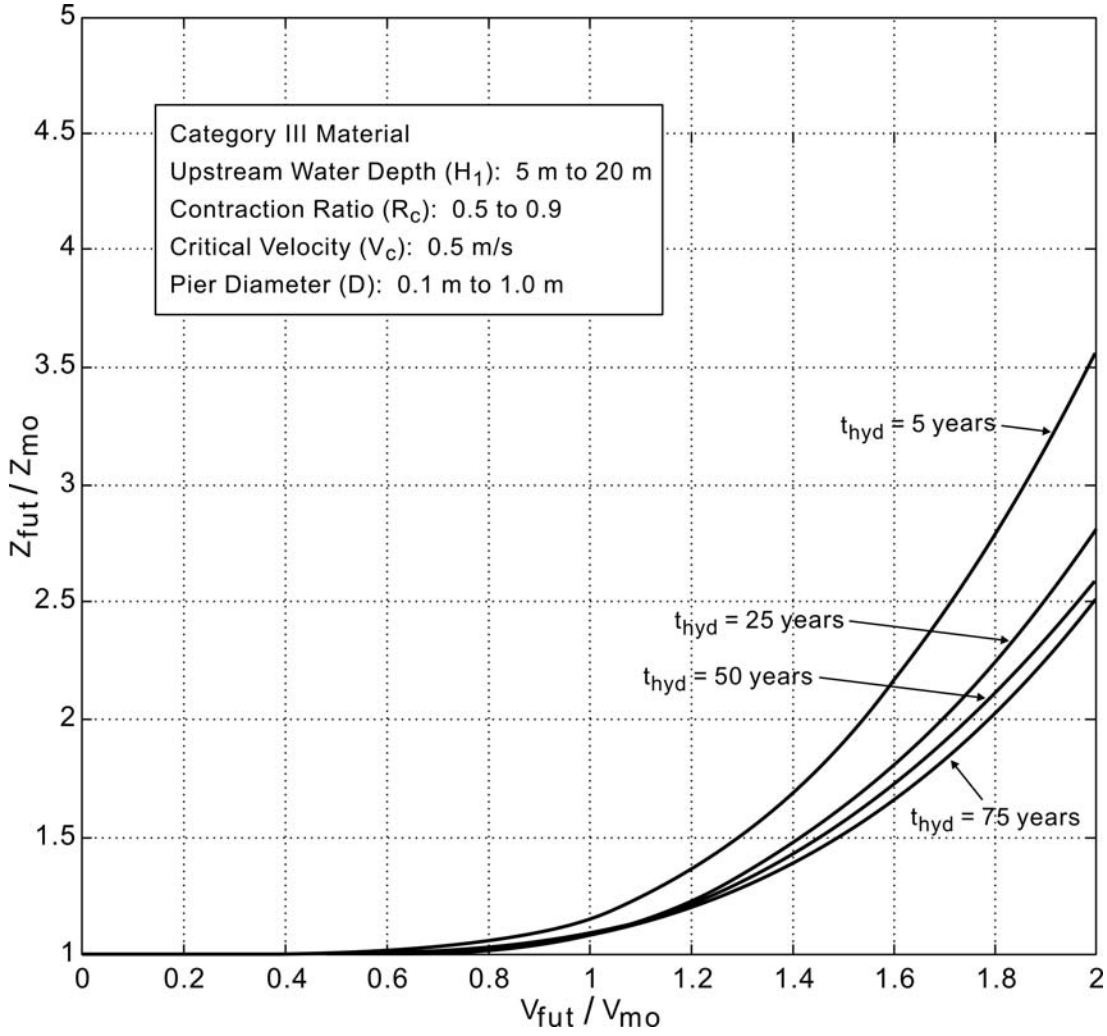

Figure 4-4. Z-Future Chart for Category III materials (Pier diameter: 0.1 m to 1.0 m).

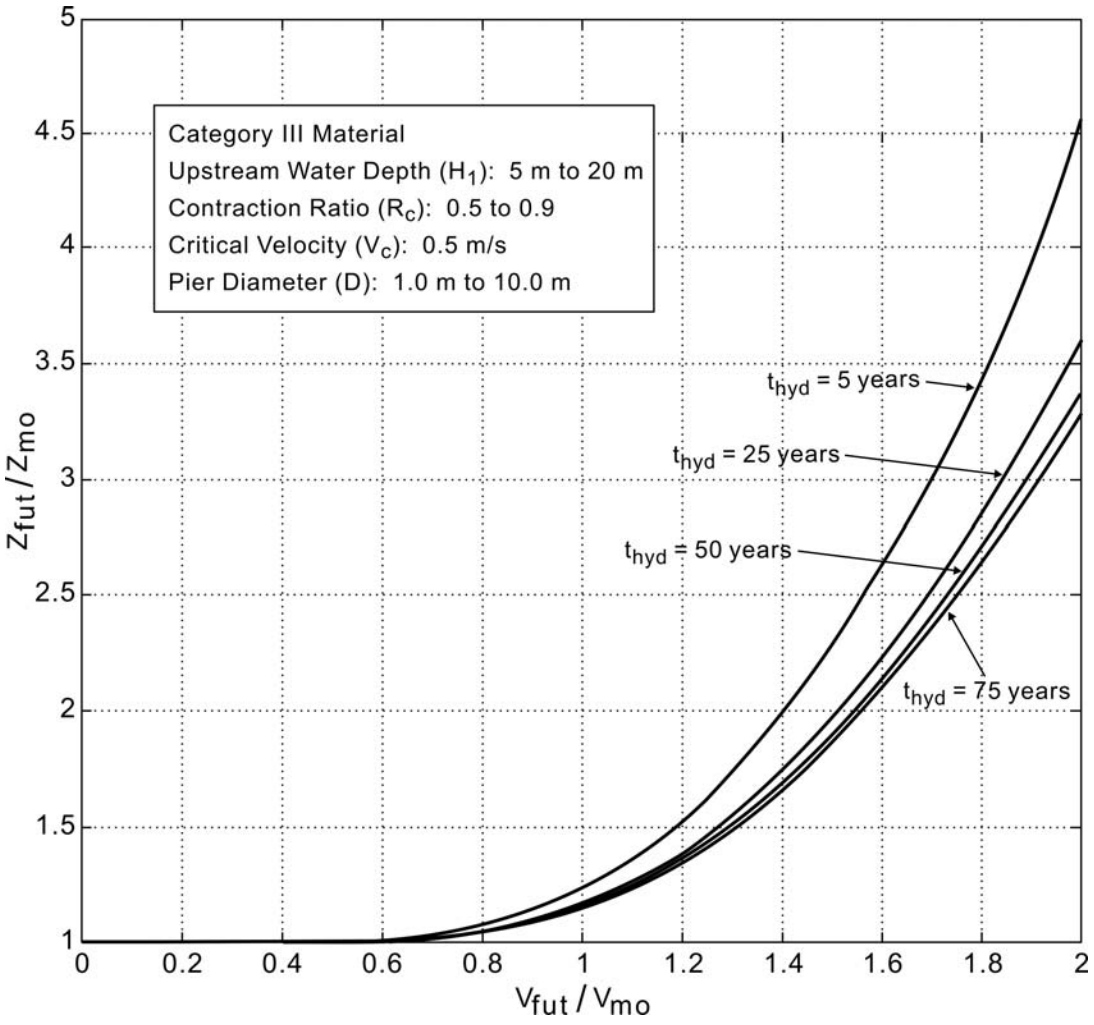

Figure 4-5. Z-Future Chart for Category III materials (Pier diameter: 1 m to 10 m).

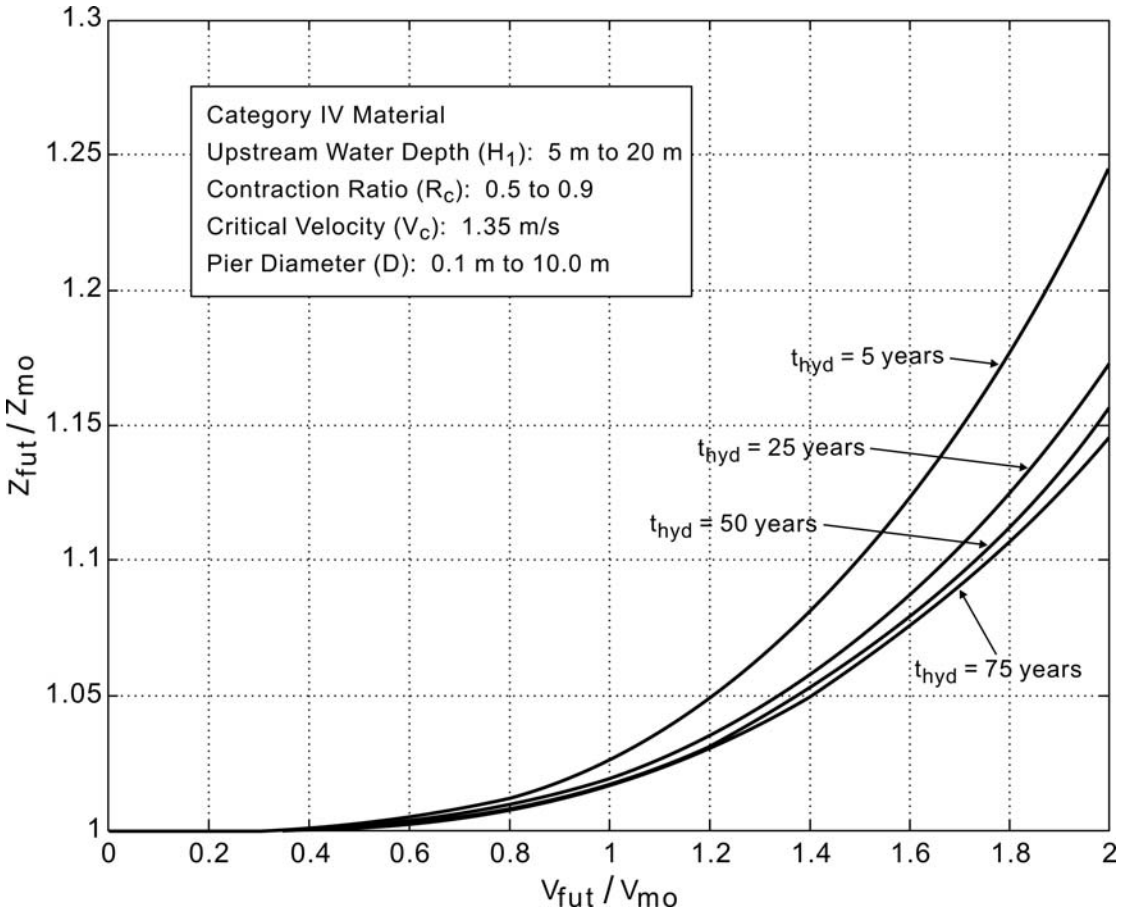

Figure 4-6. Z-Future Chart for Category IV materials.

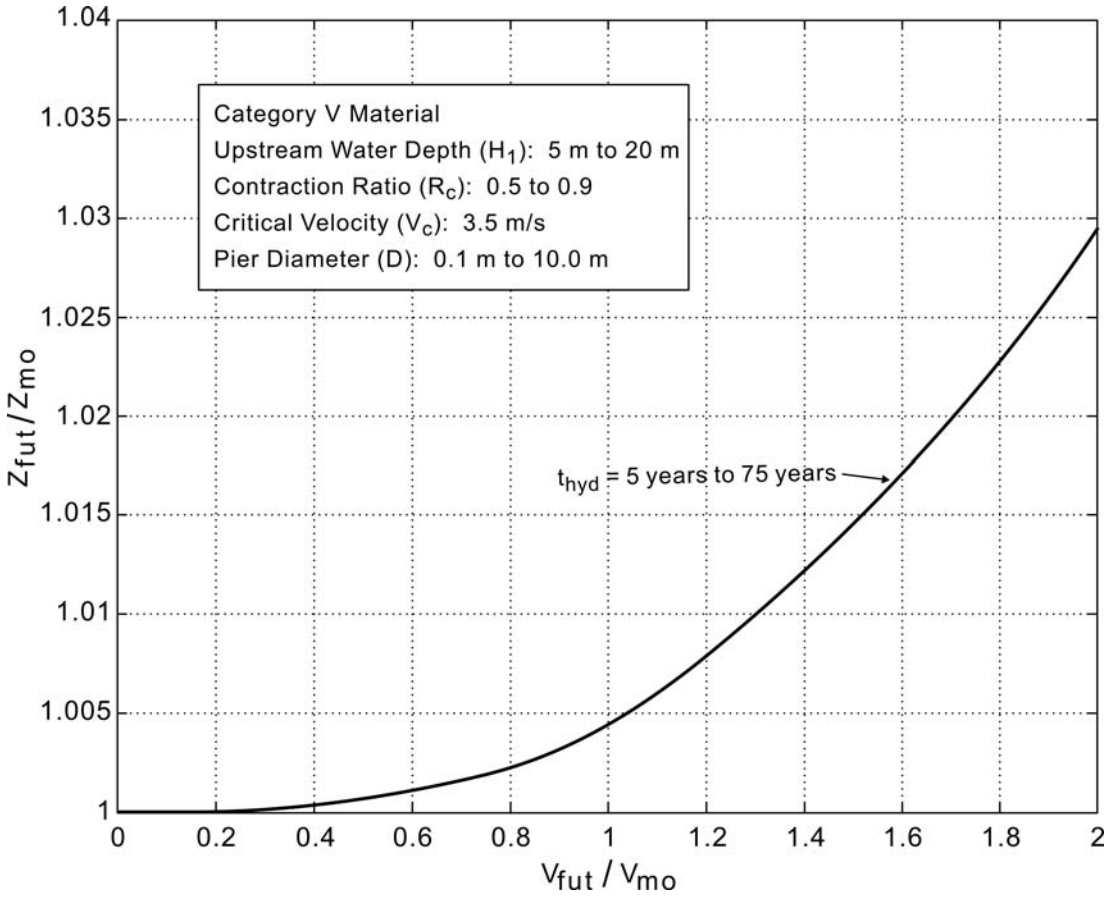

Figure 4-7. Z-Future Chart for Category V materials.

The Z-Future charts were developed using the Simple SRICOS-EFA method for pier and contraction (Briaud et al. 1999, 2005), which was detailed in Section 3. Simple SRICOS-EFA simulations were carried out by employing the equivalent time to represent the age of the bridge and varying the pier scour parameter, contraction scour parameters, and the material underlying the bridge site. The materials underlying the site are in accordance with five of the six erosion categories in the Erosion Function Charts (Figure 4-3 and Figure 4-7). These simulations computed the time-dependent scour

depth as a result of two consecutive flows having velocities V_{mo} and V_{fut}, respectively. The two general cases covered by the simulations are as follows:

1. Case 1: $V_{fut} \geq V_{mo}$

   This case represents the scenario where the bridge is being assessed for a future flood that is equal to or larger than the maximum flood it has experienced, where the velocity ratio (V_{fut}/V_{mo}) is equal to or greater than unity.

2. Case 2: $V_{fut} < V_{mo}$

   This case represents the scenario where the bridge is being assessed for a future flood that is smaller than the maximum flood it has experienced, where the velocity ratio (V_{fut}/V_{mo}) is less than unity.

The material categories involved in these simulations are Erosion Categories I through V. Category VI was omitted from the simulations as materials that fall under this category are considered non-erosive and a Simple SRICOS-EFA simulation on them would lead to no additional scour.

Simple SRICOS-EFA simulations of pier scour depth and contraction scour depth as described above were carried out by creating various combinations of the following parameters:

1. V_{fut} and V_{mo} ranging from 0.1 m/s to 3.5 m/s, which is well within the velocity range of flow of rivers in Texas.
2. Upstream water depth, H_1 ranging from 5 m to 20 m.
3. Channel contraction ratio, R_c ranging from 0.5 to 0.9.
4. Soil critical velocity, V_c according to the 5 material categories investigated, i.e. Erosion Categories I through V.

5. Pier diameter, D ranging from 0.1 m to 10.0 m. For the case of Category I and II materials, two ranges of pier diameter (0.1 m to 1.0 m and 1.0 m to 10 m) are represented by two curves on the same figure (Figure 4-3. Z-Future Chart for Category I & II materials For the case of Category III materials, the Z-Future Charts were separated into two charts, i.e. one for D ranging from 0.1 m to 1.0 m and the other for D ranging from 1.0 m to 10.0 m (Figure 4-4 and Figure 4-5). This was done because there was notable difference between the band of Z_{fut}/Z_{mo} ratios from these two ranges of pier diameters. The pier diameters for all other categories were lumped together, i.e. ranging from 0.1 m to 10.0 m as there was no significant difference due to the low erosion rates.

Simulations of pier and contraction scour depth described above were carried out for 360,000 combinations of the above parameters for each material category. The data points on Figure 4-3 through Figure 4-7 have been omitted to improve clarity of the curves but are shown in Appendix A. The Z_{fut} values were normalized with the corresponding Z_{mo} values and the V_{fut} values were normalized with the corresponding V_{mo} values and subsequently plotted against each other to form the Z-Future Charts. It should be noted that Z_{mo} in these simulations are computed values based on a given V_{mo} and other relevant parameters.

Figure 4-8 and Figure 4-9 show how two sequences of floods, i.e. the maximum flood observed at the bridge, Q_{mo} (with a corresponding V_{mo}) and the specified future flood, Q_{fut} (with a corresponding V_{fut}) are simulated. This procedure is adopted from Briaud et al. (2001b). Figure 4-8 illustrates the approach adopted for Case 1 where V_{fut} is larger than V_{mo} while Figure 4-9 shows the approach for Case 2 where V_{fut} is smaller than V_{mo}.

In general, the Z-Future Charts lead to the determination of Z_{fut} by employing the following relationship:

$$Z_{fut} = Z_{mo} \times f\left(V_{fut}/V_{mo}\right) \tag{4.1}$$

where f is some function of (V_{fut}/V_{mo}) obtained from the Z-Future Charts, and is always equal or greater than unity (for the case of clear-water scour, as considered in these simulations). The velocity ratio (V_{fut}/V_{mo}) is plugged into the chart by the user to obtain the value of the function *f*, based on the material type, age of the bridge and the pier scour and contraction scour parameters. Z_{mo} is obtained from bridge inspection and measurement records.

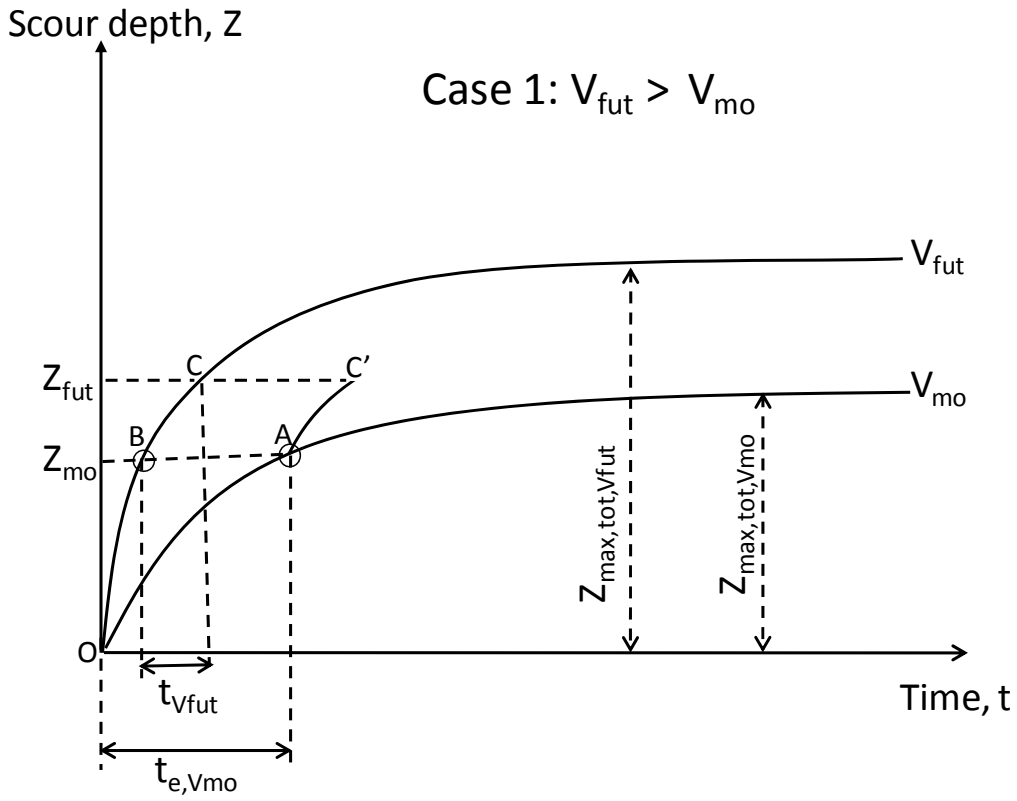

Figure 4-8. Scour caused by sequence of two flood events: Vfut > Vmo (after Briaud et al. 2001).

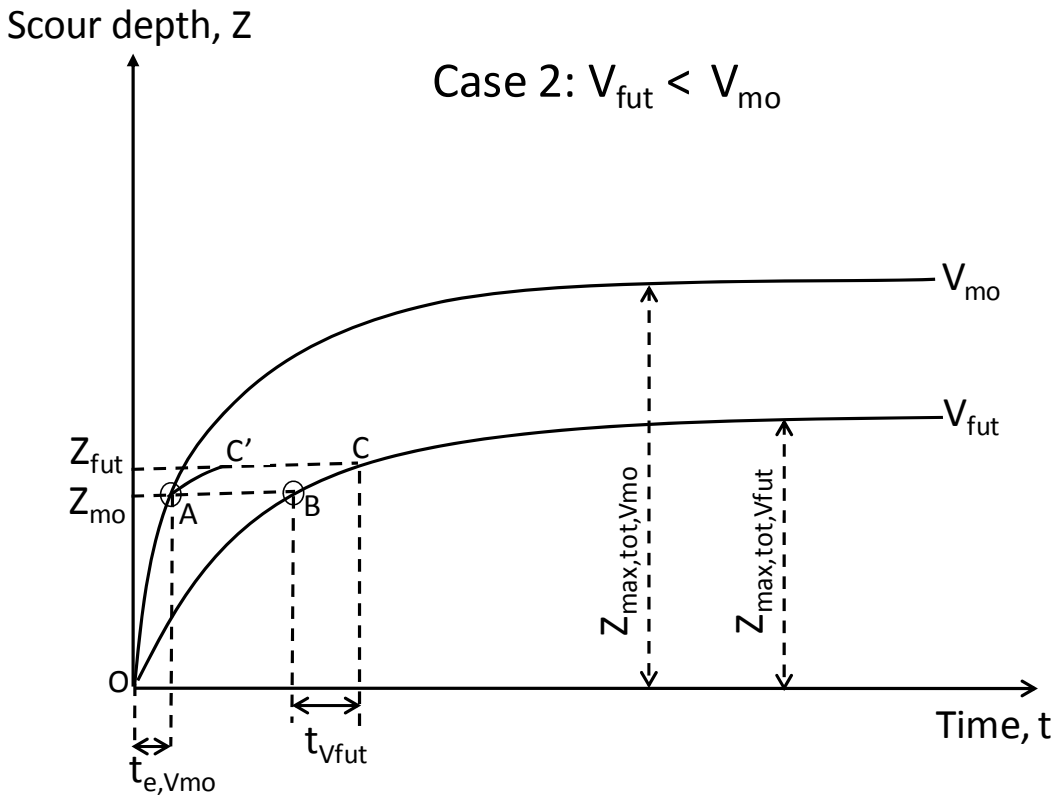

Figure 4-9. Scour caused by sequence of two flood events: $V_{fut} < V_{mo}$ (after Briaud et al. 2001).

4.2.1. Case 1: $V_{fut} > V_{mo}$

In Figure 4-8, the scour depth (Z) versus time (t) curve under V_{fut} and V_{mo} are shown. The lower curve represents the Z – t relationship for the lower velocity, V_{mo} and the upper curve represents the Z – t relationship for the higher velocity, V_{fut}. In this analysis, the velocity hydrograph at the bridge until the most recent scour measurement is converted into an equivalent time, with t_{hyd} as the hydrograph duration and V_{mo} as the maximum hydrograph velocity (Equation (2.7) and Equation (2.8)). At the start of the application of the equivalent time $t_{e,Vmo}$ and V_{mo}, the scour depth is zero (O in Figure 4-8) and progresses to Z_{mo} (Point A) at the end of $t_{e,Vmo}$. At the start of the future flood, the scour depth is translated to point B where it is still equal to Z_{mo} on the upper curve. In the development of the Z-Future Charts, the duration of the future flood is taken as 72 hours at a constant velocity, V_{fut}. This duration of the future flood is termed t_{Vfut} in Figure 4-8 and Figure 4-9. At the end of the future flood (t_{Vfut}), the scour depth would have progressed to Z_{fut} (Point C). This Z_{fut} can be equal to the maximum scour depth under the future flood ($Z_{max,tot,Vfut}$) if the time is sufficient to reach this maximum value. The combined scour depth time history for Case 1 is given by points O, A and C'.

4.2.2. Case 2: $V_{fut} < V_{mo}$

In Figure 4-9, the scour depth (Z) versus time (t) curve under V_{fut} and V_{mo} are shown. The lower curve represents the Z – t relationship for the lower velocity, V_{fut} and the upper curve represents the Z – t relationship for the higher velocity, V_{mo}. Similar to Case 1, the velocity hydrograph at the bridge until the most recent scour measurement is

converted into an equivalent time, with t_{hyd} as the hydrograph duration and V_{mo} as the maximum hydrograph velocity (Equation (2.7) and Equation (2.8)). At the start of the application of the equivalent time $t_{e,Vmo}$ and V_{mo}, the scour depth is zero (O in Figure 4-9) and progresses to Z_{mo} (Point A) at the end of $t_{e,Vmo}$. If Z_{mo} is larger than $Z_{max,tot,Vfut}$, which is the maximum scour depth possible under V_{fut}, the scour hole is already deeper than what is possible under V_{fut}, and therefore cannot create additional scour (Briaud et al. 2001b). If Z_{mo} is smaller than $Z_{max,tot,Vfut}$, the scour depth at the start of the future flood is translated to point B where it is still equal to Z_{mo} on the lower curve. At the end of the future flood the scour depth would have progressed to Z_{fut} (Point C). This Z_{fut} can be equal to the maximum scour depth under the future flood ($Z_{max,tot,Vfut}$) if the time is sufficient to reach this maximum value. The combined scour depth time history for Case 2 is given by points O, A and C'.

4.3. THE BSA 1 FLOWCHART

The boxes in the BSA 1 flowcharts (Figure 4-1and Figure 4-2) are of three shapes: rectangular, diamond, and rounded. Rectangular boxes are data collection and calculation boxes meaning that the data listed in the box needs to be collected by the user for the bridge being analyzed and then equations need to be used. Diamond boxes are "Yes-No" decision boxes. Rounded boxes are conclusion boxes. All boxes are numbered for easy reference where the first digit represents the BSA level and the second digit represents the box number.

As mentioned in the introduction of this section, the BSA 1 procedure consists of 2 flowcharts which are the BSA 1 (Uniform Deposit) and BSA 1 (Multilayer Analysis) flowcharts. BSA 1 (Uniform Deposit) is an assessment procedure for a bridge site that is underlain by a uniform deposit or when the scour depth being investigated is not expected to exceed the top layer of a multilayer deposit. BSA 1 (Multilayer Analysis) is used for layered deposits when the scour depth being investigated penetrates beyond the top layer.

4.3.1. The BSA 1 (Uniform Deposit) Flowchart and Procedure

In this procedure, the first step is to identify whether the bridge is founded in rock or not. If the bridge is indeed founded in rock, the BSA 1 then separates rock mass and rock substance controlled erosion. Rock mass controlled erosion occurs when reactions of rock materials to hydraulic stress is controlled by rock mass properties such as fracture and joint spacing, bedding planes, folding and spatial orientation (Cato 1991). In rock mass controlled erosion, the rock materials are eroded and transported as blocks. The critical velocity in rock mass erosion according to rock fracture spacing is shown in Table 4-1. The erosion categories in this table correspond to the Erosion Function Charts (Figure 3-4). Please note that Table 4-1 is preliminary in nature and should be calibrated against field behavior. The critical velocity and critical shear stress of rock as a function of fracture spacing is also shown in the Erosion Threshold Chatrs (Figure 3-18 and Figure 3-20). Rock substance controlled erosion is the erosion process that is governed by the property of the mineral grains forming the rock. These properties include density,

strength, hardness, permeability, weathering, grain size, and grain shape (Cato 1991). In BSA 1 (Uniform Deposit), scour assessments of rock materials that undergo rock mass controlled erosion are referred to other available methods for assessing scour in rock. Rock materials that undergo rock substance controlled erosion are treated as soils in BSA 1.

Table 4-1. Rock mass erosion (after Briaud 2008).

Joint spacing (mm)	Critical Velocity (m/s)	Erosion Category	Orientation of joints
< 30	0.5 – 1.35	III (Medium)	Not applicable
30 - 150	1.35 – 3.5	IV (Low)	Evaluation needed
150 – 1,500	3.5 – 10	V (Very low)	Evaluation needed
> 1,500	> 10	VI (Nonerosive)	Not applicable

Note: This table is preliminary in nature and should be calibrated against field behavior.

There are two conditions for local scour at a bridge when it concerns the presence of sediments in the flow and deposition of sediments from the flow. The first condition is termed clear-water scour and occurs when there is no movement of the bed material in the flow upstream of the bridge, or when the bed material being transported in the upstream reach is transported in suspension through the scour hole (Richardson and Davis 2001). The second condition is termed live-bed scour and occurs when there is transport of bed material from the upstream reach into the bridge crossing (Richardson and Davis 2001). Live-bed scour is cyclic in nature. The scour hole deepens during the rising stage of the flood. At the falling stage of the flood, the flow recedes and its sediment carrying capacity reduces. This results in the deposition of sediments, which

could take place in the scour hole. This could lead to infilling of the scour hole, yet is possible that the relative depth of scour is marginally affected all over the river bottom.

When live-bed scour has taken place, the depth of the scour hole measured during bridge inspections could be the scour depth after infilling has occurred. This would be the case if the bridge inspection is carried out either during the falling stage of the flood or after the flood event altogether. Because the Z-Future Charts are developed for clear-water scour conditions, if the measurements taken during the bridge inspection do not account for possible infilling, Z_{fut} would be under-predicted, as implied by Equation (4.1). This would therefore lead to an unconservative or even erroneous assessment of the bridge for scour. Several options are available in BSA 1 when infilling is expected to occur:

1. Quantifying the amount of infilling that has occurred, Z_{infill}

   The amount of infilling can be quantified from sediment transport calculations, model tests, by probing into the scour hole and roughly identifying the extent of the infilled material, or simply by engineering judgement and local experience. In this case, the value of Z_{mo} used in Equation (4.1) is the summation of the measured scour depth and Z_{infill}.

2. Taking special action

   If the amount of infilling cannot be quantified or estimated, special actions such as measuring the scour depth during and after flood events or utilization of scour monitoring methods can be adopted.

3. Carrying out BSA 2

   If the amount of infilling cannot be quantified or estimated, then BSA 2 could be undertaken to obtain the maximum scour depth

In order to obtain the scour depth ratio, Z_{fut}/Z_{mo} from the Z-Future Chart, the velocity ratio, V_{fut}/V_{mo} is required. Once the scour depth ratio is obtained from the Z-Future Chart, Z_{fut} is obtained from Equation (4.1) by plugging in the value of Z_{mo} measured in the field. If the site is underlain by a multilayer deposit and Z_{fut} extends beyond the top layer, then BSA 1 (Multilayer Analysis) should be carried out. Otherwise, if the site is underlain by a uniform deposit or if Z_{fut} does not extend beyond the top layer in a multilayer deposit, BSA 1 (Uniform Deposit) is continued. If Z_{fut} is equal or greater than the allowable scour depth, Z_{thresh}, BSA 2 should be undertaken. Otherwise the bridge is deemed as "Minimal Risk" and should undergo regular monitoring.

4.3.2. The BSA 1 (Multilayer Analysis) Flowchart and Procedure

The BSA 1 (Multilayer Analysis) is carried out if a bridge site with a multilayer deposit is found to have a Z_{fut} value according to BSA 1 (Uniform Deposit) that extends beyond the top layer of the deposit. A multilayer analysis is required because, using the maximum observed scour depth Z_{mo} in the top layer and extrapolating the scour depth to a different bottom layer could be unconservative in the case where the top layer is more erosion resistant (strong) than the bottom layer. This is because by doing so, one is expecting the less erosion resistant (weak) bottom layer to respond to hydraulic stresses in a similar manner as the strong layer. Conversely, a bridge site with a weak top layer over a strong bottom layer would be too conservative and uneconomical.

In BSA 1 (Multilayer Analysis), the calculations involved are more detailed than BSA 1 (Uniform Deposit). The underlying principle of the multilayer analysis is the determination of the time it takes to completely erode the top layer and the corresponding remaining time of the future flood duration and its impact on the bottom layer. Figure 4-10 shows an example of a multilayer analysis where V_{fut} is greater than V_{mo} and the top layer is more erosion resistant than the bottom layer. There are three $Z - t$ curves in this figure. The lowest curve is the $Z - t$ relationship for the top layer under velocity V_{mo}. The middle curve is the $Z - t$ relationship for the top layer under velocity V_{fut}. The upper curve is the $Z - t$ relationship for the bottom layer under V_{fut}. The definitions of the parameters that appear in Figure 4-10 are given in Table 4-2.

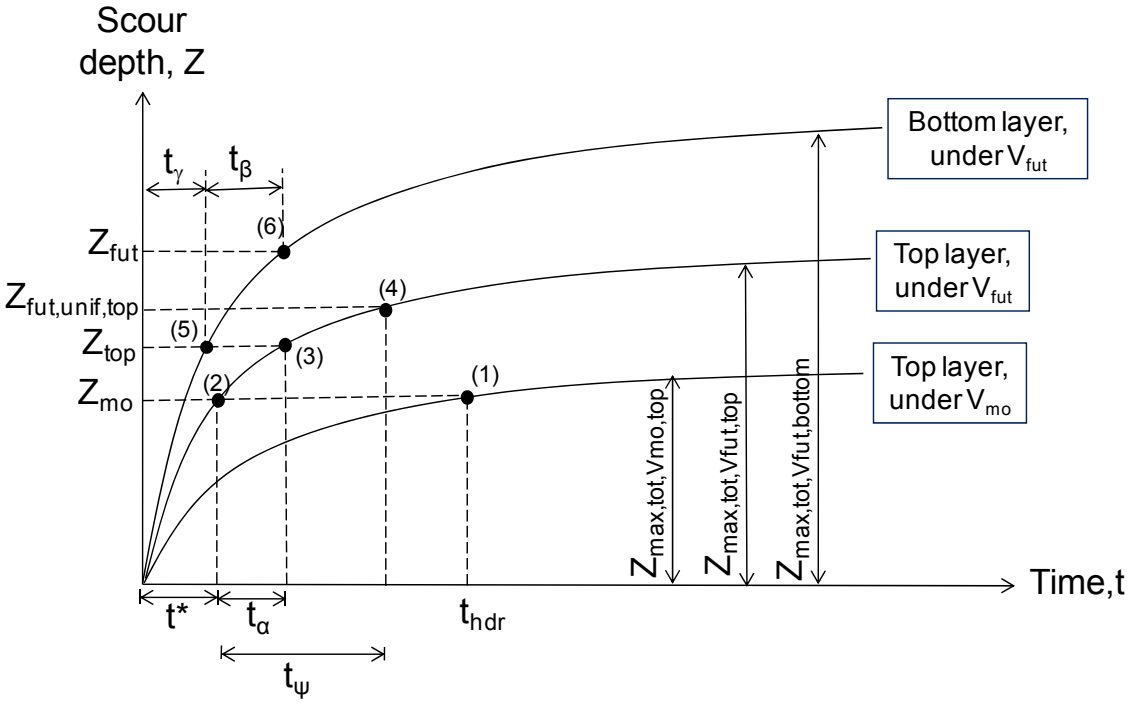

Figure 4-10. A general illustration for BSA 1 (Multilayer Analysis).

Table 4-2. Definition of terms in BSA 1 (Multilayer Analysis).

Term	Definition
Z_{mo}	The maximum observed scour depth at the bridge until the time of the most recent scour measurement.
Z_{fut}	The scour depth corresponding to the future flood velocity, V_{fut}.
$Z_{fut,unif,top}$	The scour depth at the end of the future flood assuming the site is made of the top layer material only. This parameter is obtained from the Z-Future Chart based on the material in the top layer and BSA 1 (Uniform Deposit).
Z_{top}	The depth of the lower boundary of the top layer.
$Z_{max,tot,Vmo,top}$	The maximum total scour depth in a uniform deposit comprising only of the top layer material, under the maximum observed velocity, $V_{mo.}$
$Z_{max,tot,Vfut,top}$	The maximum total scour depth in a uniform deposit made of the top layer material, under the future flood velocity, V_{fut}.
$Z_{max,tot,Vfut,bottom}$	The maximum total scour depth in a uniform deposit made of the bottom layer material, under the future flood velocity, V_{fut}.
t_{hyd}	The age of the bridge at the time Z_{mo} was measured.
t*	The time for Z_{mo} to be achieved under the future flood velocity, V_{fut}.
t_{ψ}	The duration of the future flood. In the case of this report, the duration of the future flood is chosen as 72 hours under constant velocity, V_{fut}.
t_{α}	The time it takes for the future flood to completely erode the top layer. In other words, it is the time for the scour depth to advance from Z_{mo} to Z_{top} under V_{fut}.
t_{β}	The time between the complete erosion of the top layer due to V_{fut} to the end of the future flood.
t_{γ}	The time required to develop Z_{top} in a uniform deposit made of the bottom layer material, under V_{fut}.

By rearranging the hyperbolic model presented in Equation (2.3), we obtain the time required to achieve a specified final scour depth, Z_{fin} by the following equation:

$$t = \frac{Z_{fin}\, Z_{max}}{\dot{Z}_i \left(Z_{max} - Z_{fin} \right)} \tag{4.2}$$

By using Equation (4.2), t* which is time for Z_{mo} to be achieved under V_{fut} can be determined. Point 2 in Figure 4-10 represents the scour depth Z_{mo} at time t* and is given by the following equation:

$$t^* = \frac{Z_{mo}\, Z_{max,tot,Vfut,top}}{\dot{Z}_{i,Vfut,top} \left(Z_{max,tot,Vfut,top} - Z_{mo} \right)} \tag{4.3}$$

where $Z_{max,tot,Vfut,top}$ is the maximum total scour that can occur in the top layer under V_{fut} and $\dot{Z}_{i,Vfut,top}$ is the erosion rate for the top layer corresponding to V_{fut}. The value of $\dot{Z}_{i,Vfut,top}$ is obtained from the Erosion Function Charts. The value of $Z_{max,tot,Vfut,top}$ is obtained by summing the values of maximum pier scour and contraction scour for the top layer material obtained from Equation (2.2) and Equation (2.4).

If Z_{top} is the depth of the lower boundary of the top layer and t_α is the time it takes for the scour depth to advance from Z_{mo} to Z_{top},

$$t^* + t_\alpha = \frac{Z_{top}\, Z_{max,tot,Vfut,top}}{\dot{Z}_{i,Vfut,top} \left(Z_{max,tot,Vfut,top} - Z_{top} \right)} \tag{4.4}$$

Point 3 on Figure 4-10 represents the scour depth Z_{top} at time ($t^* + t_\alpha$). Subsequently, the explicit value of t_α can be obtained from Equation (4.3) and Equation (4.4).

Here t_ψ is defined as the duration of the future flood. If it is initially assumed that the bridge site is underlain by a uniform deposit comprising only the top layer material, the scour depth corresponding to the future flood can be obtained from the Z-Future Chart. This scour depth is termed $Z_{fut,unif,top}$. Then, the value of $(t^* + t_\psi)$ is given by

$$t^* + t_\psi = \frac{Z_{fut,unif,top}\, Z_{max,tot,Vfut,top}}{\dot{Z}_{i,Vfut,top}\left(Z_{max,tot,Vfut,top} - Z_{fut,unif,top}\right)} \tag{4.5}$$

Point 4 on Figure 4-10 represents the scour depth $Z_{fut,unif,top}$ at time $(t^* + t_\psi)$. Subsequently, the explicit value of t_ψ can be obtained from Equation (4.3) and Equation (4.5).

If t_β is the duration the bottom layer is exposed to the future flood, it is given by

$$t_\beta = t_\psi - t_\alpha \tag{4.6}$$

Here t_γ is defined as time required to develop Z_{top} in a uniform deposit made of the bottom layer material, under V_{fut}. Then, t_γ is given by

$$t_\gamma = \frac{Z_{top}\, Z_{max,tot,Vfut,bottom}}{\dot{Z}_{i,Vfut,bottom}\left(Z_{max,tot,Vfut,bottom} - Z_{top}\right)} \tag{4.7}$$

where $Z_{max,tot,Vfut,bottom}$ is the maximum total scour that can occur in a uniform deposit comprising the bottom layer material, under V_{fut}. $\dot{Z}_{i,Vfut,bottom}$ is the erosion rate for the bottom layer corresponding to V_{fut}. The value of $\dot{Z}_{i,Vfut,bottom}$ is obtained from the Erosion Function Charts. The value of $Z_{max,tot,Vfut,bottom}$ is obtained by summing the values of maximum pier scour and contraction scour for the bottom layer material obtained from

Equation (2.2) and Equation (2.4). Point 5 on Figure 4-10 represents the scour depth Z_{top} at time t_γ.

The value of Z_{fut} in the multilayer deposit can now be computed using the hyperbolic model with a time input of $(t_\gamma + t_\beta)$. This is represented by Point 6 in Figure 4-10. The step-by-step procedure for BSA 1 (Uniform Deposit) is presented in Appendix B.

4.3.2.1. Sub-cases in BSA 1 (Multilayer Analysis)

In the BSA 1 (Multilayer Analysis), there are three sub-cases within Case 1 and Case 2 which address the variations in the relative positions of the Z – t curves. The variations of the relative positions of the Z – t curves are a result of the variations in the maximum total scour depth that can occur in a particular material. For example, in a situation where the top layer is strong (st) and the bottom layer is weak (w) and V_{fut} is less than V_{mo}, the maximum total scour depth of the two layers have two possible outcomes:

- Outcome 1: $Z_{max,tot,Vfut,w} > Z_{max,tot,Vmo,st}$
- Outcome 2: $Z_{max,tot,Vfut,w} < Z_{max,tot,Vmo,st}$

where $Z_{max,tot,Vfut,w}$ is the maximum total scour depth in the weak material under V_{fut} and $Z_{max,tot,Vmo,st}$ is the maximum total scour depth in the strong material under V_{mo}. These sub-cases are presented and defined in Table 4-3, and illustrated in Figure 4-11 through Figure 4-16. However, the general concept of the BSA 1(Multilayer Analysis) as presented in Figure 4-10 is applicable to all the sub-cases. The sub-cases are presented to

aid the user in understanding the different scenarios that could be encountered while using BSA 1 (Multilayer Analysis).

Table 4-3. Sub-cases within Case 1 and Case 2.

Velocity Ratio	Case	Relative Material Erodibility	Condition
≥ 1 ($V_{fut} \geq V_{mo}$)	1(a)	Strong layer over weak layer	$Z_{max,tot,Vfut,w} > Z_{max,tot,Vmo,st}$
	1(b)	Weak layer over strong layer	$Z_{max,tot,Vfut,w} > Z_{max,tot,Vmo,st}$
	1(c)		$Z_{max,tot,Vfut,w} < Z_{max,tot,Vmo,st}$
< 1 ($V_{fut} < V_{mo}$)	2(a)	Weak layer over strong layer	$Z_{max,tot,Vmo,w} < Z_{max,tot,Vfut,st}$
	2(b)		$Z_{max,tot,Vmo,w} > Z_{max,tot,Vfut,st}$
	2(c)	Strong layer over weak layer	$Z_{max,tot,Vmo,w} > Z_{max,tot,Vfut,st}$

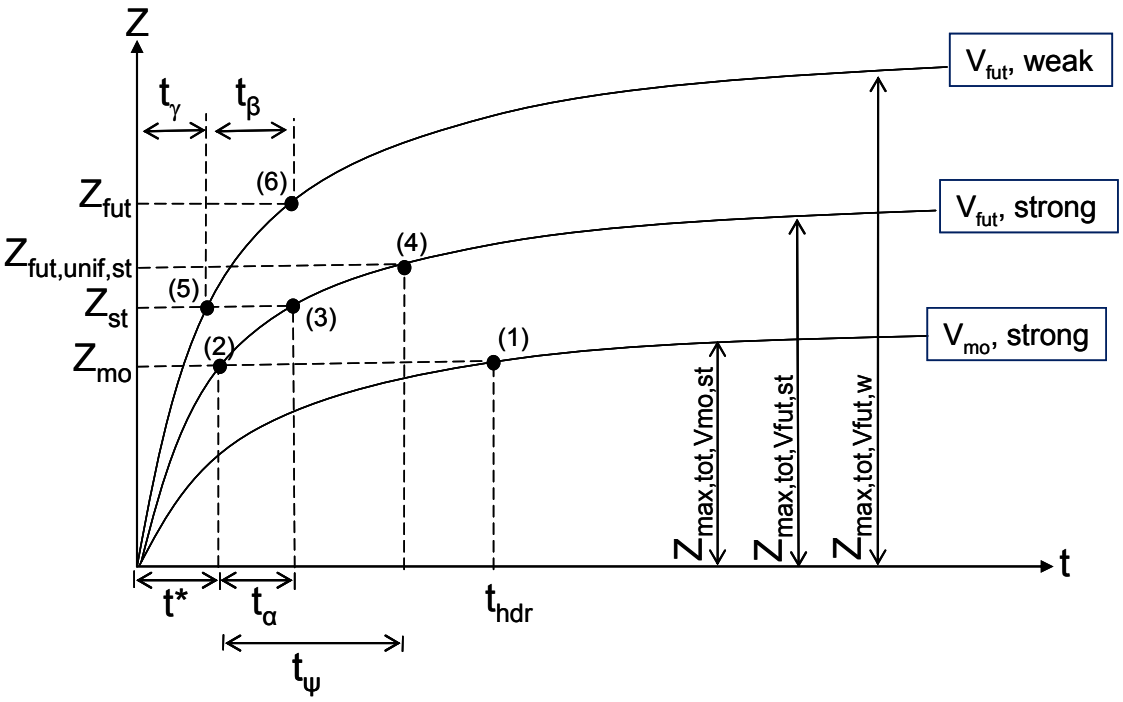

Figure 4-11. Case 1(a) for BSA 1 (Multilayer Analysis).

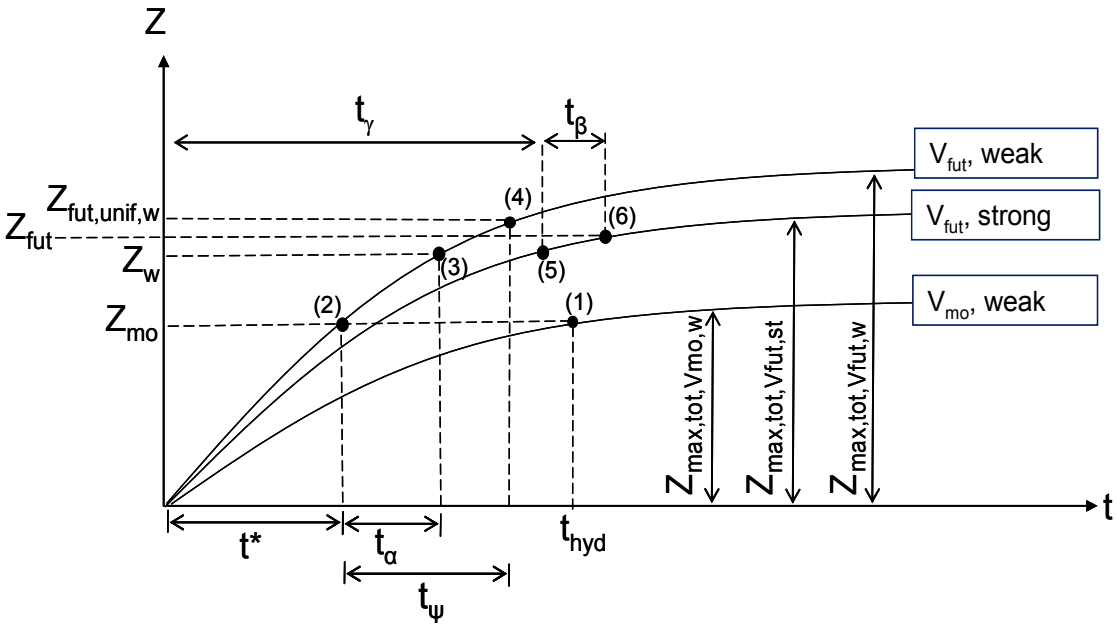

Figure 4-12. Case 1(b) for BSA 1 (Multilayer Analysis).

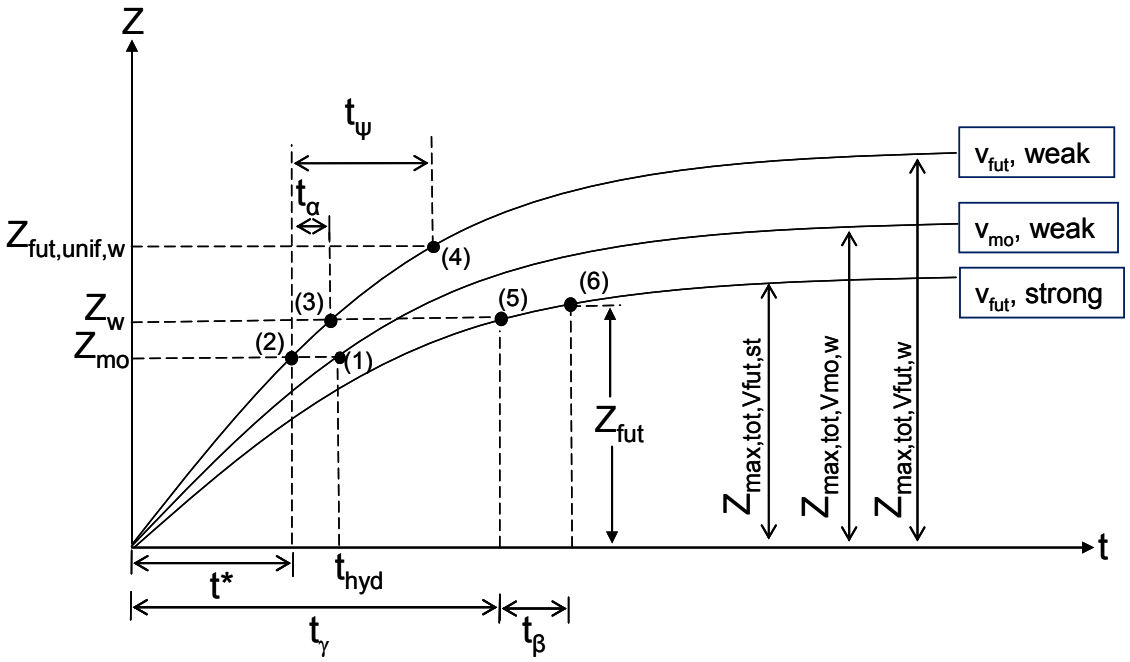

Figure 4-13. Case 1(c) for BSA 1 (Multilayer Analysis).

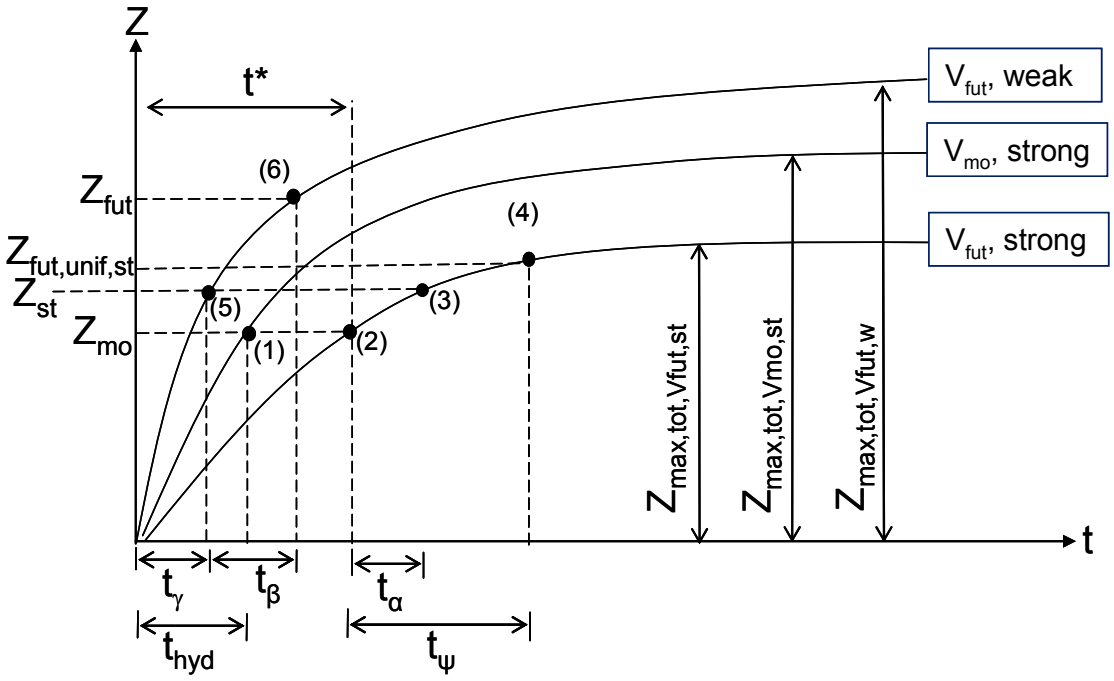

Figure 4-14. Case 2(a) for BSA 1 (Multilayer Analysis).

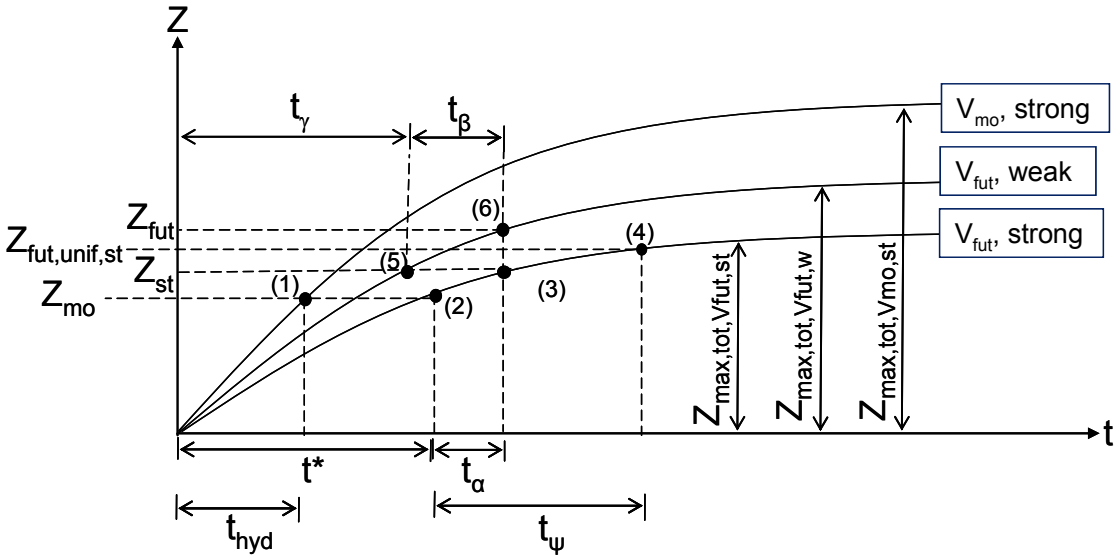

Figure 4-15. Case 2(b) for BSA 1 (Multilayer Analysis).

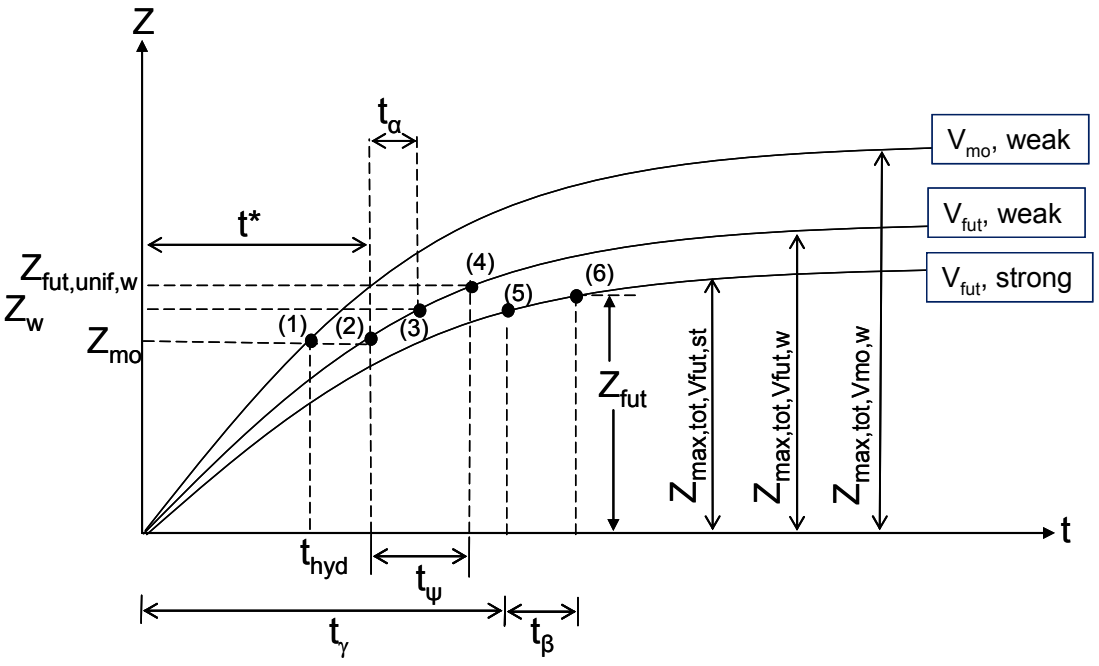

Figure 4-16. Case 2(c) for BSA 1 (Multilayer Analysis).

4.4. STEP-BY-STEP PROCEDURE FOR BSA 1

To assist the user in carrying out a BSA 1 analysis, tables detailing all the steps of the method according to flowchart box number are presented. Table 4.4 is for BSA 1 (Uniform Deposit) and Table 4.5 is for BSA 1 (Multilayer Analysis).

Table 4-4. Step-by–step procedure for BSA 1 (Uniform Deposit).

Box No.	Description
1-1	Introduction to BSA 1 (Uniform Deposit).
1-2	The decision box to determine if a bridge is founded in rock or soil. If the bridge is founded in rock, proceed to Box 1-3. Otherwise, proceed to Box 1-5.
1-3	The decision box to determine if the erosion of the rock (if applicable) is rock mass or rock substance controlled. • *Rock mass controlled* The rock is eroded and transported as blocks that are recognizable and can be identified with its parent material (Cato 1991). • *Rock substance controlled* The rock is eroded at the grain level and involves the rock substance properties such as density, strength, hardness, permeability, weathering, grain size, and grain shape (Cato 1991). • If the erosion is rock mass controlled, proceed to Box 1-4 where the user is referred to other available methods for rock scour assessment (Table 4-1, Figure 3-4, Figure 3-5, Figure 3-18, and Figure 3-20). • If the erosion is rock substance controlled, the rock is treated as soil. Proceed to Box 1-5.
1-4	The box that refers the user to other available rock scour assessment procedures to address rock mass controlled erosion (Table 4-1, Figure 3-4, Figure 3-5, Figure 3-18, and Figure 3-20).
1-5	The data collection box that gathers the maximum observed scour at the bridge, Z_{mo} and the allowable scour depth of the bridge foundation, Z_{thresh}. • Z_{mo} is the largest scour depth recorded at the bridge and is usually obtained from bridge inspection records. • Z_{thresh} is obtained from foundation bearing capacity or lateral stability analysis. Z_{thresh} is sometimes taken as half the pile embedment length.
1-6	The decision box to determine if infilling of the scour hole is expected to have occurred at the bridge site. Infilling occurs under live-bed scour conditions. If infilling is expected to have occurred, proceed to Box1-7.
1-7	The decision box to determine if the amount of infilling can be quantified, for example by local experience or engineering judgement. If the amount of infilling can be quantified, proceed to Box 1-10. Otherwise, proceed to Box 1-8.
1-8	The decision box to determine if special action is to be adopted to address the infilling issue. If yes, proceed to Box 1-9. Otherwise proceed to Box 1-20.

Table 4-4. Continued.

Box No.	Description
1-9	Conclusion box that presents options for special action to address infilling. These options are (Delphia 2008): • Measurement of scour during and after flood events • Utilization of scour monitoring methods
1-10	The data collection box for the amount of infilling, Z_{infill}.
1-11	The calculation box that updates Z_{mo} to account for infilling. This is done by adding Z_{infill} to the Z_{mo} value that did not account for infilling. Once this process is completed, proceed to Box 1-12.
1-12	The decision box to determine if Z_{mo} exceeds Z_{thresh}. Sometimes, Z_{thresh} is taken as half the pile embedment length. If yes, proceed to Box 1-13 which recommends immediate action. Otherwise, proceed to Box 1-14.
1-13	Conclusion box that recommends immediate action be taken to protect the bridge against scour related damage.
1-14	The data collection box for the velocity ratio, $V_{fut}/V_{mo.}$
1-15	The data collection box that gathers the type of geomaterial underlying the bridge site. In the case of a multilayer deposit, this box requires the geomaterial of the top layer.
1-16	The box involving the determination of Z_{fut} from the Z-Future Charts. The value of the velocity ratio, V_{fut}/V_{mo} is plugged into the appropriate Z-Future Chart to obtain the scour depth ratio, Z_{fut}/Z_{mo}. Use Equation (4.1) to obtain Z_{fut}. The Z-Future Charts were developed based on a range of pier and contraction scour parameters. These parameters are clearly indicated on the chart. The chart should not be used for cases that **DO NOT** comply with the indicated range of these parameters. If such a case arises, proceed to BSA 2.
1-17	The decision box to determine if the value of Z_{fut} as obtained in Box 1-16 extends beyond the top layer of the multilayer deposit (if applicable). If yes, proceed to the BSA 1 (Multilayer Analysis). Otherwise proceed to Box 1-19.
1-18	Lead to BSA 1 (Multilayer Analysis).
1-19	Decision box to determine if the bridge can be designated as "Minimal Risk." If Z_{fut} equals or exceeds Z_{thresh}, proceed to BSA 2 to calculate the maximum scour depth Z_{max}. Otherwise, the bridge is deemed as "Minimal Risk" and should undergo regular monitoring.
1-20	Lead to BSA 2.
1-21	Conclusion box that classifies the bridge as having minimal risk to scour. The bridge should undergo regular monitoring.

Table 4-5. Step-by–step procedure for BSA 1 (Multilayer Analysis).

Box No.	Description
1-22	Introduction to BSA 1 (Multilayer Analysis).
1-23	The data collection box that gathers the following parameters: • The velocity corresponding to the future flood, V_{fut}. • The maximum observed scour depth, Z_{mo} (including infilling if applicable) • The thickness of the top layer, Z_{top}. • The allowable scour depth, Z_{thresh} obtained from foundation bearing capacity or lateral stability analysis.
1-24	The data collection box that gathers the following information: • The erosion functions of the top and bottom layer geomaterials, obtained from the Erosion Function Charts. The erosion function can be taken as the left boundary of the erosion category that best describes the geomterial layer. • The critical velocity, V_c of the top and bottom layers. V_c is the velocity corresponding to an erosion rate of 0.1 mm/hr on the erosion function. • The initial erosion rate corresponding to V_{mo} and V_{fut} of the top and bottom layers ($\dot{Z}_{i,Vmo,top}$, $\dot{Z}_{i,Vmo,bottom}$, $\dot{Z}_{i,Vfut,top}$, and $\dot{Z}_{i,Vfut,bottom}$, respectively) • The age of the bridge, t_{hyd} in terms of equivalent time. The equivalent time for pier scour, $t_{e,p}$ is obtained from Equation (2.7). The equivalent time for contraction scour, $t_{e,c}$ is obtained from Equation (2.8). In this case, the velocity for the equivalent time equations is V_{mo}. The rate of scour is obtained from the erosion function at velocity V_{mo}.
1-25	The data collection box for pier and contraction scour parameters which are: • Approach velocity, V_{appr} • Pier diameter, D • Kinematic viscosity of water, υ ($\upsilon = 10^{-6}$ m^2/s at 20º Celsius) • Critical velocity, V_c • Upstream water depth, H_1 • Uncontracted channel width B_1 and contracted channel width B_2
1-26	The box where the future scour depth Z_{fut} for multilayer condition is calculated. Refer to the BSA 1 (Multilayer Analysis) calculation flowchart in Appendix C.
1-27	Decision box to determine if the bridge can be classified as "Minimal Risk." If Z_{fut} equals or exceeds Z_{thresh}, proceed to BSA 2 to calculate the maximum scour depth Z_{max}. Otherwise, the bridge is classified as "Minimal Risk" and should undergo regular monitoring.
1-28	Lead to BSA 2.
1-29	Conclusion box that designates the bridge as having minimal risk to scour. Here, the bridge should undergo regular monitoring.

4.5. BSA 1 (UNIFORM DEPOSIT) EXAMPLE

Problem: Determine the future scour depth corresponding to the 100-year flood for the following information that characterizes the bridge scour problem.

- Geomaterial Type: Uniform Medium Erodibility material (Category III)
- Contraction ratio $R_c = 0.85$, Upstream Water depth $H_1 = 10$ m, Pier Diameter D = 1.0 m
- Age of the bridge $t_{hyd} = 25$ years
- The bridge is not founded in rock
- The scour conditions are mostly clear-water scour and a 0.3 m infilling is estimated to occur after big floods.
- $V_{fut}/V_{mo} = V_{100}/V_{mo} = 1.4$
- Maximum observed scour depth $Z_{mo} = 2$ m
- The allowable scour depth $Z_{thresh} = 8$ m
- The bridge was built in 1981 and assessed in 2006

Solution according to BSA 1(Uniform Deposit) flowchart Box numbers:

Box 1-1 : Start of BSA 1 (Uniform Deposit). Proceed to Box 1-2

Box 1-2: The bridge is not founded in rock. Proceed to Box 1-5.

Box 1-5: $Z_{mo} = 2$ m, $Z_{thresh} = 8$ m. Proceed to Box 1-6.

Box 1-6: Infilling is estimated at 0.3 m. Proceed to Box 1-11.

Box 1-11: $Z_{mo} = 2 + 0.3 = 2.3$ m. Proceed to Box 1-12.

Box 1-12: $Z_{mo} < Z_{thresh}$. Proceed to Box 1-14.

Box 1-14: $V_{fut}/V_{mo} = V_{100}/V_{mo} = 1.4$

Box 1-15: Medium Erodibility Material (Category III). Proceed to Box 1-16

Box 1-16: From Figure 4-4, $Z_{fut}/Z_{mo} = 1.5$ for a 25 year old bridge.

$$Z_{fut} = 1.5 \times Z_{mo}$$
$$= 1.5(2.3)$$
$$= 3.5 \text{ m}$$

Proceed to Box 1-17.

Box 1-17: The bridge is founded on a uniform soil deposit. Proceed to Box 1-19

Box 1-18: $Z_{fut} = 3.5$ m, $Z_{thresh} = 8$ m. Z_{fut} is less than $Z_{thresh.}$ Proceed to Box 1-21

Box 1-21: The bridge is deemed as 'Minimal Risk' and should undergo regular monitoring.

5. BRIDGE SCOUR ASSESSMENT 2

5.1. INTRODUCTION

Bridge Scour Assessment 2 (BSA 2) is the assessment procedure that has to be carried out if a bridge is not found as either "Minimal Risk (Regular Monitoring)', "Immediate Action Required" or "Special Action" at the end of Bridge Scour Assessment 1 (BSA 1). BSA 2 is a process that determines the scour vulnerability by applying the maximum scour depth concept. The maximum bridge scour depth concept is based on the assumption that the bridge will experience the maximum possible scour depth (equilibrium scour depth) under V_{fut} within its lifetime. This might not be the case for more erosion resistant materials such as clays and some rocks. In BSA 2, the maximum scour at the bridge, termed maximum total local scour ($Z_{max,l}$) is the arithmetic sum of the three components of scour, i.e. maximum pier scour ($Z_{max,p}$), maximum contraction scour ($Z_{max,c}$) and, maximum abutment scour ($Z_{max,a}$). The vulnerability associated with scour depends on the comparison between the maximum total local scour depth and the allowable scour depth of the bridge.

5.2. THE BSA 2 FLOWCHART AND PROCEDURE

The BSA 2 flowchart is presented in Figure 5-1. The boxes in the flowchart are of four forms: rectangular, diamond, circle, and rounded. Rectangular boxes are data collection and calculation boxes, meaning that the data listed in the box needs to be collected by

the user for the bridge being analyzed and where appropriate, involve the use of equations. Diamond boxes are "Yes-No" decision boxes. The circle represents "On Page" information. Rounded boxes are conclusion boxes. All boxes are numbered for easy reference where the first digit represents the level of assessment and the second digit represents the box number.

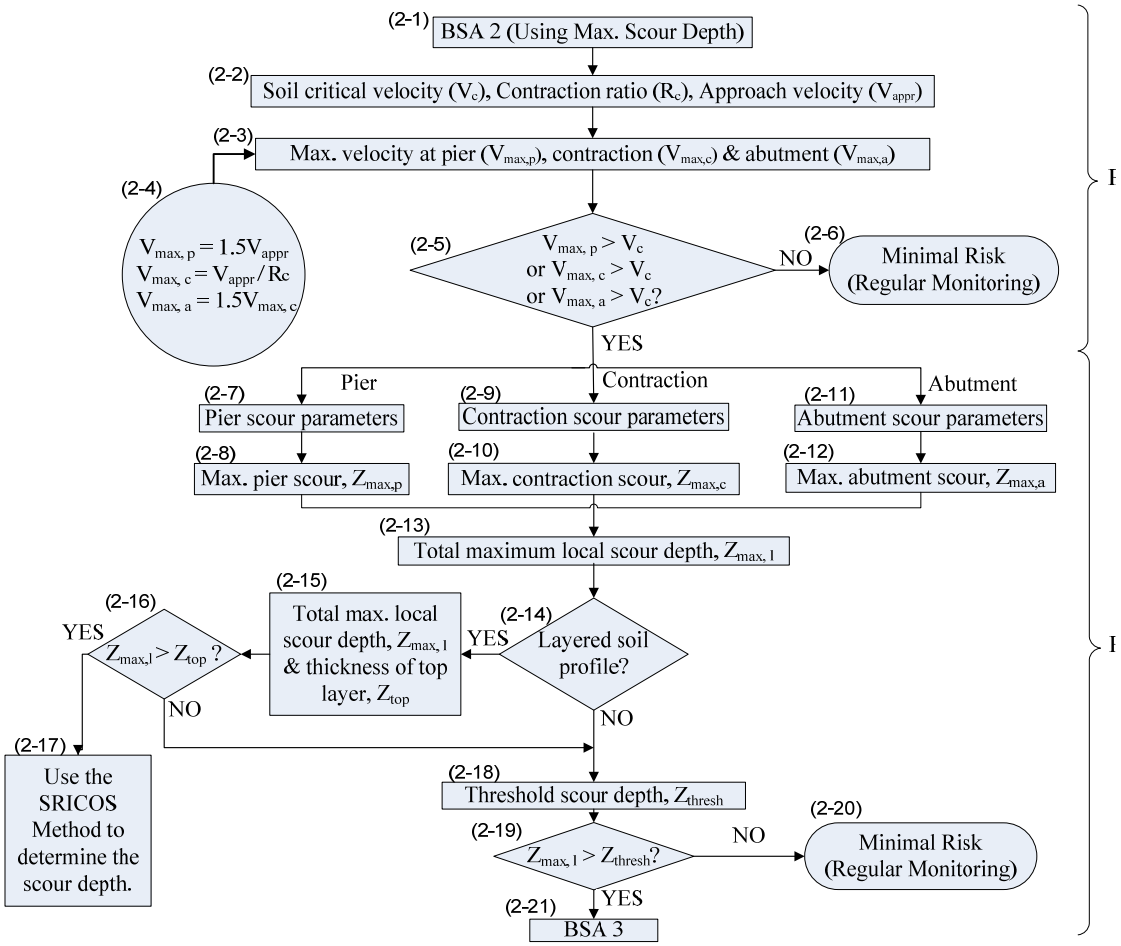

Figure 5-1. The BSA 2 flowchart.

The BSA 2 flowchart consists of two parts. Part 1 is essentially a simple filtering process that utilizes the critical velocity of the soil present at the bridge (V_c) and local velocities at the pier, contraction or abutment ($V_{max,p}$, $V_{max,c}$ and $V_{max,a}$, respectively). The critical velocity is obtained by an Erosion Function Chart developed on the basis of a database of Erosion Function Apparatus (EFA) tests (Briaud et al. 2001) and on the experience of the authors (Figure 3-4 and Figure 3-5). The Erosion Function Chart shows erosion categories for various soils and the bridge inspector can determine the relevant critical velocity. This chart essentially eliminates the need for site specific erosion testing (Govindasamy et al. 2008). The following equations for local velocities are derived from the authors' experience and numerical simulations results:

$$V_{max,p} = 1.5\ V_{appr} \tag{5.1}$$

$$V_{max,c} = V_{appr}/R_c \tag{5.2}$$

$$V_{max,a} = 1.5\ V_{max,c} \tag{5.3}$$

where V_{appr} = approach velocity upstream of the bridge and R_c is the ratio of the contracted width of the channel B_1 to the uncontracted width of the channel B_2 (Figure 2-11).

If any one of the local velocities exceeds the soil critical velocity, then Part 2 of BSA 2 is required to be carried out. Otherwise, the velocities at the obstruction are less than the velocity required to initiate significant erosion and the bridge is categorized as "Minimal Risk (Regular Monitoring)" (Govindasamy et al. 2008).

In Part 2 of BSA 2, simple calculations for maximum scour depth are carried out. The calculations for maximum pier scour and contraction scour are described in

Section 2 and detailed in Briaud et al. (1999, 2005). Calculations for maximum abutment scour are also described in Section 2 and are based on HEC-18 (Richardson and Davis 2001). The maximum total local scour depth, $Z_{max,l}$ is a summation of all three scour components:

$$Z_{max,l} = Z_{max,p} + Z_{max,c} + Z_{max,a} \tag{5.4}$$

where $Z_{max,p}$, $Z_{max,c}$ and $Z_{max,a}$ are the maximum pier scour, contraction scour and abutment scour, respectively.

The BSA 2 flowchart also addresses the presence of a layered geologic profile at the bridge site. In the case where the maximum total local scour depth, $Z_{max,l}$ exceeds the thickness of the top layer within the profile, Z_{top} the maximum scour depth concept is not applicable, requiring analysis using the Extended SRICOS-EFA Method (Briaud et al. 1999, 2005, http://ceprofs.tamu.edu/briaud/research.html) . However if $Z_{max,l}$ does not exceed Z_{top}, the maximum scour depth concept is applicable and subsequently if the value of $Z_{max,l}$ does not exceed $Z_{threshold}$, the bridge is deemed as "Minimal Risk (Regular Monitoring)". Otherwise, BSA 3 needs to be undertaken.

5.3. STEP-BY-STEP PROCEDURE FOR BSA 2

To assist the user in carrying out a BSA 2 analysis, a table detailing all the steps of the method according to the flowchart box numbers is presented below (Table 5-1).

Table 5-1. Step-by–step procedure for BSA 2.

Box No.	Description
2-1	Introduction to BSA 2. Links BSA 1 to BSA 2.
2-2	The data collection box for the following parameters: • The critical velocity, V_c which is the velocity corresponding to an erosion rate of 0.1 mm/hr on the erosion function. The erosion function can be taken as the left boundary of the erosion category that best describes the geomaterial underlying the bridge site. • Contraction ratio (R_c), which is the ratio of the width of the river in the contracted zone B_2 to the upstream channel width B_1 (Figure 2-11). • Approach velocity (V_{appr}), which is the velocity of the water directly upstream of the bridge. The approach velocity is the velocity that corresponds to the flow being considered. For example, if the flow being considered is the 100-year flood Q_{100}, then the corresponding velocity is V_{100}.
2-3	The data collection box for maximum local velocities at the pier ($V_{max,p}$), contraction ($V_{max,c}$), and abutment ($V_{max,a}$). The relationship between these parameters and the approach velocity, V_{appr} is given by Equation (5.1) through Equation (5.3).
2-4	The on page information giving the relationship between local velocities and the approach velocity, as given by Equation (5.1) through Equation (5.3)
2-5	Decision box to determine if scour would take place at the bridge based on maximum local velocities and the critical velocity. If any one of the maximum local velocities (from Box 2-3) exceeds the critical velocity (from Box 2-2), Part 2 of BSA 2 needs to be undertaken. Otherwise, the bridge can be designated as Minimal Risk and should undergo regular monitoring (Box 2-6).
2-6	Conclusion box indicating that the bridge is classified as “Minimal Risk” and should undergo regular monitoring.
2-7	The data collection box for pier scour parameters, which are: • Approach velocity, V_{appr} • Pier diameter, D • Kinematic viscosity of water, υ ($\upsilon = 10^{-6}$ m^2/s at 20º Celsius)
2-8	The calculation box for maximum pier scour depth. The maximum pier scour depth $Z_{max,\,p}$ is obtained fro Equation (2.2).
2-9	The data collection box for contraction scour parameters, which are: • Approach velocity, V_{appr} • Critical velocity, V_c (from Box 2-2). • Upstream water depth, H_1 • Contraction ratio, R_c (from Box 2-2)
2-10	The calculation box for the maximum contraction scour depth. The maximum contraction scour depth $Z_{max,\,c}$ is obtained from Equation (2.4).

Table 5.1. Continued.

Box No.	Description
2-11	The data collection box for abutment scour parameters. The HIRE equation should be used if the ratio of the projected abutment length L to the flow depth at the abutment y_1 is greater than 25. Otherwise the Froehlich equation should be used. The parameters for maximum abutment scour calculation are as follows: *Froehlich Equation* • Approach velocity, V_{appr} • Length of active flow obstructed by the embankment, L' • Average flow depth in the floodplain, y_a • Abutment shape coefficient K_1 obtained from Figure 2-15 and Table 2-4. • Coefficient for angle of embankment flow K_2 as described in Section 2.4.1 and Figure 2-14. *Hire Equation* • Approach velocity, V_{appr} • Abutment shape coefficient K_1 obtained from Figure 2-15 and Table 2-4. • Coefficient for angle of embankment flow K_2 as described in Section 2.4.1 and Figure 2-14. • Water depth of flow at the abutment on the overbank or main channel y_1
2-12	The calculation box for maximum abutment scour depth. The maximum abutment scour depth $Z_{max,\,a}$ is obtained either from Equation (2.9) or Equation (2.10).
2-13	The calculation box for the maximum local scour depth, obtained from Equation (5.4).
2-14	Decision box to determine if the bridge site has a layered deposit.
2-15	The data collection box for the thickness of the topmost layer at the bridge site Z_{top}.
2-16	The decision box to determine if the maximum local scour depth $Z_{max,l}$ is greater than the thickness of the topmost layer $Z_{top.}$ If yes, the maximum scour depth method is not applicable and the SRICOS-EFA Method needs to be used. Otherwise, the maximum scour depth method is applicable and BSA 2 is continued in Box 2-18.
2-17	Lead to the SRICOS Method (Briaud et al. 2003).
2-18	The data collection box for the allowable scour depth Z_{thresh}. This is based on the foundation element being considered.
2-19	Decision box to determine if the bridge is classified as having low scour risk or requires BSA 3 analysis. This is done by comparing the maximum local scour depth $Z_{max,l}$ against the allowable scour depth Z_{thresh}. If $Z_{max,l}$ is greater than Z_{thresh}, the analysis should proceed to BSA 3 (Time Analysis). Otherwise, the bridge is classified as "Minimal Risk" and should undergo regular monitoring.
2-20	Conclusion box indicating that the bridge is classified as "Minimal Risk" and should undergo regular bridge scour monitoring.
2-21	Lead to BSA 3.

5.4. EXAMPLE OF BSA 2 ANALYSIS

Problem: Determine the maximum scour depth corresponding to the following information that characterizes the bridge scour problem.

- Geomaterial Type: Uniform Medium Erodibility material (Category III)
- Contraction ratio: $R_c = 0.85$
- Upstream Water depth $H_1 = 10$ m
- Pier Diameter D = 1.0 m
- Approach velocity $V_{appr} = V_{100} = 2.0$ m/s
- Water depth directly upstream of abutment $y_0 = 3.0$ m
- Length of active flow obstructed by the abutment, L = 4.0 m (Figure 5-2)
- Angle of embankment flow $\theta = 30^{\circ}$ (Figure 5-2).
- Abutment Type = Vertical-wall abutment
- Kinematic viscosity of water at 20˚C, $\upsilon = 10^{-6}$ m^2/s
- Allowable scour depth $Z_{thresh} = 10$ m

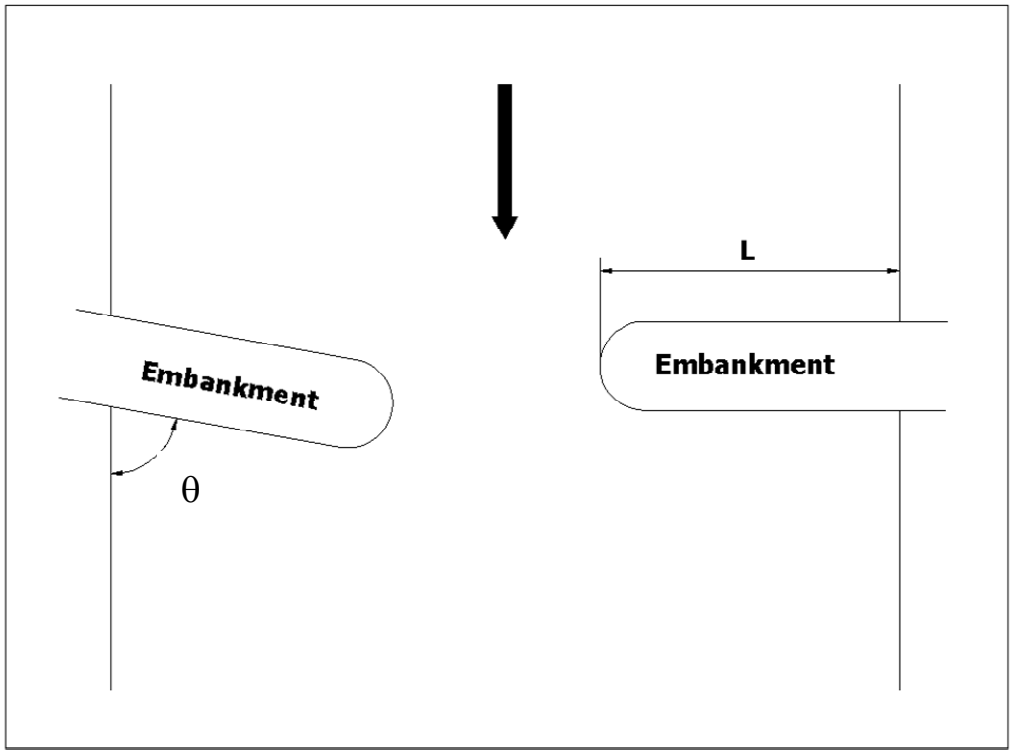

Figure 5-2. Definition of length of active flow obstructed by the abutment and angle of embankment flow.

Solution according to BSA 2 Flowchart Box numbers:

Box 2-1: Start of BSA 2.

Box 2-2: From Table 3-2, $V_c = 0.5$ m/s, $R_c = 0.85$, $V_{appr} = V_{100} = 2.0$ m/s.

Proceed to Box 2-3.

Box 2-3: From Box 2-4,

$$V_{max,p} = 1.5V_{appr} = 1.5(2.0) = 3.0 \text{ m/s}$$

$$V_{max,c} = 1.5V_{appr} = \frac{V_{appr}}{R_c} = \frac{2.0}{0.85} = 2.4 \text{ m/s}$$

$$V_{max,a} = 1.5\ (V_{max,c}) = 1.5\ (2.4) = 3.6 \text{ m/s}$$

Proceed to Box 2-5.

Box 2-5: $V_{max,p}$ is greater than $V_{c.}$

$V_{max,c}$ is greater than $V_{c.}$

$V_{max,a}$ is greater than $V_{c.}$

Proceed to Box 2-7.

Box 2-7: Pier scour parameters.

$D = 1.0$ m, $V_{appr} = V_{100} = 2.0$ m/s, $\upsilon = 10^{-6}$ m^2/s

Proceed to Box 2-8.

Box 2-8: $$Z_{max,p}(mm) = 0.18\left(\frac{V_{appr} D}{\nu}\right)^{0.635} = 1804.8$$

$$Z_{max,p}(m) = 1.8.$$

Proceed to Box 2-9.

Box 2-9: Contraction scour parameters.

$R_c = 0.85$, $H_1 = 10.0$ m, $V_{appr} = V_{100} = 2.0$ m/s, $V_c = 0.5$ m/s

Proceed to Box 2-10.

Box 2-10: $$Z_{max,c} = 1.9H_1\left[\frac{1.38V_{appr}}{R_c\sqrt{gH_1}} - \frac{V_c}{\sqrt{gH_1}}\right]$$

$$= 1.9(10.0)\left[\frac{1.38(2.0)}{0.85\sqrt{9.81 \text{ x } 10.0}} - \frac{0.5}{\sqrt{9.81 \text{ x } 10.0}}\right]$$

$$= 5.3 \text{ m}$$

Proceed to Box 2-11.

Box 2-11: Abutment scour parameters.

$y_a = 3.0$ m, $V_{appr} = V_{100} = 2.0$ m/s, $L = 4.0$ m, $\theta = 30^{\circ}$

Abutment type = Vertical –wall abutment

Proceed to Box 2-12.

$$\frac{L}{y_a} = \frac{4.0}{3.0} = 1.33 > 2.5$$

Box 2-12: Since $\frac{L}{y_a} > 2.5$, use the Froehlich Equation.

$$\frac{Z_{max,a}}{y_a} = 2.27\, K_1\, K_2 \left(\frac{L}{y_a}\right)^{0.43} F^{0.61}$$

From Table 2-4, $K_1 = 1.00$

$$K_2 = \left(\frac{\theta}{90}\right)^{0.13} = \left(\frac{30}{90}\right)^{0.13} = 0.87$$

$$Z_{max,a} = 2.27\, y_a K_1\, K_2 \left(\frac{L}{y_a}\right)^{0.43} \left(\frac{V_{appr}}{\sqrt{g y_a}}\right)^{0.61}$$

$$= 2.27\,(3.0)\,(1.00)\,(0.87) \left(\frac{4.0}{3.0}\right)^{0.43} \left(\frac{2.0}{\sqrt{9.81 \text{ x } 3.0}}\right)^{0.61}$$

$$= 3.6 \text{ m}$$

Proceed to Box 2-13.

Box 2-13: $Z_{max,l} = Z_{max,p} + Z_{max,c} + Z_{max,a}$

$= 1.8 + 5.3 + 3.6$

$= 10.7$ m

Proceed to Box 2-14

Box 2-14: The bridge is not underlain by a layered profile. Proceed to Box 2-18

Box 2-18: $Z_{thresh} = 10$ m. Proceed to Box 2-19.

Box 2-19: Z_{max} is greater than $Z_{thresh.}$ Proceed to Box 2-21.

Box 2-21: BSA 3 needs to be carried out.

6. BRIDGE SCOUR ASSESSMENT 3

6.1. INTRODUCTION

Bridge Scour Assessment 3 (BSA 3) is the assessment procedure that has to be carried out if a bridge is not found as "Minimal Risk (Regular Monitoring)" at the end of Bridge Scour Assessment 2 (BSA 2). BSA 3 involves the calculation of time dependent scour depth, which is the scour depth after a specified time rather than simply using the maximum scour depth. This method is valuable in the case of clays and rocks that have high erosion resistance (low erosion rate) and do not achieve the maximum scour depth as computed in BSA 2 within the lifetime of the bridge. The time dependent scour depth is termed the final scour depth, Z_{fin}. In BSA 3, the total final local scour depth at the bridge, termed the final local scour ($Z_{fin,l}$) is the arithmetic sum of the three components of scour., i.e. final pier scour ($Z_{fin,p}$), final contraction scour ($Z_{fin,c}$), and final abutment scour ($Z_{fin,a}$). Similar to BSA 2, the vulnerability associated with scour depends on the comparison between the total final scour depth, $Z_{fin,l}$ and the allowable scour depth of the bridge, Z_{thresh}.

6.2. THE BSA 3 FLOWCHART AND PROCEDURE

The BSA 3 flowchart is shown in Figure 6-1. The boxes in the flowchart are of three forms: rectangular, diamond, and rounded. Rectangular boxes are data collection and calculation boxes meaning that the data listed in the box needs to be collected by the

user for the bridge being analyzed and where appropriate, involve the use of equations. Diamond boxes are "Yes-No" decision boxes. Rounded boxes are conclusion boxes. All boxes are numbered for easy reference, where the first digit represents the BSA level and the second digit represents the box number.

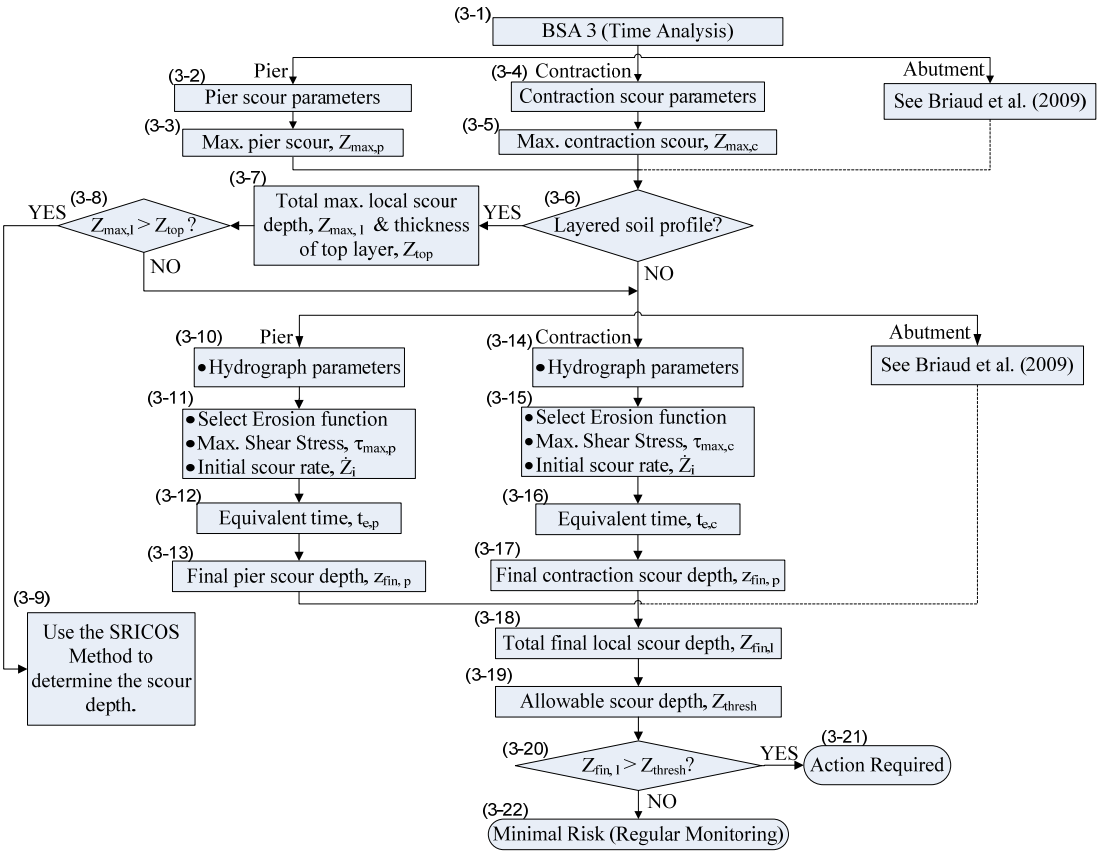

Figure 6-1. The BSA 3 (Time Analysis) flowchart.

In the BSA 3 analysis, the scour depth versus time is modeled as a hyperbola. Equation (2.3) and Equation (2.6) show the hyperbolic model for pier and contraction scour, respectively (Briaud, et al. 1999, 2005). These models have been described in Section 2 under the section on SRICOS methods for pier and contraction scour. Similar to the total maximum local scour depth in BSA 2, the time dependent scour local depth at the end of a specified time, termed the total final local scour depth, $Z_{fin,l}$ is summation of the final scour depths of the three components of time dependent scour:

$$Z_{fin,l} = Z_{fin,p} + Z_{fin,c} + Z_{fin,a} \tag{6.1}$$

where $Z_{fin,p}$, $Z_{fin,c}$ and $Z_{fin,a}$ are the pier scour, contraction scour and abutment scour after a specified time, respectively. The process of determining the time dependent abutment scour, $Z_{fin,a}$ is ongoing at Texas A&M University, under the leadership of Dr. Jean-Louis Briaud. The procedure to determine final abutment scour depth is being published as Briaud et al. (2009).

The first step in BSA 3 is the determination of the maximum scour depth of the various components of scour, i.e. pier scour, contraction scour and, abutment scour. The calculations could have been carried out in BSA 2. The calculations for maximum pier and contraction scour are described in Section 2 and detailed in Briaud et al. (1999, 2005). Calculations for abutment scour is being published as Briaud et al. (2009). If the geologic profile underlying the bridge is layered, the topmost layer is used in the calculation of maximum scour depth. If the total maximum scour depth based on the topmost layer extends beyond that layer, then the Extended SRICOS-EFA Method should be used to determine the time dependent scour depth (Briaud et al. 1999, 2005,

http://ceprofs.tamu.edu/briaud/research.html). Otherwise the BSA 3 (Time Analysis) is continued.

In the BSA 3 (Time Analysis), the hydrograph parameters, i.e. the duration of the hydrograph (t_{hyd}) and the maximum hydrograph velocity (V_{max}) are obtained to determine the equivalent time, as detailed in Section 2 and defined by Equation (2.7) and Equation (2.8). In addition to this, the initial rate of scour, $\dot{Z}_i$ is obtained from the appropriate erosion function selected from the Erodibility Charts (Figure 3-4 and Figure 3-5). The initial rate of scour, $\dot{Z}_i$ is the scour rate that corresponds to the approach velocity being considered. The total final pier and contraction scour depths ($Z_{fin,p}$ and $Z_{fin,c}$, respectively) are obtained using Equations (2.3) and Equation (2.6), respectively. If the final local scour depth, $Z_{fin,l}$ does not exceed the allowable scour depth, Z_{thresh}, the bridge is designated as "Minimal Risk" and should undergo regular monitoring. Otherwise immediate action is required.

6.3. STEP-BY-STEP PROCEDURE FOR BSA 3

To assist the user in carrying out a BSA 3 analysis, a table detailing all the steps of the method according to flowchart box number is presented (Table 6-1).

Table 6-1. Step-by–step procedure for BSA 3 (Time Analysis).

Box No.	Description
3-1	Introduction to BSA 3 (Time Analysis). Links BSA 2 to BSA 3.
3-2	The data collection box for parameters required to determine the maximum pier scour. These parameters are as follows: • Approach velocity, V_{appr} • Pier diameter, D • Kinematic viscosity of water, υ which is 10^{-6} m^2/s at 20º Celsius.
3-3	Calculation box for the maximum pier scour depth from Equation (2.2).
3-4	The data collection box for parameters required to determine the maximum contraction scour depth. These parameters are as follows: • Approach velocity, V_{appr} • The critical velocity, V_c which is the velocity corresponding to an erosion rate of 0.1 mm/hr on the erosion function. The erosion function can be taken as the left boundary of the erosion category that best describes the geomaterial underlying the bridge site. • Upstream water depth, H_1 • Uncontracted channel width, B_1 • Contracted channel width, B_2
3-5	Calculation box for the maximum contraction scour depth from Equation (2.4).
3-6	Decision box to determine wether the bridge site is underlain by a layered geologic profile. If yes, the maximum local scour depth $Z_{max,l}$ is compared with the thickness of the topmost layer, Z_{top} in Box 3.8.
3-7	The calculation box for the maximum local scour depth, $Z_{max,l}$ and input for the thickness of the topmost geomaterial layer underlying the bridge site, Z_{top}.
3-8	Decision box to determine if the maximum local scour depth $Z_{max,l}$ is greater than the thickness of the topmost geomaterial layer layer, $Z_{top.}$ If yes, the SRICOS Method needs to be used (Briaud et al. 2003).
3-9	Lead to the SRICOS Method (Briaud et al. 2003).
3-10	The collection box for hydrograph parameters. These parameters are as follows: • Hydrograph duration, t_{hdr} • Maximum velocity appearing in the hydrograph, V_{appr}

Table 6.1. Continued.

Box No.	Description
3-11	The box for determination of the initial scour rate, $\dot{Z}_i$ that is to be used in computing the equivalent time for pier scour, $t_{e,p}$ (Equation (2.7)). This is done by carrying out the following steps: • Select the erosion function for the material underlying the bridge site using the Erosion Function Chart (Figure 3-4). The erosion function can be taken as the left boundary of the erosion category that best describes the geomaterial underlying the bridge site. • Get the erosion rate corresponding to the maximum hydrograph velocity, V_{appr} (or V_{max}) on the selected erosion function. This erosion rate is the initial scour rate, $\dot{Z}_i$.
3-12	Box for the computation of the equivalent time for pier scour $t_{e,p}$ using Equation (2.7).
3-13	The box for determination of the final pier scour depth $Z_{fin,p}$ using the hyperbolic model (Equation (2.3)).
3-14	Collection of hydrograph parameters. This box is identical to Box 3-10.
3-15	The box for the determination of the initial scour rate, $\dot{Z}_i$ that is to be used in computing the equivalent time for contraction scour, $t_{e,c}$ (Equation (2.8)). The steps to determine $\dot{Z}_i$ here are the same as the steps to determine $\dot{Z}_i$ in Box 3-11.
3-16	Box for the computation of the equivalent time for contraction scour $t_{e,c}$ using Equation (2.8).
3-17	Box for the determination of the final contraction scour depth $Z_{fin,c}$ using the hyperbolic model (Equation (2.6)).
3-18	The determination of the total final scour depth, $Z_{fin,l}$. The total final scour depth is given by Equation (6.1).
3-19	Box for the input of allowable scour depth, Z_{thresh}. This is based on the foundation element being considered.
3-20	The decision box to determine if the bridge is can be classified as having low scour risk or requires action against scour damage. This is done by comparing the values of total final local scour depth $Z_{fin,l}$ against the allowable scour depth, Z_{thresh}. If $Z_{fin,l}$ is greater than Z_{thresh}, the bridge is classified as "Action Required." Otherwise, the bridge is classified as "Minimal Risk" and should undergo regular monitoring.
3-21	Box indicating that the bridge is susceptible to scour related damage and requires immediate action.
3-22	Box indicating that the bridge is deemed as having low scour risk and should undergo regular bridge scour monitoring.

6.4. EXAMPLE OF BSA 3 ANALYSIS

Problem: Determine the maximum scour depth corresponding to the following information that characterizes the bridge scour problem.

- Geomaterial Type: Uniform Medium Erodibility material (Category III)
- Contraction ratio $R_c = 0.85$, upstream water depth $H_1 = 10$ m
- Pier Diameter D = 1.0 m
- Maximum hydrograph velocity $V_{max} = 2.0$ m/s
- Kinematic viscosity of water at 20˚C, $\upsilon = 10^{-6}$ m^2/s
- Allowable scour depth $Z_{thresh} = 6.0$ m
- Age of the bridge $t_{hyd} = 25$ years

Solution according to BSA 3 Flowchart Box numbers:

Box 3-1: Start of BSA 3. Proceed to Box 3-2.

Box 3-2: Pier scour parameters.

$D = 1.0$ m, $V_{appr} = 2.0$ m/s, $\upsilon = 10^{-6}$ m^2/s

Proceed to Box 3-3

Box 3-3:
$$Z_{max,p}(\text{mm}) = 0.18\left(\frac{V_{appr}\, D}{\nu}\right)^{0.635}$$

$$= 1804.8$$

$$Z_{max,p}(\text{m}) = 1.8$$

Proceed to Box 3-4.

Box 3-4: Contraction scour parameters.

$R_c = 0.85$, $H_1 = 10.0$ m, $V_{appr} = 2.0$ m/s, $V_c = 0.5$ m/s

Proceed to Box 3-5.

Box 3-5: $$Z_{max,c} = 1.9H_1\left[\frac{1.38V_{appr}}{R_C\sqrt{gH_1}} - \frac{V_c}{\sqrt{gH_1}}\right]$$

$$= 1.9(10.0)\left[\frac{1.38(2.0)}{0.85\sqrt{9.81 \text{ x } 10.0}} - \frac{0.5}{\sqrt{9.81 \text{ x } 10.0}}\right]$$

$$= 5.3 \text{ m}$$

Proceed to Box 3-6.

Box 3-6: The bridge is founded on a uniform profile. Proceed to Box 3-10.

Box 3-10: Hydrograph Parameters.

$V_{max} = V_{appr} = 2$ m/s, $t_{hyd} = 25$ yrs.

Proceed to Box 3-11

Box 3-11: From Figure 3-4, $\dot{Z}_i$ corresponding to V_{max} = 2.0 m/s is 150 mm/hr.

Proceed to Box 3-12.

Box 3-12: $$t_{e,p}(\text{hrs}) = 73\left[t_{hyd}(\text{years})\right]^{0.126}\left[V_{max}(\text{m/s})\right]^{1.706}\left[\dot{Z}_i(\text{mm/hr})\right]^{-0.20}$$

$$= 73[25]^{0.126}[2.0]^{1.706}[150]^{-0.20}$$
$$= 131.16 \text{hrs}$$

Proceed to Box 3-13.

Box 3-13: $$Z_{fin,p} = \frac{t_{eq,p}}{\frac{1}{Z_i} + \frac{t_{eq,p}}{Z_{max,p}}}$$

$$= \frac{131.16}{\frac{1}{(150/1000)} + \frac{131.16}{1.8}}$$

$$= 1.6 \text{ m}$$

Proceed to Box 3-14.

Box 3-14: Same as Box 3-10. Proceed to Box 3-15.

Box 3-15: Same as Box 3-11. Proceed to Box 3-16.

Box 3-16: $t_{eq,c}\,(\text{hrs}) = 644.32\,[t_{hyd}\,(\text{yrs})]^{0.4242}\,[V_{max}\,(\text{m/s})]^{1.648}\,[\dot{Z}_i\,(\text{mm/hr})]^{-0.605}$

$$= 644.32[25]^{0.4242}[2.0]^{1.648}[150]^{-0.605}$$
$$= 381.7 \text{ hrs}$$

Proceed to Box 3-17.

Box 3-17: $$Z_{fin,c} = \frac{t_{eq,c}}{\frac{1}{Z_i} + \frac{t_{eq,c}}{Z_{max,c}}}$$

$$= \frac{381.7}{\frac{1}{(150/1000)} + \frac{381.7}{5.3}}$$
$$= 4.9 \text{ m}$$

Proceed To Box 3-18.

Box 3-18: $$Z_{fin,l} = Z_{fin,p} + Z_{fin,c}$$

$$= 1.6 + 4.9$$

$$= 6.5 \text{ m}$$

Proceed To Box 3-19.

Box 3-19: $Z_{thresh} = 6.0$ m. Proceed to Box 3-20

Box 3-20: $Z_{fin,l}$ is greater than Z_{thresh}. Proceed to Box 3-21.

Box 3-21: Immediate action is required at this bridge to mitigate scour related failure.

7. CASE HISTORIES AND VALIDATION

7.1. INTRODUCTION

In order to develop and validate the simplified method for estimating scour, 11 case histories in Texas were chosen. These cases were used to develop and validate the procedures in BSA 1, 2 and 3. The collection of the data for the case histories was carried out by contacting the relevant Texas Department of Transportation (TxDOT) district offices to obtain copies of the bridge folders maintained by TxDOT. These bridge folders contain bridge foundation information, scour measurements and soil information. However, the extent of the information and its clarity varies from folder to folder due to the fact that the bridges can be quite old (up to approximately 80 years old) and that the practice of performing bridge scour measurements was not routine before the early nineties.

7.2. CRITERIA FOR SELECTION

There are several criteria that were identified to make a bridge suitable as a case history for the validation process. In order to develop a set of case histories that was suitable, it was essential to obtain cases that covered the widest variety of conditions, i.e. soil types, foundation types, location within the state of Texas and scour status. However, there were limitations in some of the cases where there was inadequate availability of data.
The general criteria for selection are based on the following items:

1. Channel profile measurement records
2. Flow data

3. Soil information
4. Foundation information
5. Current scour status

7.3. THE BRIDGES SELECTED AS CASE HISTORIES

7.3.1. Overview and Location

Figure 7-1 shows the locations of these bridges on the map of Texas. Table 7-1 summarizes the 11 bridges selected for validation. Out of the 11 bridges selected for validation, 10 are scour critical, and the remaining 1 is stable for calculated scour conditions. Data on the 11 case histories are presented in detail in Appendix C which also includes cross-section drawings of the bridges.

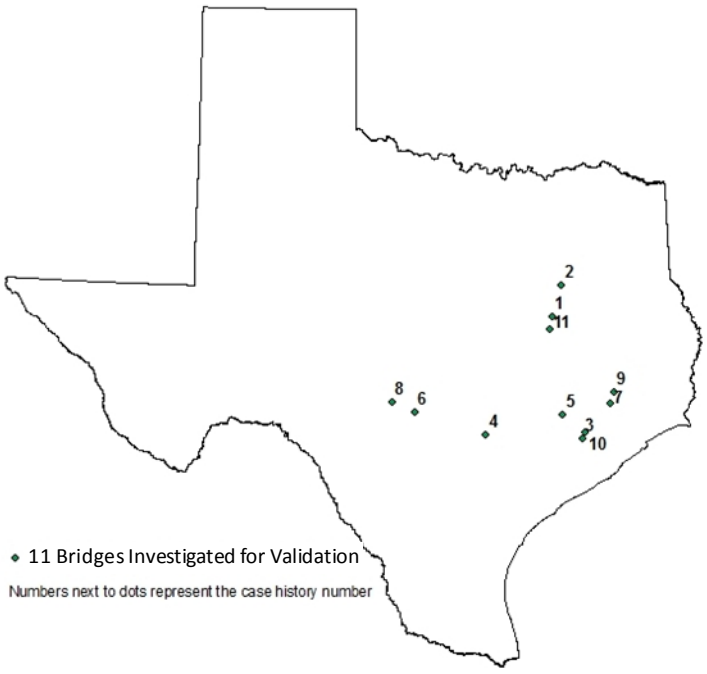

Figure 7-1. Location of the 11 case histories selected for validation.

Table 7-1. Summary of the 11 case histories selected for validation.

No.	Latitude	Longitude	Waterway	Highway	Scour Status	EFA Test Data Status	Flow Data Status
1	31.47056308	-96.29239209	Sanders Creek	FM39	Critical	Available	Not Available
2	31.97030066	-96.08752535	Alligator Creek	US287	Critical	Available	Not Available
3	29.47641599	-95.81304823	Big Creek	SH36	Critical	Not Available	Available
4	29.59232540	-97.58796201	San Marcos River	FM2091	Critical	Not Available	Available
5	29.86972042	-96.15511481	Mill Creek	FM331	Critical	Not Available	Available
6	29.96498001	-98.89669924	Guadalupe River	US87	Critical	Not Available	Available
7	30.02640843	-95.25897002	San Jacinto River	US59SB	Critical	Not Available	Available
8	30.13653693	-99.31566628	Dry Branch Creek	SH27	Critical	Not Available	Available
9	30.20833445	-95.18168475	Peach Creek	US59 @ Creekwood Dr.	Critical	Not Available	Available
10	29.58279722	-95.75768056	Brazos River	US90A (WB)	Critical	Available	Available
11	31.25425278000	-96.33052778	Navasota River	SH7	Stable	Available	Available

7.3.2. Case by Case Description of Bridges

The general description of the bridges, such as the the number of spans, foundation type and geomaterials underlying the bridge site are given in this section. As mentioned above, more detailed information on the bridges is given in Appendix C.

7.3.2.1. Case History No. 1: Bridge on Highway FM 39 Crossing Sanders Creek

This bridge is located in Limestone County within the Waco district in Texas. The TxDOT structure number for this bridge is 0643-02-038. The bridge is on Highway FM 39 and crosses Sanders Creek. The bridge was built in 1977 and has a length of 316 ft. It has 6 spans and is founded on 2.5 ft diameter drilled shafts that vary between 15 ft to 22.5 ft in length. The drilled shafts are embedded mainly in sand and silty sand. This bridge has been deemed scour critical by a concise analysis. This case history does not have flow records but does have site-specific EFA test data.

7.3.2.2. Case History No. 2: Bridge on Highway US 287 Crossing Alligator Creek

This bridge is located in Freestone County within the Bryan district in Texas. The TxDOT structure number for this bridge is 0122-03-036. The bridge is on Highway US 287 and crosses Alligator Creek. The bridge was built in 1984 and has a length of 292 ft. It has 7 spans and is founded on 2 ft diameter drilled shafts that have a minimum length of 24 ft. The soil at the site is clay and sand. This bridge has been deemed scour critical by a concise analysis. This case history does not have flow records but does have site-specific EFA test data.

7.3.2.3. Case History No. 3: Bridge on Highway SH 36 Crossing Big Creek

This bridge is located in Fort Bend County within the Houston district in Texas. The TxDOT structure number for this bridge is 0188-02-023. The bridge is on Highway SH 36 and crosses Big Creek. The bridge was built in 1932 and has a length of 257 feet. It has 9 spans and is founded on 14 inch concrete piles that vary between 25 ft to 35 ft in

length. The soil at the site is a deep sand deposit, extending beyond 40 ft below the channel bottom. This bridge is stable in terms of scour. This case history has flow records but does not have site-specific EFA test data.

7.3.2.4. Case History No. 4: Bridge on Highway FM 2091 Crossing San Marcos River

This bridge is located in Gonzales County within the Yoakum district in Texas. The TxDOT structure number for this bridge is 2080-01-005. The bridge is on Highway FM 2091 and crosses the San Marcos River. The bridge was built in 1960 and has a length of 382 feet. It has 6 spans and is founded on 15-inch wide, 32 ft long precast concrete piles and 14-inch wide, 33 ft long steel H-piles. The soil at the site is clay and sand. This bridge is on the scour critical list. This case history has flow records but does not have site-specific EFA test data.

7.3.2.5. Case History No. 5: Bridge on Highway FM 331 Crossing Mill Creek

This bridge is located in Austin County within the Austin district in Texas. The TxDOT structure number for this bridge is 0408-05-019. The bridge is on Highway FM 331 and crosses Mill Creek. The bridge was built in 1951 and has a length of 271 feet. It has 6 spans and is founded on 18 inch wide precast concrete piles with a minimum length of 20 ft. The soil at the site is clay and silty sand. This bridge has been deemed scour critical by a concise analysis. This case history has flow records but does not have site-specific EFA test data.

7.3.2.6. Case History No. 6: Bridge on Highway US 87 Crossing Guadalupe River

This bridge is located in Kendall County within the San Antonio district in Texas. The TxDOT structure number for this bridge is 0072-04-020. The bridge is on Highway US 87 and crosses the Guadalupe River. The bridge was built in 1932 and has a length of 1434 feet. It has 34 spans and is founded on 16 inch wide concrete square piles that are vary between 36 ft to 50 ft in length. The bridge was widened in 1984, where the widened section is on 6 ft diameter drilled shafts that are approximately 17 ft long. The soil at the site is clay and sandy gravel. This bridge has been deemed scour critical by a concise analysis. This case history has flow records but does not have site-specific EFA test data.

7.3.2.7. Case History No. 7: Bridge on Highway US 59(SB) Crossing West Fork San Jacinto River

This bridge is located in Harris County within the Houston district in Texas. The TxDOT structure number for this bridge is 0177-06-081. The bridge is on Highway US 59(SB) and crosses the West Fork San Jacinto River. The bridge was built in 1961 and has a length of 1645 feet. It is founded on 16 inch square concrete piles with a minimum length of 10 ft. The soil at the site is sand. This bridge has been deemed scour critical by a concise analysis. This case history has flow records but does not have site-specific EFA test data.

7.3.2.8. Case History No. 8: Bridge on Highway SH 27 Crossing Dry Branch Creek

This bridge is located in Kerr County within the San Antonio district in Texas. The TxDOT structure number for this bridge is 0142-03-008. The bridge is on Highway SH 27 and crosses Dry Branch Creek. The bridge was built in 1935 and has a length of 142 feet. It has 5 spans and is founded on spread footings that are embedded approximately between 10 ft to 15 ft bellow the channel bottom. The bridge was widened in 1963 where the widened section is on 2 ft diameter drilled shafts that are approximately 15 ft long. The soil at the site is clay, shale and limestone. This bridge has been deemed scour critical by a concise analysis. This case history has flow records but does not have site-specific EFA test data.

7.3.2.9. Case History No. 9: Bridge on Highway US 59 at Creekwood Drive Crossing Peach Creek

This bridge is located in Montgomery County within the Houston district in Texas. The TxDOT structure number for this bridge is 170-0177-05-119. The bridge is on Highway US 59 at Creekwood Drive and crosses Peach Creek. The bridge was built in 1970 and has a length of 120 feet. It has 3 spans and is founded on 16 inch wide, approximately 35 ft long square piles. The soil at the site is sand. This bridge has been deemed scour critical by a concise analysis. This case history has flow records but does not have site-specific EFA test data.

7.3.2.10. Case History No. 10: Bridge on Highway US 90A (WB) Crossing Brazos River

This bridge is located in the Houston district in Texas. The TxDOT structure number for this bridge is 0027-08-092. The bridge is on Highway US 90A (WB) and crosses the Brazos River. The bridge was built in 1965 and has a length of 942 feet. It has 10 spans and is founded on 16 inch to 20 inch square piles. The pile lengths vary between 70 ft to 78 ft. The soil at the site is silty sand and clayey sand. This bridge has been deemed scour critical by a concise analysis. This case history has both flow records and site-specific EFA test data.

7.3.2.11. Case History No. 11: Bridge on Highway SH 7 Crossing Navasota River

This bridge is located in Leon County within the Bryan district in Texas. The TxDOT structure number for this bridge is 0382-05-021. The bridge is on Highway SH7 and crosses the Navasota River. The bridge was built in 1956 and has a length of 271 feet. It has 7 spans and is founded on 14 inch wide concrete piles that vary between 28 ft to 50 ft in length. The soil at the site is sand. This bridge has been deemed stable by a concise analysis. This case history has both flow records and site-specific EFA test data.

7.4. VALIDATION OF THE SIMPLIFIED METHOD

7.4.1. Validation of BSA 1

The validation of BSA 1 is aimed at evaluating how well results of the proposed BSA 1 method match actual field measurements. This is carried out by using both flow records

and scour measurements at a particular case history bridge. In this investigation, 9 bridge case histories were selected for validation. These are the case histories that have flow records. In order to carry out a meaningful validation, actual flow records recorded by a suitable flow gage were used. The validation process is summarized as follows:

1. The validation procedure starts at the time the first scour measurement was taken at a particular case history bridge. This time is called T_1 and could represent a particular date, for example August 21, 1952 or even a year, say 1952.

2. From the measured velocity time history, the maximum flow velocity experienced by the bridge until T_1, termed V_{mo1} is obtained. The scour depth measured at the bridge, Z_{mo1} at time T_1 is obtained from bridge inspection records.

3. A "mock" scour prediction is made at T_1 for a future flood event with velocity V_{fut1} over the next scour measurement interval time, t_{meas1}. It is required that there be actual scour measurements taken at the bridge site at time $T_1 + t_{meas1}$. V_{fut1} is the maximum velocity obtained between T_1 and $T_1 + t_{meas1}$.

4. The Z-Future chart is then used to obtain the scour depth ratio Z_{fut}/Z_{mo} by using the velocity ratio V_{fut}/V_{mo}. In this case, Z_{mo} is Z_{mo1}, V_{fut} is V_{fut1} and V_{mo} is V_{mo1}. Z_{fut} is obtained using equation 5.1. This Z_{fut} is termed $Z_{fut,predict1}$. Then, $Z_{fut,predict1}$ is compared with the actual measured scour depth, $Z_{fut,meas1}$.

5. The process is continued by replacing T_1 with $T_2 = T_1 + t_{meas1}$. T_2 is the time when the next scour measurement was taken at the bridge.

6. From the measured velocity time history, the maximum flow velocity experienced by the bridge until T_2, V_{mo2} is obtained. The scour depth measured at the bridge, Z_{mo2} at time T_2 is obtained from bridge inspection records.

7. A "mock" scour prediction is made at T_2 for a future flood event with velocity V_{fut2} over the next scour measurement interval time, t_{meas2}. It is required that there be actual scour measurements taken at the bridge site at time $T_2 + t_{meas2}$. V_{fut2} is the maximum velocity obtained between T_2 and $T_2 + t_{meas2}$.

8. The Z-Future chart is then used to obtain the scour depth ratio Z_{fut}/Z_{mo} by plugging in the velocity ratio V_{fut}/V_{mo}. In this case, Z_{mo} is Z_{mo2}, V_{fut} is V_{fut2} and V_{mo} is V_{max2}. Z_{fut} is obtained using equation 5.1. This Z_{fut} is now termed $Z_{fut,predict2}$. Then, $Z_{fut,predict2}$ is compared with the actual measured scour depth, $Z_{fut,meas2}$.

9. Steps 1 through 4 are repeated for the remaining bridge inspection records.

The validation process might yield one or more sets of predicted and measured scour depth for each of the selected bridge case histories. The bridge records had limited bridge scour measurements. In fact, there were no bridge scour measurements taken before the year 1991. Because most of the bridges were reasonably old, they had experienced the largest flow velocity prior to the first bridge scour measurement. This resulted in all the cases having a V_{fut}/V_{mo} ratio of equal or less than unity. Results of the validation are shown in Figure 7-2 where they are plotted against the equal value line. Figure 7-2 shows a good agreement between the two values. However, it should be noted that this validation is only for V_{fut}/V_{mo} ratios equal or less than unity.

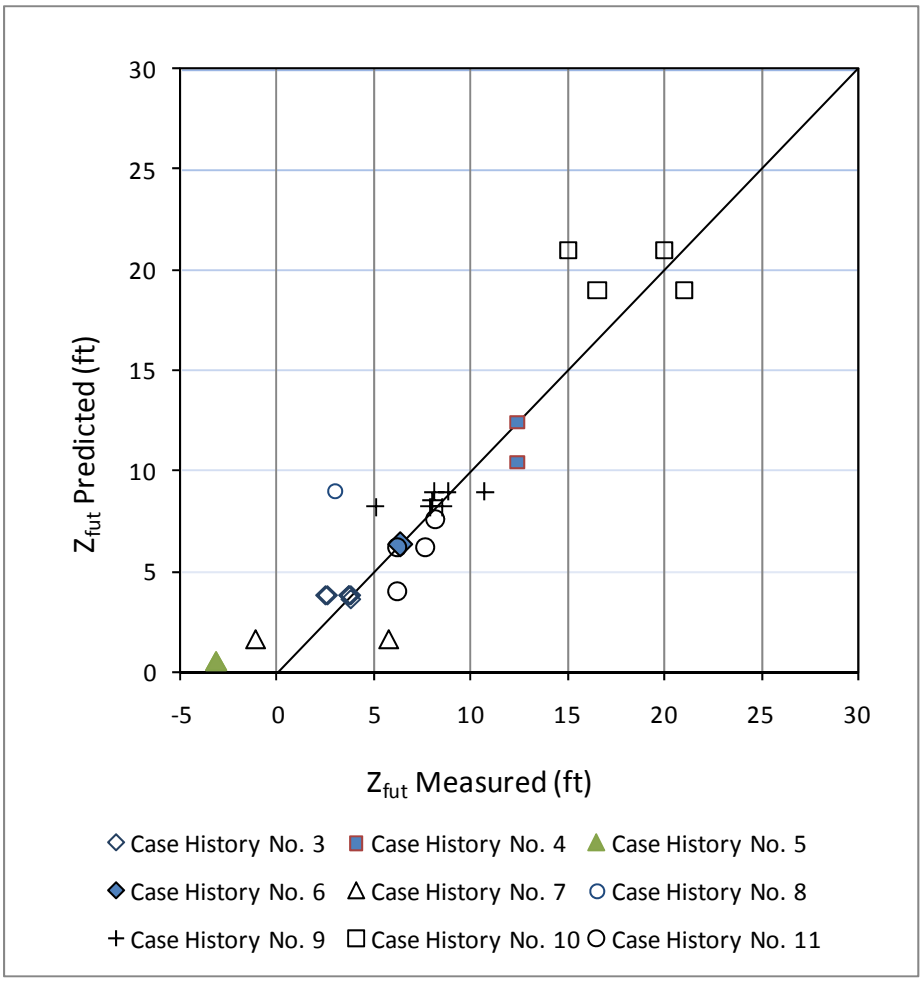

Figure 7-2. Comparison between Z_{fut} values predicted by BSA 1 and corresponding field measurements.

7.4.2. Validation of BSA 2

The validation of BSA 2 is aimed at comparing the maximum scour depth predicted by this method and maximum scour depths obtained by the SRICOS-EFA method. For validating BSA 2, 3 case histories were selected. The flow velocity corresponding to the 100-year flood was used as the input velocity to obtain the maximum scour depth. The 100-year flood is obtained based on flow records until the most recent scour depth measurements carried out and recorded in the case history bridge folders. The three case histories are ones that have EFA test data.

First, the maximum pier and contraction scour depths are computed using Equation (2.2) and Equation (2.4). The EFA data is used to obtain the critical velocity of the geomaterial underlying the bridge site. The critical velocity is a required input in Equation (2.4). The total maximum scour depth is the sum of the maximum pier and contraction scour. The total maximum scour depth using the EFA data is termed $Z_{max,l\text{-}EFA.}$

Subsequently, the maximum scour depth is obtained using BSA 2. In this case, the only difference is the critical velocity used in Equation (2.4) which instead is obtained from the Erosion Function Charts for the material concerned. The critical velocities are obtained from the mean of the EFA test data on CL, CH, and SC soils (Figure 3-6, Figure 3-7, and Figure 3-11). The maximum scour depth using BSA 2 is termed $Z_{max,l\text{-}BSA2.}$ The values of $Z_{max,l\text{-}EFA}$ and $Z_{max,l\text{-}BSA2}$ were then compared with each other for the 3 case histories. To investigate the outcome of both methods, the input

parameters for the calculations of maximum scour depth were varied as indicated below, resulting in 144 data sets:

1. Approach velocity, V_{appr} = 0.5 m/s and 3.5 m/s
2. Upstream water depth, H_1 = 10 m and 20 m
3. Pier diameter, D = 0.1 m, 1.0 m and 10 m
4. Contraction ratio, R_c = 0.5 and 0.9

Figure 7-3 shows the comparison between $Z_{max,l\text{-}EFA}$ and $Z_{max,l\text{-}BSA2}$ against the equal value line. The calculation results are presented in Appendix C. This validation exercise shows a good agreement between both methods.

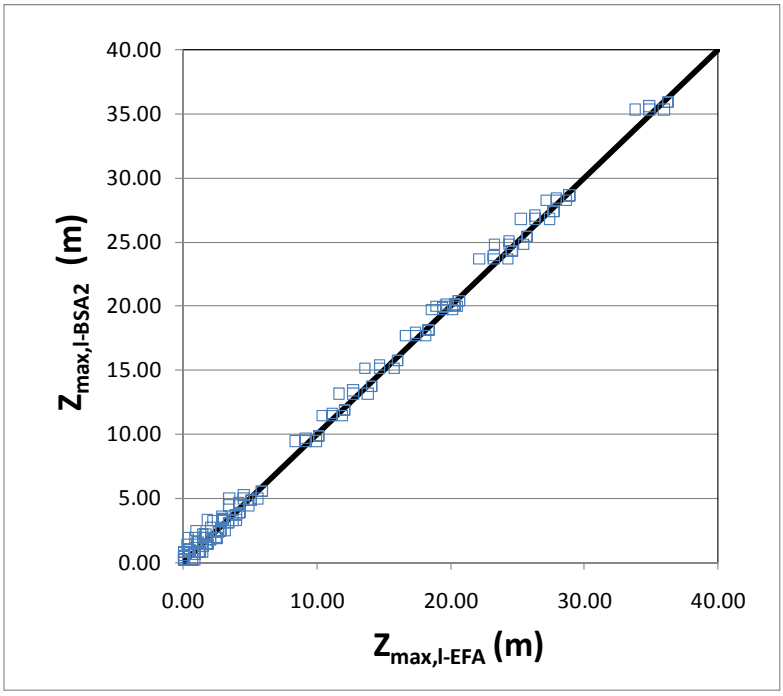

Figure 7-3. Comparison of maximum scour depth obtained using EFA test data and the Erosion Function Chart.

7.4.3. Validation of BSA 3

The validation of BSA 3 is aimed at comparing the time dependent scour depth, Z_{fin} predicted by this method and bridge scour measurements. Only 3 case histories were validated for BSA 3. This was because out of the 11 case histories, only 3 cases had flow data and all the available parameters for BSA 3 analysis. Table 7-2 shows the results of the BSA 3 validation.

Table 7-2. Results of BSA 3 validation.

Case History No.	Z_{max} (ft) (from BSA 2)	Z_{BSA3} (ft) (final scour depth)	$Z_{measured}$ (ft)
3	12.7	11.0	3.6
7	30.7	29.0	5.7
11	24.5	20.5	13.6

The validation results show that BSA 3 tends to overestimate the scour depth. This could be due to the fact that there are only 3 data points (3 cases). In addition to this, the poor agreement between the predicted and measured values could be due to some unknown conditions in the field. However, BSA 3 produces scour depths that are approximately 2 ft to 4 ft lower than the maximum scour depth, Z_{max}.

7.5. SCHOHARIE CREEK REVISITED

As a supplement to the 11 case histories, the Schoharie Creek Bridge failure in 1987 was investigated (Figure 7-4). The bridge was a 5-span, 540 ft long highway bridge over the Schoharie Creek in Montgomery County near Amsterdam, New York (National Transportation Safety Board or NTSB, 1987). The bridge was built in 1954 and was

founded on spread footings that were approximately 19 ft wide and 5 ft thick. On April 5th, 1987 one of the piers of the bridge, (Pier 3) collapsed, causing two spans of the bridge to plunge into the creek (Figure 7-5). This was followed by the collapse of an adjacent pier (Pier 2). The failure of this bridge caused the deaths of 10 people. The cause of the failure was attributed to scour (NTSB 1987, Resource Consultants and Colorado State University, 1987, Wiss, Janney, Elstner Associates and Mueser Rutledge Consulting Engineers, 1987).

Figure 7-4. The 1987 Schoharie Creek Bridge failure.

Figure 7-5. One of the Schoharie Creek Bridge spans plunging into the river.

The bridge experienced its largest flood in 1955. The second largest flood was the flood that took place in 1987 during the failure of the bridge. According to the NTSB (1987), the magnitudes of both floods (peak) were $Q_{peak,1955} = 73{,}600$ cfs and $Q_{peak,1987} = 62{,}100$ cfs, respectively. The flow velocities at Pier 3 were obtained from the one-dimensional flow computer model, Water-Surface PROfile Computations (WSPRO) developed by USGS. The computer simulations were carried out by Resource Consultants, Inc. and presented in NTSB (1987) as follows:

Table 7-3. Peak discharge versus WSPRO mean velocity at Schoharie Creek Pier 3 (after NTSB 1987).

Peak discharge (cfs)	WSPRO mean velocity (ft/s)
10,000	3.6
20,000	5.5
30,000	7.0
40,000	8.2
50,000	9.4
60,000	10.3

The flow-velocity data shown in Table 7-3 was plotted and shown in Figure 7-6. A regression was performed on the data to obtain the flow-velocity relationship. The regression produced an R^2 value of 0.99. Using the relationship shown in Figure 7-6, the flow values $Q_{peak,1955} = 73{,}600$ cfs and $Q_{peak,1987} = 62{,}100$ cfs translate into velocities $V_{peak,1955} = 3.6$ m/s and $V_{peak,1987} = 3.2$ m/s, respectively.

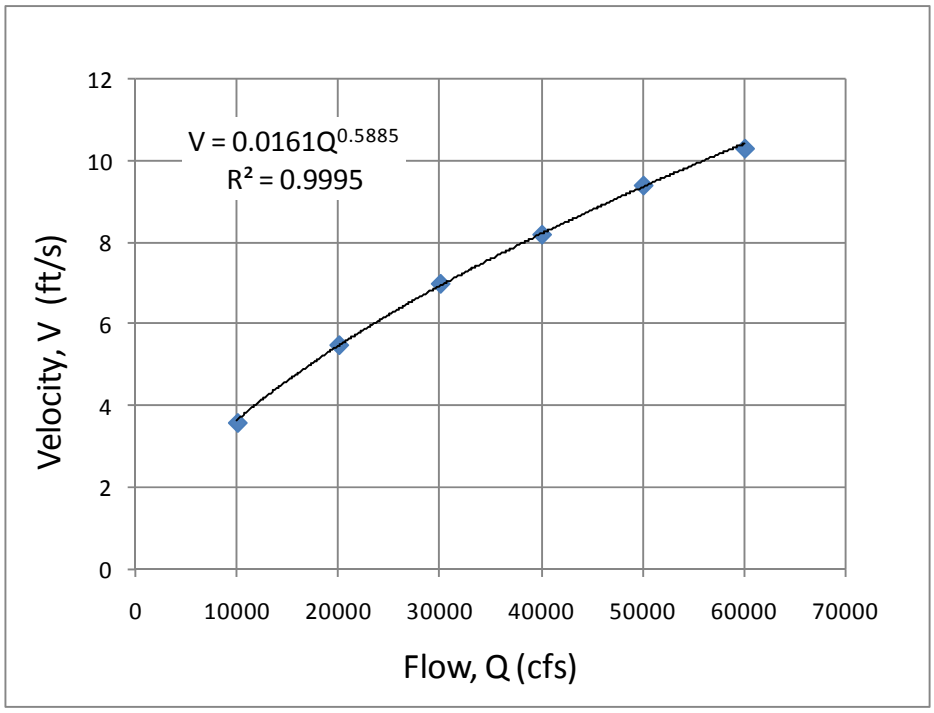

Figure 7-6. Flow-velocity relationship for Schoharie Creek Pier 3.

Prior investigations into the failure revealed that riprap was placed at the bridge piers prior to 1955 as protection against scour. NTSB (1987) states that "At Piers 2 and 3, riprap was installed from bottom of footing (elevation 270 ft) sloping to elevation 279.5 ft prior to the 1955 flood. Therefore, at Pier 3 the thickness of the riprap was approximately 9.5 ft (Figure 7-7). Photos taken on October 30th 1956 showed riprap movement at Piers 2 and 3. Various photographs taken from 1954 to 1977 during low water showed that some of the rocks had moved northward (downstream) during that time. Photographic analysis of Pier 2 (aided by computers) confirms the downstream movement of rock at Pier 2 from 1954 to 1977." Figure 7-8, Figure 7-9, and Figure 7-10

show photos of Pier 2 taken in 1956, 1977, and 1987. Figure 7-11 shows a photo of Pier 3 taken in 1987 after the failure of the bridge.

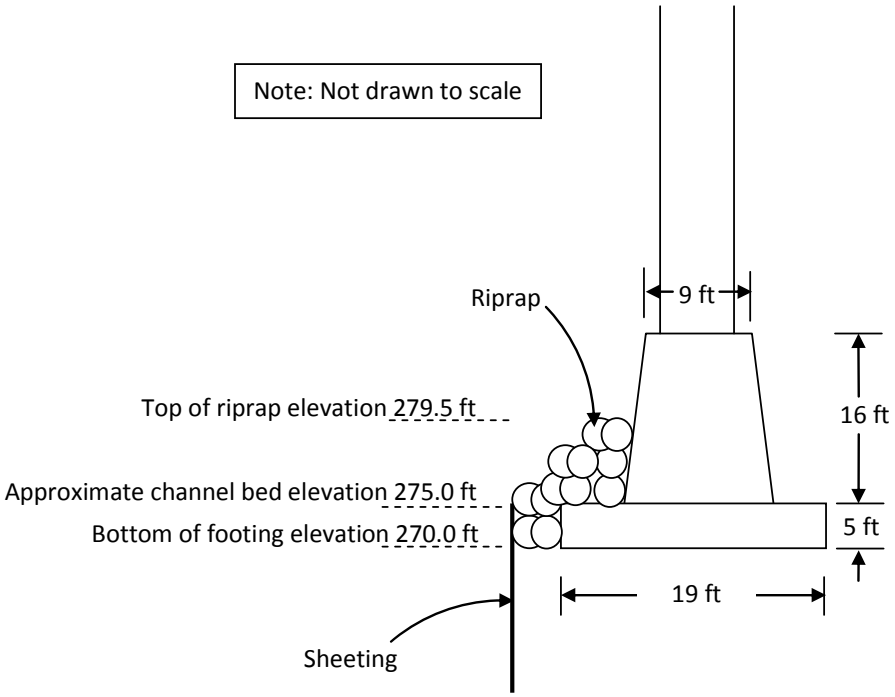

Figure 7-7. Schoharie Creek Pier 3 (after NTSB 1987).

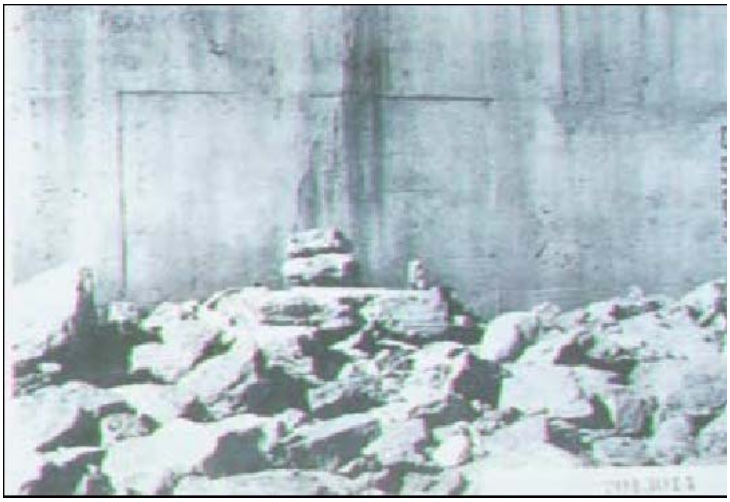

Figure 7-8. Photo of Pier 2 taken in 1956.

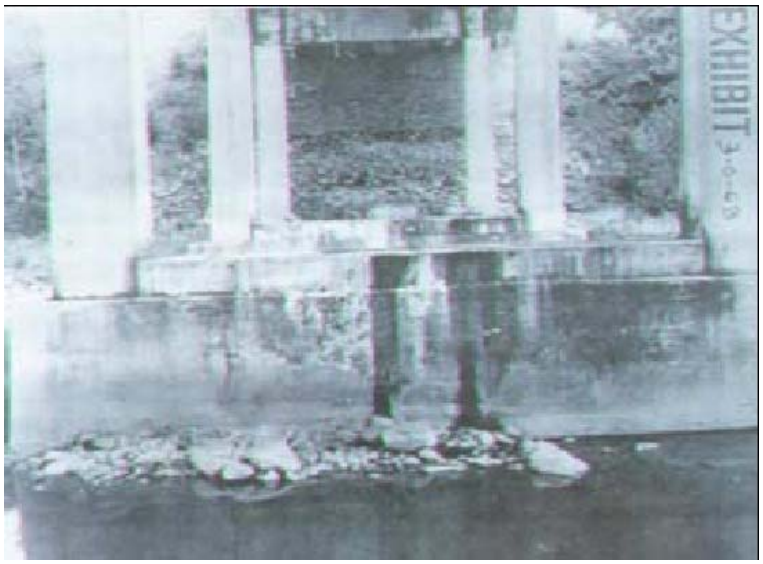

Figure 7-9. Photo of Pier 2 taken in 1977.

Figure 7-10. Photo of Pier 2 taken in 1987 after the failure.

Figure 7-11. Photo of Pier 3 taken in 1987 after the failure.

Regarding the riprap placed at the bridge prior to the 1955 flood, NTSB (1987) states that, "The only riprap dimensions specified in the bridge plans should be a minimum thickness of 8 inches and a maximum thickness of 15 inches. The plans also call for the riprap to be an Item 80 riprap according to the New York Department of Public Works (DPW) specifications. An Item 80 riprap should have at least 50% of the stones weighing in excess of 300 lbs each."

According to the Erosion Threshold Chart (Figure 3-18), for D_{50} = 8 inches = 203 mm,

$$V_c(\text{m/s}) = 0.35[D_{50}(\text{mm})]^{0.45}$$
$$= 0.35(203)^{0.45}$$
$$= 3.8\text{m/s}$$

For a DPW Item 80 riprap, assuming the weight of a spherical piece of riprap with a diameter D_{50} = 300 lbs and it's specific gravity S_g=2.65,

$$\text{Weight (lbs)} = \text{Density(lb/ft}^3\text{)} \times \text{Volume(ft}^3\text{)}$$
$$300 \text{ lbs} = 2.65 \times 62.4(\text{lb/ft}^3) \times \frac{4}{3}\pi\left(\frac{D_{50}}{2}\right)^3$$
$$D_{50} = 2.4\text{ft} = 731 \text{ mm}$$

Again from the Erosion Threshold Chart,

$$V_c(\text{m/s}) = 0.35[D_{50}(\text{mm})]^{0.45}$$
$$= 0.35(731)^{0.45}$$
$$= 6.8 \text{ m/s}$$

However, since the NTSB (1987) states that "field observations and photographs indeed showed movement of riprap between 1954 to 1977, the critical velocity, V_c of the riprap should be less than 3.6 m/s, which is the largest flood velocity experienced at the Schoharie Creek bridge." It goes on to state that, "it is evident that there was riprap movement between 1956 and 1977." The maximum flow between 1956 and 1977 was 40,400 cfs (NTSB 1987), which corresponds to an approach velocity of 8.3 ft/s or 2.5 m/s. Therefore, it is reasonable to assume that the critical velocity of the riprap should be below 1.5 times the approach velocity, 3.75 m/s. This is the local velocityr at

the pier and is given by Equation (5.1). Taking V_c of the riprap as 3.5 m/s (below 3.75 m/s), we take the upper boundary of a Category V material as the erosion function of the riprap. This is shown in the Figure 7-12. According to Resource Consultants and Colorado State University (1987), V_c of the glacial till = 4.9 f/s = 1.5 m/s. The upper boundary of a Category IV material is translated to the right so that the critical velocity corresponds to the critical velocity of the glacial till (Figure 7-12).

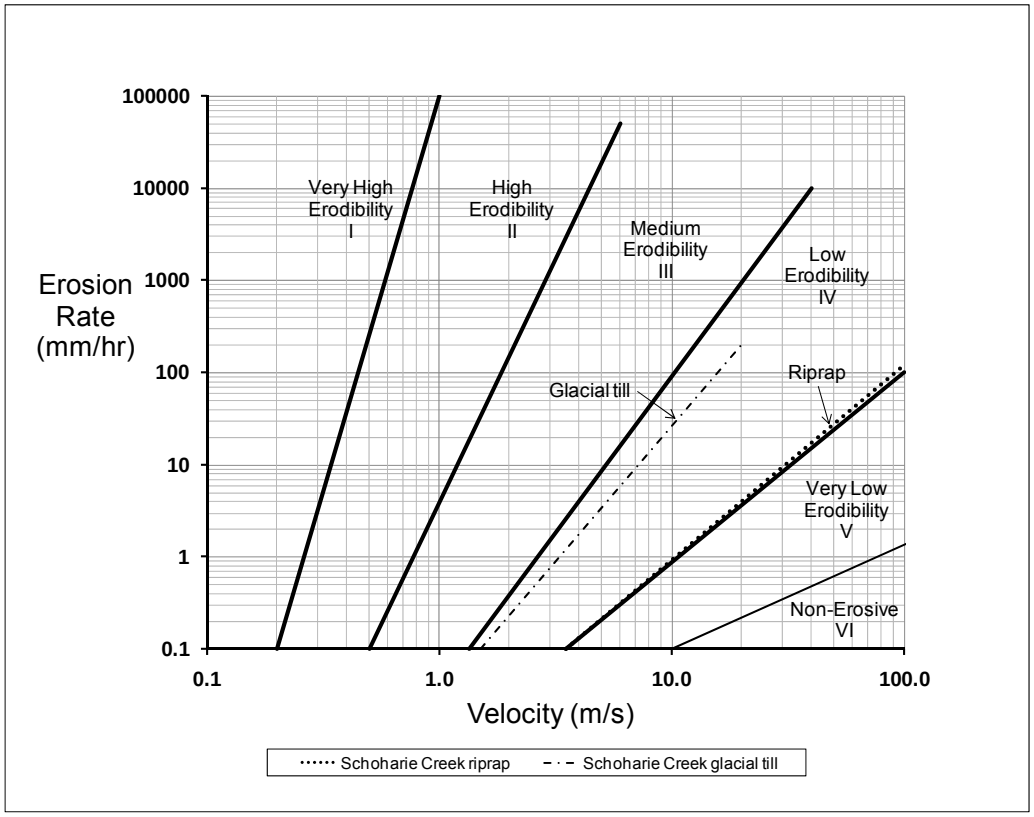

Figure 7-12. Estimated erosion functions for the Schoharie Creek riprap and glacial till.

Through prior investigations into the Schoharie Creek bridge failure, it was found that the 1955 flood and following smaller floods cause the riprap to move between 1955 and prior to the 1987 collapse. Because the riprap was placed down to the bottom level of the footing, it is believed that there was still some remaining riprap just prior to the 1987 flood. Otherwise, the erosion would have undermined the footing before the 1987 flood. Since the velocity of the 1987 flood was greater than V_c of the riprap, it is highly likely that the 1987 flood moved the remaining riprap, thus exposing the more erodible glacial till beneath. As shown in Figure 7-12, the till was more erodible than the riprap. Therefore, once the till was exposed, the footing was undermined very rapidly causing the bridge to fail.

Therefore, the reason for the Schoharie Creek Bridge failure under a lesser flood in 1987 than the flood of 1955 is that of a multilayer deposit response and not one of a uniform deposit response. Indeed, during the 1955 event, the scour hole remained in the riprap while in 1987 it eroded what was left of the riprap (strong layer) and rapidly advanced in the glacial till below (weak layer).

8. APPLICATION TO SCOUR CRITICAL BRIDGES

8.1. INTRODUCTION

A total number of 16 bridges were selected as an example of the proposed bridge scour assessment method in this report. Out of these 16 bridges, 11 were the same bridges selected as case histories for validation and 5 are additional bridges selected solely for the purpose of evaluating the proposed bridge scour assessment method. Of the bridges selected for applications, the 12 are scour critical and 4 are stable according to current TxDOT designation. A combination of both scour critical and stable was selected to be able to test all possible outcome of the proposed bridge scour assessment method against the TxDOT scour designation. In these applications, the future flow is taken as the 100-year flood with a corresponding velocity, V_{100}. A summary of the information on the 16 bridges is provided in Table 8-1. The results of the application of BSA 1 are compared with the current TxDOT scour designation of the bridges and presented in Subsection 8.1.2.

Table 8-1. Bridges selected for application using the proposed bridge scour assessment method.

Application No.	Latitude	Longitude	Waterway	Highway	Scour Status	EFA Test Data Status	Flow Data Status
1	31.47056308000	-96.29239209000	Sanders Creek	FM39	Critical	Available	Not Available
2	31.97030066000	-96.08752535000	Alligator Creek	US287	Critical	Available	Not Available
3	29.47641599000	-95.81304823000	Big Creek	SH36	Critical	Not Available	Available
4	29.59232540000	-97.58796201000	San Marcos River	FM2091	Critical	Not Available	Available
5	29.86972042000	-96.15511481000	Mill Creek	FM331	Critical	Not Available	Available
6	29.96498001000	-98.89669924000	Guadalupe River	US87	Critical	Not Available	Available
7	30.02640843000	-95.25897002000	San Jacinto River	US59SB	Critical	Not Available	Available
8	30.13653693000	-99.31566628000	Dry Branch Creek	SH27	Critical	Not Available	Available
9	30.20833445000	-95.18168475000	Peach Creek	US59 @ Creekwood Dr.	Critical	Not Available	Available
10	29.58279722000	-95.75768056000	Brazos River	US90A (WB)	Critical	Available	Available
11	31.25425278000	-96.33052778000	Navasota River	SH7	Stable	Available	Available
12	31.91973292000	-97.66186263000	North Bosque River	SH 22	Critical	Available	Not Available
13	29.59945278000	-97.65082500000	San Marcos River	SH 80	Stable	Available	Not Available
14	29.82402778000	-95.28920000000	Sims Bayou	SH 35 NB	Stable	Available	Not Available
15	30.90126667000	-95.77777500000	Bedias Creek	US 75	Stable	Available	Available
16	30.91262222000	-95.91015278000	Bedias Creek	SH 90	Stable	Available	Not Available

8.1.1. Case by Case Description of Bridges

The general description of the bridges, such as the type of bridge, foundation type and geomaterials underlying the bridge site are given in this section. As mentioned above, detailed information on the bridges is given in Appendix C.

8.1.1.1. Application No. 1: Bridge on Highway FM 39 Crossing Sanders Creek

This bridge is located in Limestone County within the Waco district in Texas. The TxDOT structure number for this bridge is 0643-02-038. The bridge is on Highway FM 39 and crosses Sanders Creek. The bridge was built in 1977 and has a length of 316 ft. It has 6 spans and is founded on 2.5 ft diameter drilled shafts that vary between 15 ft to 22.5 ft in length. The drilled shafts are embedded mainly in sand and silty sand. This bridge has been deemed scour critical by a concise analysis. This case history does not have flow records but does have site-specific EFA test data.

8.1.1.2. Application No. 2: Bridge on Highway US 287 Crossing Alligator Creek

This bridge is located in Freestone County within the Bryan district in Texas. The TxDOT structure number for this bridge is 0122-03-036. The bridge is on Highway US 287 and crosses Alligator Creek. The bridge was built in 1984 and has a length of 292 ft. It has 7 spans and is founded on 2 ft diameter drilled shafts that have a minimum length of 24 ft. The soil at the site is clay and sand. This bridge has been deemed scour critical by a concise analysis. This case history does not have flow records but does have site-specific EFA test data.

8.1.1.3. Application No. 3: Bridge on Highway SH 36 Crossing Big Creek

This bridge is located in Fort Bend County within the Houston district in Texas. The TxDOT structure number for this bridge is 0188-02-023. The bridge is on Highway SH 36 and crosses Big Creek. The bridge was built in 1932 and has a length of 257 feet. It has 9 spans and is founded on 14 inch concrete piles that vary between 25 ft to 35 ft in length. The soil at the site is a deep sand deposit, extending beyond 40 ft below the channel bottom. This bridge is stable in terms of scour. This case history has flow records but does not have site-specific EFA test data.

8.1.1.4. Application No. 4: Bridge on Highway FM 2091 Crossing San Marcos River

This bridge is located in Gonzales County within the Yoakum district in Texas. The TxDOT structure number for this bridge is 2080-01-005. The bridge is on Highway FM 2091 and crosses the San Marcos River. The bridge was built in 1960 and has a length of 382 feet. It has 6 spans and is founded on 15-inch wide, 32 ft long precast concrete piles and 14-inch wide, 33 ft long steel H-piles. The soil at the site is clay and sand. This bridge is on the scour critical list. This case history has flow records but does not have site-specific EFA test data.

8.1.1.5. Application No. 5: Bridge on Highway FM 331 Crossing Mill Creek

This bridge is located in Austin County within the Austin district in Texas. The TxDOT structure number for this bridge is 0408-05-019. The bridge is on Highway FM 331 and crosses Mill Creek. The bridge was built in 1951 and has a length of 271 feet. It has 6

spans and is founded on 18 inch wide precast concrete piles with a minimum length of 20 ft. The soil at the site is clay and silty sand. This bridge has been deemed scour critical by a concise analysis. This case history has flow records but does not have site-specific EFA test data.

8.1.1.6. Application No. 6: Bridge on Highway US 87 Crossing Guadalupe River

This bridge is located in Kendall County within the San Antonio district in Texas. The TxDOT structure number for this bridge is 0072-04-020. The bridge is on Highway US 87 and crosses the Guadalupe River. The bridge was built in 1932 and has a length of 1434 feet. It has 34 spans and is founded on 16 inch wide concrete square piles that vary between 36 ft to 50 ft in length. The bridge was widened in 1984, where the widened section is on 6 ft diameter drilled shafts that are approximately 17 ft long. The soil at the site is clay and sandy gravel. This bridge has been deemed scour critical by a concise analysis. This case history has flow records but does not have site-specific EFA test data.

8.1.1.7. Application No. 7: Bridge on Highway US 59(SB) Crossing West Fork San Jacinto River

This bridge is located in Harris County within the Houston district in Texas. The TxDOT structure number for this bridge is 0177-06-081. The bridge is on Highway US 59(SB) and crosses the West Fork San Jacinto River. The bridge was built in 1961 and has a length of 1645 feet. It is founded on 16 inch square concrete piles with a minimum length of 10 ft. The soil at the site is sand. This bridge has been deemed scour critical by

a concise analysis. This case history has flow records but does not have site-specific EFA test data.

8.1.1.8. Application No. 8: Bridge on Highway SH 27 Crossing Dry Branch Creek

This bridge is located in Kerr County within the San Antonio district in Texas. The TxDOT structure number for this bridge is 0142-03-008. The bridge is on Highway SH 27 and crosses Dry Branch Creek. The bridge was built in 1935 and has a length of 142 feet. It has 5 spans and is founded on spread footings that are embedded approximately between 10 ft to 15 ft bellow the channel bottom. The bridge was widened in 1963 where the widened section is on 2 ft diameter drilled shafts that are approximately 15 ft long. The soil at the site is clay, shale and limestone. This bridge has been deemed scour critical by a concise analysis. This case history has flow records but does not have site-specific EFA test data.

8.1.1.9. Application No. 9: Bridge on Highway US 59 at Creekwood Drive Crossing Peach Creek

This bridge is located in Montgomery County within the Houston district in Texas. The TxDOT structure number for this bridge is 170-0177-05-119. The bridge is on Highway US 59 at Creekwood Drive and crosses Peach Creek. The bridge was built in 1970 and has a length of 120 feet. It has 3 spans and is founded on 16 inch wide, approximately 35 ft long square piles. The soil at the site is sand. This bridge has been deemed scour

critical by a concise analysis. This case history has flow records but does not have site-specific EFA test data.

8.1.1.10. Application No. 10: Bridge on Highway US 90A (WB) Crossing Brazos River

This bridge is located the Houston district in Texas. The TxDOT structure number for this bridge is 0027-08-092. The bridge is on Highway US 90A (WB) and crosses the Brazos River. The bridge was built in 1965 and has a length of 942 feet. It has 10 spans and is founded on 16 inch to 20 inch square piles. The pile lengths vary between 70 ft to 78 ft. The soil at the site is silty sand and clayey sand. This bridge has been deemed scour critical by a concise analysis. This case history has both flow records and site-specific EFA test data.

8.1.1.11. Application No. 11: Bridge on Highway SH 7 Crossing Navasota River

This bridge is located in Leon County within the Bryan district in Texas. The TxDOT structure number for this bridge is 0382-05-021. The bridge is on Highway SH7 and crosses the Navasota River. The bridge was built in 1956 and has a length of 271 feet. It has 7 spans and is founded on 14 inch wide concrete piles that vary between 28 ft to 50 ft in length. The soil at the site is sand. This bridge has been deemed stable by a concise analysis. This case history has both flow records and site-specific EFA test data.

8.1.1.12. Application No. 12: Bridge on Highway SH 22 Crossing North Bosque River

This bridge is located in Bosque County within the Waco district in Texas. The TxDOT structure number for this bridge is 0121-01-038. The bridge is on Highway SH 22 and crosses the North Bosque River. The bridge was built in 1940 and has a length of 566 ft. It has 12 spans and is founded on 4 ft thick footings embedded 15 ft to 35 ft below the channel bottom. The footings for 9 of the 11 piers are supported by steel piling that is set into shale and soft sandstone. The remaining 2 piers are on footings embedded approximately 1 ft into shale and soft sandstone. Generally, the geomaterial at the site is sand, gravel, soft sandstone and shale. The material within the depth of interest is however the sand and gravel which extend approximately 3 ft below the top of footing level. This bridge is on the scour critical list.

8.1.1.13. Application No. 13: Bridge on Highway SH 80 Crossing San Marcos River

This bridge is located in the Austin district in Texas. The TxDOT structure number for this bridge is 028-01-014. The bridge is on Highway SH 80 and crosses the San Marcos River. The bridge was built in 1939 and has a length of 579 feet. It has 11 spans and is founded on 16 inch wide concrete piles that vary between 20 ft to 50 ft in length. The soil in the site is silty sand and sand. This bridge is not on the scour critical list.

8.1.1.14. Application No. 14: Bridge on Highway SH 35 NB Crossing Sims Bayou

This bridge is located in the Houston district in Texas. The TxDOT structure number for this bridge is 178-01-060. The bridge is on Highway SH 35 NB and crosses Sims Bayou.

The bridge was built in 1948 and has a length of 200 feet. It has 5 spans and is founded on 30 inch diameter drilled shafts that vary between 35 ft to 55 ft in length. The soil at the site is clay and sand. This bridge is not on the scour critical list.

8.1.1.15. Application No. 15: Bridge on Highway US 75 Crossing Bedias Creek

This bridge is located in the Bryan district in Texas. The TxDOT structure number for this bridge is 166-07-047. The bridge is on Highway US 75 and crosses Bedias Creek. The bridge was built in 1947 and has a length of 892 feet. It has 29 spans and is founded on precast concrete piles and spread footings. The piles are 16 inches wide and embedded a minimum 30 ft below ground level. The spread footings are embedded 15 ft to 24 ft below the channel bed. The soil at the site is sand and sandy clay. This bridge is on the scour critical list.

8.1.1.16. Application No. 16: Bridge on Highway SH 90 Crossing Bedias Creek

This bridge is located in the Bryan district in Texas. The TxDOT structure number for this bridge is 315-01-070. The bridge is on Highway SH 90 and crosses Bedias Creek. The bridge was built in 1976 and has a length of 200 feet. It has 5 spans and is founded on 28 inch to 32 inch treated timber piles that vary between 30 ft to 35 ft in length. The site is underlain by sandy clay and silty. This bridge is not on the scour critical list.

8.1.2. Results of Application

The results of the application of BSA 1 on scour critical bridges are shown in Table 8-2. Out of the 16 bridges, 6 bridges that were designated as scour critical by TxDOT were found to be stable by BSA 1. Of the 16, 3 bridges could not be evaluated due to reasons explained in the footnotes of Table 8-2. The remaining 7 bridges had outcomes similar to the TxDOT designation. Out of the 7 bridges that had similar outcomes for both BSA 1 and the TxDOT designation, 3 were stable and 4 were scour critical. So, 6 of the 10 bridges that were originally scour critical and had sufficient information were found to be stable after BSA 1 according to the stability criterion.

Table 8-2. Comparison between BSA 1 outcome and the current TxDOT scour designation for the 18 bridges.

Application No.	Waterway	Highway	Scour Location	Z_{mo} (ft)	Z_{thresh} (ft)	V_{100}/V_{mo}	Z_{100}/Z_{mo} (from chart)	Z_{100} (ft)	Outcome of BSA 1	Current TxDOT Scour Status
1	Sanders Creek	FM39	Bent 5	1.5	11.3	1.05	1.10	1.7	Stable	Critical
2	Alligator Creek	US287	Bent 3	13.1	16	1.04	1.20	15.7	Stable	Critical
3	Big Creek	SH36	Bent 5	3.8	11	1.00	1.00	3.8	Stable	Critical
4	San Marcos River[§]	FM2091	Bent 5	12.4	16	0.95	§	§	§	Critical
5	Mill Creek	FM331	Bent 4	0.8	1.5	1.33	1.50	1.2	Stable	Critical
6	Guadalupe River	US87	Bent 27	6.3	8.5	1.11	1.20	7.6	Stable	Critical
7	San Jacinto River	US59SB	Bent 15	5.7	0	1.11	1.20	6.8	Critical	Critical
8	Dry Branch Creek	SH27	Bent 4	9	7.4	1.11	†	†	†	Critical
9	Peach Creek	US59 @ Creekwood Dr.	Bent 2	8.5	17.5	1.20	1.35	11.5	Stable	Critical
			Bent 3	12.1	17.5			16.3		
10	Brazos River	US90A (WB)	Bent 3	21	39	1.67	2.15	45.1	Critical	Critical
11	Navasota River	SH7	Bent 5	8.1	17.5	1.17	1.35	11.0	Stable	Stable
12	North Bosque River	SH 22	Bent 8	5	16	1.43	1.55	7.8	Critical	Critical
			Bent 9	8	12			12.4		
13	San Marcos River	SH 80	Bent 8	7.5	12	0.95	1.00	7.5	Stable	Stable
			Bent 9	10	12.5			10		
14	Sims Bayou	SH 35 NB	Bent 4	4	20	1.11	1.20	4.8	Stable	Stable
15	Bedias Creek	US 75	Bent 26	8	8	1.18	1.30	10.4	Critical	Critical
16	Bedias Creek[*]	SH 90	*	*	*	*	*	*	*	Stable

Notes:

[§] A large caisson was added in 1995 at the scour critical pier. It was not possible to extrapolate Z_{mo} that corresponds to a smaller pier size to obtain Z_{fut} for a larger pier size.

[†] Z_{mo} exceeds Z_{thresh}. The 9 ft of scour was obtained in 1996. However, the channel backfilled by 6 ft in 1998 and this did not change until 2006.

[*] Channel excavation was carried out and no corresponding date was indicated in the bridge folder.

9. CONCLUSIONS

9.1. GENERAL

The topic addressed is the assessment of bridges for scour. The scour components included are pier and contraction scour. Abutment scour was not included because the Texas Department of Transportation elects not to include abutment scour in their bridge scour assessment (Texas Department of Transportation 2006). The proposed method eliminates site specific erosion testing and uses actual measured scour data. It is economical, relatively simple, and improves on the over-conservative nature of previous bridge scour assessment procedures especially in erosion resistant soils.

9.2. ERODIBILITY OF GEOMATERIALS

The erodibility of soil or rock is defined as the relationship between the erosion rate, $\dot{Z}$ and the velocity of water, V at the soil / rock - water interface. This definition however is not very satisfactory because the velocity varies in direction and intensity in the flow field (Briaud 2008). To be exact, the velocity of water is zero at the soil/rock interface. A more adequate definition is the relationship between the erosion rate $\dot{Z}$ and the shear stress τ at the soil/rock interface. However, the velocity is often used as it is easier to gauge an erosion problem from a velocity standpoint.

One of the most important material parameters in soil erosion is the threshold of erosion (Briaud 2008). Below the threshold value, erosion does not take place. Once the

applied hydraulic shear stress (or more simply the velocity) exceeds the threshold value, erosion is initiated until the equilibrium scour depth is obtained. The threshold values for erosion in terms of shear stress is the critical shear stress τ_c and in terms of velocity is the critical velocity V_c. Important parameters that assist in describing the erosion function include the threshold value, the initial rate of scour and the equilibrium scour depth. The erosion rate in clays and rocks can be many times smaller than the erosion rate in sands.

9.3. BRIDGE SCOUR ASSESSMENT 1

Bridge Scour Assessment 1 (BSA 1) is a bridge scour assessment procedure that makes use of existing data collected either from bridge records maintained by the authorities or by site visit (Govindasamy et al. 2008). It is the first level of bridge scour assessment within the bridge scour assessment framework proposed in this report. The main idea behind the BSA 1 procedure is that the scour depth corresponding to a specified future flood event is obtained from historical and site specific scour depth observations (Z_{mo}), from historical and site specific maximum flood observations (V_{mo}), and extrapolation charts that relate the future scour depth ratio (Z_{fut}/Z_{mo}) to the future velocity ratio (V_{fut}/V_{mo}). Here, Z_{fut} is the scour depth corresponding to a specified future flood, Z_{mo} is the maximum observed scour at the bridge, V_{fut} is the velocity corresponding to the specified future flood, and V_{mo} is the maximum velocity ever observed at the bridge until the time Z_{mo} is measured. The extrapolation charts are termed the Z-Future Charts. The vulnerability associated with scour depends on the comparison between Z_{fut} and the

allowable scour depth of the foundation, Z_{thresh}. BSA 1 is summarized in two flowcharts that are presented in a decision tree format: BSA 1 (Uniform Deposit) and BSA 1 (Multilayer Analysis).

9.4. BRIDGE SCOUR ASSESSMENT 2

Bridge Scour Assessment 2 (BSA 2) is the assessment procedure that has to be carried out if BSA 1 did not conclude with a specific plan of action for the bridge. The plan of action could be in the form of a recommendation for regular monitoring if the bridge is found to have minimal risk, special action such as specialized scour monitoring or immediate action to prevent scour induced failure. BSA 2 is a process that determines the scour vulnerability by first calculating the maximum scour depth. The maximum bridge scour depth concept is based on the assumption that the bridge will experience the maximum possible scour depth (equilibrium scour depth) within its lifetime. This might not be the case for some more erosion resistant materials such as clays and some rocks. In BSA 2, the maximum scour at the bridge, termed maximum total local scour ($Z_{max,l}$) is the arithmetic sum of the three components of scour, i.e. maximum pier scour ($Z_{max,p}$), maximum contraction scour ($Z_{max,c}$) and, maximum abutment scour ($Z_{max,a}$). The vulnerability associated with scour depends on the comparison between the maximum total local scour depth and the allowable scour depth of the bridge. BSA 2 is represented by a flowchart that is presented in decision tree format.

9.5. BRIDGE SCOUR ASSESSMENT 3

Bridge Scour Assessment 3 (BSA 3) is the assessment procedure that has to be carried out if BSA 2 did not conclude with a specific plan of action for the bridge. The plan of action could be in the form of recommendation for regular monitoring if the bridge is found to have minimal risk, special action such as specialized scour monitoring or immediate action to prevent scour induced failure. BSA 3 analysis also has to be carried out if the maximum calculated scour depth in BSA 2 extends beyond the topmost layer in the presence of a layered geologic profile. BSA 3 involves the calculation of time dependent scour depth, which is the scour depth after a specified time rather than simply using the maximum scour depth. This method is valuable in the case of clays and some rocks that have high erosion resistance (low erosion rate) and do not achieve the maximum scour depth as computed in BSA 2 within the lifetime of the bridge. The time dependent scour depth is termed the final scour depth, Z_{fin}. In BSA 3, the total final local scour depth at the bridge, termed the final local scour ($Z_{fin,l}$) is the arithmetic sum of the three components of scour., i.e. final pier scour ($Z_{fin,p}$), final contraction scour ($Z_{fin,c}$), and final abutment scour ($Z_{fin,a}$). Similar to BSA 2, the vulnerability associated with scour depends on the comparison between the total final scour depth, $Z_{fin,l}$ and the allowable scour depth of the bridge, Z_{thresh}. BSA 3 is represented by two flowcharts that are presented in decision tree format: BSA 3 (Time Analysis) and BSA 3 (Multilayer Time Analysis). The outcome of BSA 3 will be a conclusive plan of action for the bridge.

9.6. VALIDATION OF THE PROPOSED ASSESSMENT METHOD

Several full case histories were selected for the validation of the proposed bridge scour assessment procedure. The required information was soil data, flow data, age of the bridge, foundation type and dimensions, and scour depths. There were 11 cases that were considered adequate and suitable, and were used in the validation process.

The bridge records for the case histories had limited bridge scour measurements. In fact, there were no bridge scour measurements taken before the year 1991. Because most of the bridges were reasonably old (up to approximately 80 years old), they had experienced the largest flow velocity prior to the first bridge scour measurement. This resulted in all the cases having a V_{fut}/V_{mo} ratio equal to or less than unity for the BSA 1 validation. Results of the BSA 1 validation, shown in Figure 7-2 shows good agreement between predicted and measured values. However, this validation is only for V_{fut}/V_{mo} ratios equal to or less than unity. From Figure 7-3, it can be observed that the results of the validation of BSA 2 show good agreement between the BSA 2 method and the SRICOS-EFA Method. The validation of BSA 3 indicates that BSA 3 tends to overestimate the scour depth when compared to field measurements. This could be because the selection of erosion categories on the basis of soil type is very conservative (by design). However, BSA 3 does improve on the over-estimation of scour depth by 2 ft to 4 ft when compared to maximum scour depths.

9.7. APPLICATION TO SCOUR CRITICAL BRIDGES

The results of the application of BSA 1 on scour critical bridges are shown in Table 8-2. Out of the 16 bridges, 6 bridges that were designated as scour critical by TxDOT were found to be stable by BSA 1. Of the 16, 3 bridges could not be evaluated due insufficient information or unsuitable field conditions. The remaining 7 bridges had outcomes similar to the TxDOT designation. Out of the 7 bridges that had similar outcomes for both BSA 1 and the TxDOT designation, 3 were stable and 4 were scour critical. So, 6 of the 10 bridges that were originally scour critical and had sufficient information were found to be stable after BSA 1 according to the stability criterion.

9.8. RECOMMENDATIONS

It is recommended that

- Studies be carried out to quantify the amount of infilling that takes place in live-bed scour conditions. This could be in the form of scour monitoring methods or sediment transport analysis.
- The level of risk associated with employing BSA 1 be studied and addressed. It would be meaningful to determine the probability of the Z_{fut}/Z_{mo} ratios predicted using BSA 1 exceeding field values.
- The time dependent abutment scour depth be addressed and included in BSA 1 and BSA 3.

REFERENCES

Adams, L., Palmer, R.N., and Turkiyyah, G. (1995). "An expert system for evaluating scour potential and stream stability at bridges." *Proc., 22nd Annual National Conf.*, Water Resources Planning and Management Division, ASCE, Cambridge, Massachusetts, 786-789.

Ayres Associates (2004). "Plans of action for scour critical bridges." *Office Manual*, Idaho Transportation Department, Boise, Idaho.

Briaud, J.-L., Ting, F.C.K., Chen, H.-C., Gudavalli, R., Perugu, S., and Wei, G. (1999). "SRICOS: Prediction of scour rate in cohesive soils at bridge piers." *Journal of Geotechnical and Geoenvironmental Engineering*, 125(4), 237-246.

Briaud, J.-L., Ting, F.C.K., Chen, H.-C., Cao, Y., Han, S.W., and Kwak, K.W. (2001a). "Erosion function apparatus for scour rate predictions." *Journal of Geotechnical and Geoenvironmental Engineering*, 127(2), 105-113.

Briaud, J.-L., Chen, H.-C., Kwak, K.W., Han, S.W., and Ting, F.C.K. (2001b). "Multiflood and multilayer method for scour rate prediction at bridge piers." *Journal of Geotechnical and Geoenvironmental Engineering*, 127(2), 114-125.

Briaud, J.-L., Chen, H.-C., Li, Y., Nurtjahyo, P., and Wang, J. (2003). "Complex pier scour and contraction scour in cohesive soils." *NCHRP Report 24-15,* National Cooperative Highway Research Program, Transportation Research Board, National Research Council, Washington D.C., <http://ceprofs.civil.tamu.edu/briaud/sricos-efa.htm> (Jan. 25, 2008).

Briaud, J.-L., Chen, H.-C., Li, Y., Nuttjahyo, P. and Wang, J. (2004). "Pier and contraction scour in cohesive soils" *National Cooperative Highway Research Program Report 516*, Transportation Research Board, Washington, D.C., 118.

Briaud, J.-L., Chen, H.-C., Li, Y., Nurtjahyo, P., and Wang, J. (2005). "SRICOS-EFA method for contraction scour in cohesive soils." *Journal of Geotechnical and Geoenvironmental Engineering*, Vol. 131(10), 1283-1294.

Briaud, J.-L. (2008). "Case histories in soil and rock erosion: Woodrow Wilson Bridge, Brazos River meander, Normandy Cliffs, and New Orleans levees - 2007 Ralph B. Peck Lecture." *Journal of Geotechnical and Geoenvironmental Engineering*, 134(10), 1425-1447.

Briaud J.-L., Chen H.-C., Chang K.-A, Oh S., and Chen X. (2009). "Abutment scour in cohesive soils." *NCHRP Report 24-15(2)*, Transportation Research Board, National Academy of Sciences, Washington, DC.

California Department of Transportation (2007). "Scour plan of action." Division of Maintenance, <http://www.dot.ca.gov/hq/structur/strmaint/scour.htm#SamplePOA> (Nov. 4, 2008)

Cao, Y., Wang, J., Briaud, J.L., Chen, H.C., Li, Y., and Nurtjahyo, P. (2002). "Erosion function apparatus overview and discussion of influence factors on cohesive soil erosion rate in the EFA test." *Proc., 1st Int. Conf. on Scour of Foundations*, Texas A&M University, College Station, Texas, 459-470.

Cato, K.D. (1991). "Performance of geologic materials under hydraulic stress." Ph.D. dissertation, Department of Geology, Texas A&M University, College Station, Texas.

Colorado Highway Department (1990). "Colorado bridge safety assurance procedure for Colorado Highway Department." *Ref. 1514*, Colorado.

Delphia J. (2008). Written communication, E-mail to Anand V Govindasamy on May 6, 2008.

Federal Highway Administration (1991). "Evaluating scour at bridges" *Technical Advisory T 5140.23*, Washington, D.C., <http://www.fhwa.dot.gov/legsregs/directives/techadvs/t514023.htm>, (Jan. 8, 2008).

Federal Highway Administration (2004). *National bridge inspection standards*, Washington D.C., <http://www.fhwa.dot.gov/Bridge/nbis.htm>, (Jun. 6, 2008).

Froehlich, D.C. (1989a). "Abutment scour prediction." *Presentation*, Transportation Research Board, Washington, D.C.

Froehlich, D.C. (1989b). "Local scour at bridge abutments" *Proc., 1989 National Conf. on Hydraulic Engineering*, ASCE, New Orleans, Louisiana, 13-18.

Govindasamy, A.V., Briaud, J.-L., Chen, H.-C., Delphia, J., Elsbury, K., Gardoni, P., Herrman, G., Kim, D., Mathewson, C.C., McClelland, M., and Olivera, F. (2008). "Simplified method for estimating scour at bridges." *GeoCongress 2008*, New Orleans, Louisiana, 385-393.

Gudavalli, R., Ting, F., Chen, H.C., Perugu, S., and Wei, G. (1997). "Flume tests to study scour rate of cohesive soils." *Research Report Prepared for Texas Department of Transportation*, Department of Civil Engineering, Texas A&M University, College Station, Texas.

Haas, C., Weissmann, J., and Groll, T. (1999). "Remote bridge scour monitoring: A prioritization and implementation guideline." *Report No. TX-00/0-3970-1*, Texas

Department of Transportation Research and Technology Transfer Section - Construction Division, Austin, Texas, 180.

Harmsen, P. Palmer, R., and Turkiyyah, G. (2001). "Development and application of an expert system for evaluation of scour and stream stability." *Civil and Environmental Systems*, Overseas Publishers Association, 18(3), 171-192.

Hjulström, F. (1935). "The morphological activity of rivers as illustrated by river Fyris." *Bulletin of the Geological Institute Uppsala No. 25*, Chapter 3, 221.

Holnbeck, S.R. and Parrett, C. (1997). "Method for rapid estimation of scour at highway bridges based on limited site data." *Water-Resources Investigations Report 96-4310*, United States Geological Survey, Helena, Montana, 79.

Huizinga, R.J. and Rydlund, P.H. (2004). "Potential-scour assessments and estimates of scour depth using different techniques at selected bridge sites in Missouri." *Scientific Investigations Report 2004-5213*, United States Geological Survey and Missouri Department of Transportation, Reston, Virginia, 42.

Johnson, P.A. (2005). "Preliminary assessment and rating of stream channel stability near bridges." *Journal of Hydraulic Engineering*, 131(10), 845-852.

Jones, J. Sterling and Ortiz, Jorge E. Pagán (2002). "Approach to developing a plan of action for scour critical bridges." Presentation, *Transportation Research Board Annual Meeting*, Washington D.C.

Kattell, J. and Eriksson, M. (1998). *Bridge scour evaluation: Screening, analysis and countermeasures*, United States Department of Agriculture Forest Service, San Dimas, California.

Lagasse, P.F., Schall, J.D., Johnson, F., Richardson, E.V., and Chang, F. (1995). "Stream stability at highway structures." *Federal Highway Administration Report No. FHWA-IP-90-014 (HEC-20)*, Washington D.C., 144.

Leung, A. (1996). "Perfecting bridge inspecting." *Civil Engineering*, 66(3), 59 – 60.

Olona, S. B. (1992). "Texas bridge scour evaluation program." *Proc., Hydraulic Engineering Sessions - Water Forum '92*, New York, 70-75.

Palmer, R., Turkiyyah, G., Harmsen, P., Owens, D., Quan, S., Adams, L., Pollen, S., Shepard, J., and Landrum, D. (1997). "CAESAR: An expert system for cataloging and expert evaluation of scour risk and river stability at bridge sites." *Draft User's Guide*, Department of Civil Engineering, University of Washington, Seattle, Washington, 51.

Palmer, R., Turkiyyah, G., and Harmsen, P. (1999).”CAESAR: An expert system for evaluation of scour and stream stability.” *National Cooperative Highway Research Program Report 426*, Transportation Research Board, National Research Council, National Academy Press, Washington, D.C., 54.

Pearson, D., S. Stein, and J. S. Jones (2000). “HYRISK methodology and user’s guide.” *Report FHWA-RD-02-XXX,* Federal Highway Administration, Washington, D.C.

Richardson, E. V., and Davis, S. M. (2001). “Evaluating scour at bridges.” *Publication No. FHWA NHI 01-001 (HEC No. 18)*, United States Department of Transportation, Washington, D.C., 378.

Richardson, E.V., D.B. Simons, and P.F. Lagasse (2001). “River engineering for highway encroachments - Highways in the river environment” *FHWA NHI 01-004 Hydraulic Series No. 6*, Federal Highway Administration, Washington, D.C.,644.

Shields, A. (1936). “Anwendung der aehnlichkeitsmechanik und der turbulenzforschung auf die geschiebebewegung.” Doktor-Ingenieurs dissertation, Technischen Hochschule, Berlin (in German).

Simon, A., Outlaw, G. S., and, Thoman, R. (1989). “Evaluation, modeling and mapping of potential bridge scour, West Tennessee.” *Proc., Bridge Scour Symp.*, Federal Highway Administration and United States Geological Survey, 112-139.

Texas Department of Transportation (1993). “Texas secondary evaluation and analysis for scour.” Texas Bridge Scour Program, Division of Bridges and Structures, Austin, Texas, 12.

United States Army Corps of Engineers (1995). “Constructing quality management.” *Engineering Regulation No. 1180-1-6*, Washington D.C.

United States Geological Survey (1993). “Aspects of the Tennessee Level 1 bridge scour assessment methodology applicable to the Texas secondary evaluation and analysis for scour,” prepared in Cooperation with Design Division, Texas Department of Transportation, Austin, Texas, 18.

Wang, J. (2004). “The SRICOS-EFA method for complex pier and contraction scour.” Ph.D. dissertation, Texas A&M University, College Station ,Texas.

Wei, G., Chen, H.C., Ting, F.,Briaud, J.L., Gudavalli, R., and Perugu, S. (1997). “Numerical simulation to study scour rate in cohesive soils.” *Research Report to the Texas Department of Transportation*, Department of Civil Engineering, Texas A&M University, College Station, Texas.

APPENDIX A

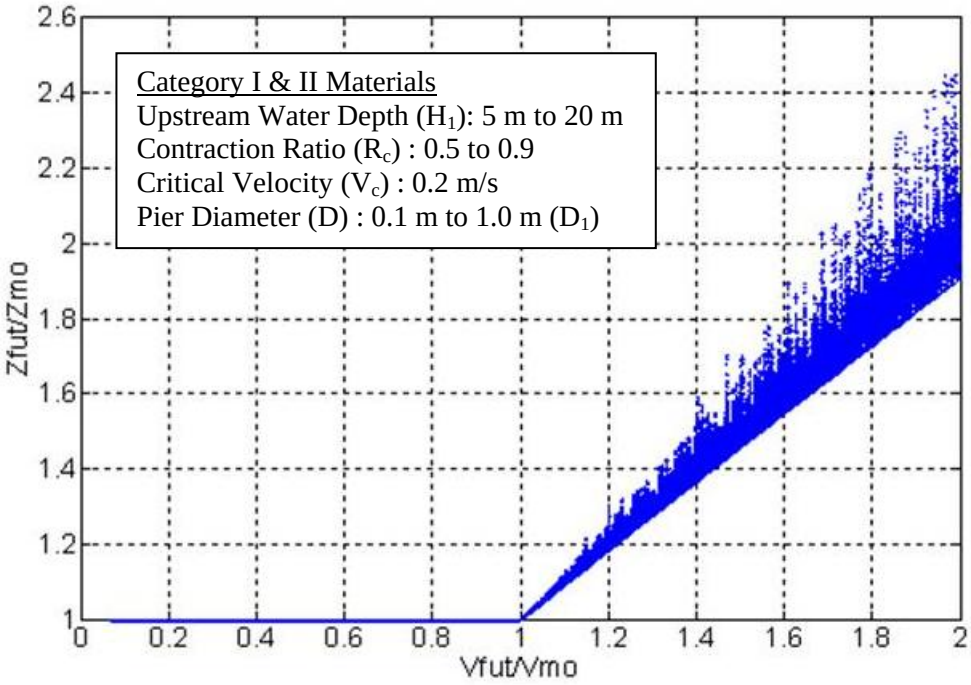

Figure A-1. Z-Future Chart simulation data for Category I & II materials (0.1 m ≤ D ≤ 1.0 m).

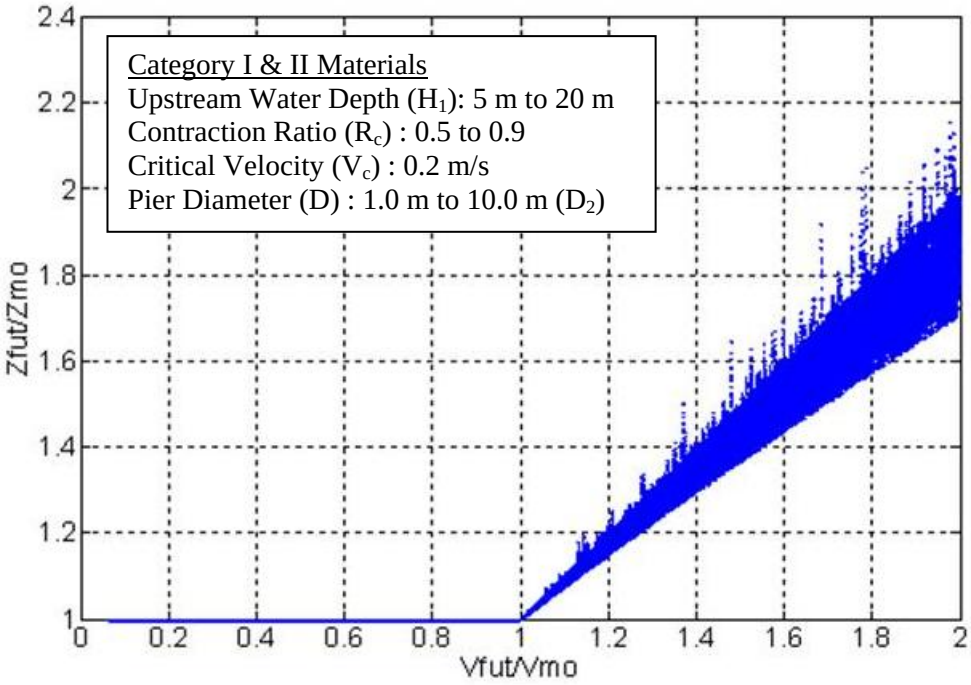

Figure A-2. Z-Future Chart simulation data for Category I & II materials (1.0 m ≤ D ≤ 10.0 m).

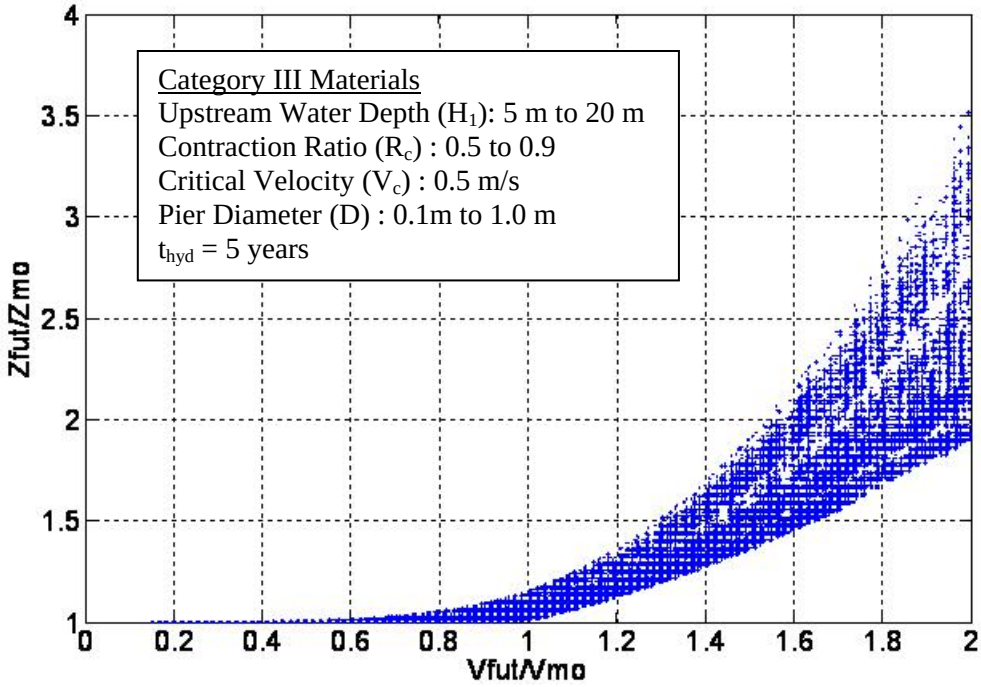

Figure A-3. Z-Future Chart simulation data for Category III materials (0.1 m ≤ D ≤ 1.0 m).

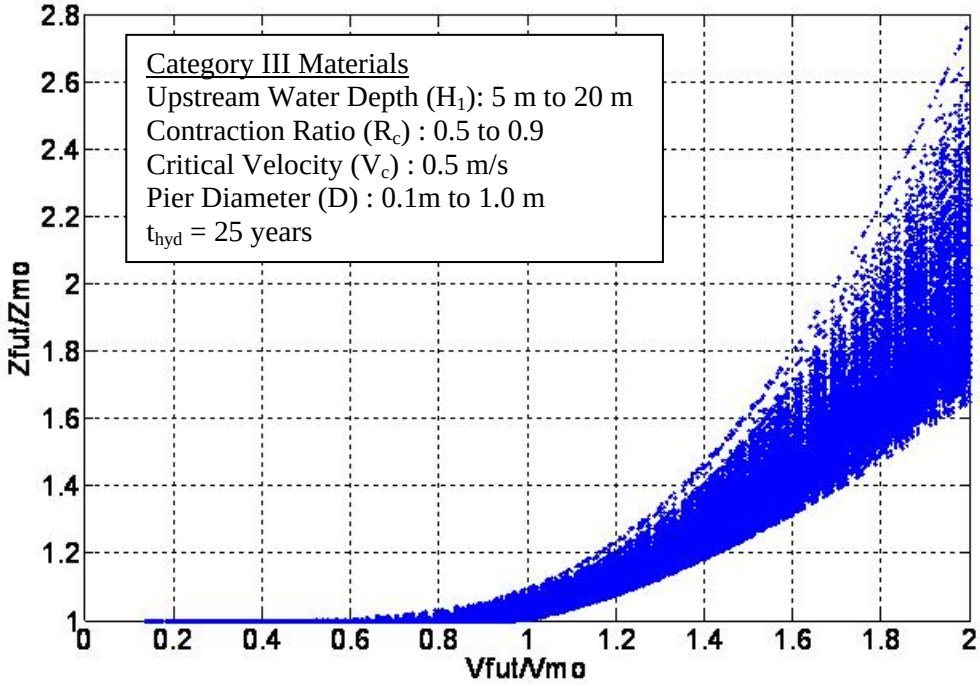

Figure A-4. Z-Future Chart simulation data for Category III materials (0.1 m ≤ D ≤ 1.0 m).

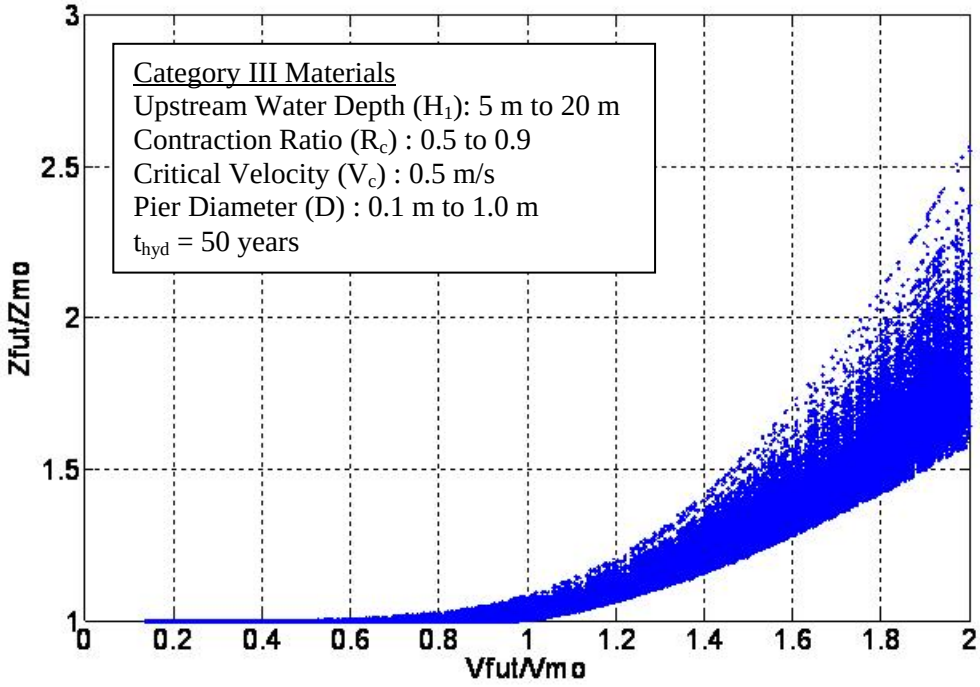

Figure A-5. Z-Future Chart simulation data for Category III materials (0.1 m ≤ D ≤ 1.0 m).

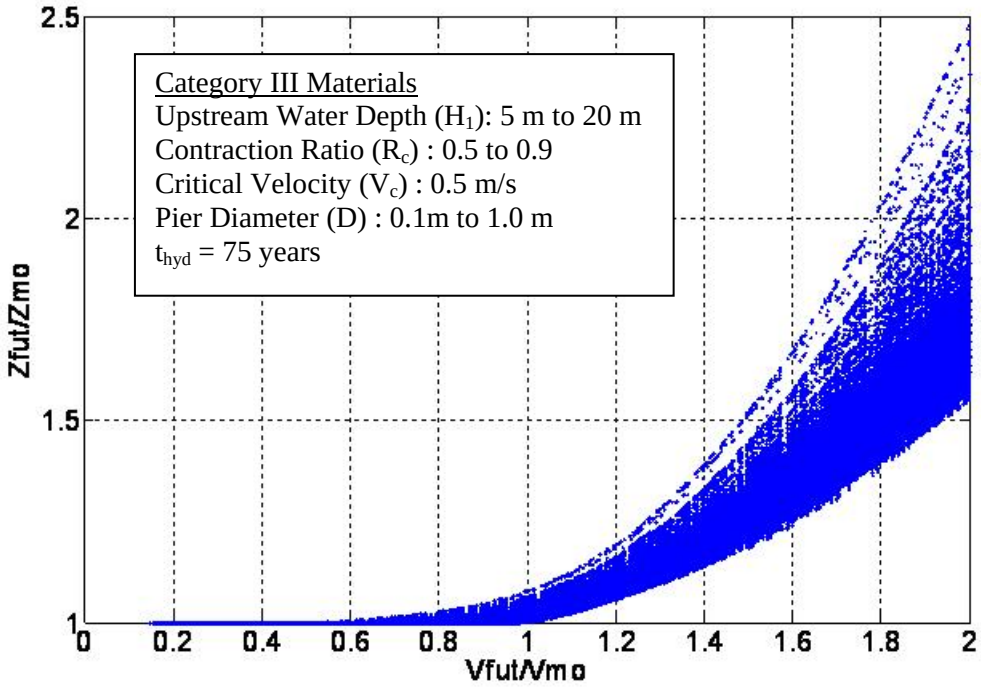

Figure A-6. Z-Future Chart simulation data for Category III materials (0.1 m ≤ D ≤ 1.0 m).

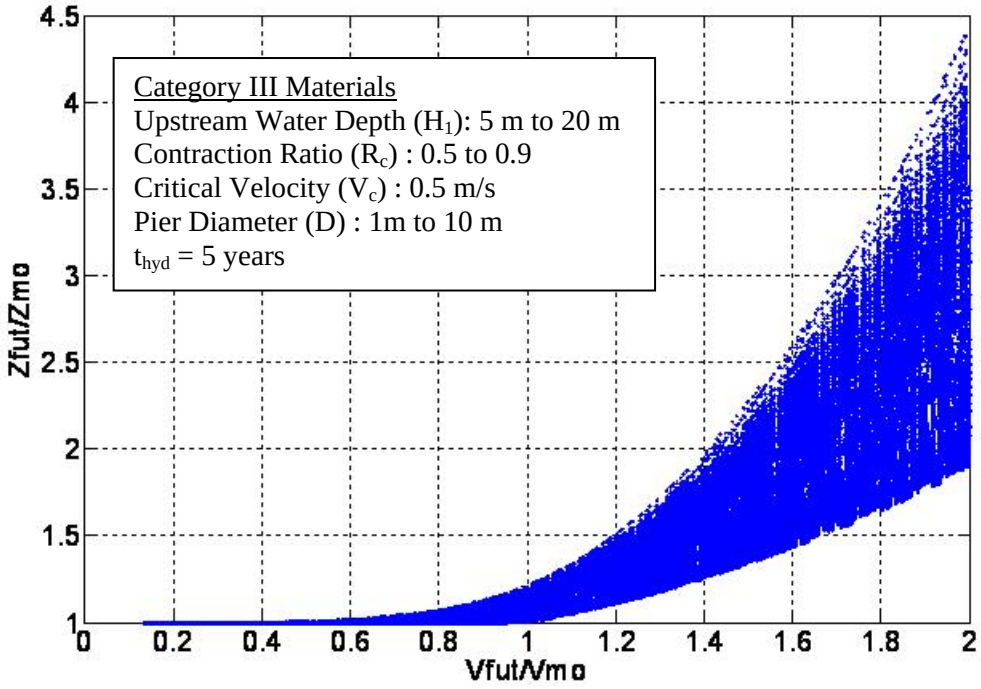

Figure A-7. Z-Future Chart simulation data for Category III materials (1.0 m ≤ D ≤ 10.0 m).

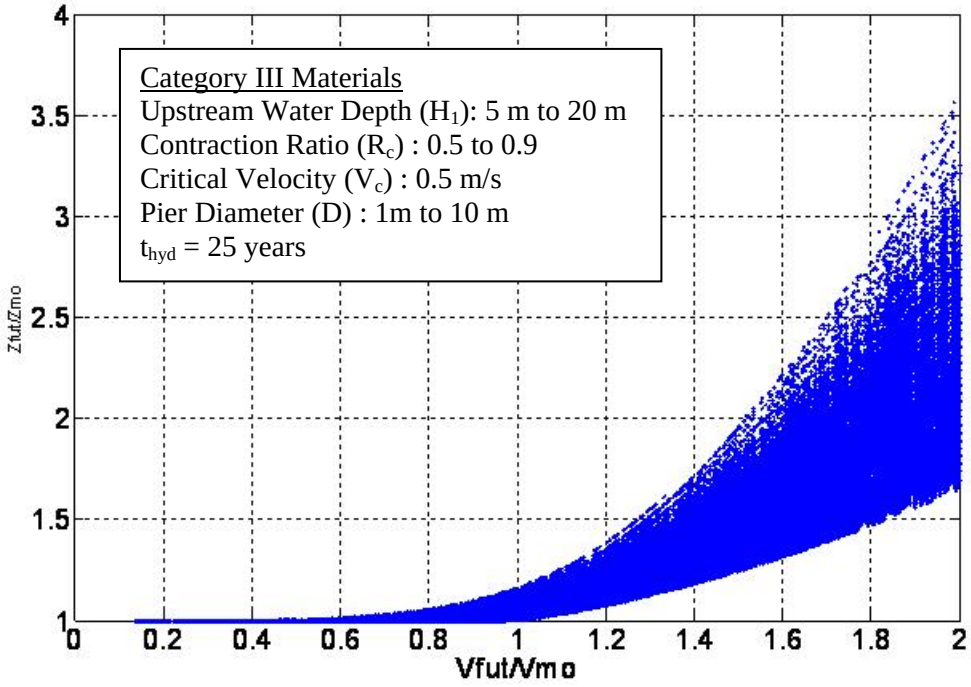

Figure A-8. Z-Future Chart simulation data for Category III materials (1.0 m ≤ D ≤ 10.0 m).

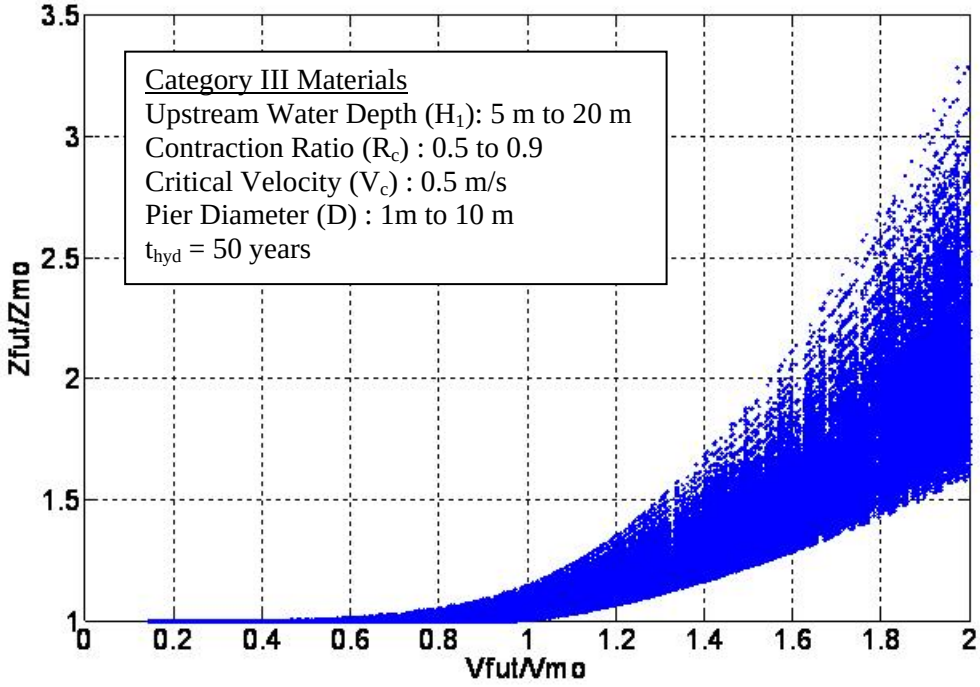

Figure A-9. Z-Future Chart simulation data for Category III materials (1.0 m ≤ D ≤ 10.0 m).

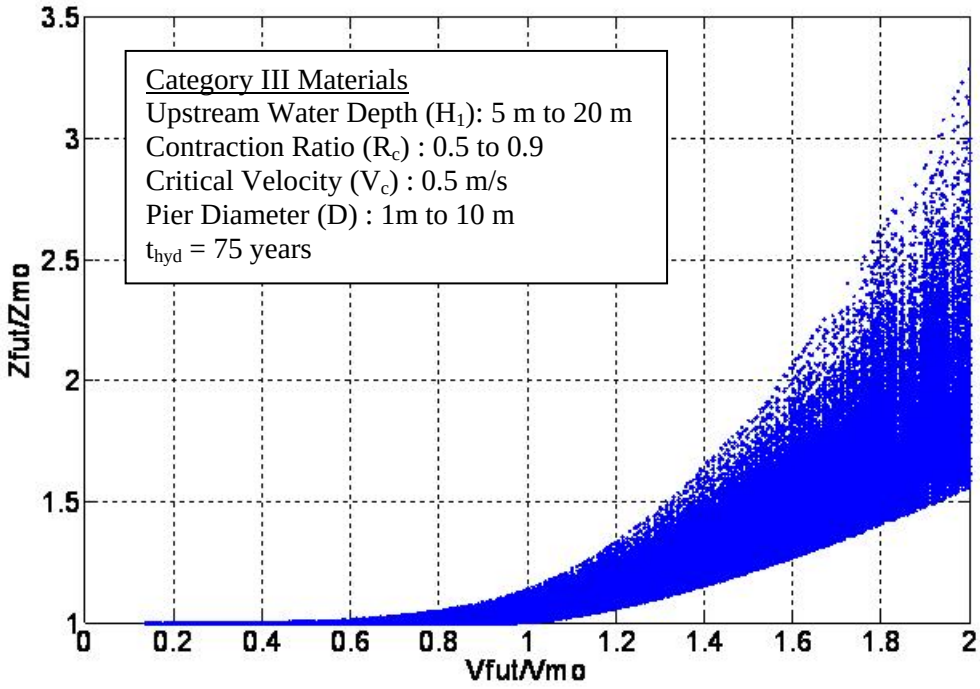

Figure A-10. Z-Future Chart simulation data for Category III materials (1.0 m ≤ D ≤ 10.0 m).

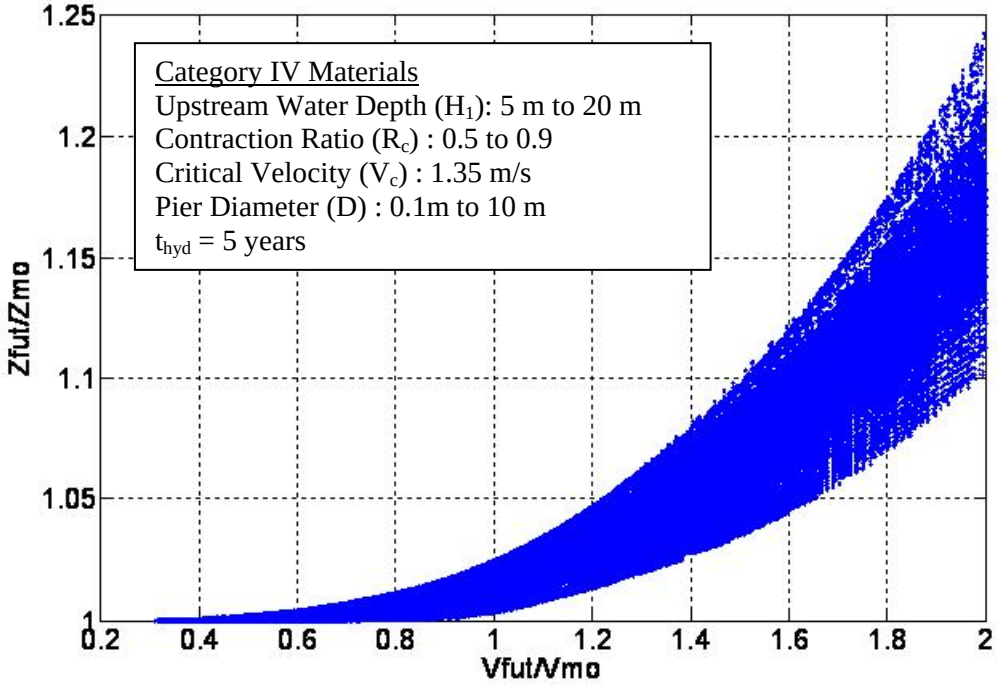

Figure A-11. Z-Future Chart simulation data for Category IV materials (0.1 m ≤ D ≤ 10.0 m).

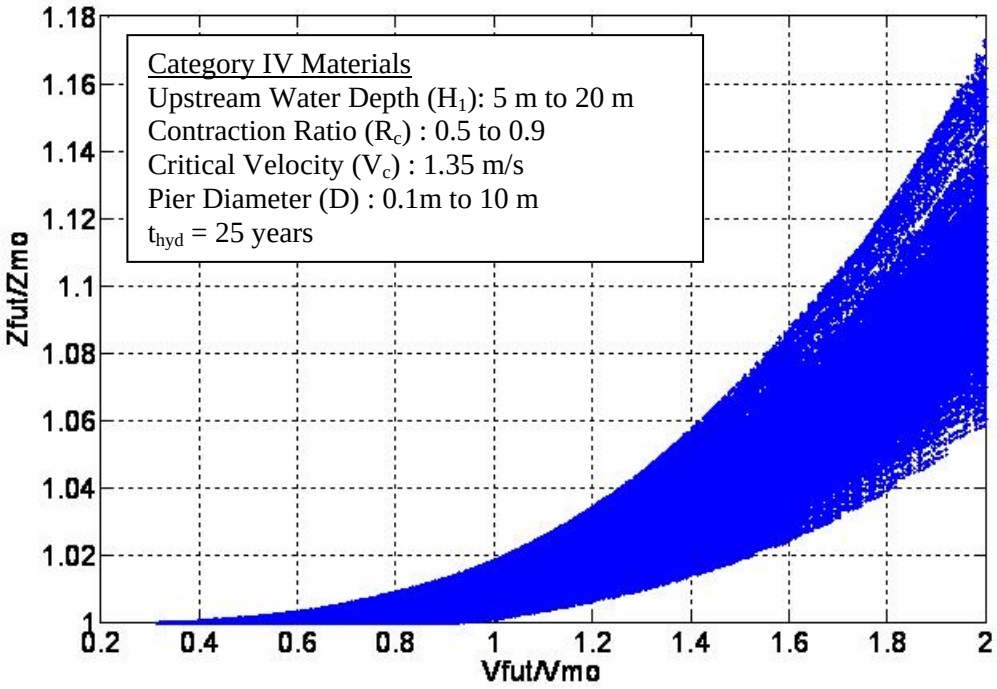

Figure A-12. Z-Future Chart simulation data for Category IV materials (0.1 m ≤ D ≤ 10.0 m).

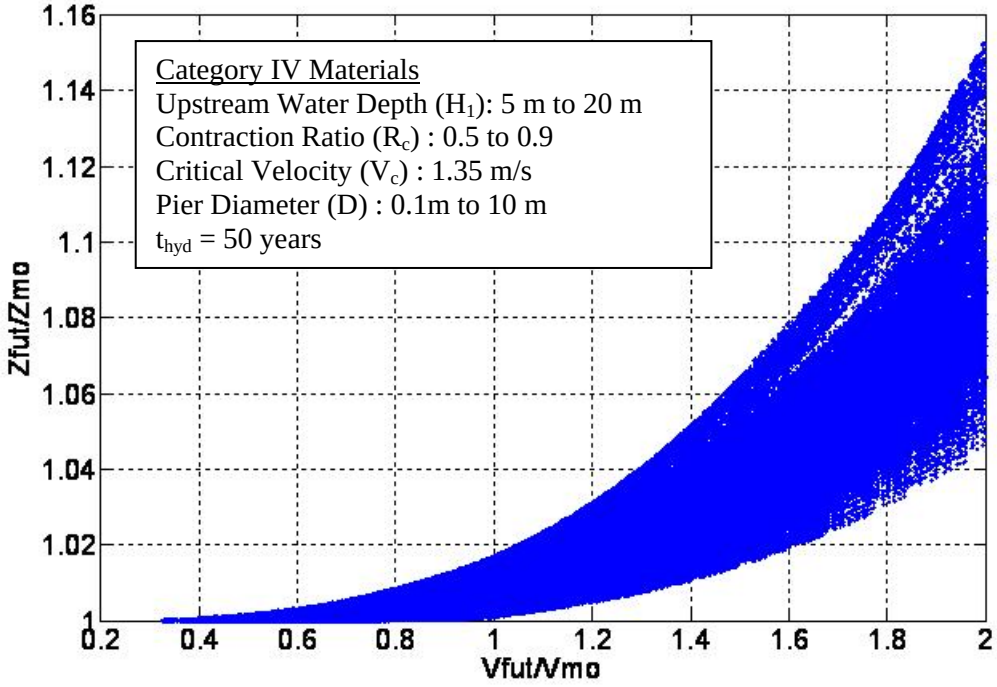

Figure A-13. Z-Future Chart simulation data for Category IV materials (0.1 m ≤ D ≤ 10.0 m).

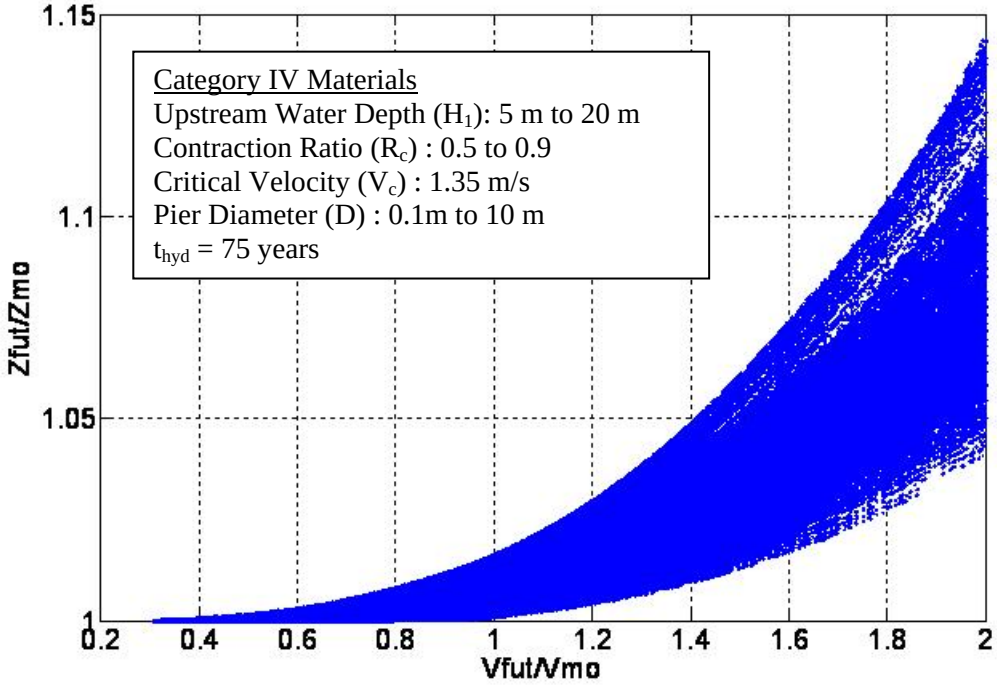

Figure A-14. Z-Future Chart simulation data for Category IV materials (0.1 m ≤ D ≤ 10.0 m).

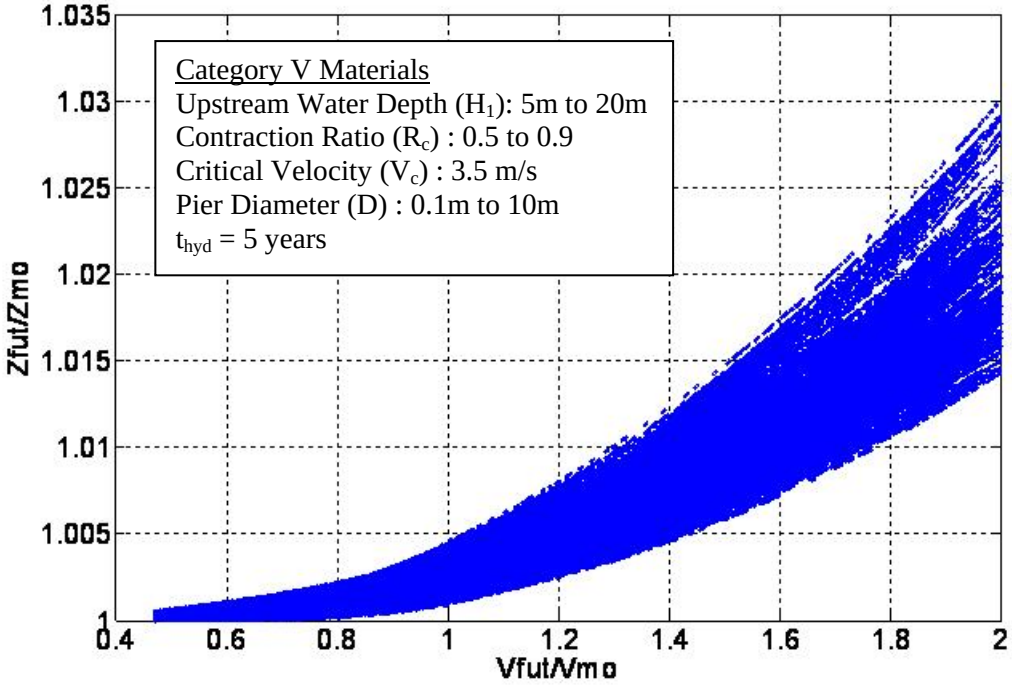

Figure A-15. Z-Future Chart simulation data for Category V materials (0.1 m ≤ D ≤ 10.0 m).

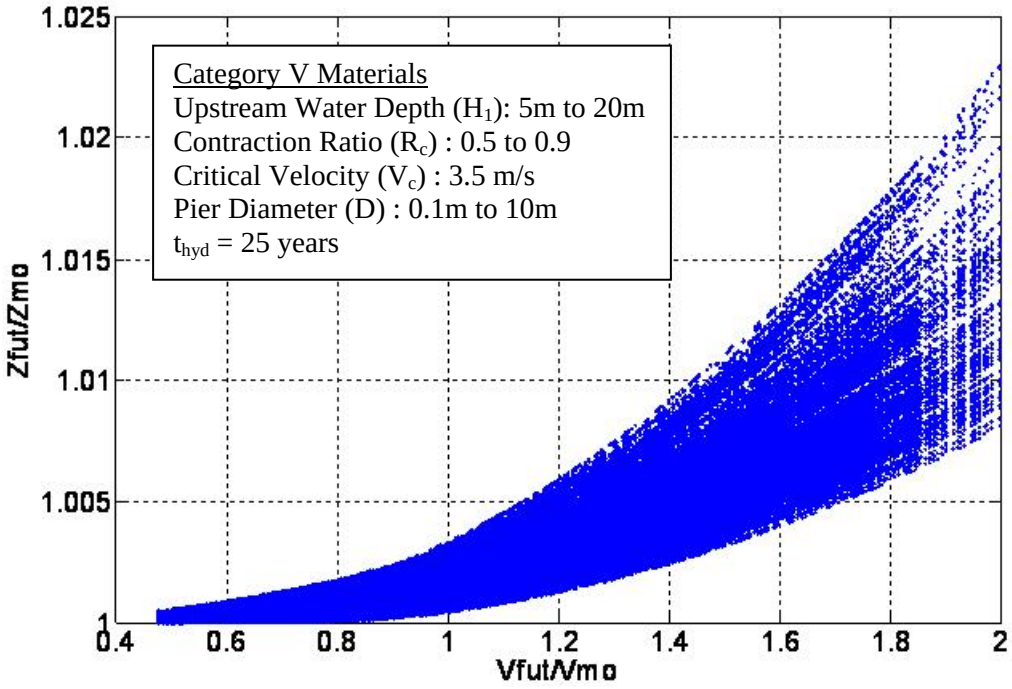

Figure A-16. Z-Future Chart simulation data for Category V materials (0.1 m ≤ D ≤ 10.0 m).

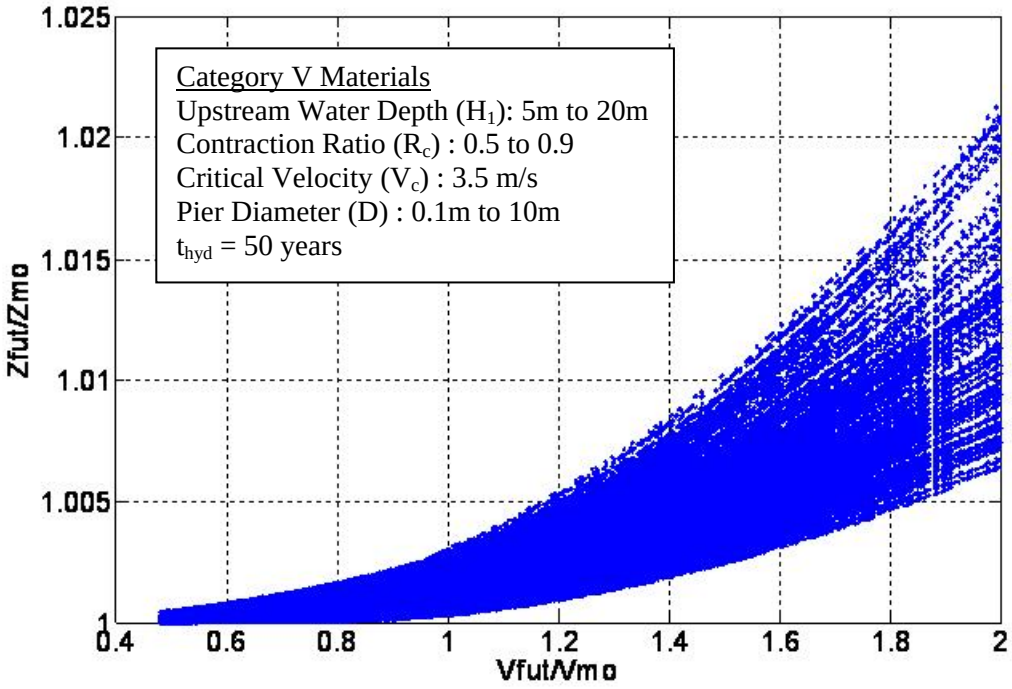

Figure A-17. Z-Future Chart simulation data for Category V materials (0.1 m ≤ D ≤ 10.0 m).

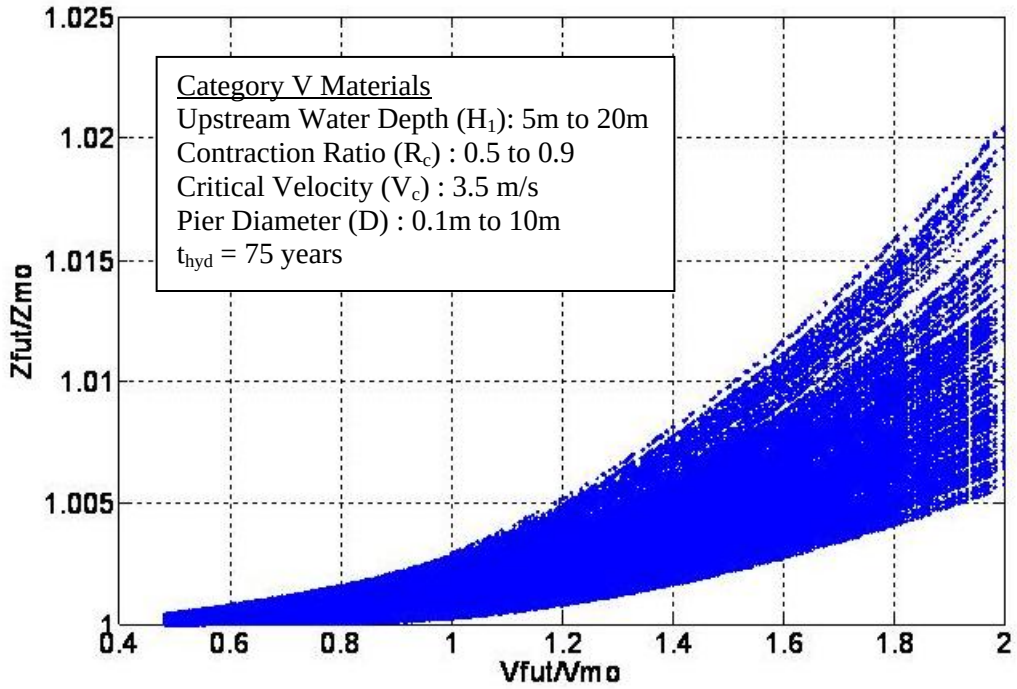

Figure A-18. Z-Future Chart simulation data for Category V materials (0.1 m ≤ D ≤ 10.0 m).

APPENDIX B

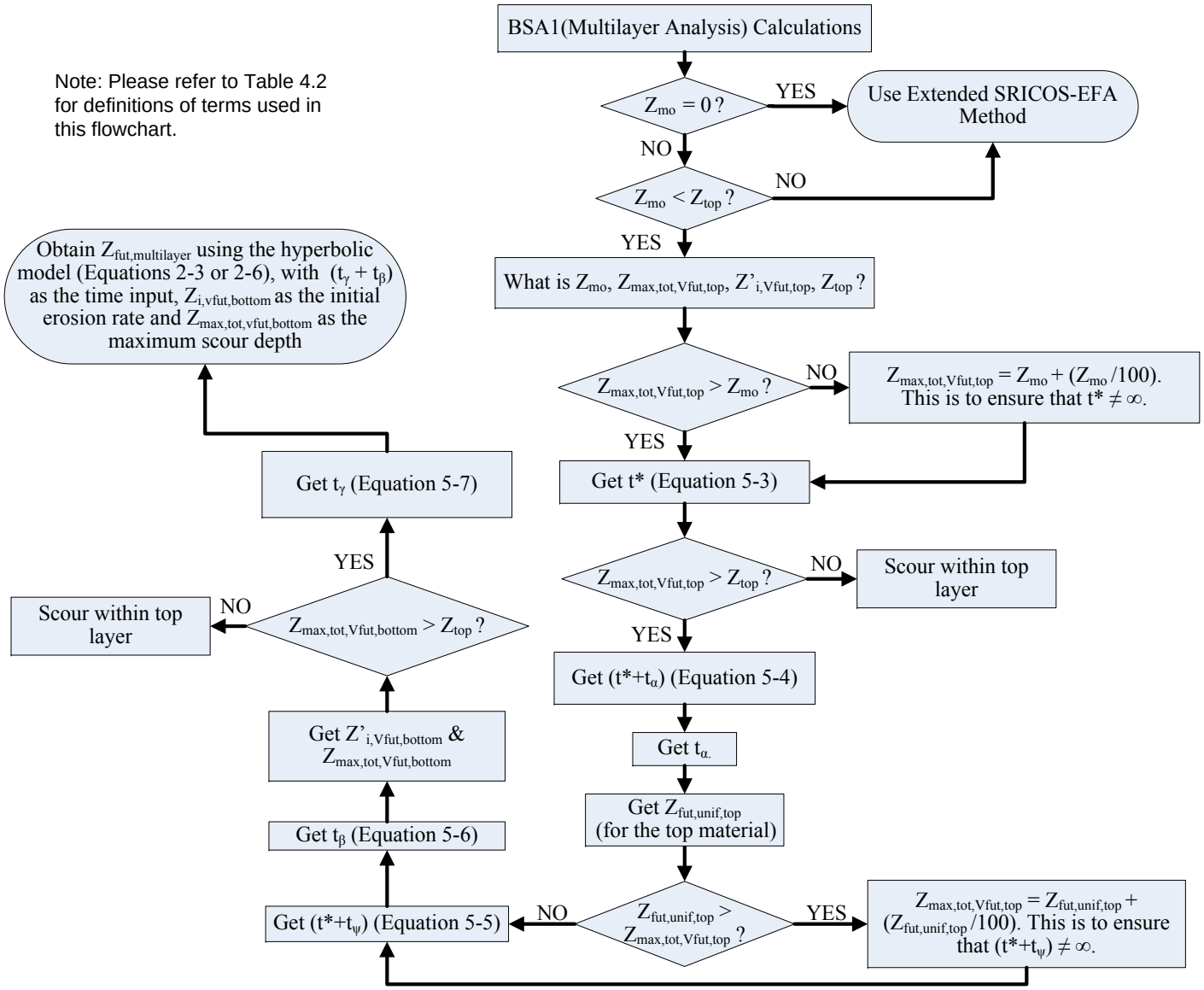

Figure B-1. BSA 1 (Multilayer Analysis) calculation flowchart.

APPENDIX C

Table C-1. Case History No. 1.

District:	Waco (9)
County:	Limestone
Structure No.:	0643-02-038
Source:	Anand4
Highway:	FM 39
River:	Sanders Creek
Status:	Unstable by Concise Analysis
Foundation	Drilled shafts
Pier/Foundation Dimensions:	2.5 ft diameter drilled shaft with approximately 22.5 ft embedment at Bents 5 and 6 (Secondary Scour Evaluation Sheet, Nov. 25, 1996 and Channel Profile Drawing).
Upstream Channel Width:	Not available
Channel Width at Bridge:	Main channel width is approximately 60 ft and total channel width (including left and right overbank) is approximately 315 ft (Channel Profile Drawing)
Material:	Dense sand begins approximately 20 ft below channel bottom. The overlying material is loose, silty sand. (Bridge Scour Action Plan, Nov 25, 1996) and clay (soil boring carried out for the present research)
Year built:	1977
Length:	316 ft
No. of Spans	6-span prestressed concrete box beam superstructure
$Z_{thresh\ 1}$:	11.3 ft based on bearing stability at Bent 5 (Bridge Scour Action Plan, Nov 25, 1996).
$Z_{thresh\ 2}$:	N/A
Critical Scour Location:	Bent 5 (Channel Profile Drawing)

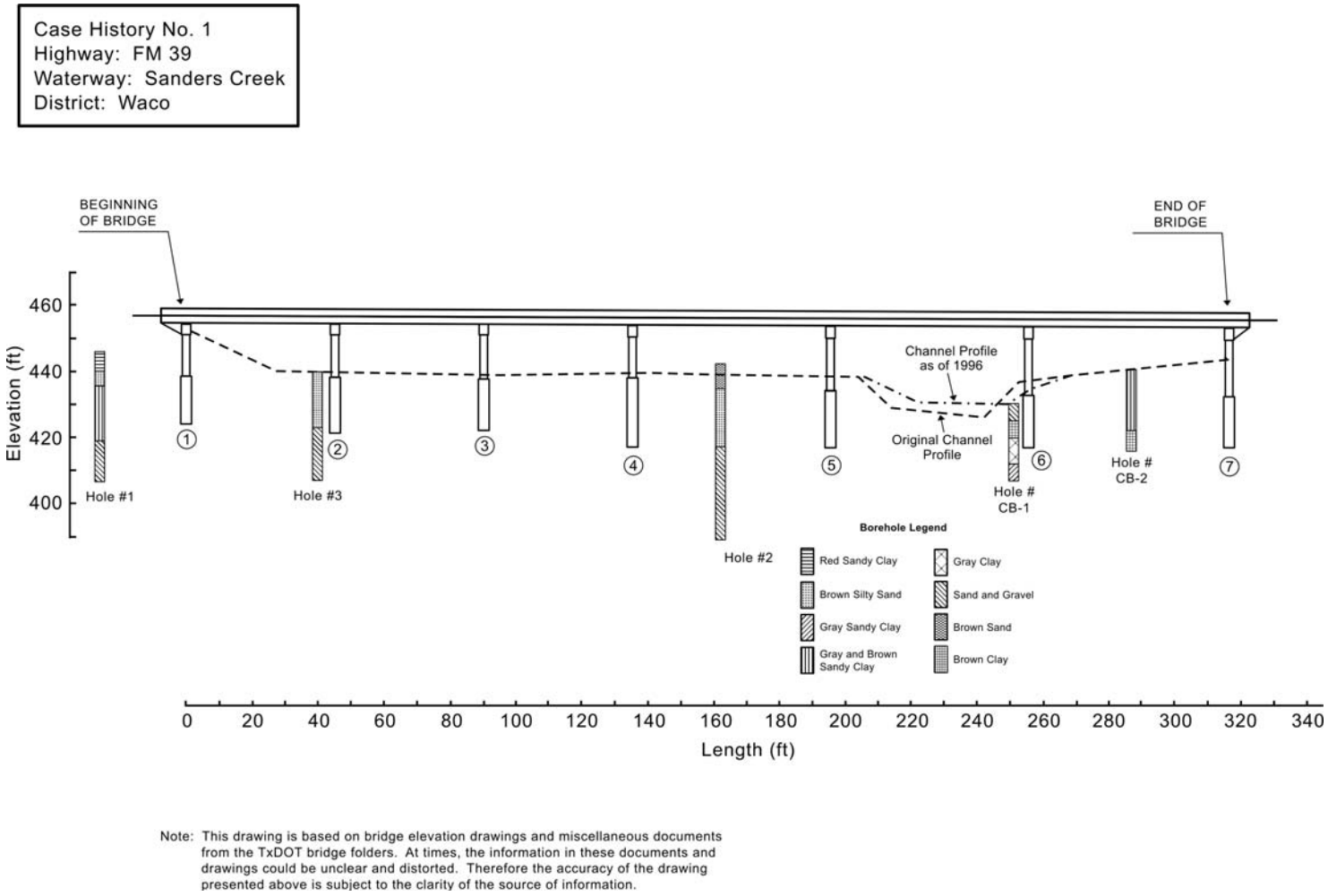

Note: This drawing is based on bridge elevation drawings and miscellaneous documents from the TxDOT bridge folders. At times, the information in these documents and drawings could be unclear and distorted. Therefore the accuracy of the drawing presented above is subject to the clarity of the source of information.

Figure C-1. Case History No. 1 – Bridge Cross-Section.

Table C-2. Case History No. 2.

District:	Bryan (17)
County:	Freestone (082)
Structure No.:	0122-03-036
Source:	Anand4
Highway:	US 287
River:	Alligator Creek (Trinity River Relief)
Status:	Unstable by Concise Analysis
Foundation:	Drilled shafts (Bridge Scour Action Plan 8/6/96)
Pier/Foundation Dimensions:	Drilled shafts that extend a minimum 24 ft below the 8/6/96 channel bed elevation (Bridge Scour Action Plan 8/6/96). The drilled shaft diameter is 2 ft (TSEAS Scour evaluation form Pg. B-1)
Upstream Channel Width:	36 ft (Live Bed Contraction Scour calculation sheet)
Channel Width at Bridge:	32 ft (Live Bed Contraction Scour calculation sheet)
Material:	14 ft of clay underlain by thick sand layer (Bridge Scour Action Plan 8/6/96)
Year built:	1984
Length:	292 ft
No. of Spans:	7 span girder superstructure
$Z_{thresh\ 1}$:	16 ft based on bearing stability (Bridge Scour Action Plan 8/6/96).
$Z_{thresh\ 2}$:	-
Critical Scour Location:	None (Bridge Scour Action Plan 8/6/96)

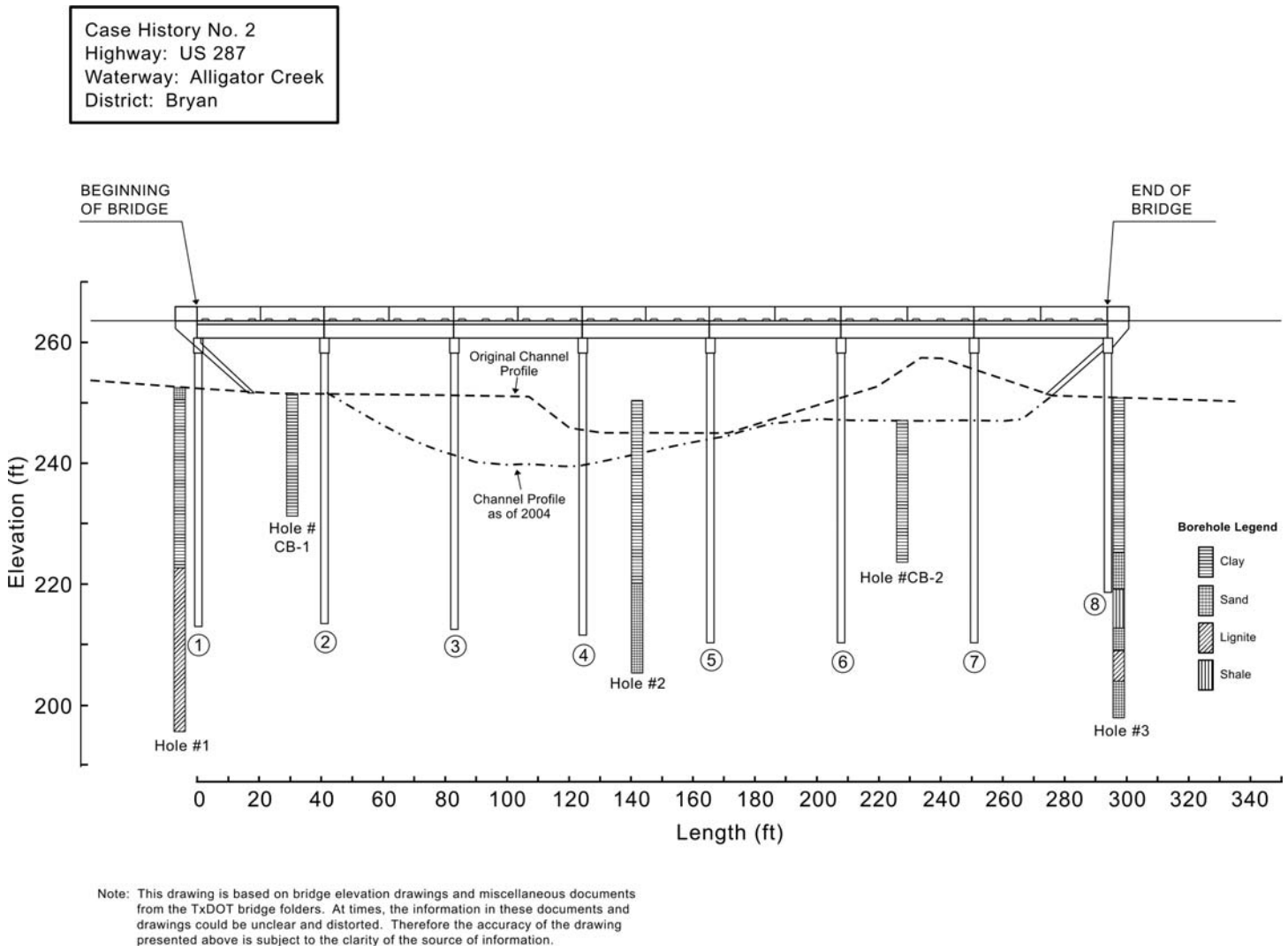

Note: This drawing is based on bridge elevation drawings and miscellaneous documents from the TxDOT bridge folders. At times, the information in these documents and drawings could be unclear and distorted. Therefore the accuracy of the drawing presented above is subject to the clarity of the source of information.

Figure C-2. Case History No. 2 – Bridge Cross-Section.

Table C-3. Case History No. 3.

District:	Houston (12)
County:	Fort Bend (80)
Structure No.:	0188-02-023
Source:	DK20
Highway:	SH 36
River:	Big Creek
Status:	Unstable by Concise Analysis
Foundation:	Concrete piles (Secondary Scour Evaluation, 5/16/94)
Pier /Foundation Dimensions :	14 inch wide concrete piles at Bent 5 (Secondary Scour Evaluation Notes). The concrete piles are approximately 25 ft to 35 ft long (Channel Profile Drawing)
Upstream Channel Width:	40.0 ft (Secondary Scour Evaluation Worksheet 4, 5/10/94)
Channel Width at Bridge:	37.6 ft (Secondary Scour Evaluation Worksheet 4, 5/10/94)
Material:	Deep sand deposit extending 40 ft below the channel bottom (Secondary Scour Evaluation, 5/16/94)
Year built:	1932 (Form 113.2-Bridge Scour Survey, 6/18/91)
Length:	257 (Form 113.2-Bridge Scour Survey, 6/18/91)
No. of Spans:	9 ft (Secondary Scour Evaluation, 5/16/94)
$Z_{thresh\ 1}$:	11 ft at Bent 5 (Secondary Scour Evaluation Notes 1, 5/10/94)
$Z_{thresh\ 2}$:	N/A
Critical Scour Location:	Bents 4, 5 & 6 (Secondary Scour Evaluation, 5/16/94)

Ref. No. (for Z_{thresh})	Measurement Date	Source	Scour depth (ft)	Location	V_{fut} (ft/s)	V_{mo} (ft/s)	V_{fut}/V_{mo}	Z_{mo} (ft)	Z_{fut}/Z_{mo}		$Z_{fut,\ model}$ (ft)	$Z_{fut,field}$ (ft)	$Z_{fut,model}$ /$Z_{fut\ field}$
									Ratio	Notes			
1	1994	CPDM	3.6	Bent 5	-	-	-	-	-	-	-	-	-
1	1995	CPDM	3.8	Bent 5	5.7	6.9	0.83	3.6	1	-	3.6	3.8	0.95
1	1997	CPDM	3.8	Bent 5	4.2	6.9	0.61	3.8	1	-	3.8	3.8	1.0
1	1998	CPDM	3.7	Bent 5	5.1	6.9	0.74	3.8	1	-	3.8	3.7	1.03
1	2001	CPDM	3.5	Bent 5	4.6	6.9	0.66	3.8	1	-	3.8	3.5	1.09
1	1/9/2005	CPDM	2.6	Bent 5	5	6.9	0.72	3.8	1	-	3.8	2.6	1.46
1	1/21/2007	CPDM	2.5	Bent 5	5	6.9	0.72	3.8	1	-	3.8	2.5	1.52

Note: CPDM = Channel Profile Drawings and Channel Profile Measurements

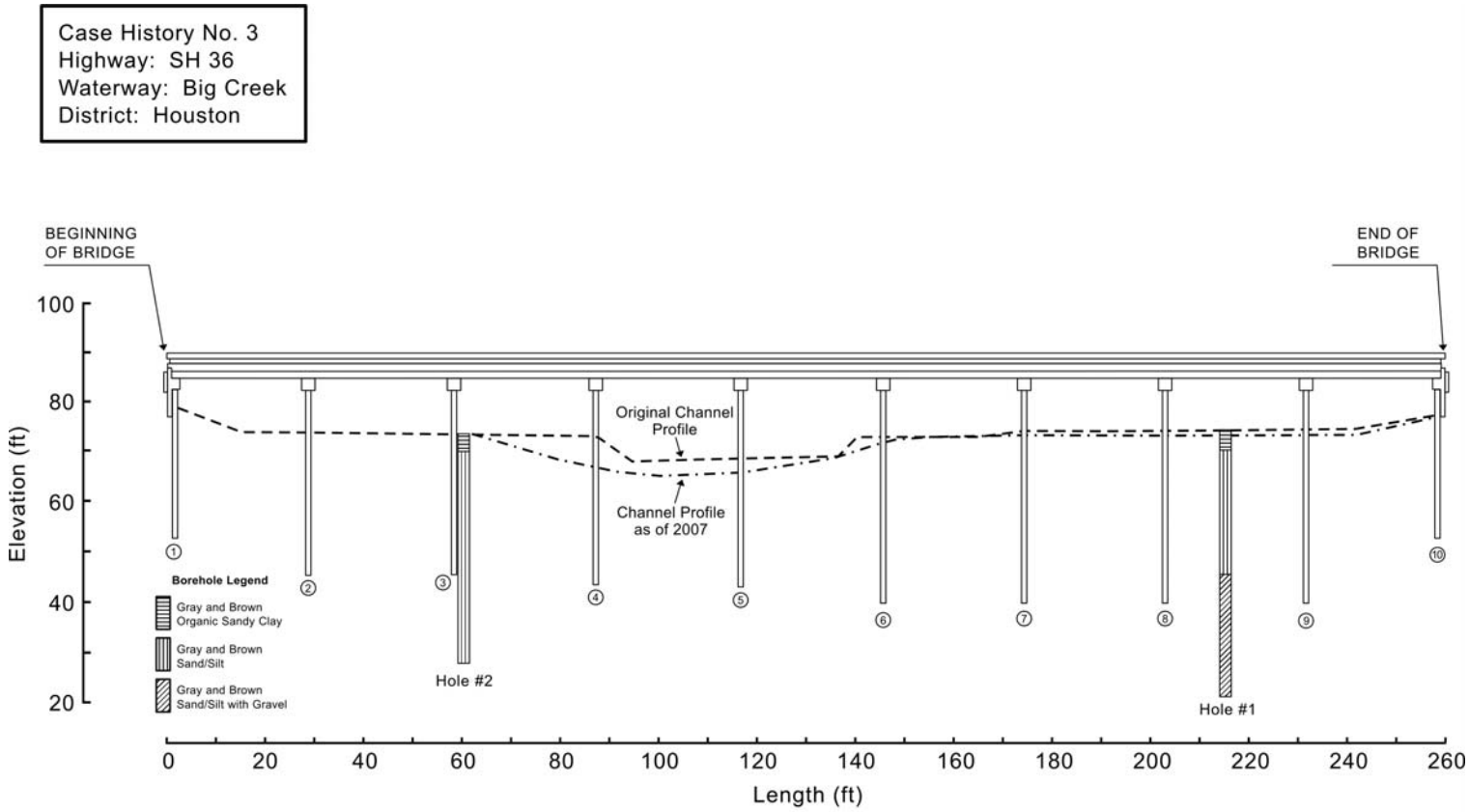

Note: This drawing is based on bridge elevation drawings and miscellaneous documents from the TxDOT bridge folders. At times, the information in these documents and drawings could be unclear and distorted. Therefore the accuracy of the drawing presented above is subject to the clarity of the source of information.

Figure C-3. Case History No.3 – Bridge Cross-Section.

Table C-4. Case History No. 4.

District	Yoakum (13)
County	Gonzales
Structure No.:	090-2080-01-005
Source:	DK20
Highway:	FM 2091
River:	San Marcos River
Status:	On the scour critical list
Foundation:	Precast concrete square piles, steel H-piles and caisson
Pier/Foundation Dimensions:	Bents 2, 3, 4, 7 & 8 consist of concrete caps founded on three 15 inch wide square precast concrete piles that are 32 ft long. Bents 5 & 6 consist of concrete caps, each on two circular columns that are founded on four 14 inch steel H-piles that are 33 ft long. Caisson was added at Bent 5 in 1995.
Upstream Channel Width:	Not available.
Channel Width at Bridge:	40 ft (Computer generated channel profile drawing on 3/23/94)
Material:	Clay and sand.
Year built:	1960
Length:	381.5 ft
No. of Spans:	5 simple spans, 1 continuous span
$Z_{thresh\ 1}$:	16.5 ft (33 ft pile length x 0.5, assumed)
$Z_{thresh\ 2}$:	15 ft (30 ft caisson length x 0.5, assumed)
Critical Scour Location:	Bents 5 and 6 (Underwater inspection report)

Ref. No. (for Z_{thresh})	Measurement Date	Source	Scour depth (ft)	Location	V_{fut} (ft/s)	V_{mo} (ft/s)	V_{fut}/V_{mo}	Z_{mo} (ft)	Z_{fut}/Z_{mo}		$Z_{fut,\ model}$ (ft)	$Z_{fut,\ field}$ (ft)	$Z_{fut,\ model}$ / $Z_{fut\ field}$
									Ratio	Notes			
1	8/2/91	CPD	9 ft	Bent 5	-	-	-	-	-	-	-	-	-
1	1/9/92	CPD	12.4 ft	Bent 5	11.3	12.0	0.94	9	1.15		10.4	12.4	0.84
1	1993	CPD	12.4 ft	Bent 5	7.3	12.0	0.61	12.4	1.00		12.4	12.4	1.00
Caisson added at Bent 5 in 1995.													
2	1997	CPD	-5 ft (deposition)	Bent 5	9.6	12.0	0.80	-	-	-	-	-	-
2	1999	CPD	-1 ft (4 ft of scour compared to 1997)	Bent 6	8.0	12.0	0.66	-	-	-	-	-	-

Note: CPD = Channel Profile Drawings

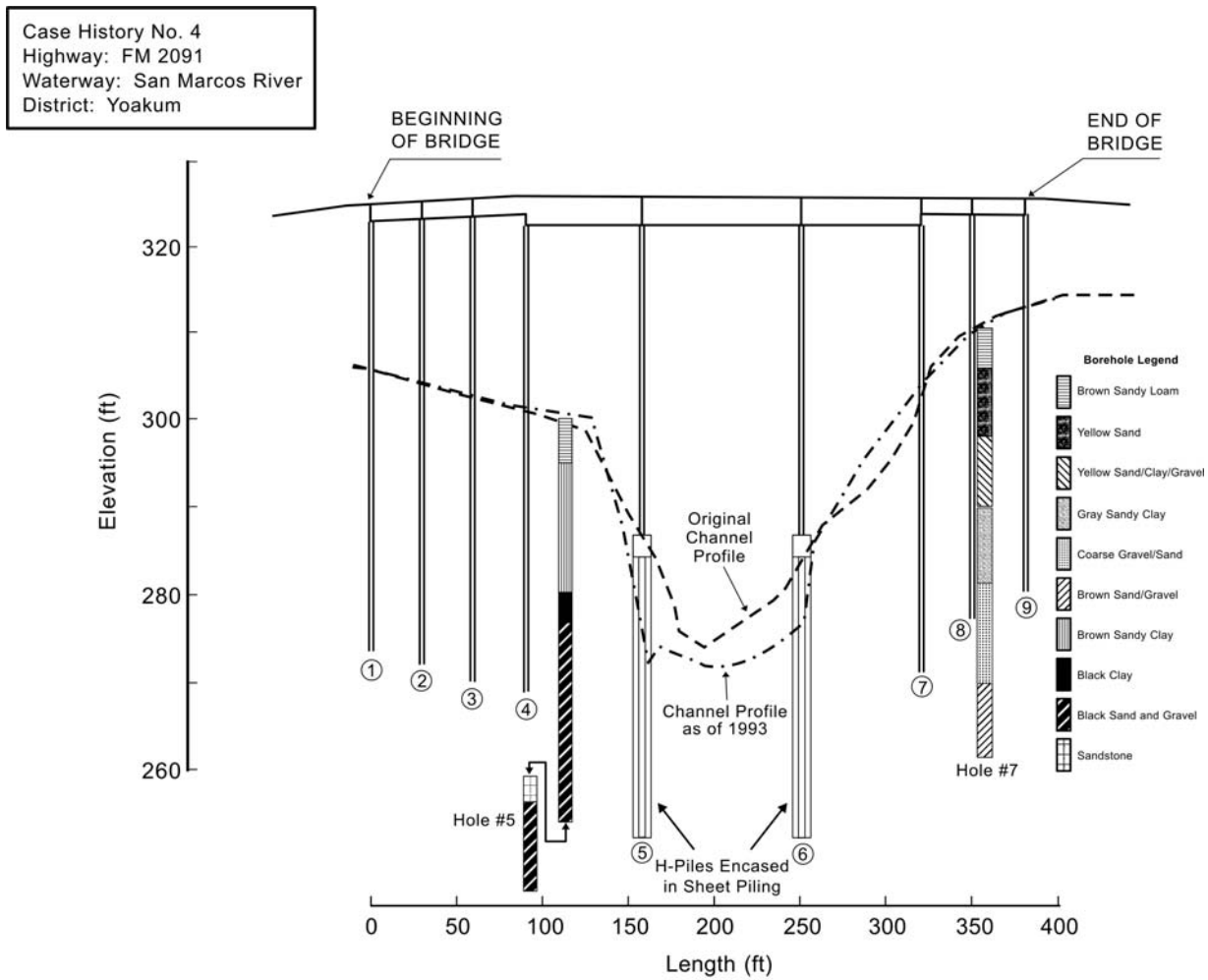

Note: This drawing is based on bridge elevation drawings and miscellaneous documents from the TxDOT bridge folders. At times, the information in these documents and drawings could be unclear and distorted. Therefore the accuracy of the drawing presented above is subject to the clarity of the source of information.

Figure C-4. Case History No.4 – Bridge Cross-Section.

Table C-5: Case History No. 5.

District:	Austin (13)
County:	Austin (08)
Structure No.:	0408-05-019
Source:	DK20
Highway:	FM 331
River:	Mill Creek
Status:	Unstable by Concise Analysis
Foundation:	Precast concrete piles
Pier/Foundation Dimensions:	18 inch wide precast concrete piles that are embedded a minimum 20 ft into the channel bed (Secondary Scour Evaluation - Allowable Scour Depth Worksheet for Bent 4)
Upstream Channel Width:	Not available.
Channel Width at Bridge:	210 ft (HEC-RAS figure)
Material:	Silty sand and clay. It is assumed that at Bent 4, all scour took place in the sand.
Year built:	1951
Length:	271 ft
No. of Spans:	3 simple prestressed concrete beam main spans and 3 pan girder approach spans on concrete pile bents.
$Z_{thresh\ 1}$:	1.46 ft (Allowable scour depth based on lateral stability at Bent 4, Secondary Scour Evaluation Worksheet 1 Notes, Landtech Consultants)
$Z_{thresh\ 2}$:	N/A
Critical Scour Location:	Bent 4 (Secondary Scour Evaluation - Allowable Scour Depth Worksheet 1)

Ref. No. (for Z_{thresh})	Measurement Date	Source	Scour depth (ft)	Location	V_{fut} (ft/s)	V_{mo} (ft/s)	V_{fut}/V_{mo}	Z_{mo} (ft)	Z_{fut}/Z_{mo}		$Z_{fut,\ model}$ (ft)	$Z_{fut,\ field}$ (ft)	$Z_{fut,\ model}$ / $Z_{fut\ field}$
									Ratio	Notes			
1	6/10/93	CPD	0.5	Bent 4	-	-	-	-	-	-	-	-	-
1	6/95	CPD	-3.2 (deposition)	Bent 4	-	-	-	-	-	-	-	-	-
1	4/20/2001	CPD	-3.2 (deposition)	Bent 4	9.43	9.6	0.98	0.5	1.0	-	0.5	-3.2	-0.16
1	7/18/2003	CPD	-3.2 (deposition)	Bent 4	4.69	9.6	0.49	0.5	1.0	-	0.5	-3.2	-0.16

Note: CPD = Channel Profile Drawings

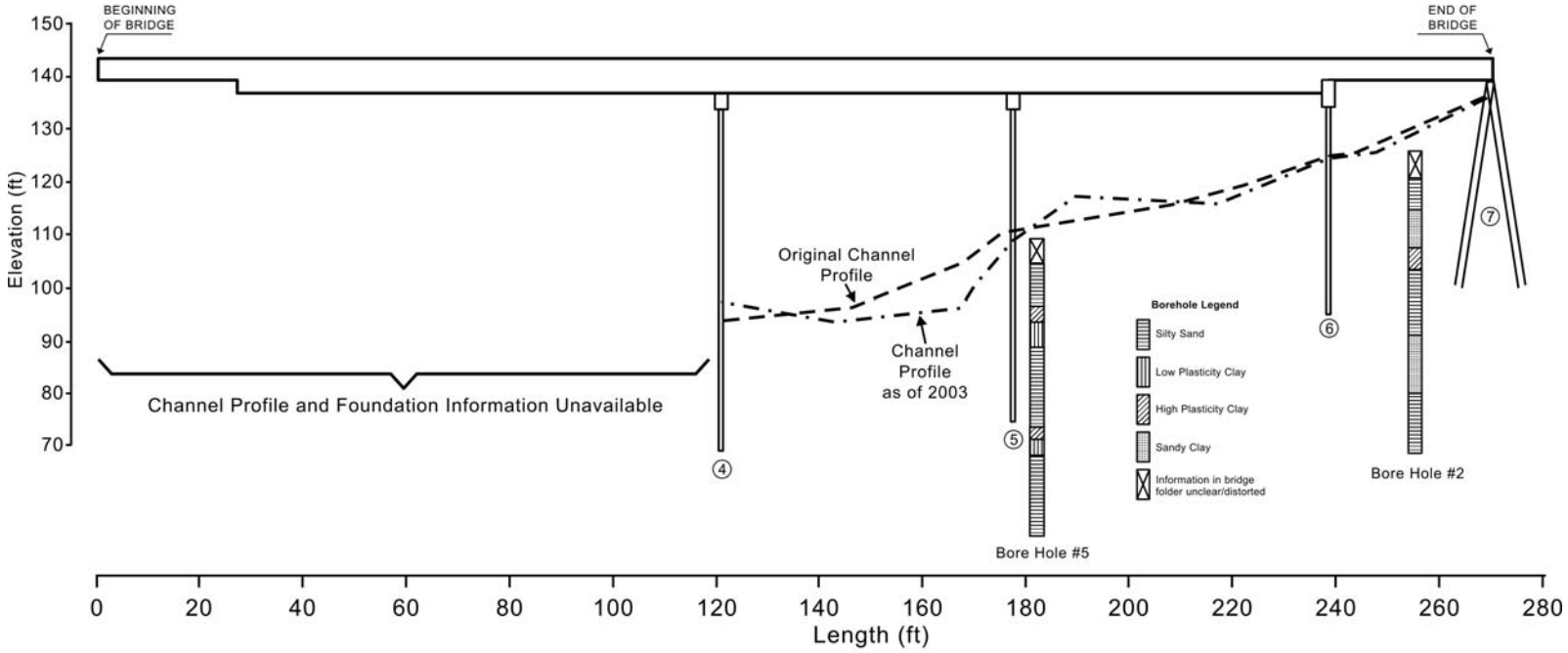

Note: This drawing is based on bridge elevation drawings and miscellaneous documents from the TxDOT bridge folders. At times, the information in these documents and drawings could be unclear and distorted. Therefore the accuracy of the drawing presented above is subject to the clarity of the source of information.

Figure C-5. Case History No.5 – Bridge Cross-Section.

Table C-6. Case History No. 6.

District:	San Antonio
County:	Kendall (131)
Structure No.:	0072-04-020
Source:	DK20
Highway:	US87
River:	Guadalupe River
Status:	Unstable by Concise Analysis
Foundation:	Square piles. Drilled shaft at Bent 27.
Foundation Dimensions :	16 inch wide, 36 ft to 50 ft long concrete square piles (Channel Profile Drawing). 6 ft diameter, 17 ft long drilled shaft at Bent 27 (Secondary Scour Evaluation Worksheet 1)
Channel Upstream Width (ft):	1616.3 (HEC-RAS Output, Page A2)
Channel Width at Bridge (ft):	1199.5 (HEC-RAS Output, Page A2)
Material:	Poor materials, i.e. clay and sandy gravel (Bridge Scour Action Plan 11/30/99).
Year built:	1932. Widened in 1984 (Bridge Scour Action Plan 11/30/99)
Length (ft):	1434 (Channel. Profile dwg)
No. of Spans:	29 concrete slab and girder spans, 2 steel stringer spans, 3 span continuous steel plate girder. (Bridge Scour Action Plan 11/30/99)
$Z_{thresh\ 1}$ (ft)	8.5 (Bridge Scour Action Plan 11/30/99)
$Z_{thresh\ 2}$ (ft)	N/A
Critical Scour Location:	Bent 27 (Bridge Scour Action Plan 11/30/99)

Ref. No. (for Z_{thresh})	Measurement Date	Source	Scour depth (ft)	Location	V_{fut} (ft/s)	V_{mo} (ft/s)	V_{fut}/V_{mo}	Z_{mo} (ft)	Z_{fut}/Z_{mo}		$Z_{fut,\ model}$ (ft)	$Z_{fut,\ field}$ (ft)	$Z_{fut,\ model}/Z_{fut\ field}$
									Ratio	Notes			
1	1998	CPD	6.3	Bent 27	-	-	-	-	-	-	-	-	-
1	2000	CPD	6.3	Bent 27	6.82	25.83	0.26	6.3	1	-	6.3	6.3	1.00

Note: CPD = Channel Profile Drawings

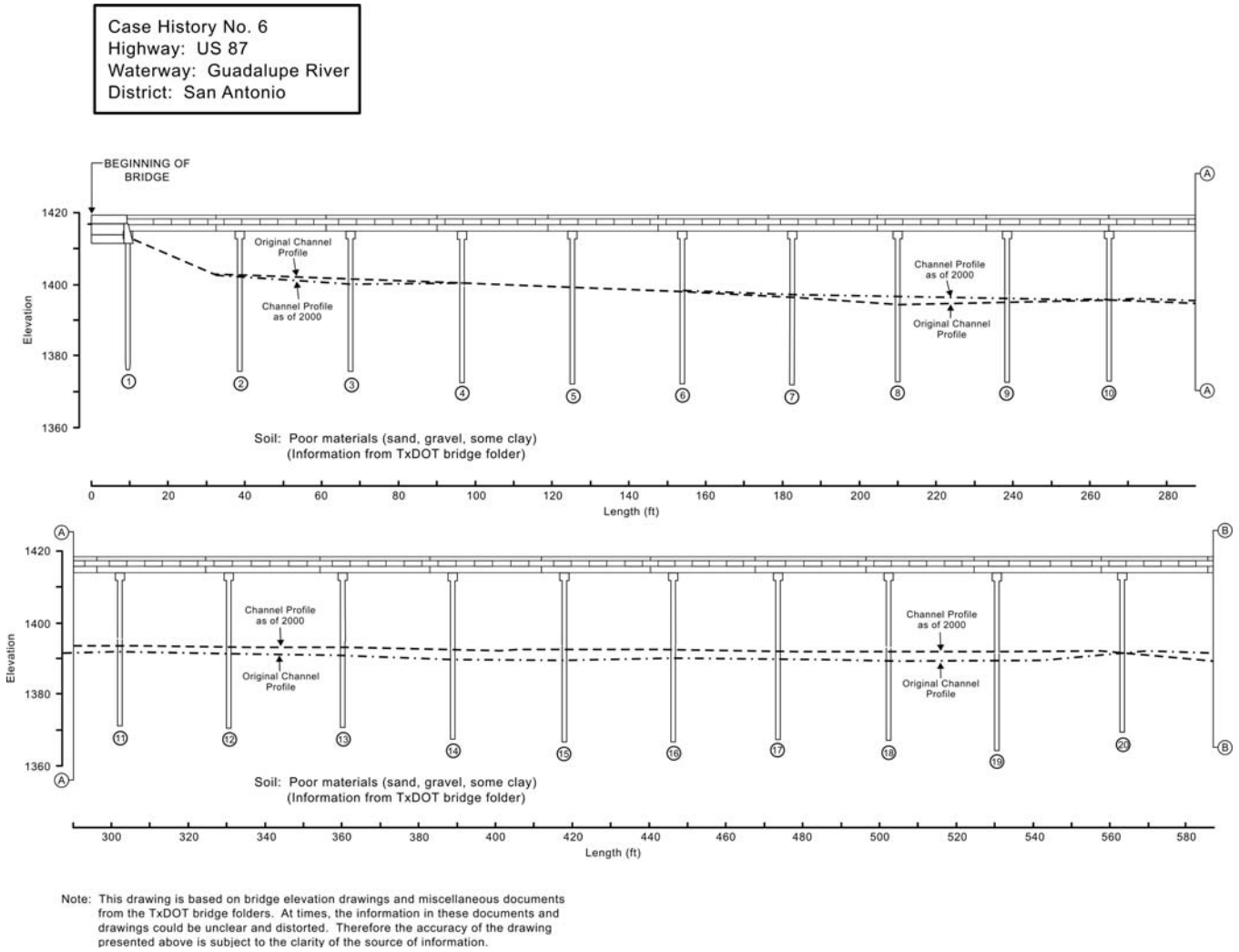

Figure C-6. Case History No. 6 – Bridge Cross-Section Part 1.

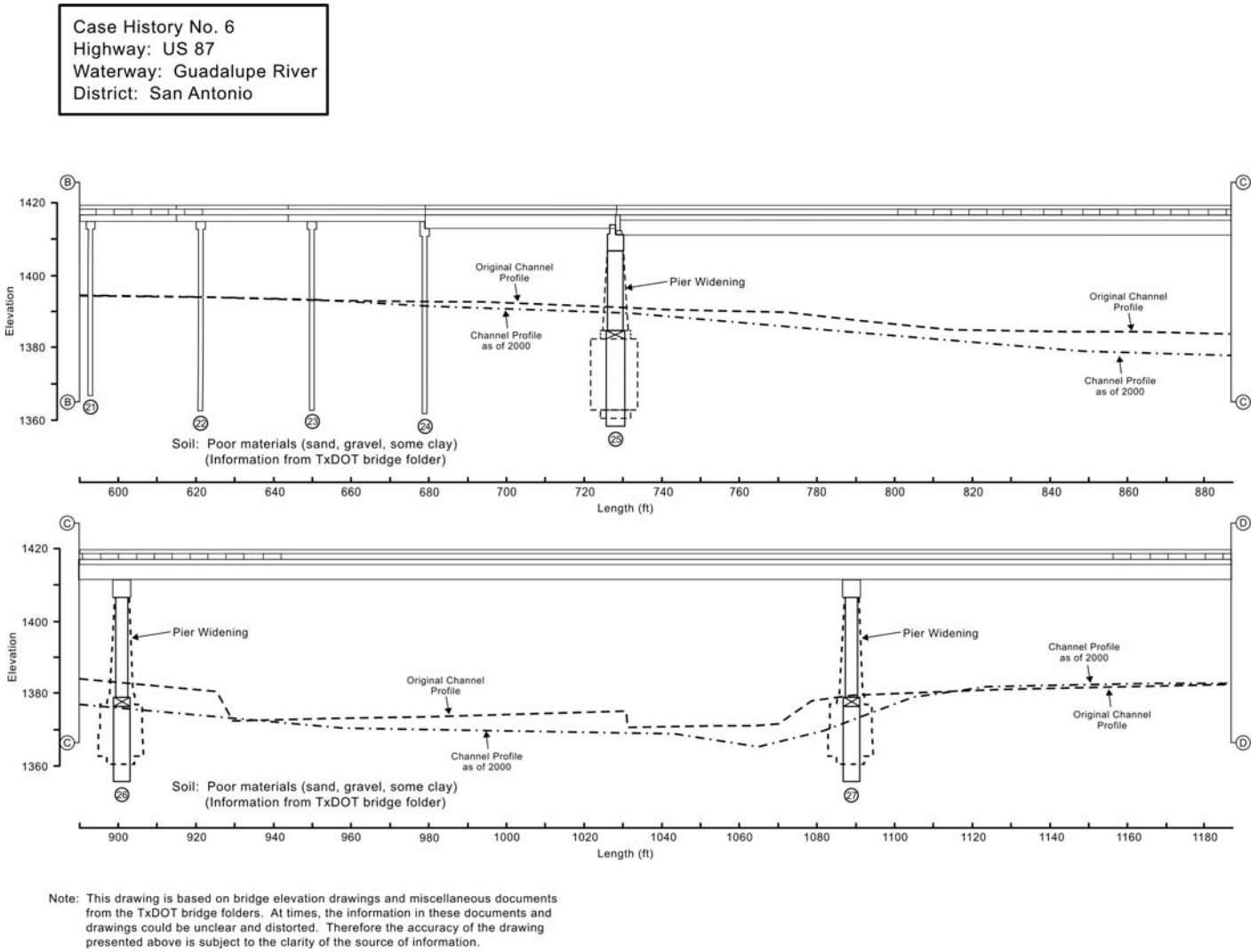

Note: This drawing is based on bridge elevation drawings and miscellaneous documents from the TxDOT bridge folders. At times, the information in these documents and drawings could be unclear and distorted. Therefore the accuracy of the drawing presented above is subject to the clarity of the source of information.

Figure C-6. Case History No. 6 – Bridge Cross-Section Part 2.

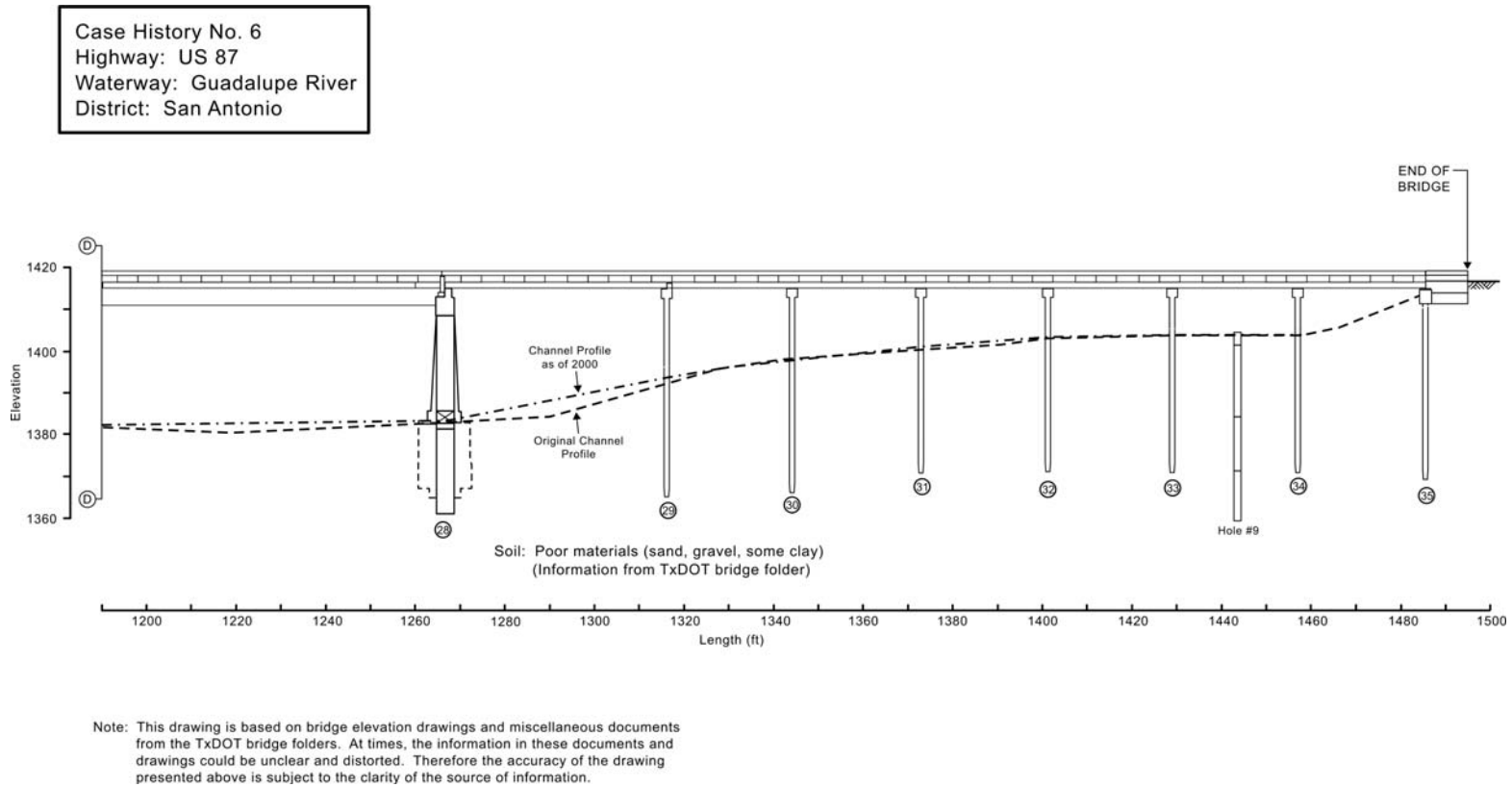

Note: This drawing is based on bridge elevation drawings and miscellaneous documents from the TxDOT bridge folders. At times, the information in these documents and drawings could be unclear and distorted. Therefore the accuracy of the drawing presented above is subject to the clarity of the source of information.

Figure C-6. Case History No. 6 – Bridge Cross-Section Part 3.

Table C-7. Case History No. 7.

District:	Houston (12)
County:	Harris
Structure No.:	0177-06-081
Source:	DK20
Highway:	US59 South Bound
River:	West Fork San Jacinto River
Status:	Unstable by Concise Analysis
Foundation:	Concrete square piles (Summary of Concise Analysis Results, 5/27/94)
Pier/Foundation Dimensions :	16 inch wide concrete square piles with a minimum length of 10 ft (Summary of Concise Analysis Results, 5/27/94)
Upstream Channel Width:	270 ft (Secondary Scour Evaluation Worksheet 4)
Channel Width at Bridge:	187 ft (Secondary Scour Evaluation Worksheet 4)
Material:	Foundation is embedded in more than 10 ft of sand (Summary of Results of Secondary Screening and Field Visit, 3/30/94)
Year built:	1961 (Form 113.2 - Bridge scour survey, 6/12/91)
Length:	1645 (Form 113.2 - Bridge scour survey, 6/12/91)
No. of Spans:	26
$Z_{thresh\ 1}$:	0 ft (Summary of Concise Analysis Results, 5/27/94)
$Z_{thresh\ 2}$:	N/A
Critical Scour Location:	Bent 15 (TSEAS Secondary Scour Evaluation Worksheet 1)

Ref. No. (for Z_{thresh})	Measurement Date	Source	Scour depth (ft)	Location	V_{fut} (ft/s)	V_{mo} (ft/s)	V_{fut}/V_{mo}	Z_{mo} (ft)	Z_{fut}/Z_{mo}		$Z_{fut,model}$ (ft)	$Z_{fut,\ field}$ (ft)	$Z_{fut,model}/Z_{fut\ field}$
									Ratio	Notes			
1	2/10/95	CCMR	0	Bent 15	-	-	-	-	-	-	-	-	-
1	1/29/97	CCMR	-0.3	Bent 15	11.1	9.8	1.13	0	1.5	-	-	-	-
1	1999	CCMR	1.6	Bent 15	7.4	11.1	0.67	0	1	-	-	-	-
1	1/2003	CCMR	-1.1	Bent 15	9	11.1	0.81	1.6	1	-	1.6	-1.1	-1.45
1	2/28/2007	CPD	5.7	Bent 15	7.8	11.1	0.70	1.6	1	-	1.6	5.7	0.28

Note: CCMR = Channel Cross-section Measurement Records; CPD = Channel Profile Drawing

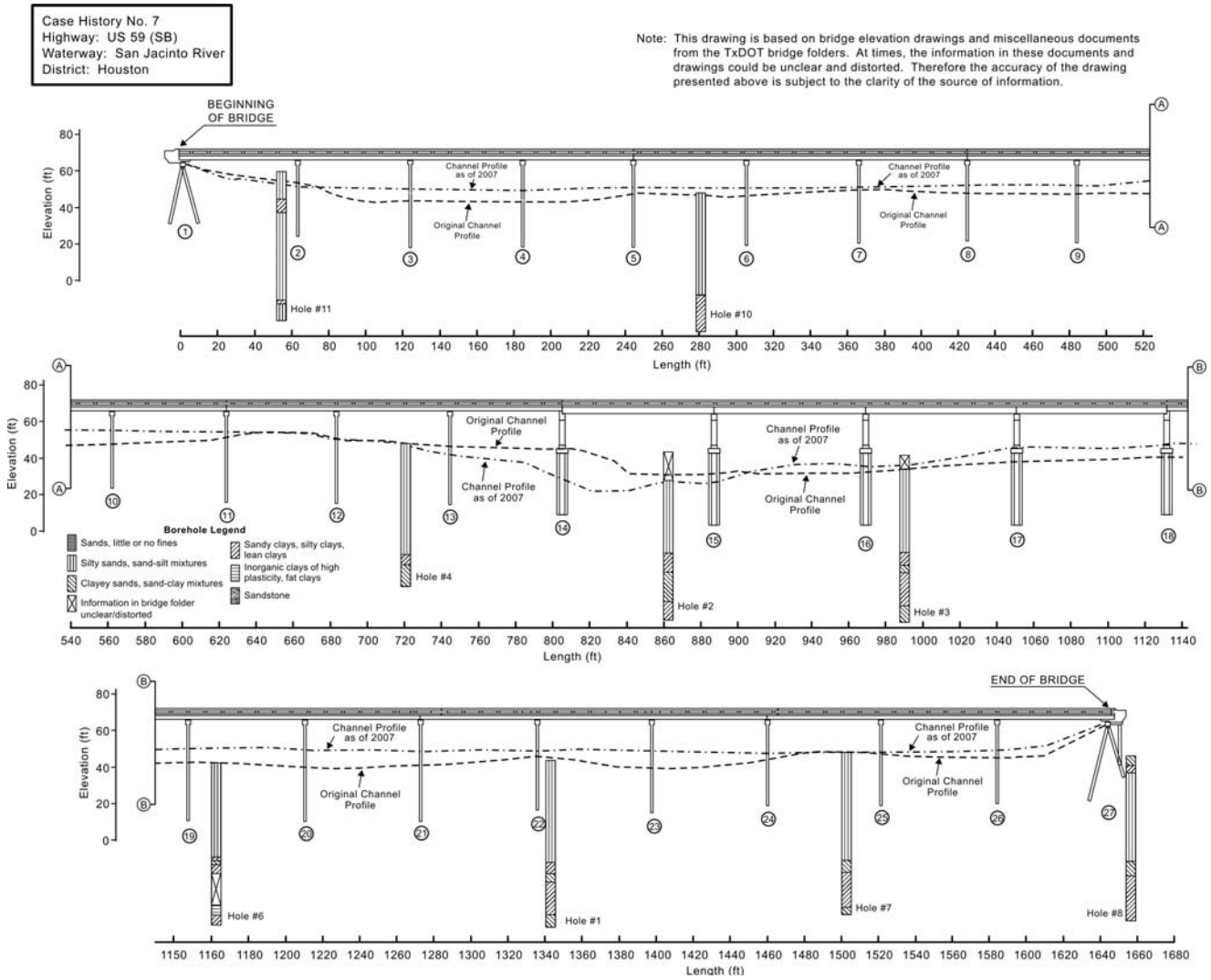

Figure C-7. Case History No. 7 – Bridge Cross-Section.

Table C-8. Case History No. 8.

District:	San Antonio (15)
County:	Kerr (133)
Structure No.:	0142-03-008
Source:	DK20
Highway:	SH 27
River:	Dry Branch Creek
Status:	Unstable by Concise Analysis
Foundation:	Original bridge is on spread footings in shale clay. Widened portion of the bridge is on drilled shafts embedded in limestone or shale (Bridge Scour Action Plan, 11/15/99)
Pier/Foundation Dimensions :	2 ft diameter drilled shafts (Secondary Scour Evaluation Worksheet 2 (A6) - at Bent 4). The length of the drilled shafts are approximately 15 ft. The spread footings are embedded approximately 10 ft to 15 ft below the channel bottom (Channel Profile Drawing)
Upstream Channel Width:	84.11 ft (Secondary Scour Evaluation Worksheet 4)
Channel Width at Bridge:	78.11 ft (Secondary Scour Evaluation Worksheet 4)
Material:	Clay, shale, limestone (Bridge Scour Action Plan, 11/15/99)
Year built:	1935, widened in 1963
Length:	142 ft (Bridge Scour Action Plan)
No. of Spans:	5 span concrete slab
$Z_{thresh\ 1}$:	7.43 ft at Bent 4 (Bridge Scour Action Plan, 11/15/99)
$Z_{thresh\ 2}$:	N/A
Critical Scour Location:	Bent 4 (Bridge Scour Action Plan, 11/15/99)

Ref. No. (for Z_{thresh})	Measurement Date	Source	Scour depth (ft)	Location	V_{fut} (ft/s)	V_{mo} (ft/s)	V_{fut}/V_{mo}	Z_{mo} (ft)	Z_{fut}/Z_{mo}		$Z_{fut,\ model}$ (ft)	$Z_{fut,\ field}$ (ft)	$Z_{fut,\ model}/Z_{fut\ field}$
									Ratio	Notes			
1	1996	CPD	9	Bent 4	Data missing between 1994 and 1999	-	-	-	-	-	-	-	-
1	1998	CPD	3	Bent 4		-	-	-	-	-	-	-	-
1	2000	CPD	3	Bent 4	-	-	-	-	-	-	-	-	-
1	2003	CPD	3	Bent 4	11.6	16.9	0.69	9	1	-	9	3	3
1	2004	CPD	3	Bent 4	10.4	16.9	0.62	9	1	-	9	3	3
1	2006	CPD	3	Bent 4	2.87	16.9	0.17	9	1	-	9	3	3

Note: CPD = Channel Profile Drawings

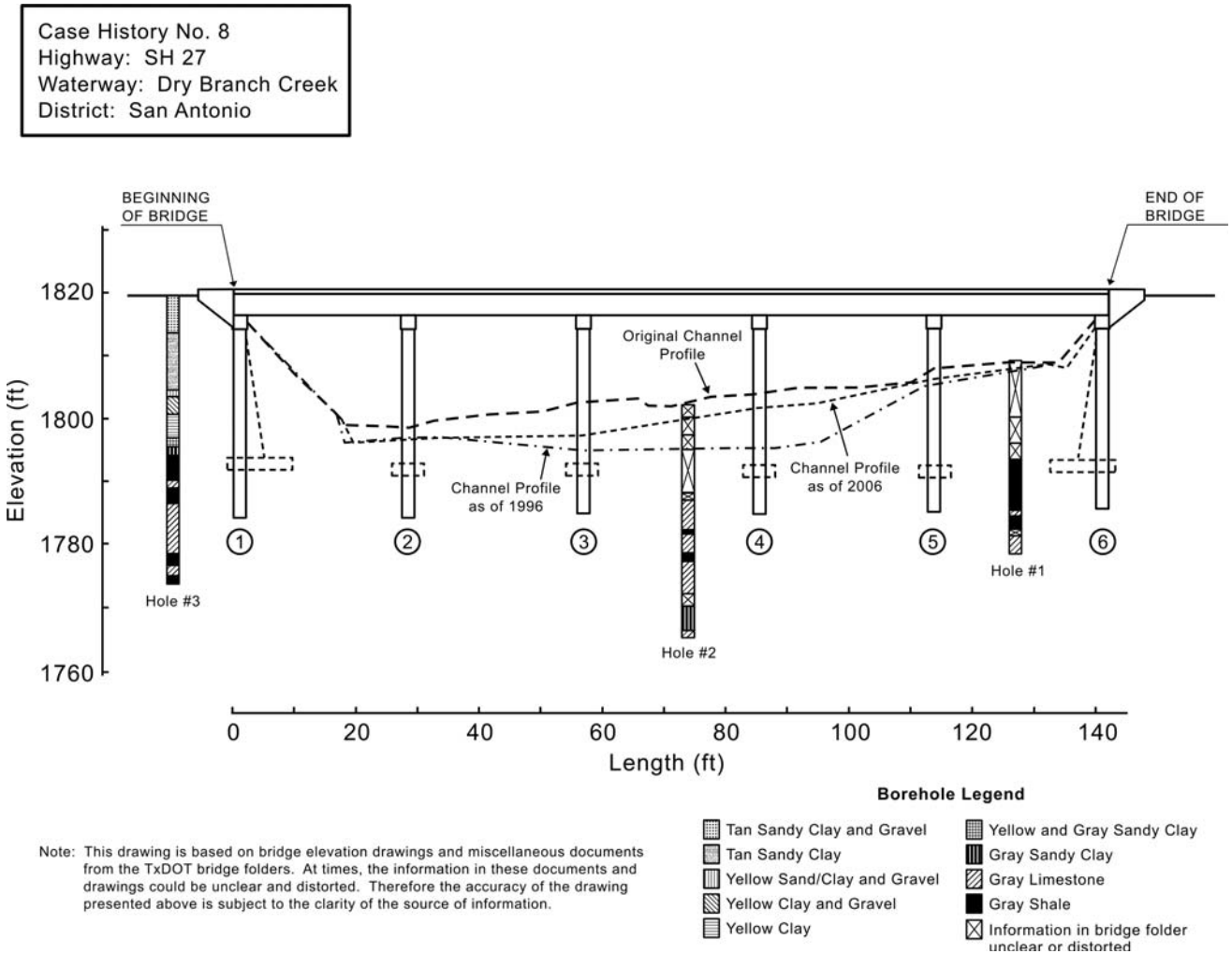

Figure C-8. Case History No. 8 – Bridge Cross-Section.

Table C-9: Case History No. 9.

District:	Houston (12)
County:	Montgomery
Structure No.:	170-0177-05-119
Source:	DK20
Highway:	US59 @ Creekwood Drive
River:	Peach Creek
Status:	Unstable by Concise Analysis
Foundation:	Concrete square piles (Form 113.2 - Bridge Scour Survey)
Pier/Foundation Dimensions :	16 inch wide concrete square piles that are approximately 35 ft long (Secondary Scour Evaluation Sheet, 5/25/94 and Channel Profile Drawing)
Upstream Channel Width:	650 ft (Secondary Scour Evaluation Worksheet s 4, 5/25/1994)
Channel Width at Bridge:	Information unclear
Material:	10 ft of sand (Secondary Scour Evaluation Cover Sheet, 3/31/94)
Year built:	1970 (Form 113.2 - Bridge Scour Survey)
Length:	120 ft (Form 113.2 - Bridge Scour Survey)
No. of Spans:	3 (Channel Profile Dwg.)
$Z_{thresh\ 1}$:	17.5 ft at Bents 2 & 3 (Secondary Scour Evaluation Sheet, 5/25/94)
$Z_{thresh\ 2}$:	N/A
Critical Scour Location:	Bents 2 & 3 (Secondary Scour Evaluation Sheet, 5/25/94 & Channel Profile Drawing)

Ref. No. (for Z_{thresh})	Measurement Date	Source	Scour depth (ft)	Location	V_{fut} (ft/s)	V_{mo} (ft/s)	V_{fut}/V_{mo}	Z_{mo} (ft)	Z_{fut}/Z_{mo}		$Z_{fut,\ model}$ (ft)	$Z_{fut,\ field}$ (ft)	$Z_{fut,\ model}$ / $Z_{fut\ field}$
									Ratio	Notes			
1	1/7/1999	CPDM	8.2	Bent 2	-	-	-	-	-	-	-	-	-
1	1/19/2001	CPDM	5.1	Bent 2	4.5	13.7	0.33	8.2	1	-	8.2	5.1	1.6
1	1/2/2003	CPDM	7.9	Bent 2	8.6	13.7	0.63	8.2	1	-	8.2	7.9	1.0
1	1/21/2005	CPDM	8.5	Bent 2	8.1	13.7	0.60	8.2	1	-	8.2	8.5	1.0
1	12/4/2006	CPD	8	Bent 2	6.5	13.7	0.47	8.5	1	-	8.5	8	1.1
1	1/19/2001	CPDM	9	Bent 3	-	-	-	-	-	-	-	-	-
1	1/2/2003	CPDM	8.8	Bent 3	8.6	13.7	0.63	9	1	-	9	8.8	1.0
1	1/21/2005	CPDM	8.1	Bent 3	8.1	13.7	0.59	9	1	-	9	8.1	1.1
1	12/4/2006	CPD	10.7	Bent 3	6.5	13.7	0.47	9	1	-	9	10.7	0.8

Note: CPDM = Channel Profile Drawings and Channel Profile Measurements; CPD = Channel Profile Drawings

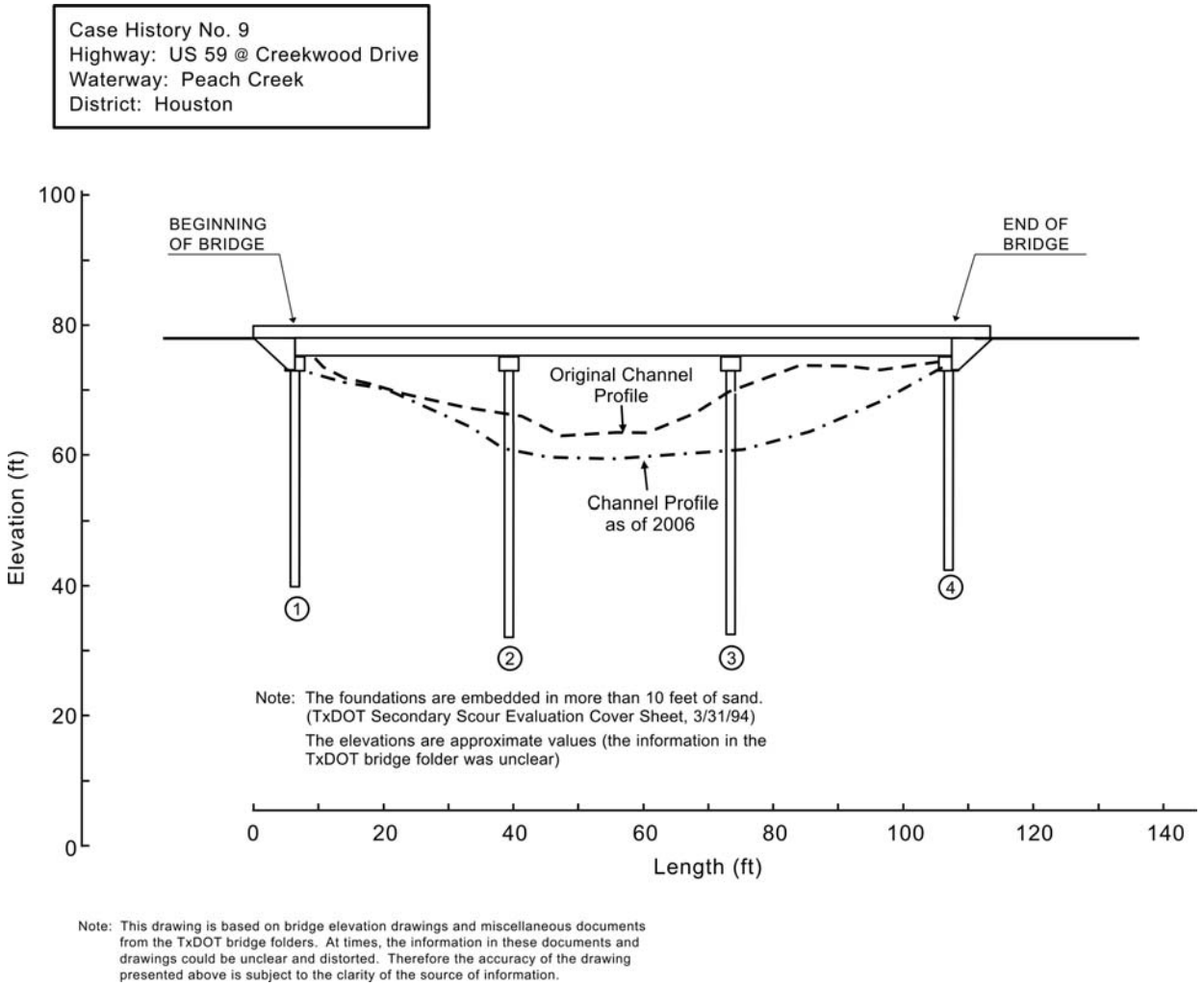

Figure C-9. Case History No. 9 – Bridge Cross-Section.

Table C-10. Case History No. 10.

District:	Houston (12)
County:	80
Structure No.:	0027-08-092
Source:	DK20
Highway:	US90A (WB)
River:	Brazos River
Status:	On the scour critical list
Foundation:	Square piles (Channel Profile Drawing, Russell -Veteto Engineering)
Pier/Foundation Dimensions :	16 inch to 20 inch wide square piles that are approximately 70 ft to 78 ft long (Channel Profile Drawing, Russell-Veteto Engineering)
Upstream Channel Width:	Not available
Channel Width at Bridge:	Not available
Material:	Silty sand, clayey sand (Channel Profile Drawing)
Year built:	1965 (Form 113.2-Bridge Scour Survey, 6/17/91)
Length:	942 ft (Form 113.2-Bridge Scour Survey, 6/17/91)
No. of Spans:	10 (Bridge Inspection Record, 2/4/07)
$Z_{thresh\ 1}$:	39 ft at Bent 3 (Taken as half pile length obtained from Channel Profile Drawing, Russell-Veteto Engineering)
$Z_{thresh\ 2}$:	N/A
Critical Scour Location:	Not specified

Ref. No. (for Z_{thresh})	Measurement Date	Source	Scour depth (ft)	Location	V_{fut} (ft/s)	V_{mo} (ft/s)	V_{fut}/V_{mo}	Z_{mo} (ft)	Z_{fut}/Z_{mo}		$Z_{fut,\ model}$ (ft)	$Z_{fut,\ field}$ (ft)	$Z_{fut,\ model}/Z_{fut\ field}$
									Ratio	Notes			
1	1992	CPD	19	Bent 3	-	-	-	-	-	-	-	-	-
1	3/28/1997	CPD	16.5	Bent 3	13.5	13.9	0.97	19	1	-	19	16.5	1.2
1	1999	CPD	21	Bent 3	11.9	13.9	0.86	19	1	-	19	21	0.9
1	2000	CPD	15	Bent 3	13.2	13.9	0.95	21	1	-	21	15	1.4
1	2002	CPD	15	Bent 3	11.5	13.9	0.83	21	1	-	21	15	1.4
1	2/4/07	CPD	20	Bent 3	13.1	13.9	0.94	21	1	-	21	20	1.05

Note: CPD = Channel Profile Drawings

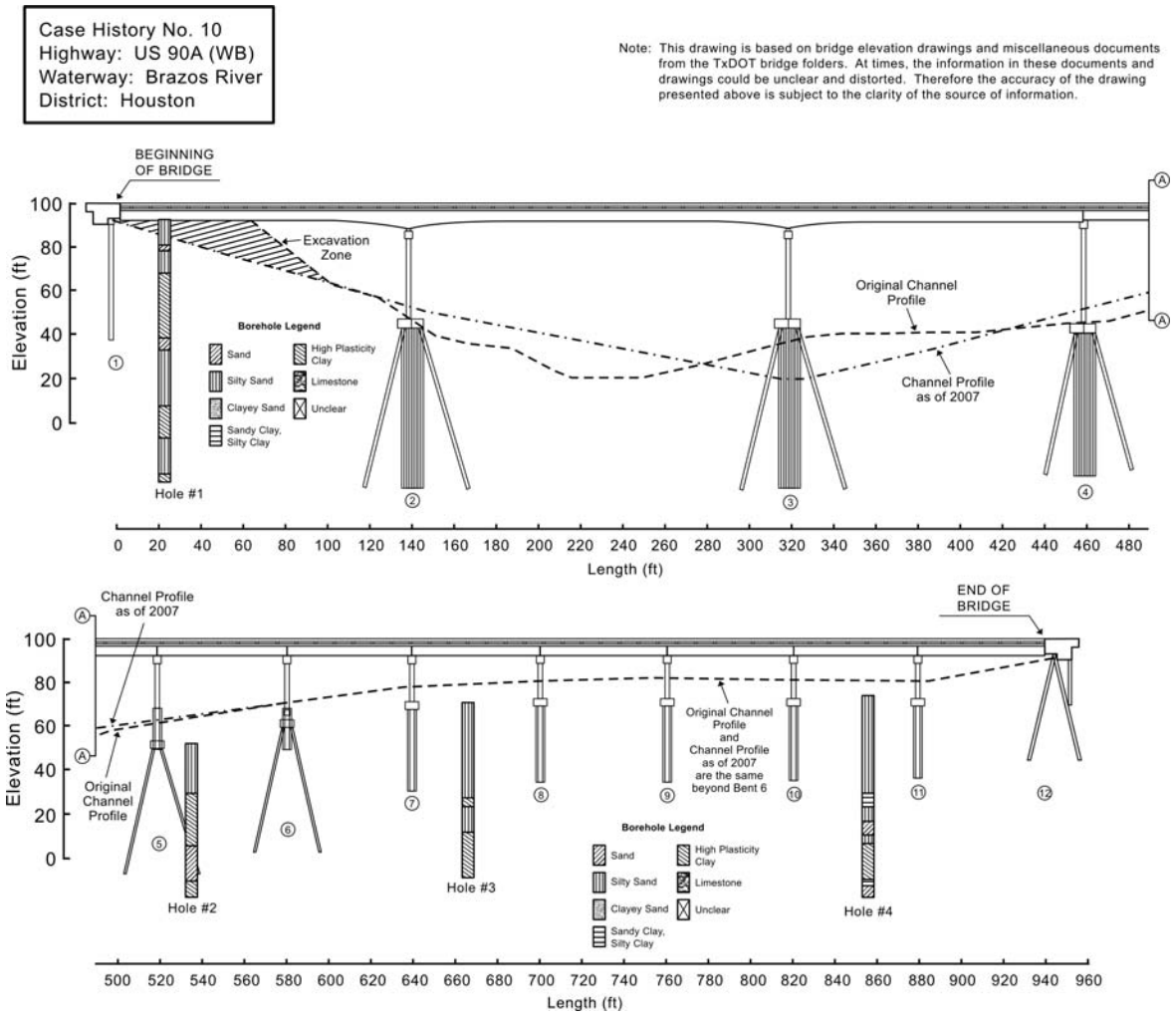

Figure C-10. Case History No.10 – Bridge Cross-Section.

Table C-11. Case History No. 11.

District:	Bryan (17)
County:	Leon (145)
Structure No.:	0382-05-021
Source:	Kiseok8
Highway:	SH7 (8 miles downstream of Lake Limestone dam and reservoir - Bridge Scour Action Plan)
River:	Navasota River
Status:	Stable by Concise Analysis
Foundation:	Concrete piles (Bridge Inventory Record, 1/18/99)
Pier/Foundation Dimensions :	14 inch diameter concrete piles that are approximately 28 ft to 50 ft long (Pier Scour Calculation Sheet, 8/1/96 and Channel Profile Drawing)
Upstream Channel Width:	70 ft (Contraction Scour Calculation Sheet, 8/1/96)
Channel Width at Bridge:	50 ft (Contraction Scour Calculation Sheet, 8/1/96)
Material:	Sand (Bridge Scour Action Plan, 8/6/96)
Year built:	1956 (Bridge Scour Action Plan, 8/6/96)
Length:	271 ft (Bridge Scour Action Plan, 8/6/96)
No. of Spans:	7 (Bridge Scour Action Plan, 8/6/96)
$Z_{thresh\ 1}$:	17.5 ft (Taken as half pile embedment length, from Channel Profile Drawing)
$Z_{thresh\ 2}$:	N/A
Critical Scour Location:	Bent 5 (Bridge Scour Action Plan, 8/6/96)

Ref. No. (for Z_{thresh})	Measurement Date	Source	Scour depth (ft)	Location	V_{fut} (ft/s)	V_{mo} (ft/s)	V_{fut}/V_{mo}	Z_{mo} (ft)	Z_{fut}/Z_{mo}		$Z_{fut,\ model}$ (ft)	$Z_{fut,\ field}$ (ft)	$Z_{fut,\ model}/Z_{fut\ field}$
									Ratio	Notes			
1	11/1994	CPD	4.0	Bent 5	-	-	-	-	-	-	-	-	-
1	1996	CPDM	6.2	Bent 5	3.7	5.9	0.63	4.0	1	-	4.0	6.2	0.7
1	12/14/1998	CPDM	6.2	Bent 5	4.6	5.9	0.78	6.2	1	-	6.2	12.5	0.9
1	4/16/01	CPDM	6.2	Bent 5	5	5.9	0.85	6.2	1	-	6.2	6.2	1
1	3/13/2003	CPDM	7.6	Bent 5	4.5	5.9	0.76	6.2	1	-	6.2	7.6	0.8
1	3/17/05	CPDM	8.1	Bent 5	3.4	5.9	0.58	7.6	1	-	7.6	8.1	0.9

Note: CPDM = Channel Profile Drawings and Channel Profile Measurements; CPD = Channel Profile Drawings

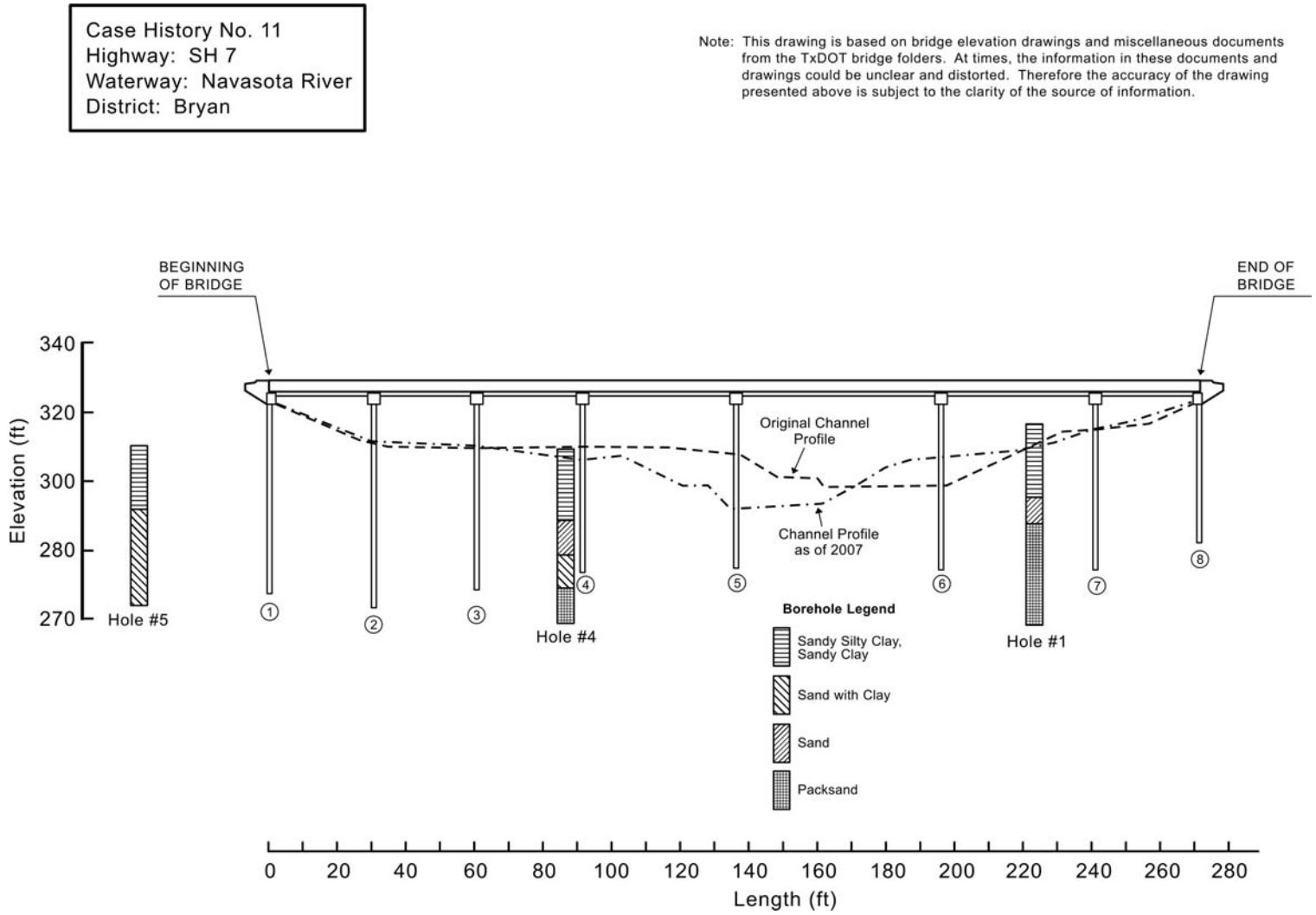

Figure C-11. Case History No.11 – Bridge Cross-Section.

Table C-12. Results of validation of BSA 2 for Case History No. 1.

Case History No.	Waterway	Highway	Sample No.	Sample Type	$V_{c,test}$ (m/s)	$V_{c,chart}$ (m/s)	V_{appr} (m/s)	Pier Diameter (m)	Upstream Water Depth (m)	Contraction Ratio	$Z_{max,I\text{-}EFA}$ (m)	$Z_{max,I\text{-}BSA2}$ (m)	$Z_{max,I\text{-}BSA2}$ / $Z_{max,I\text{-}EFA}$
1	Sanders Creek	FM 39	1464	CL	0.4	0.51	0.5	0.1	10	0.5	2.05	1.84	0.90
							3.5	0.1	10	0.5	18.36	18.15	0.99
							0.5	1	10	0.5	2.63	2.42	0.92
							3.5	1	10	0.5	20.34	20.13	0.99
							0.5	10	10	0.5	5.11	4.90	0.96
							3.5	10	10	0.5	28.87	28.66	0.99
							0.5	0.1	20	0.5	2.83	2.53	0.89
							3.5	0.1	20	0.5	25.72	25.42	0.99
							0.5	1	20	0.5	3.41	3.11	0.91
							3.5	1	20	0.5	27.70	27.40	0.99
							0.5	10	20	0.5	5.89	5.59	0.95
							3.5	10	20	0.5	36.23	35.93	0.99
							0.5	0.1	10	0.9	0.88	0.67	0.76
							3.5	0.1	10	0.9	10.12	9.91	0.98
							0.5	1	10	0.9	1.45	1.24	0.85
							3.5	1	10	0.9	12.10	11.89	0.98
							0.5	10	10	0.9	3.93	3.72	0.95
							3.5	10	10	0.9	20.64	20.43	0.99
							0.5	0.1	20	0.9	1.17	0.87	0.74
							3.5	0.1	20	0.9	14.07	13.77	0.98
							0.5	1	20	0.9	1.74	1.44	0.83
							3.5	1	20	0.9	16.05	15.75	0.98
							0.5	10	20	0.9	4.22	3.93	0.93
							3.5	10	20	0.9	24.59	24.29	0.99
1	Sanders Creek	FM 39	1466	CH	0.9	0.73	0.5	0.1	10	0.5	1.09	1.42	1.30
							3.5	0.1	10	0.5	17.40	17.73	1.02
							0.5	1	10	0.5	1.67	2.00	1.20
							3.5	1	10	0.5	19.38	19.71	1.02
							0.5	10	10	0.5	4.15	4.48	1.08
							3.5	10	10	0.5	27.92	28.24	1.01
							0.5	0.1	20	0.5	1.48	1.94	1.31
							3.5	0.1	20	0.5	24.36	24.82	1.02
							0.5	1	20	0.5	2.05	2.51	1.22
							3.5	1	20	0.5	26.34	26.80	1.02
							0.5	10	20	0.5	4.53	4.99	1.10
							3.5	10	20	0.5	34.88	35.34	1.01
							0.5	0.1	10	0.9	0.00	0.24	243.77
							3.5	0.1	10	0.9	9.17	9.49	1.04
							0.5	1	10	0.9	0.49	0.82	1.66
							3.5	1	10	0.9	11.14	11.47	1.03
							0.5	10	10	0.9	2.97	3.30	1.11
							3.5	10	10	0.9	19.68	20.01	1.02
							0.5	0.1	20	0.9	0.00	0.27	272.90
							3.5	0.1	20	0.9	12.71	13.18	1.04
							0.5	1	20	0.9	0.39	0.85	2.19
							3.5	1	20	0.9	14.69	15.15	1.03
							0.5	10	20	0.9	2.87	3.33	1.16
							3.5	10	20	0.9	23.23	23.69	1.02

Table C-13. Results of validation of BSA 2 for Case History No. 2.

Case History No.	Waterway	Highway	Sample No.	Sample Type	$V_{c,test}$ (m/s)	$V_{c,chart}$ (m/s)	V_{appr} (m/s)	Pier Diameter (m)	Upstream Water Depth (m)	Contraction Ratio	$Z_{max,I\text{-}EFA}$ (m)	$Z_{max,I\text{-}BSA2}$ (m)	$Z_{max,I\text{-}BSA2}$ / $Z_{max,I\text{-}EFA}$
2	Alligator Creek	US 287	1460	CH	1.3	0.73	0.5	0.1	10	0.5	0.33	1.42	4.34
							3.5	0.1	10	0.5	16.63	17.73	1.07
							0.5	1	10	0.5	0.90	2.00	2.21
							3.5	1	10	0.5	18.61	19.71	1.06
							0.5	10	10	0.5	3.38	4.48	1.32
							3.5	10	10	0.5	27.15	28.24	1.04
							0.5	0.1	20	0.5	0.39	1.94	4.96
							3.5	0.1	20	0.5	23.28	24.82	1.07
							0.5	1	20	0.5	0.97	2.51	2.60
							3.5	1	20	0.5	25.25	26.80	1.06
							0.5	10	20	0.5	3.45	4.99	1.45
							3.5	10	20	0.5	33.79	35.34	1.05
							0.5	0.1	10	0.9	0.00	0.24	243.77
							3.5	0.1	10	0.9	8.40	9.49	1.13
							0.5	1	10	0.9	0.00	0.82	818.71
							3.5	1	10	0.9	10.38	11.47	1.11
							0.5	10	10	0.9	2.21	3.30	1.50
							3.5	10	10	0.9	18.91	20.01	1.06
							0.5	0.1	20	0.9	0.00	0.27	272.90
							3.5	0.1	20	0.9	11.63	13.18	1.13
							0.5	1	20	0.9	0.00	0.85	847.85
							3.5	1	20	0.9	13.61	15.15	1.11
							0.5	10	20	0.9	1.78	3.33	1.87
							3.5	10	20	0.9	22.14	23.69	1.07
2	Alligator Creek	US 287	1462	CH	0.5	0.73	0.5	0.1	10	0.5	1.86	1.42	0.76
							3.5	0.1	10	0.5	18.17	17.73	0.98
							0.5	1	10	0.5	2.44	2.00	0.82
							3.5	1	10	0.5	20.15	19.71	0.98
							0.5	10	10	0.5	4.92	4.48	0.91
							3.5	10	10	0.5	28.68	28.24	0.98
							0.5	0.1	20	0.5	2.56	1.94	0.76
							3.5	0.1	20	0.5	25.45	24.82	0.98
							0.5	1	20	0.5	3.14	2.51	0.80
							3.5	1	20	0.5	27.43	26.80	0.98
							0.5	10	20	0.5	5.62	4.99	0.89
							3.5	10	20	0.5	35.96	35.34	0.98
							0.5	0.1	10	0.9	0.68	0.24	0.36
							3.5	0.1	10	0.9	9.93	9.49	0.96
							0.5	1	10	0.9	1.26	0.82	0.65
							3.5	1	10	0.9	11.91	11.47	0.96
							0.5	10	10	0.9	3.74	3.30	0.88
							3.5	10	10	0.9	20.45	20.01	0.98
							0.5	0.1	20	0.9	0.90	0.27	0.30
							3.5	0.1	20	0.9	13.80	13.18	0.95
							0.5	1	20	0.9	1.47	0.85	0.58
							3.5	1	20	0.9	15.78	15.15	0.96
							0.5	10	20	0.9	3.95	3.33	0.84
							3.5	10	20	0.9	24.31	23.69	0.97

Table C-14. Results of validation of BSA 2 for Case History No. 11.

Case History No.	Waterway	Highway	Sample No.	Sample Type	$V_{c,test}$ (m/s)	$V_{c,chart}$ (m/s)	V_{appr} (m/s)	Pier Diameter (m)	Upstream Water Depth (m)	Contraction Ratio	$Z_{max,I\text{-}EFA}$ (m)	$Z_{max,I\text{-}BSA2}$ (m)	$Z_{max,I\text{-}BSA2}$ / $Z_{max,I\text{-}EFA}$
11	Navasota River	SH 7	Navasota Layer 1	SC	0.9	0.63	0.5	0.1	10	0.5	1.09	1.61	1.47
							3.5	0.1	10	0.5	17.40	17.92	1.03
							0.5	1	10	0.5	1.67	2.19	1.31
							3.5	1	10	0.5	19.38	19.90	1.03
							0.5	10	10	0.5	4.15	4.67	1.12
							3.5	10	10	0.5	27.92	28.43	1.02
							0.5	0.1	20	0.5	1.48	2.21	1.50
							3.5	0.1	20	0.5	24.36	25.09	1.03
							0.5	1	20	0.5	2.05	2.78	1.36
							3.5	1	20	0.5	26.34	27.07	1.03
							0.5	10	20	0.5	4.53	5.26	1.16
							3.5	10	20	0.5	34.88	35.61	1.02
							0.5	0.1	10	0.9	0.00	0.44	435.60
							3.5	0.1	10	0.9	9.17	9.68	1.06
							0.5	1	10	0.9	0.49	1.01	2.05
							3.5	1	10	0.9	11.14	11.66	1.05
							0.5	10	10	0.9	2.97	3.49	1.17
							3.5	10	10	0.9	19.68	20.20	1.03
							0.5	0.1	20	0.9	0.00	0.54	544.19
							3.5	0.1	20	0.9	12.71	13.45	1.06
							0.5	1	20	0.9	0.39	1.12	2.89
							3.5	1	20	0.9	14.69	15.42	1.05
							0.5	10	20	0.9	2.87	3.60	1.26
							3.5	10	20	0.9	23.23	23.96	1.03
11	Navasota River	SH 7	Navasota Layer 2	CL	0.4	0.51	0.5	0.1	10	0.5	2.05	1.84	0.90
							3.5	0.1	10	0.5	18.36	18.15	0.99
							0.5	1	10	0.5	2.63	2.42	0.92
							3.5	1	10	0.5	20.34	20.13	0.99
							0.5	10	10	0.5	5.11	4.90	0.96
							3.5	10	10	0.5	28.87	28.66	0.99
							0.5	0.1	20	0.5	2.83	2.53	0.89
							3.5	0.1	20	0.5	25.72	25.42	0.99
							0.5	1	20	0.5	3.41	3.11	0.91
							3.5	1	20	0.5	27.70	27.40	0.99
							0.5	10	20	0.5	5.89	5.59	0.95
							3.5	10	20	0.5	36.23	35.93	0.99
							0.5	0.1	10	0.9	0.88	0.67	0.76
							3.5	0.1	10	0.9	10.12	9.91	0.98
							0.5	1	10	0.9	1.45	1.24	0.85
							3.5	1	10	0.9	12.10	11.89	0.98
							0.5	10	10	0.9	3.93	3.72	0.95
							3.5	10	10	0.9	20.64	20.43	0.99
							0.5	0.1	20	0.9	1.17	0.87	0.74
							3.5	0.1	20	0.9	14.07	13.77	0.98
							0.5	1	20	0.9	1.74	1.44	0.83
							3.5	1	20	0.9	16.05	15.75	0.98
							0.5	10	20	0.9	4.22	3.93	0.93
							3.5	10	20	0.9	24.59	24.29	0.99

APPENDIX D

Table D-1. Summary of EFA test data and associated soil classification tests.

No.	Soil Classification	Sample No.	Data Source	Liquid Limit (%)	Plastic Limit (%)	Plasticity Index (%)	Unit Weight, γ (kN/m^3)	Water Content (%)	Undrained Shear Strength (kPa)	% Passing #200 Sieve	Mean Particle Diameter, D_{50} (mm)	Critical Shear Stress, τ_c (Pa)	Critical Velocity, V_c (m/s)
1	CH	S1-B1-(0-2ft)-TW	ILIT 2006 (Katrina)	65	22	43	20.2	31.7	-	89.9	-	12.0	1.5
2	CH	S2-B1-(0-2ft)-TW	ILIT 2006 (Katrina)	49	17	32	19.7	16.1	-	67.2	-	11.3	1.5
3	CH	S7-B1-(0-2ft)-TW	ILIT 2006 (Katrina)	78	32	46	17.4	26.7	-	90.1	-	4.7	1.0
4	CH	S8-B1-(0-2ft)-TW	ILIT 2006 (Katrina)	85	36	49	17.7	32.3	-	97.3	-	5.0	1.0
5	SP	S11-(0-0.5ft)-LC-TW	ILIT 2006 (Katrina)	-	-	-	12.3	1.0	-	-	-	0.2	0.2
6	SP	S11-(0-0.5ft)-HC-TW	ILIT 2006 (Katrina)	-	-	-	13.3	1.0	-	-	-	0.6	0.3
7	CH	S12-B1-(0-2ft)-TW	ILIT 2006 (Katrina)	67	21	46	14.8	44.9	-	92.0	-	0.7	0.4
8	SC	Navasota Layer 1	Kwak, K. 2000, p.81 & 82	28	14	14	18.0	28.5	-	26.2	0.125	4.0	0.9
9	CL	Navasota River Layer 2	Kwak, K. 2000, p.81 & 83	26	6	20	18.8	26.6	32.1	57.7	-	0.7	0.4
10	SC	Brazos Layer 1	Kwak, K. 2000, p.81 & 83	24	9	15	20.2	17.3	-	30.0	0.265	0.4	0.3
11	SC	Brazos Layer 2	Kwak, K. 2000, p.81 & 84	24	9	15	20.2	17.3	-	30.0	0.265	0.7	0.4
12	CL	San Jacinto Layer 1	Kwak, K. 2000, p.81 & 84	22	9	13	19.6	151.6	23.9	50.4	-	1.0	0.5
13	CL	San Jacinto Layer 2	Kwak, K. 2000, p.81 & 85	22	9	13	19.6	151.6	23.9	50.4	-	0.2	0.2
14	Clay /Silt	San Jacinto Layer 3	Kwak, K. 2000, p.81 & 85	-	-	-	16.7	26.9	4.8	60.7	-	1.0	0.4
15	CL	San Jacinto Layer 4	Kwak, K. 2000, p.81 & 86	38	13	25	20.8	27.8	21.5	94.5	-	4.3	0.9
16	CH	Sims	Kwak, K. 2000, p.81 & 88	84	16	68	19.6	25.3	23.0	99.1	0.0012	2.9	0.8
17	Fine Gravel	Trinity Layer 1	Kwak, K. 2000, p.81 & 86	-	-	-	22.0	7.7	-	11.5	6	1.0	0.5
18	CL	Trinity Layer 2	Kwak, K. 2000, p.81 & 87	42	9	33	22.1	22.2	11.5	68.4	-	4.2	0.9
19	CL	San Marcos Layer 1	Kwak, K. 2000, p.81 & 87	41	17	24	19.6	22.0	27.3	78.3	-	0.3	0.2
20	CL	San Marcos Layer 2	Kwak, K. 2000, p.81 & 88	40	19	21	20.2	24.4	29.7	73.4	-	1.1	0.5
21	CL	Bedias (75) Layer 1	Kwak, K. 2000, p.81 & 89	48	14	34	20.0	18.1	10.0	86.8	0.048	1.7	0.6
22	Fine Sand with Clay/Silt	Bedias (75) Layer 2	Kwak, K. 2000, p.81 & 89	-	-	-	21.3	17.5	-	35.1	0.13	0.3	0.2
23	CH	Bedias (90)	Kwak, K. 2000, p.81 & 90	55	16	39	19.6	23.6	62.0	91.3	0.04	0.2	0.3
24	ML	LAR 1F-08-01-PT2	Sacramento - Ayres	49	35	14	113.5	37.7	-	97.6	0.018	6.0	1.2
25	ML	LAR 1F-08-02-PT1	Sacramento - Ayres	42	37	5	117.2	31.4	-	97.0	0.03	8.0	1.2
26	MH	LAR 1F-08-03-PT2	Sacramento - Ayres	51	45	6	109.7	44.4	-	91.4	0.044	88.3	4.5
27	ML	LAR 1F-08-04-PT2	Sacramento - Ayres	39	35	4	98.8	36.2	-	88.4	0.06	31.4	1.8
28	CL	Porcelain Clay	(TTI Rpt 2937-1, 1999, p. 21, 79)	34	20	14	18.0	28.5	12.5	100.0	0.0062	0.9	0.4
29	SP	Coarse Sand	(TTI Rpt 2937-1, 1999, p. 11 & 58)	-	-	-	13.8	-	-	-	3.375	2.2	0.6
30	CL	1454	SSSRICOS	35	14	21	19.2	20.0	-	76.0	0.028	0.4	0.4
31	CL	1456	SSSRICOS	39	13	26	19.7	21.8	-	60.2	0.046	1.6	0.7
32	CH	1459	SSSRICOS	57	15	42	18.5	28.8	-	83.2	0.004	0.6	0.5
33	CH	1460	SSSRICOS	70	20	50	17.0	36.0	-	94.8	0.001	9.4	1.3
34	CH	1462	SSSRICOS	64	17	47	17.9	29.1	-	87.2	0.004	2.2	0.5
35	CL	1464	SSSRICOS	42	25	17	19.1	26.7	-	96.4	0.011	2.0	0.4
36	ML	1465	SSSRICOS	47	29	18	19.3	28.7	-	99.4	0.01	0.4	0.3
37	CH	1466	SSSRICOS	54	25	29	19.3	22.4	-	99.4	0.009	3.7	0.9
38	CL-ML	1467	SSSRICOS	20	13	7	22.1	11.4	-	50.2	0.073	0.2	0.2
39	SC	1468	SSSRICOS	15	13	2	20.4	17.3	-	33.6	0.13	0.3	0.2
40	CH	EFA-1	TxDOT	99	77	22	18.0	32.6	-	98.3	-	0.4	0.3
41	CL	EFA-2	TxDOT	32	21	11	19.9	30.3	20.9	64.7	-	4.9	1.0

Table D-1. Continued.

No.	Soil Classification	Sample No.	Data Source	Liquid Limit (%)	Plastic Limit (%)	Plasticity Index (%)	Unit Weight, γ (kN/m^3)	Water Content (%)	Undrained Shear Strength (kPa)	% Passing #200 Sieve	Mean Particle Diameter, D_{50} (mm)	Critical Shear Stress, τ_c (Pa)	Critical Velocity, V_c (m/s)
42	CL	EFA-3	TxDOT	47	34	13	19.5	28.1	13.6	100.0	-	0.5	0.3
43	CL	EFA-4	TxDOT	47	35	12	17.8	25.4	-	94.3	-	2.6	0.6
44	CL	EFA-5	TxDOT	35	24	11	21.1	16.5	54.4	75.9	-	0.4	0.3
45	CH	EFA-6	TxDOT	88	70	18	17.0	32.9	51.3	97.4	-	5.0	1.1
46	CH	EFA-7	TxDOT	74	58	16	17.5	37.8	49.2	86.9	-	3.4	0.8
47	CH	EFA-8	TxDOT	74	58	16	18.5	20.4	17.8	86.9	-	0.3	0.3
48	CL	EFA-9	TxDOT	37	24	13	19.8	23.7	57.6	83.7	-	0.5	0.3
49	CL	EFA-10	TxDOT	35	25	10	19.8	18.8	28.3	84.6	-	1.6	0.6
50	SC	EFA-11	TxDOT	43	30	13	18.5	42.1	6.3	11.6	-	0.2	0.2
51	CL	EFA-12	TxDOT	36	25	11	20.8	21.6	30.3	38.7	-	0.3	0.2
52	CH	EFA-13	TxDOT	69	53	16	18.2	13.9	0.7	93.3	-	5.5	1.0
53	CL	EFA-14	TxDOT	49	30	19	18.9	31.8	13.6	96.5	-	0.4	0.3
54	CH	EFA-15	TxDOT	80	48	32	17.5	39.1	44.5	94.4	-	0.5	0.3
55	CH	EFA-17	TxDOT	59	37	22	19.1	24.9	38.7	90.7	-	9.9	1.5
56	CL	EFA-18	TxDOT	47	32	15	19.8	24.2	6.3	90.7	-	2.0	0.6
57	CH	EFA-19	TxDOT	74	55	19	17.8	44.5	31.4	93.7	-	1.0	0.4
58	SC	EFA-20	TxDOT	27	16	11	19.6	17.8	15.7	15.4	-	1.6	0.6
59	SM-SC	EFA-21	TxDOT	23	18	5	18.0	20.5	37.2	43.9	-	1.9	0.7
60	CH	EFA-22	TxDOT	81	25	56	18.8	30.4	26.2	85.3	-	2.8	0.8
61	CL	EFA-23	TxDOT	38	14	24	19.9	20.0	62.3	82.7	-	1.6	0.6
62	SM-SC	EFA-24	TxDOT	19	13	6	19.0	21.7	22.0	32.3	-	4.0	0.9
63	CL	EFA-25	TxDOT	45	12	33	19.1	24.0	6.3	77.9	-	1.6	0.6
64	CL	EFA-26	TxDOT	28	12	16	15.6	35.9	8.9	58.7	-	1.6	0.6
65	CH	EFA-27	TxDOT	54	18	36	16.7	28.5	21.5	81.2	-	1.6	0.6
66	SC	EFA-28	TxDOT	38	16	22	22.0	9.5	32.4	43.1	-	9.9	1.5
67	CL	EFA-29	TxDOT	38	16	22	19.2	19.0	32.4	56.9	-	2.1	0.7
68	SC	EFA-30	TxDOT	38	15	23	21.5	12.8	44.0	39.9	-	4.4	1.0
69	CL-ML	EFA-35	TxDOT	22	16	6	19.6	20.7	22.0	68.7	-	4.4	1.0
70	CL	EFA-36	TxDOT	26	17	9	20.4	16.2	-	77.1	-	4.4	1.0
71	CL	EFA-37	TxDOT	26	19	7	17.7	21.8	70.1	94.4	-	4.4	1.0
72	CH	EFA-38	TxDOT	66	19	47	24.3	35.4	-	77.8	-	4.4	1.0
73	CH	B1-(30-32)	Meander Migration	66	20	46	20.5	28.2	83.0	-	-	0.4	0.3
74	CL	B1-(40-42)	Meander Migration	32	13	19	20.3	30.0	34.0	-	-	0.1	0.1
75	CL	B2-(30-32)	Meander Migration	39	15	23	20.8	21.7	43.0	-	-	0.4	0.4
76	SP	B2-(48-50)	Meander Migration	-	-	-	20.6	19.6	-	-	-	0.3	0.2
77	SC	B3-(10-12)	Meander Migration	-	-	-	23.3	12.1	-	-	-	0.2	0.2
78	CL	B3-(20-22)	Meander Migration	47	13	34	20.4	23.3	92.0	-	-	0.5	0.3
79	CH	B3-(30-32)	Meander Migration	64	24	40	21.2	25.5	140.0	-	-	0.5	0.3
80	CH	B3-(38-40)	Meander Migration	82	26	56	19.3	29.9	140.0	-	-	0.3	0.3
81	CH	B3-(48-50)	Meander Migration	85	29	56	20.1	31.6	140.0	-	-	0.2	0.3

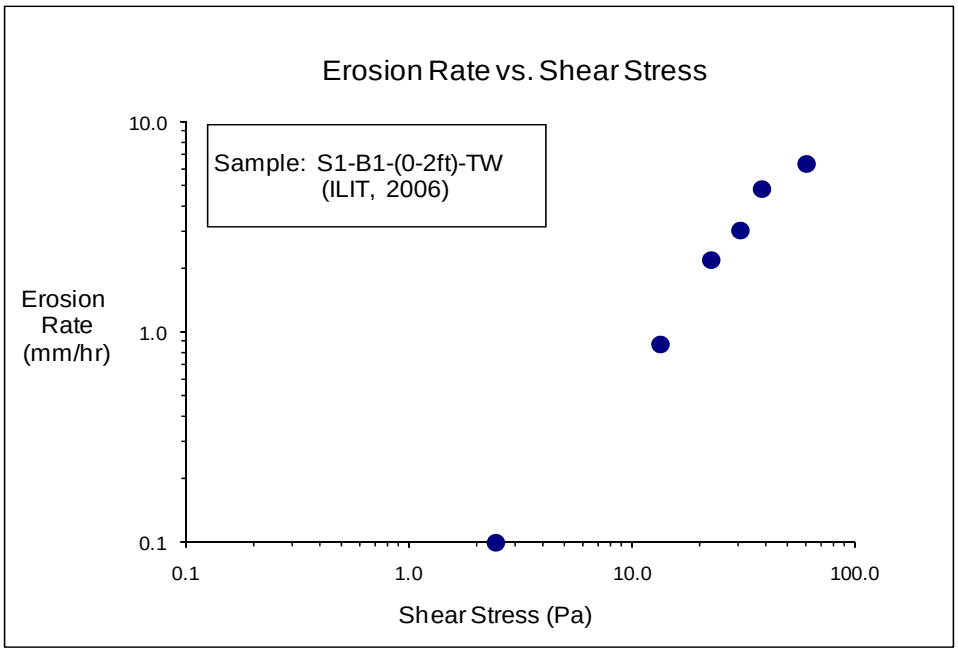

Figure D-1(a). EFA test results for soil sample S1-B1-(0-2ft)-TW (Shear Stress).

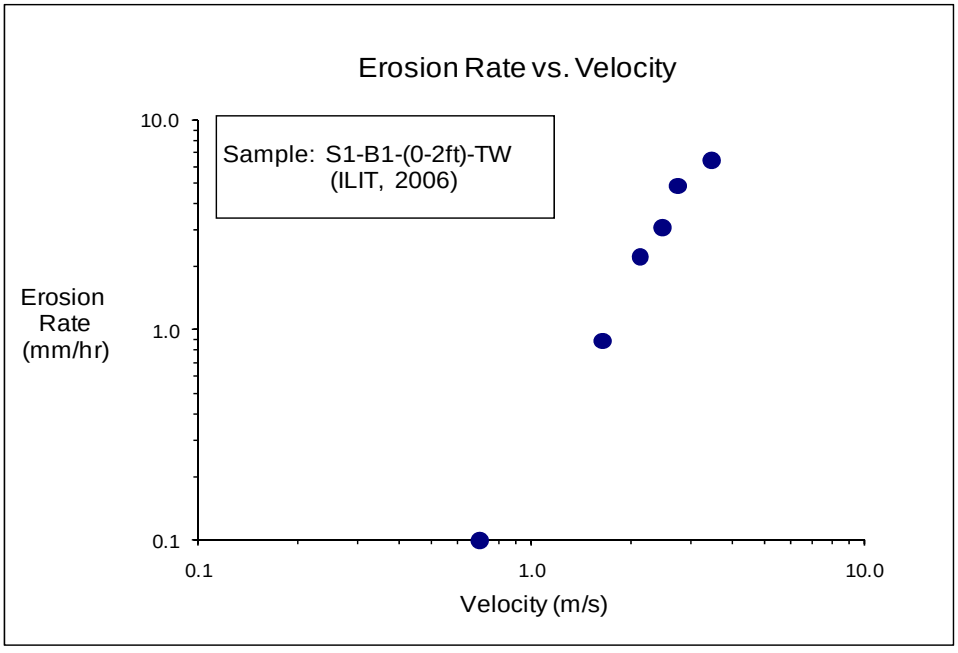

Figure D-1(b). EFA test results for soil sample S1-B1-(0-2ft)-TW (Velocity).

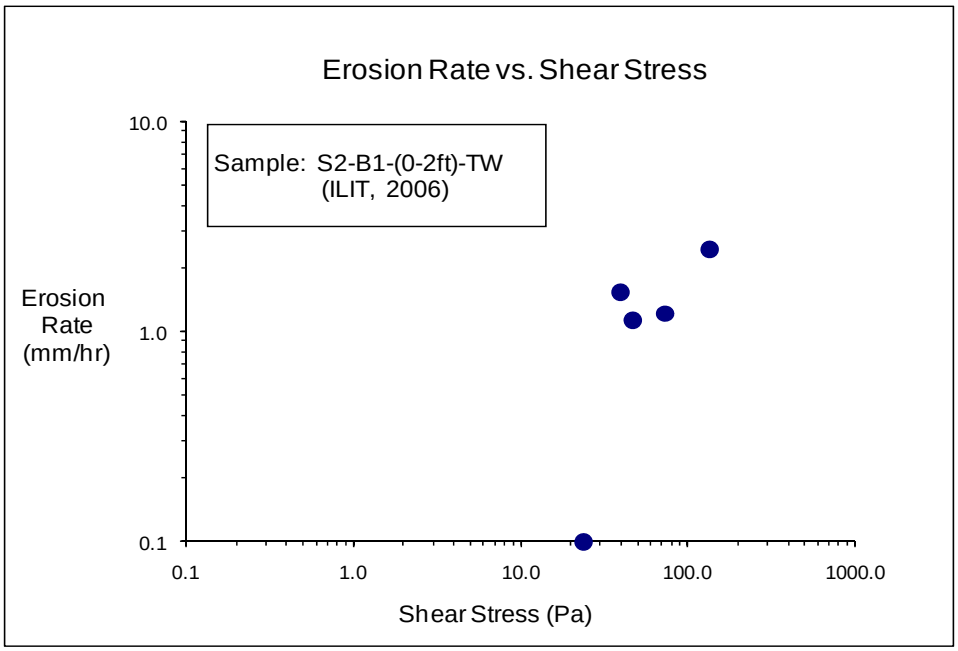

Figure D-2(a). EFA test results for soil sample S2-B1-(0-2ft)-TW (Shear Stress).

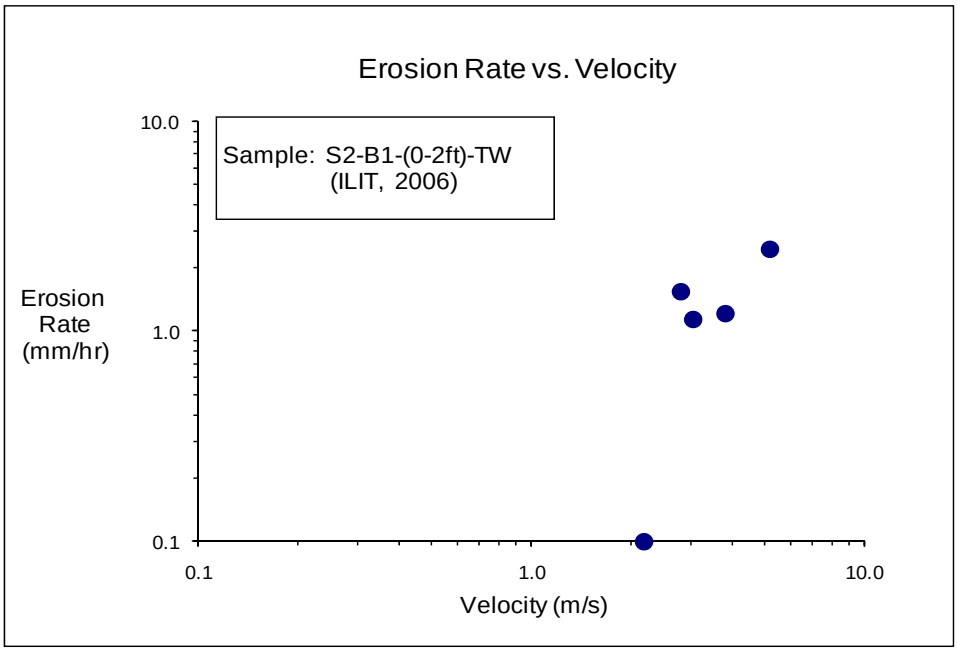

Figure D-2(b). EFA test results for soil sample S2-B1-(0-2ft)-TW (Velocity).

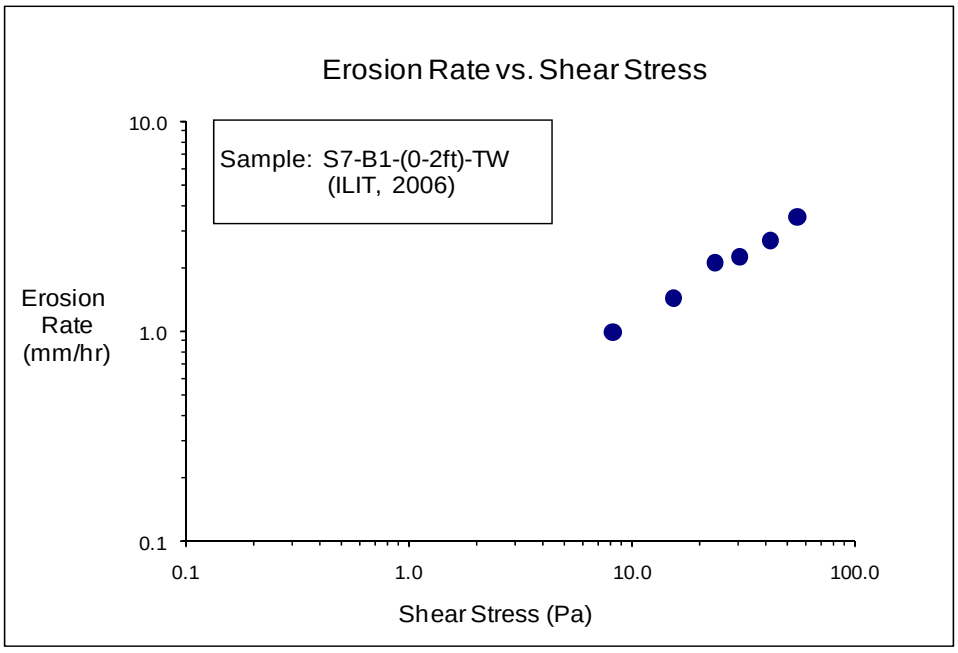

Figure D-3(a). EFA test results for soil sample S7-B1-(0-2ft)-TW (Shear Stress).

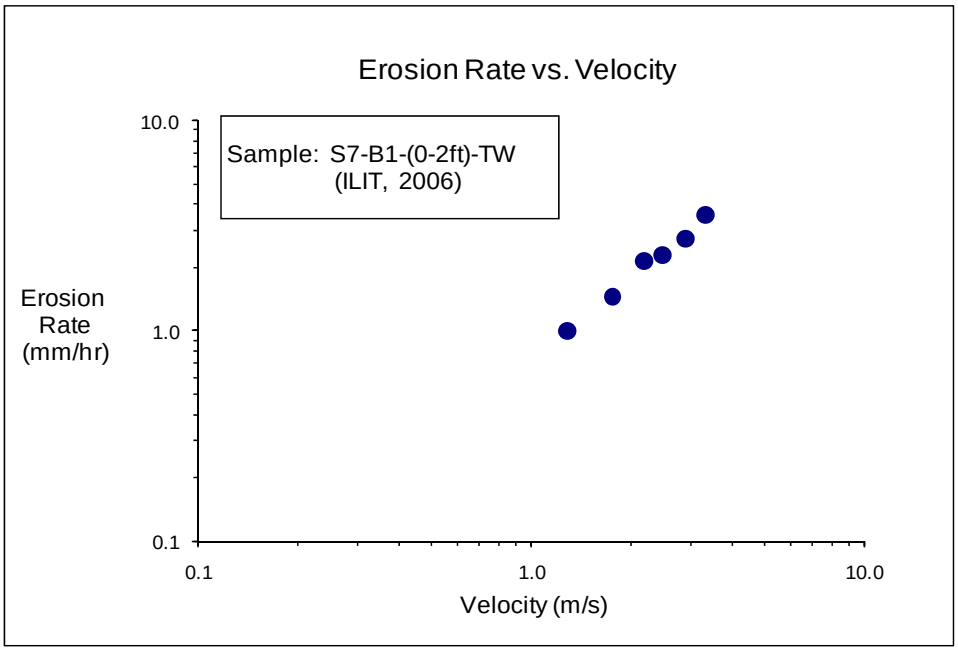

Figure D-3(b). EFA test results for soil sample S7-B1-(0-2ft)-TW (Velocity).

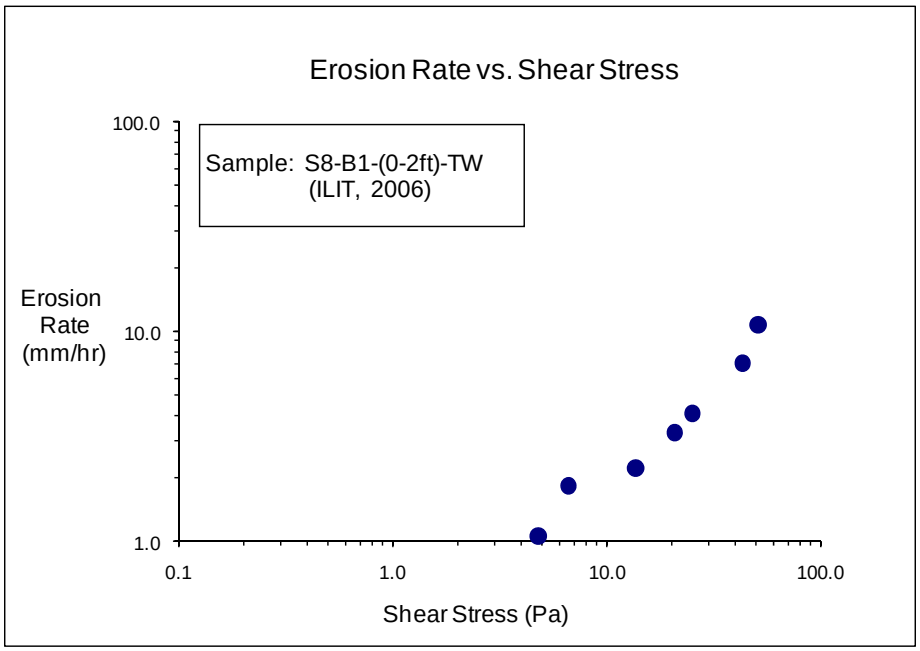

Figure D-4(a). EFA test results for soil sample S8-B1-(0-2ft)-TW (Shear Stress).

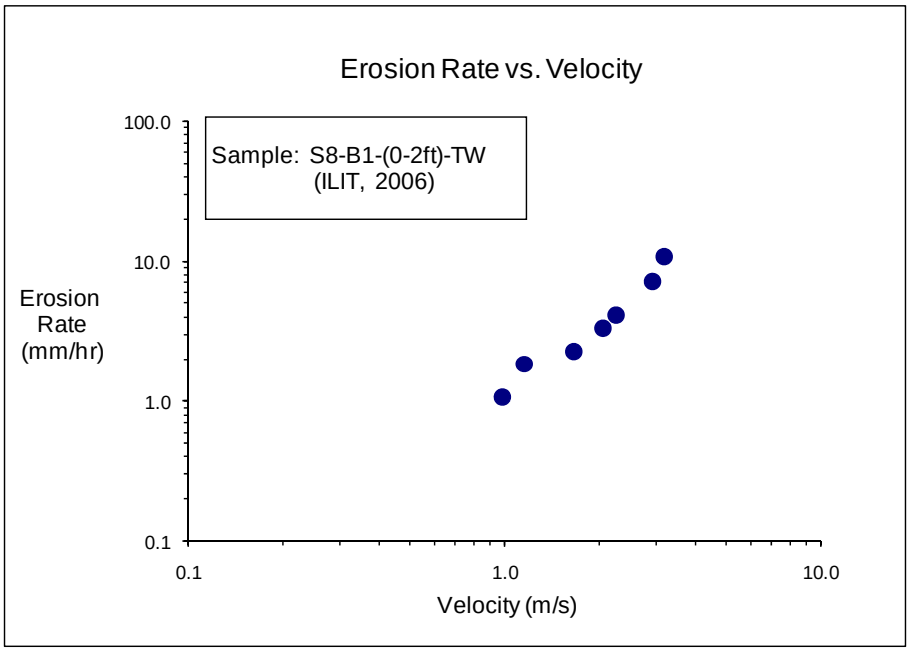

Figure D-4(b). EFA test results for soil sample S8-B1-(0-2ft)-TW (Velocity).

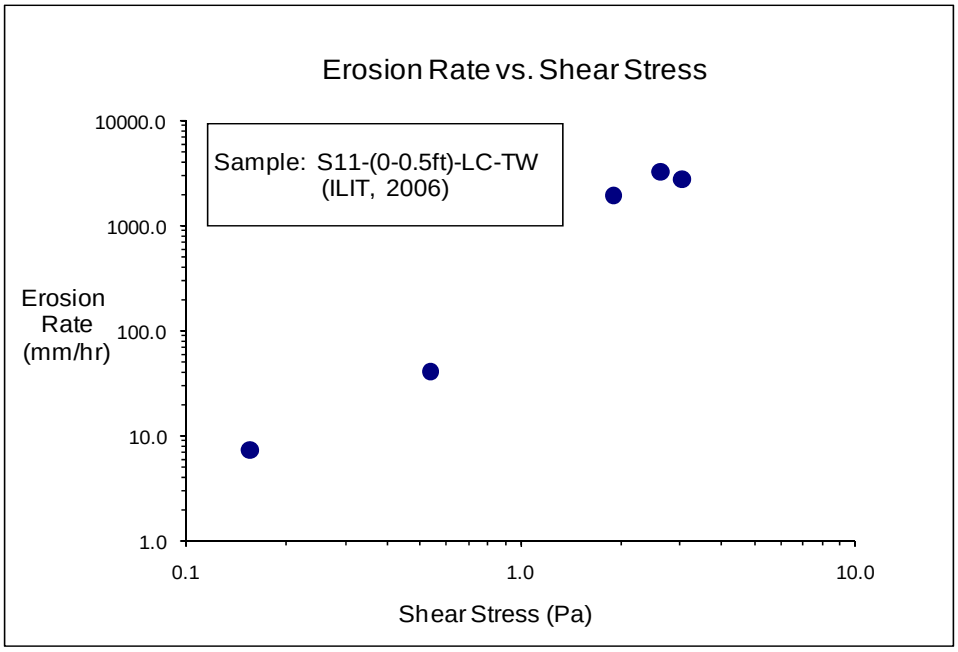

Figure D-5(a). EFA test results for soil sample S11-(0-0.5ft)-LC-TW (Shear Stress).

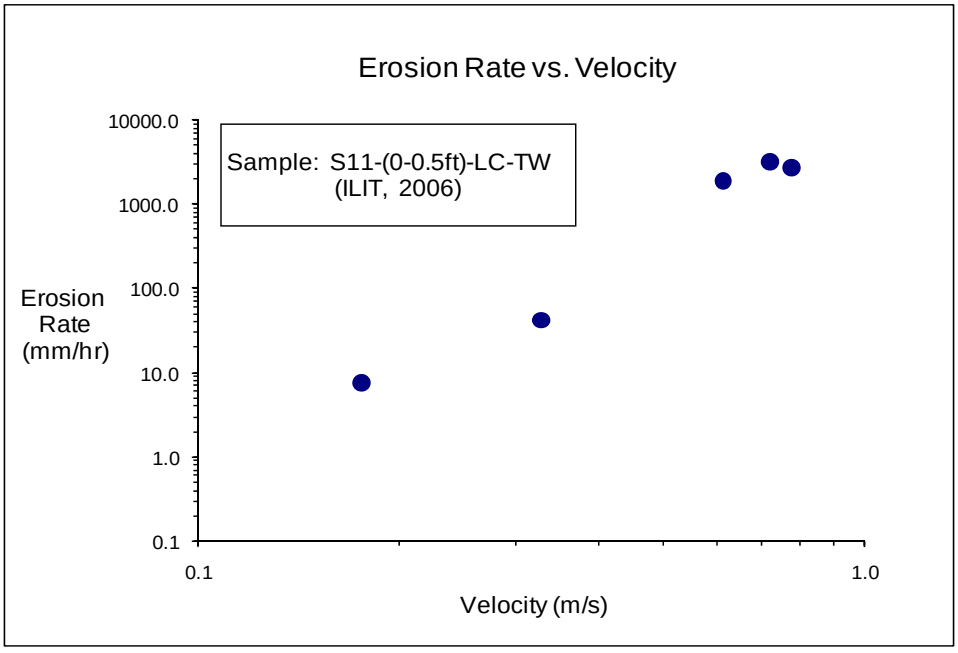

Figure D-5(b). EFA test results for soil sample S11-(0-0.5ft)-LC-TW (Velocity).

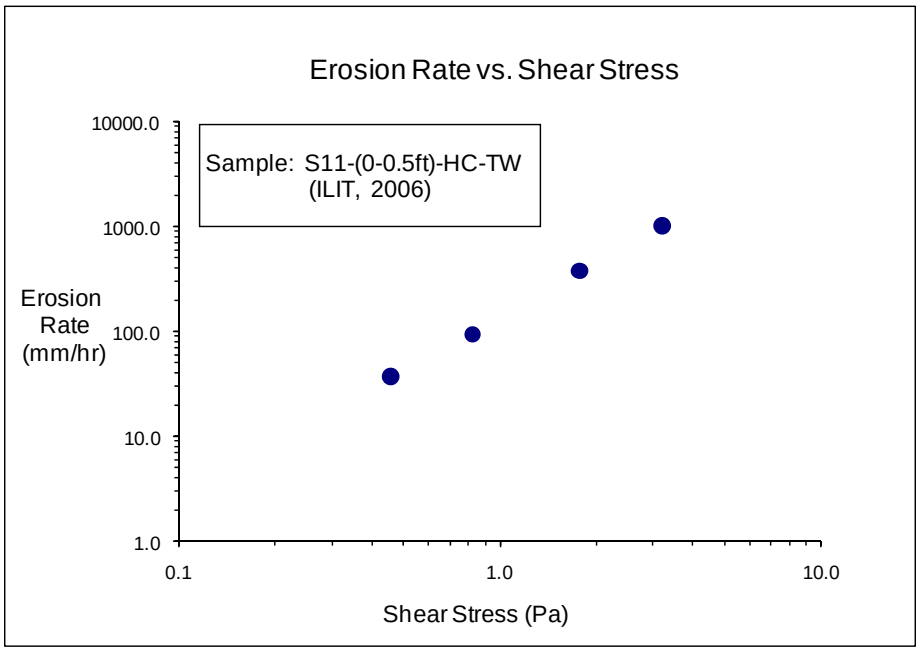

Figure D-6(a). EFA test results for soil sample S11-(0-0.5ft)-HC-TW (Shear Stress).

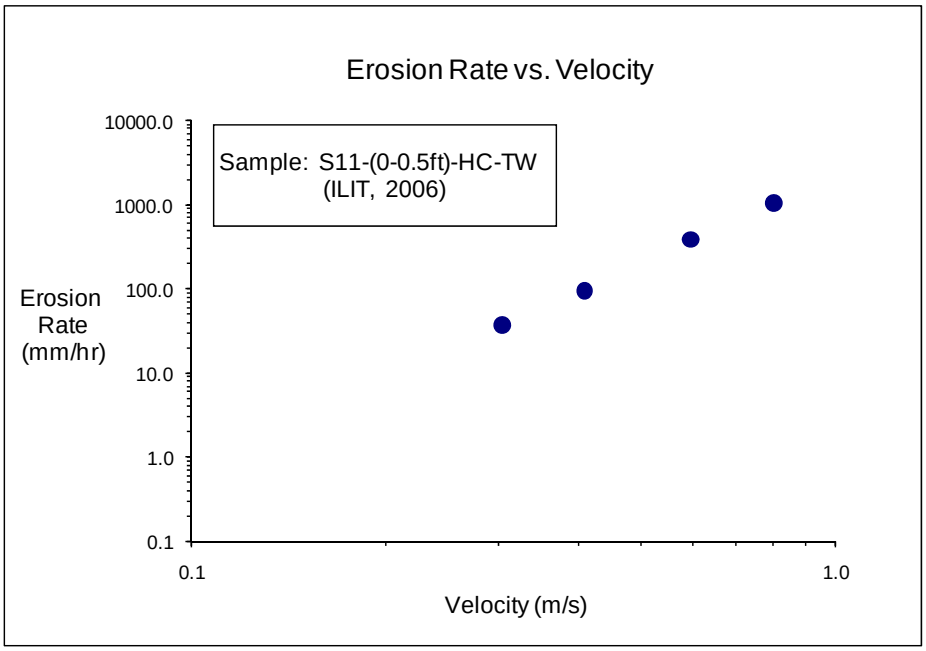

Figure D-6(b). EFA test results for soil sample S11-(0-0.5ft)-HC-TW (Velocity).

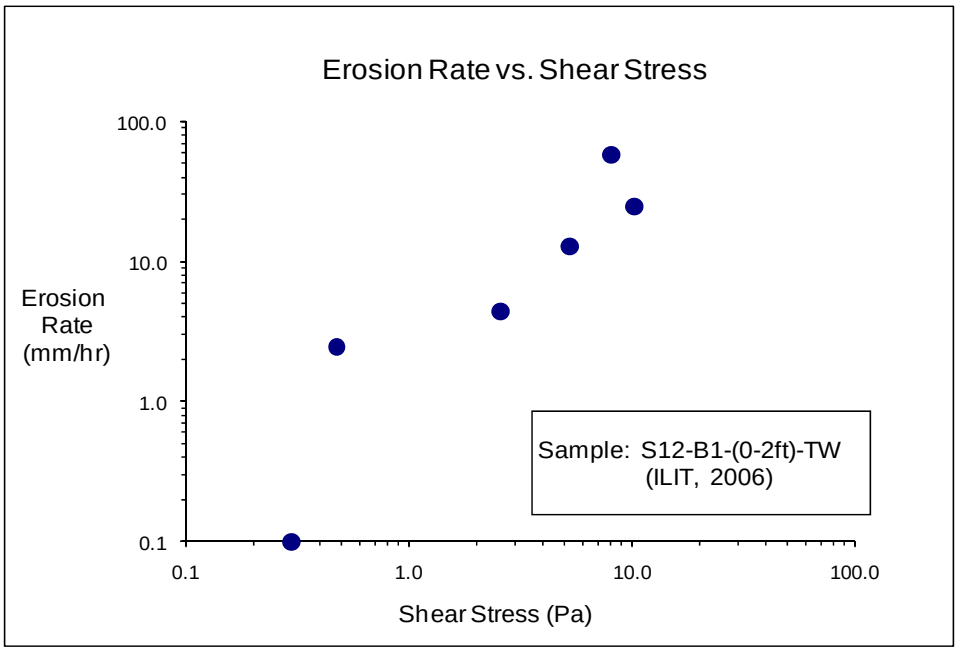

Figure D-7(a). EFA test results for soil sample S12-B1-(0-2ft)-TW (Shear Stress).

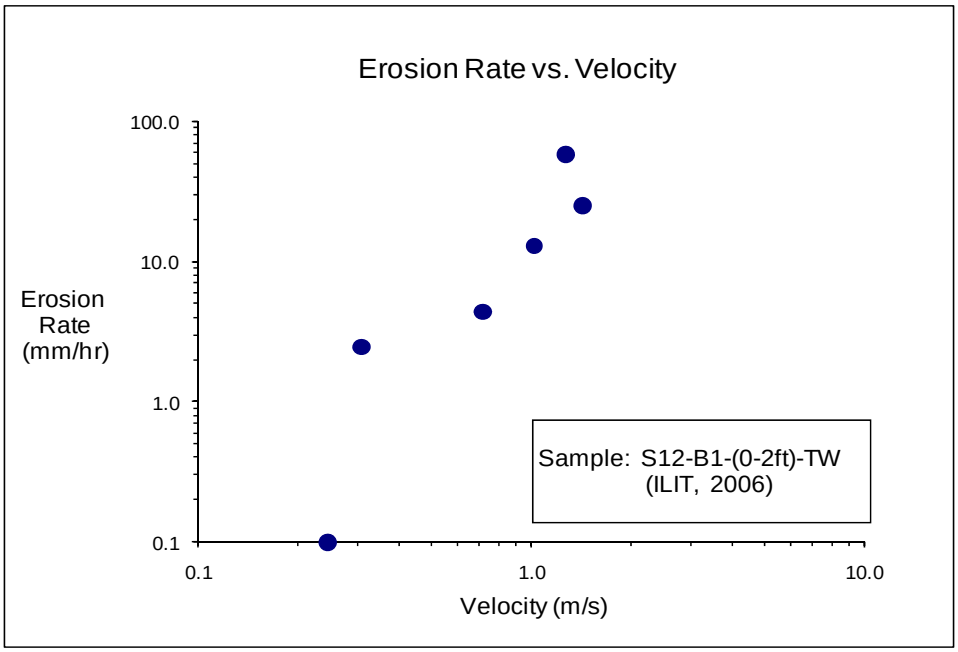

Figure D-7(b). EFA test results for soil sample S12-B1-(0-2ft)-TW (Velocity).

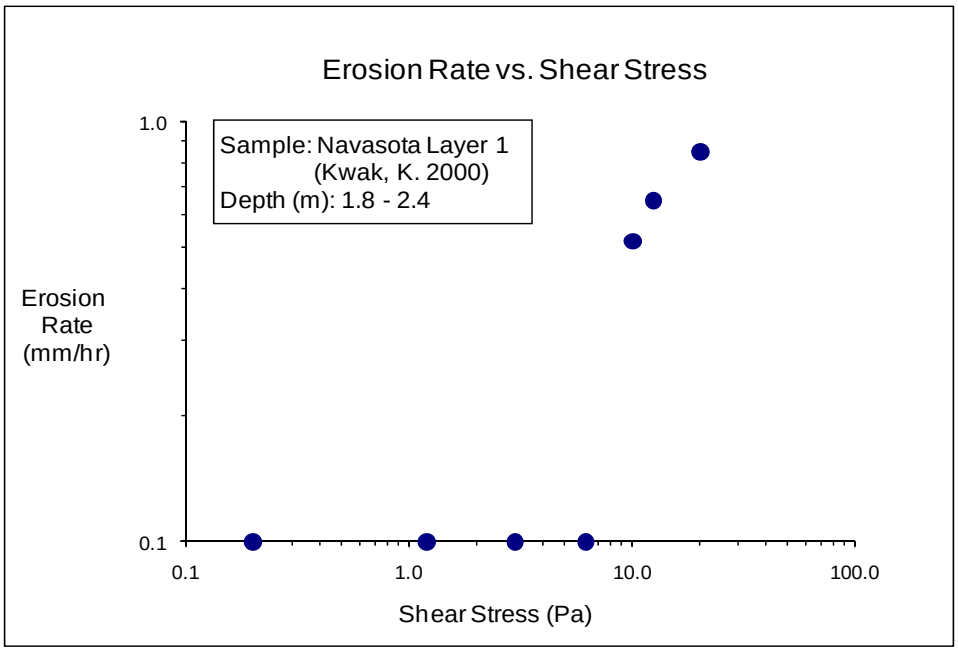

Figure D-8(a). EFA test results for soil sample Navasota Layer 1(Shear Stress).

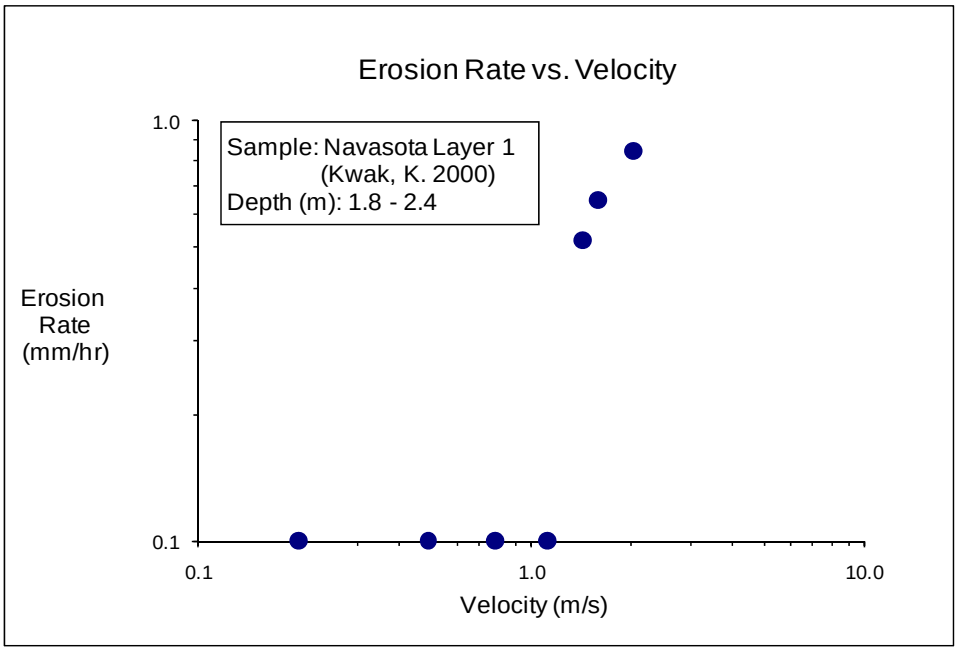

Figure D-8(b). EFA test results for soil sample Navasota Layer 1 (Velocity).

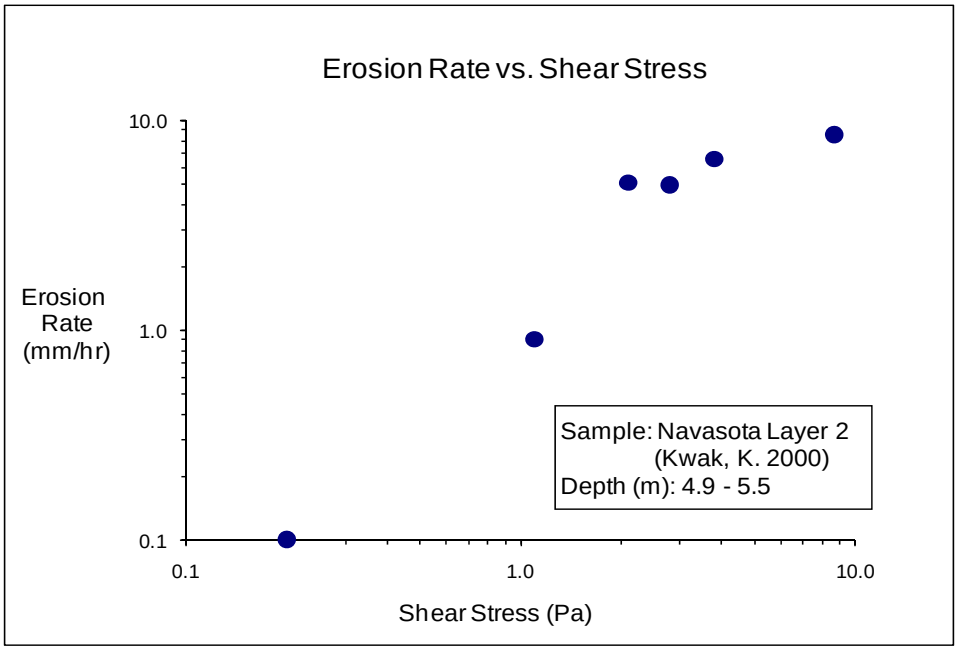

Figure D-9(a). EFA test results for soil sample Navasota Layer 2 (Shear Stress).

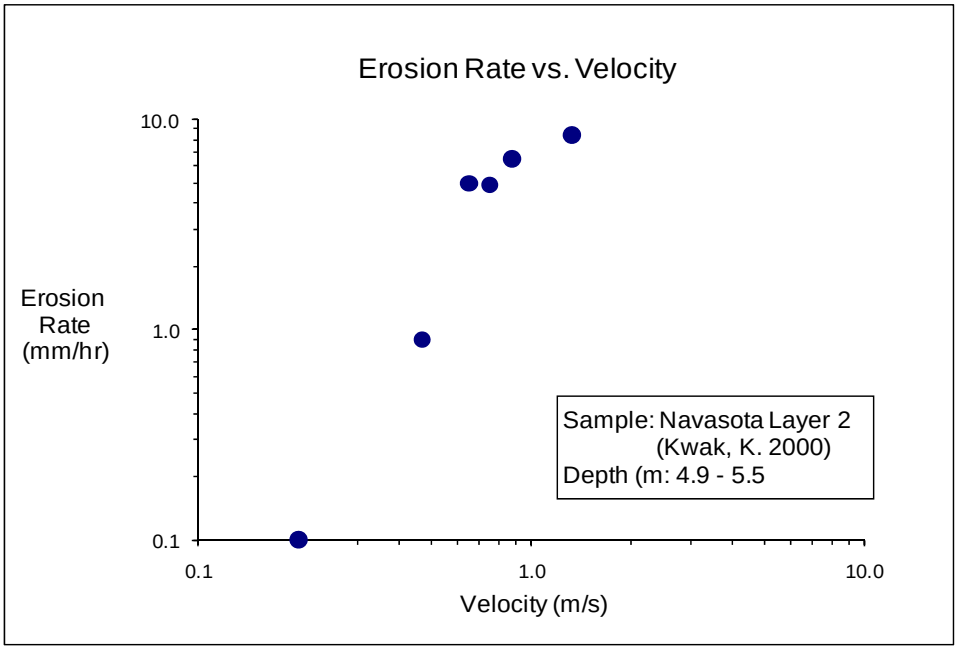

Figure D-9(b). EFA test results for soil sample Navasota Layer 2 (Velocity).

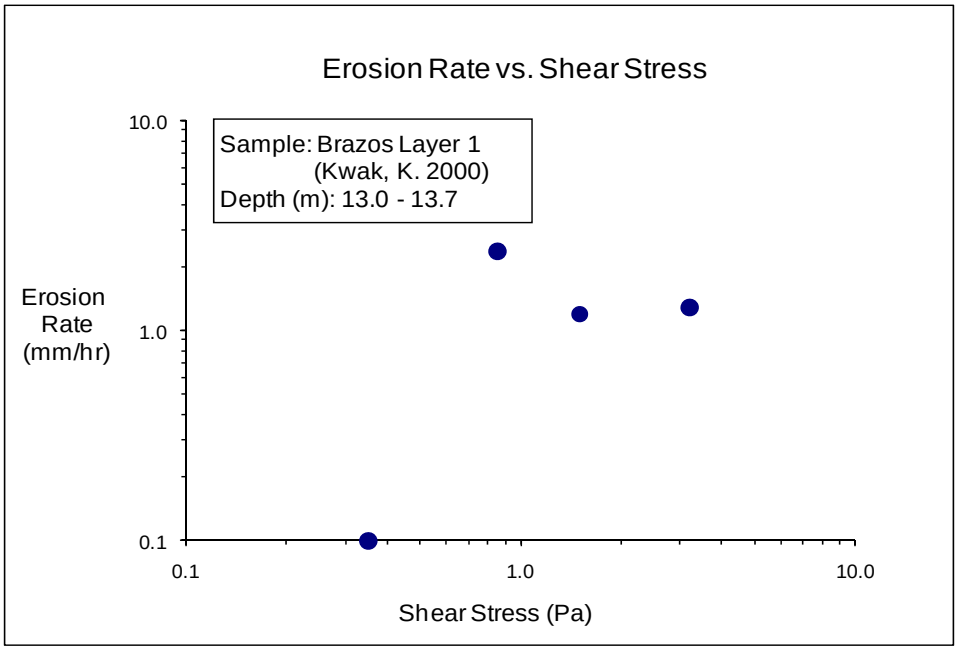

Figure D-10(a). EFA test results for soil sample Brazos Layer 1 (Shear Stress).

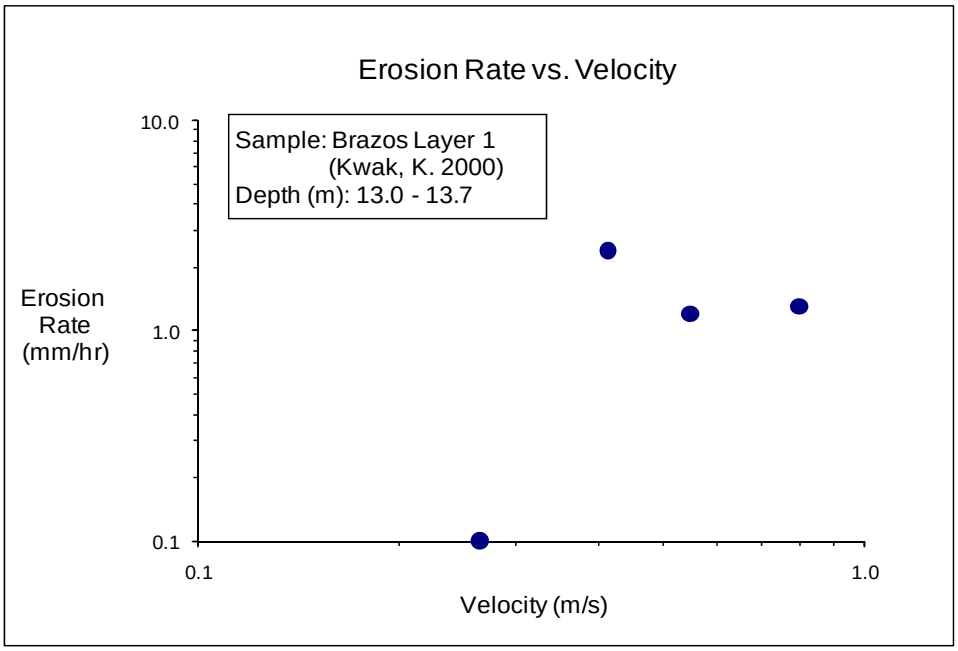

Figure D-10(b). EFA test results for soil sample Brazos Layer 1 (Velocity).

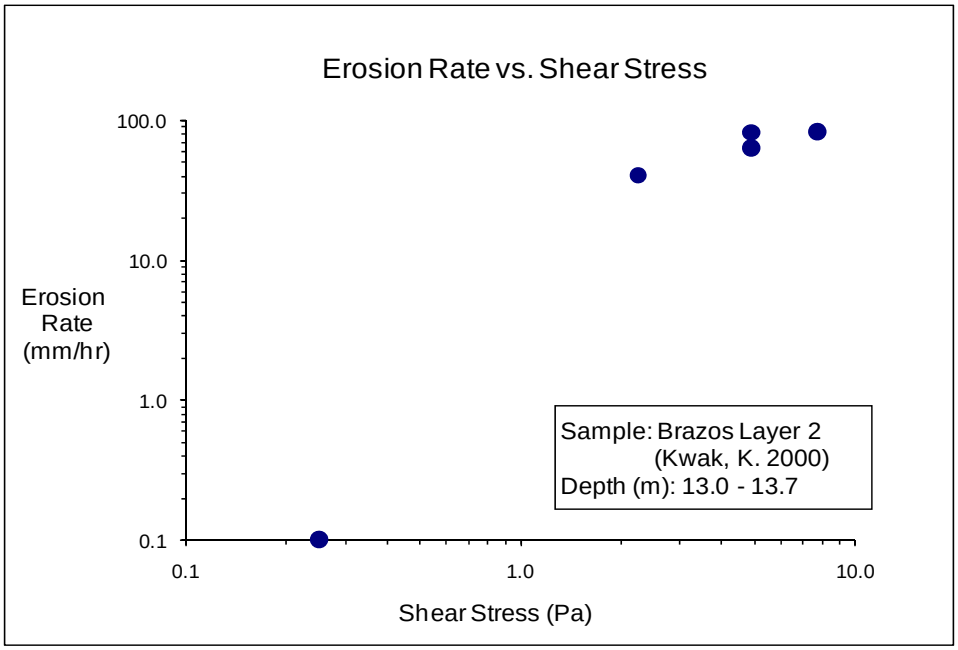

Figure D-11(a). EFA test results for soil sample Brazos Layer 2 (Shear Stress).

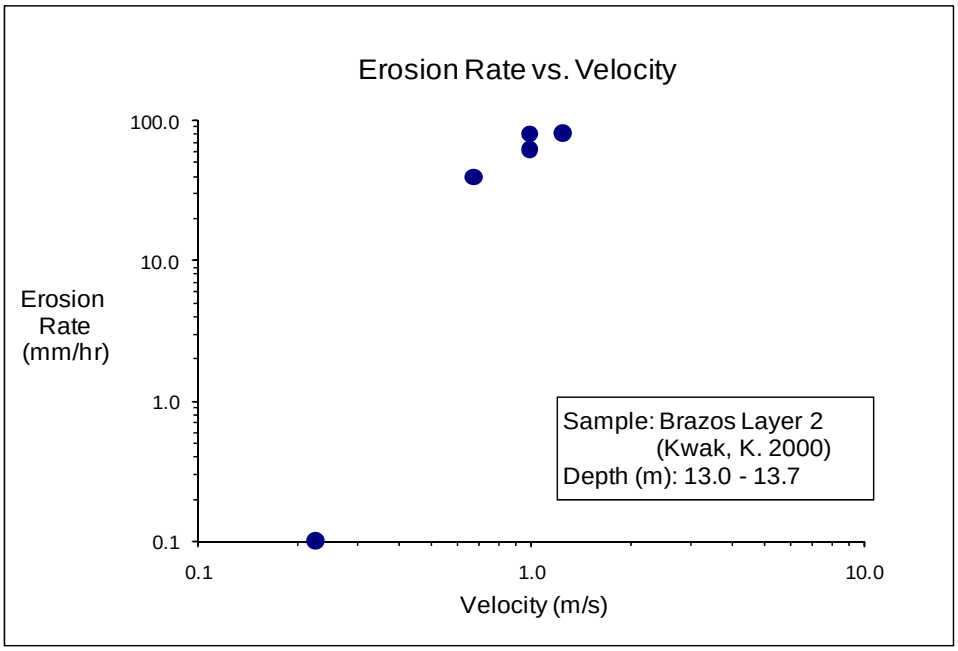

Figure D-11(b). EFA test results for soil sample Brazos Layer 2 (Velocity).

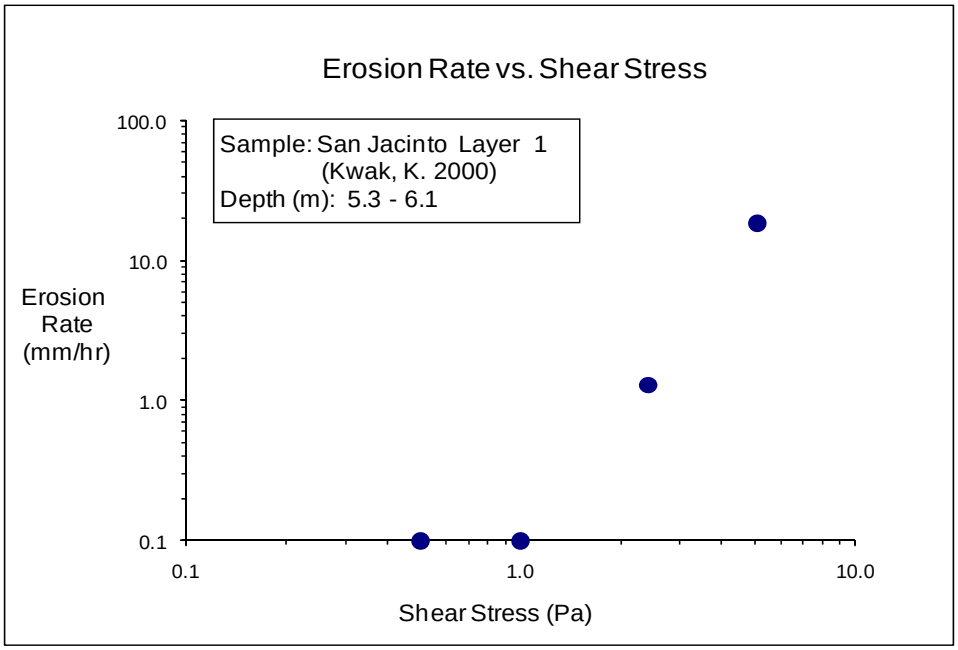

Figure D-12(a). EFA test results for soil sample San Jacinto Layer 1 (Shear Stress).

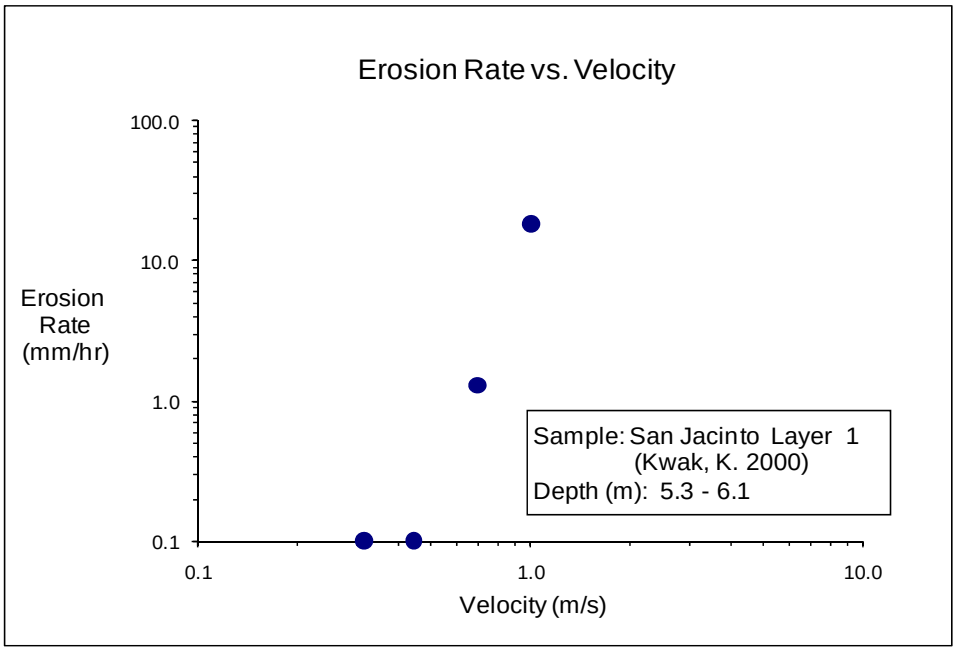

Figure D-12(b). EFA test results for soil sample San Jacinto Layer 1 (Velocity).

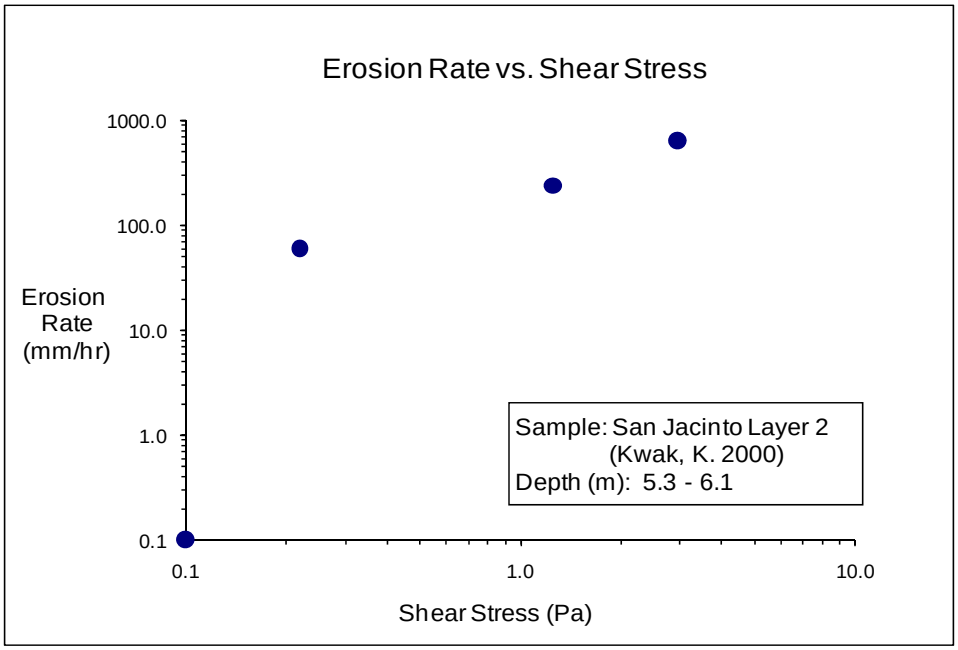

Figure D-13(a). EFA test results for soil sample San Jacinto Layer 2 (Shear Stress).

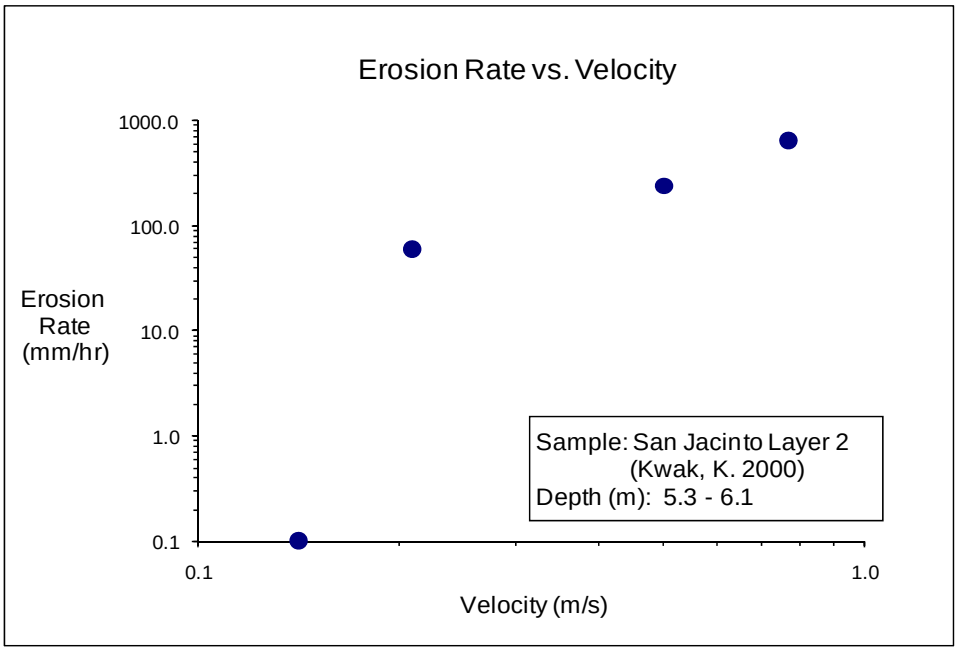

Figure D-13(b). EFA test results for soil sample San Jacinto Layer 2 (Velocity).

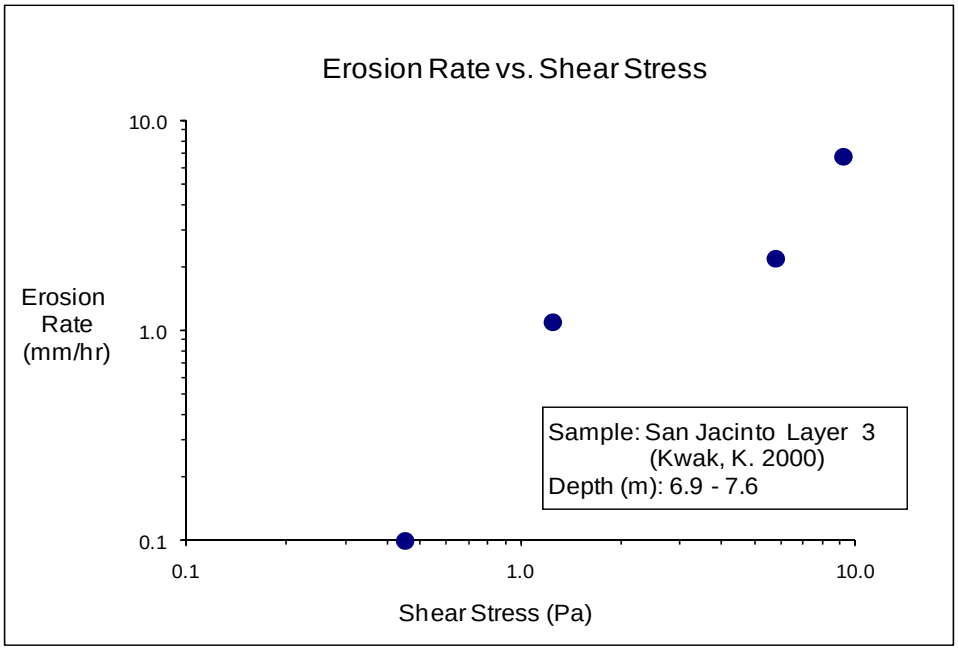

Figure D-14(a). EFA test results for soil sample San Jacinto Layer 3 (Shear Stress).

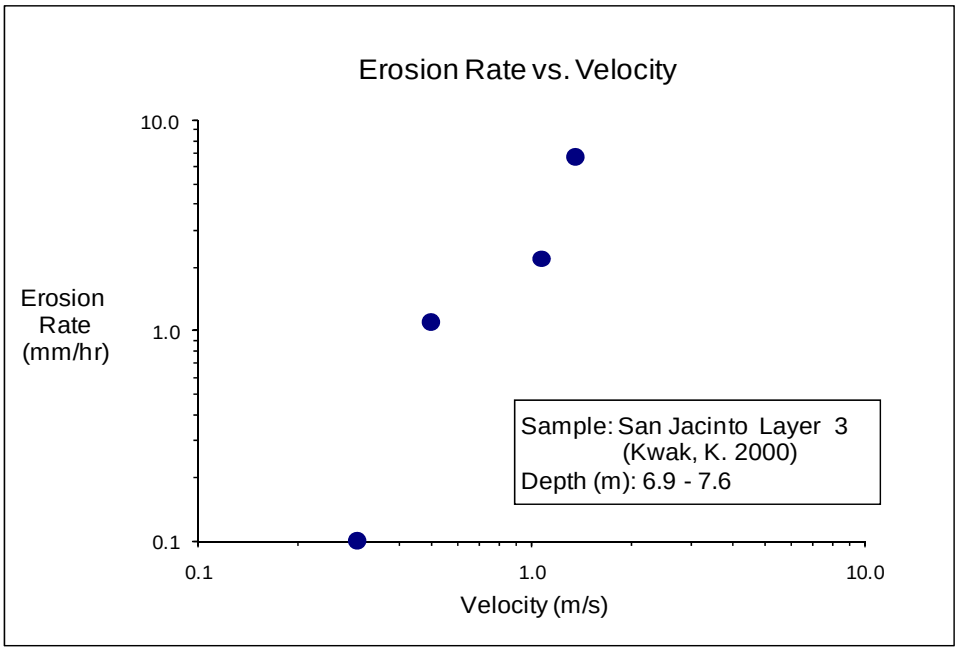

Figure D-14(b). EFA test results for soil sample San Jacinto Layer 3 (Velocity).

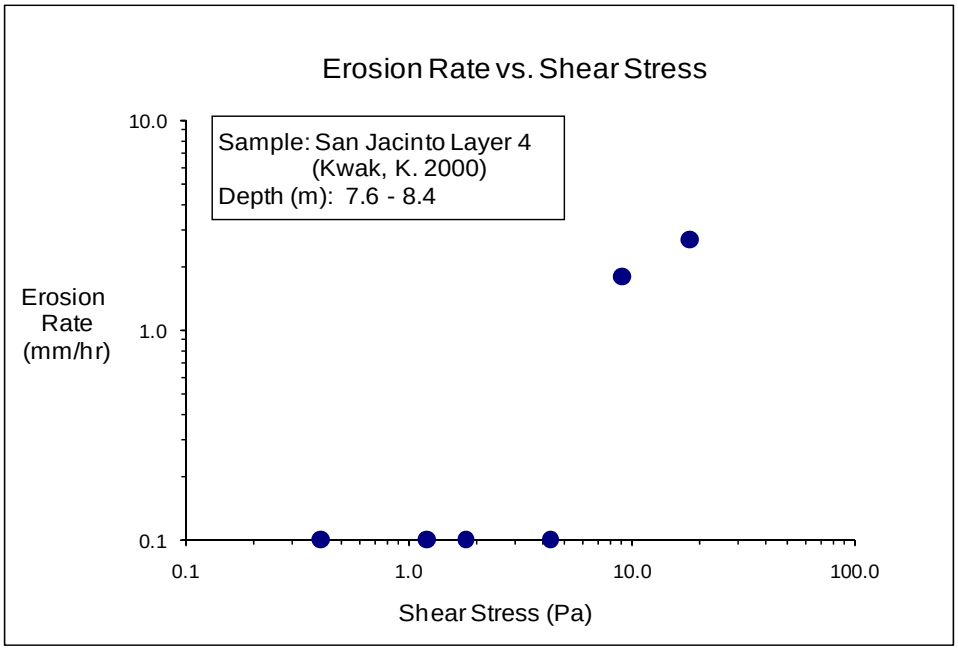

Figure D-15(a). EFA test results for soil sample San Jacinto Layer 4 (Shear Stress).

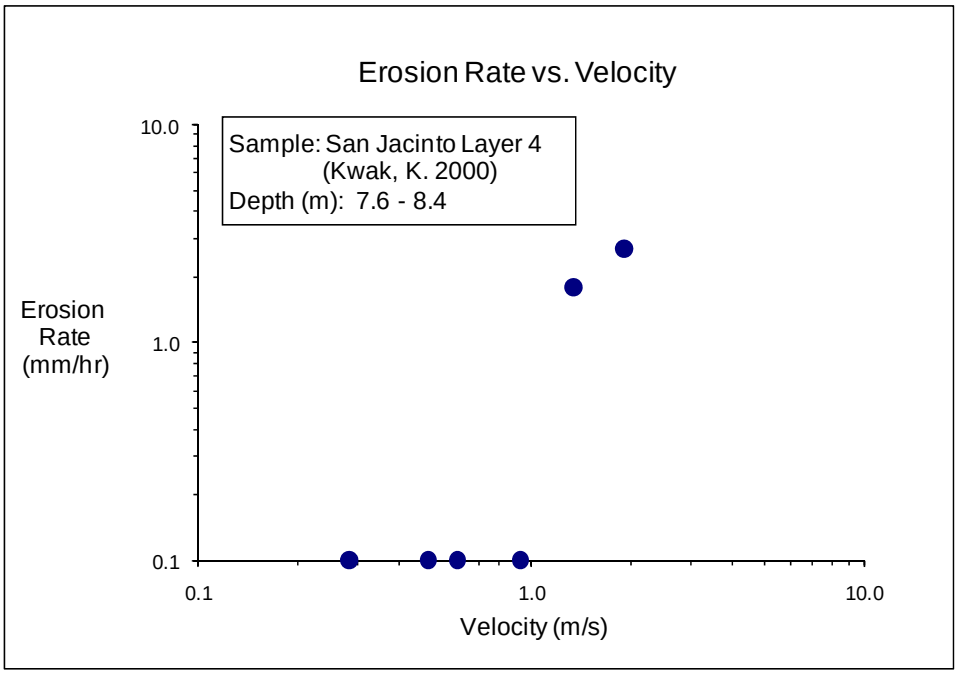

Figure D-15(b). EFA test results for soil sample San Jacinto Layer 4 (Velocity).

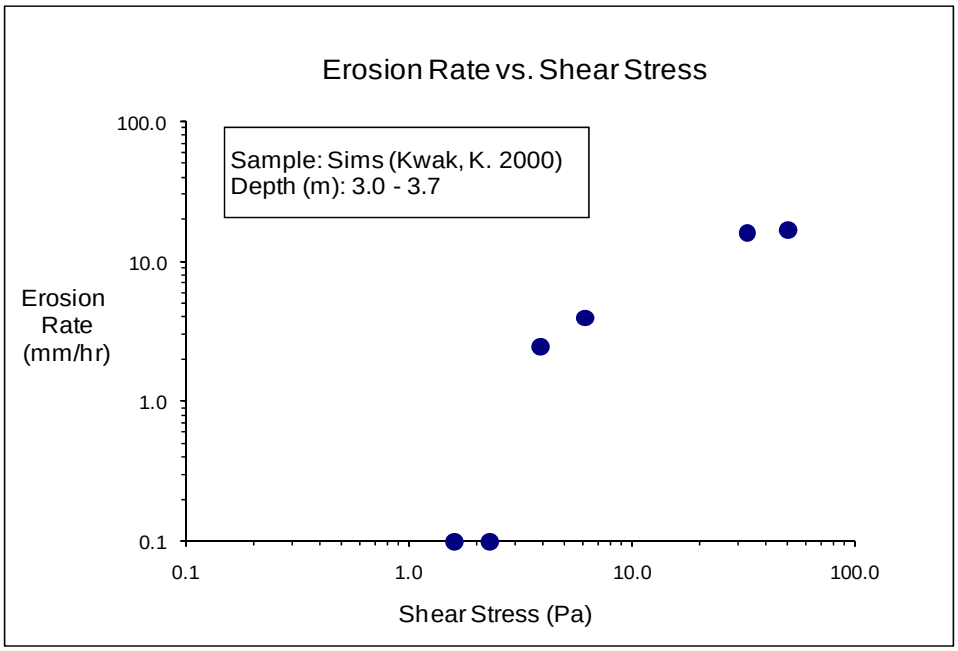

Figure D-16(a). EFA test results for soil sample Sims (Shear Stress).

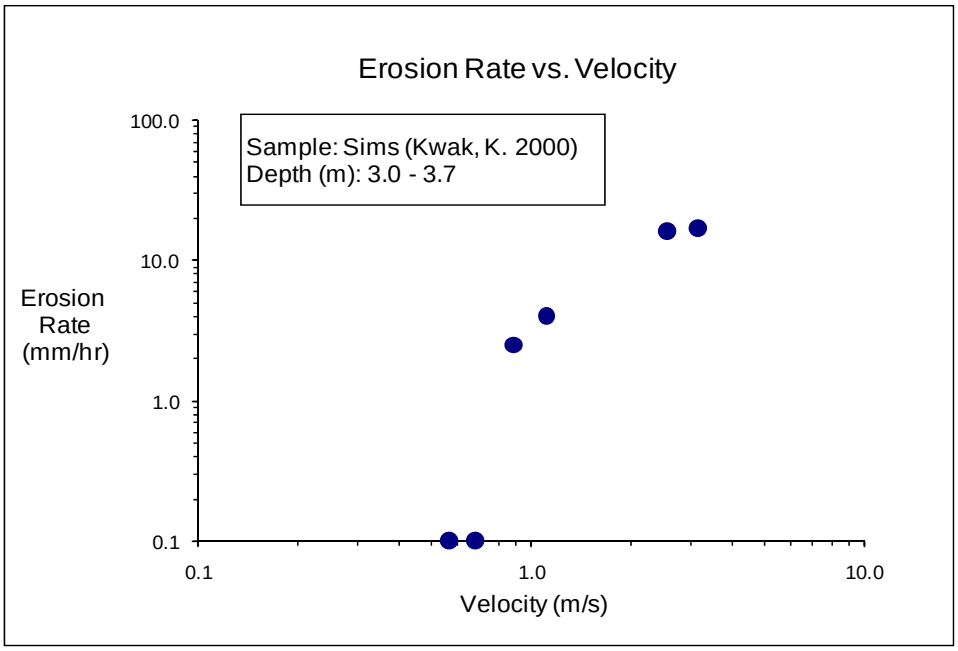

Figure D-16(b). EFA test results for soil sample Sims (Velocity).

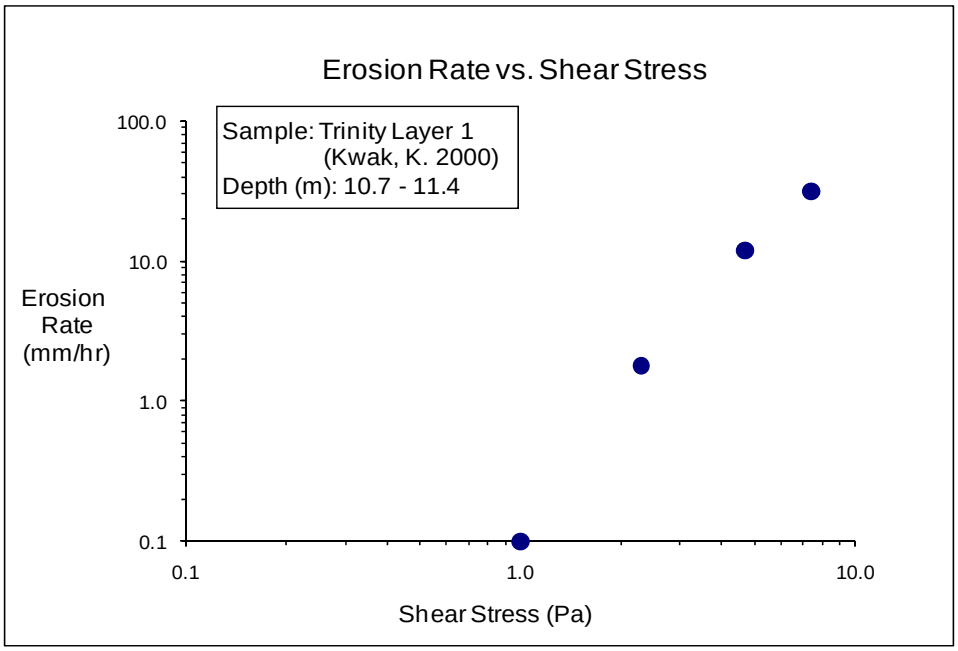

Figure D-17(a). EFA test results for soil sample Trinity Layer 1 (Shear Stress).

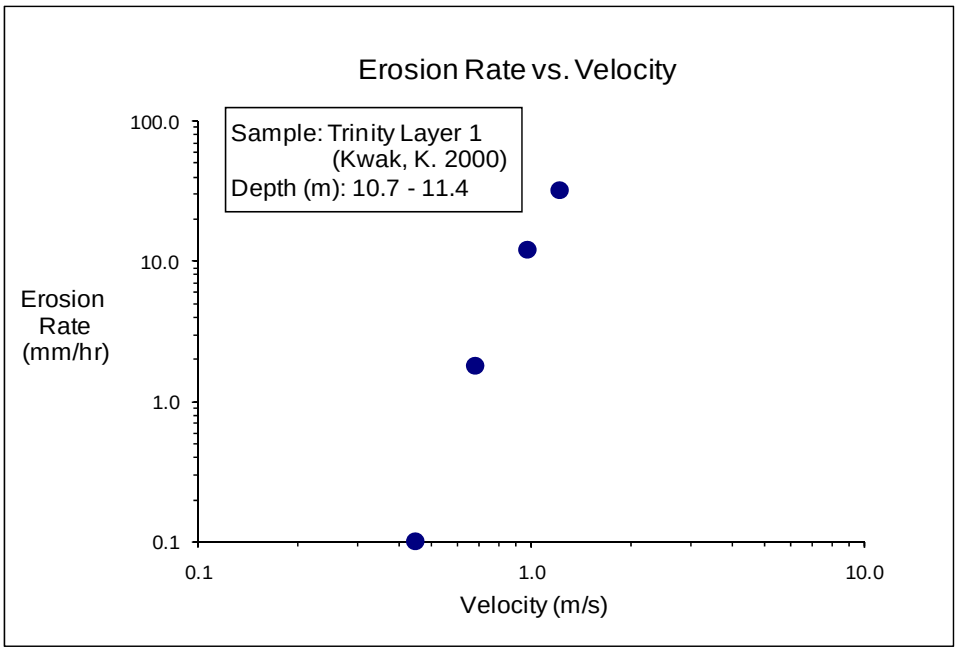

Figure D-17(b). EFA test results for soil sample Trinity Layer 1 (Velocity).

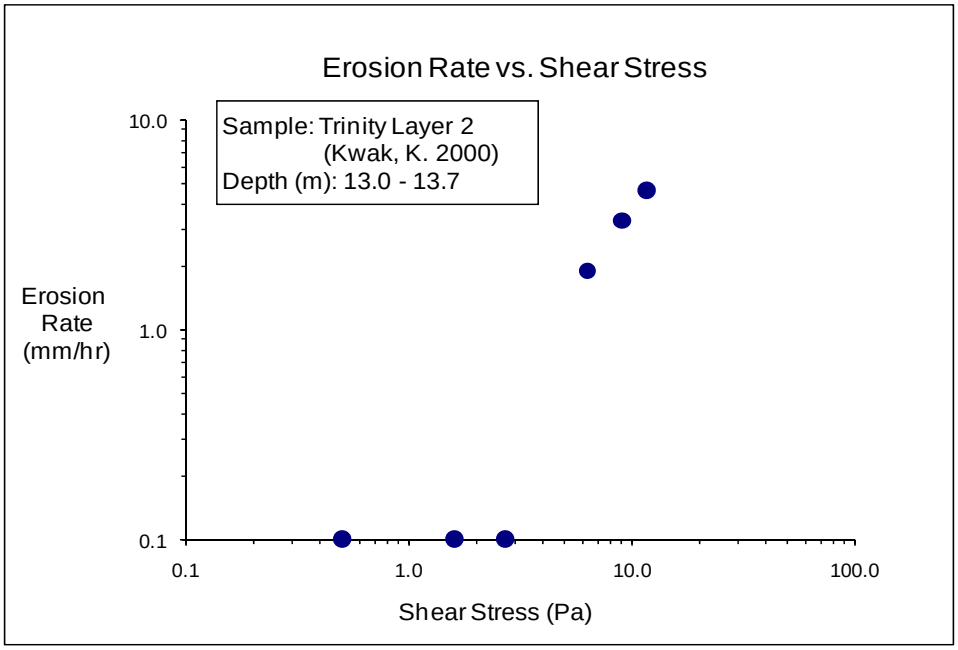

Figure D-18(a). EFA test results for soil sample Trinity Layer 2 (Shear Stress).

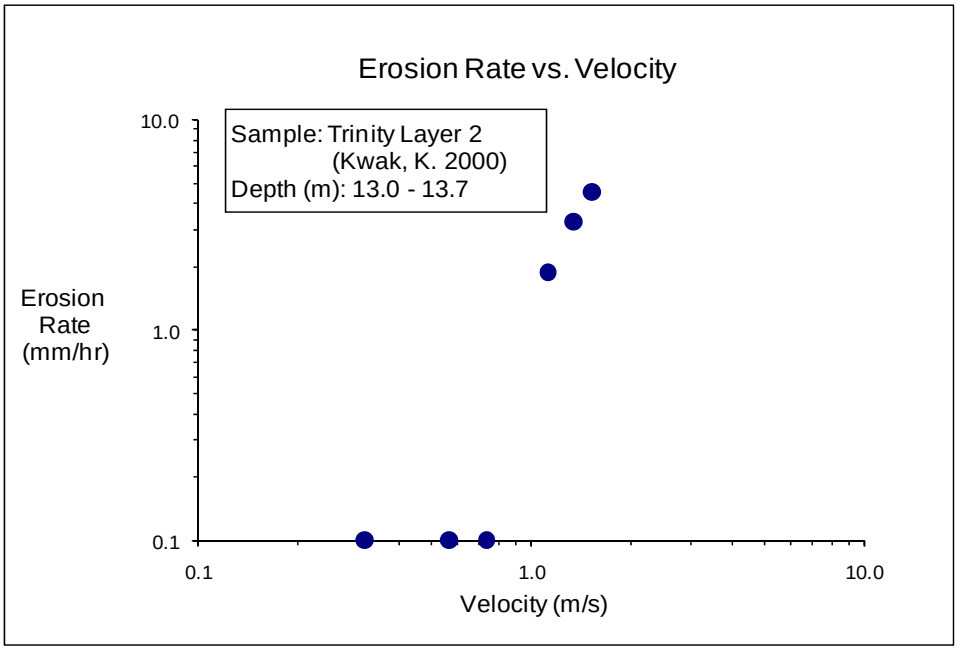

Figure D-18(b). EFA test results for soil sample Trinity Layer 2 (Velocity).

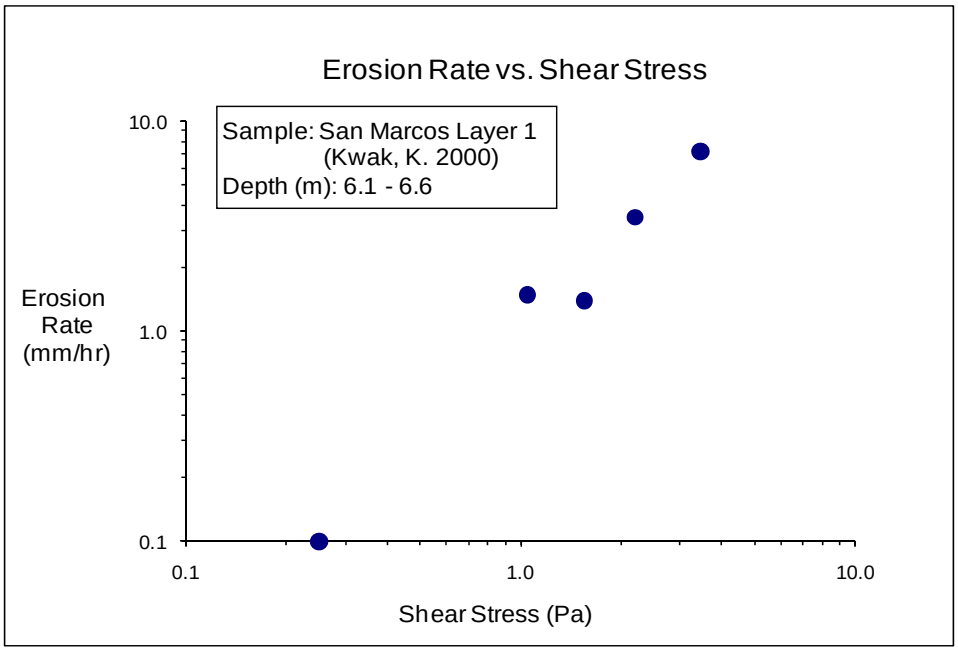

Figure D-19(a). EFA test results for soil sample San Marcos Layer 1 (Shear Stress).

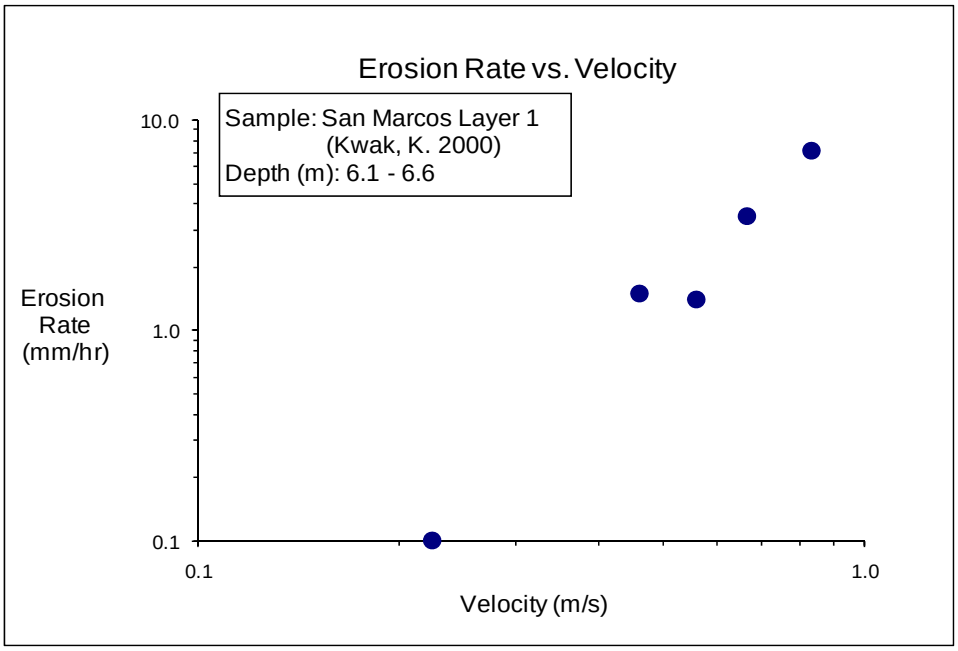

Figure D-19(b). EFA test results for soil sample San Marcos Layer 1 (Velocity).

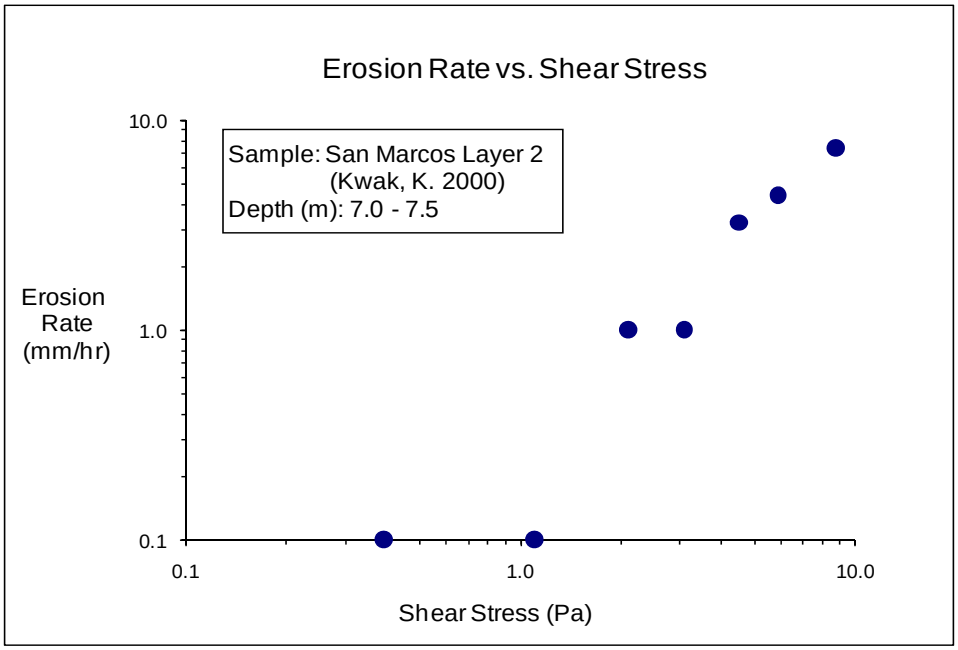

Figure D-20(a). EFA test results for soil sample San Marcos Layer 2 (Shear Stress).

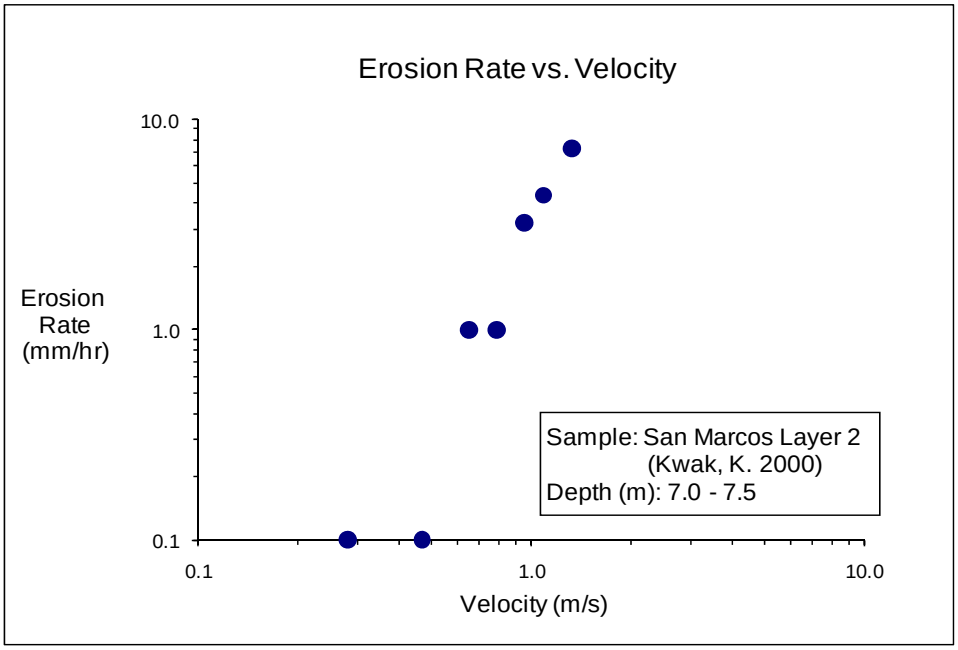

Figure D-20(b). EFA test results for soil sample San Marcos Layer 2 (Velocity).

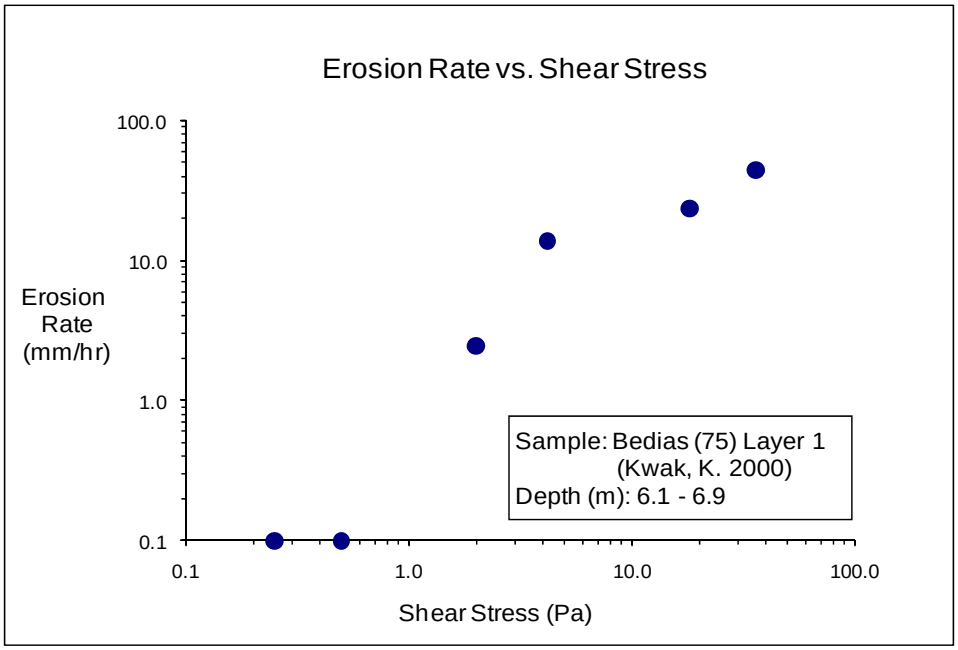

Figure D-21(a). EFA test results for soil sample Bedias (75) Layer 1 (Shear Stress).

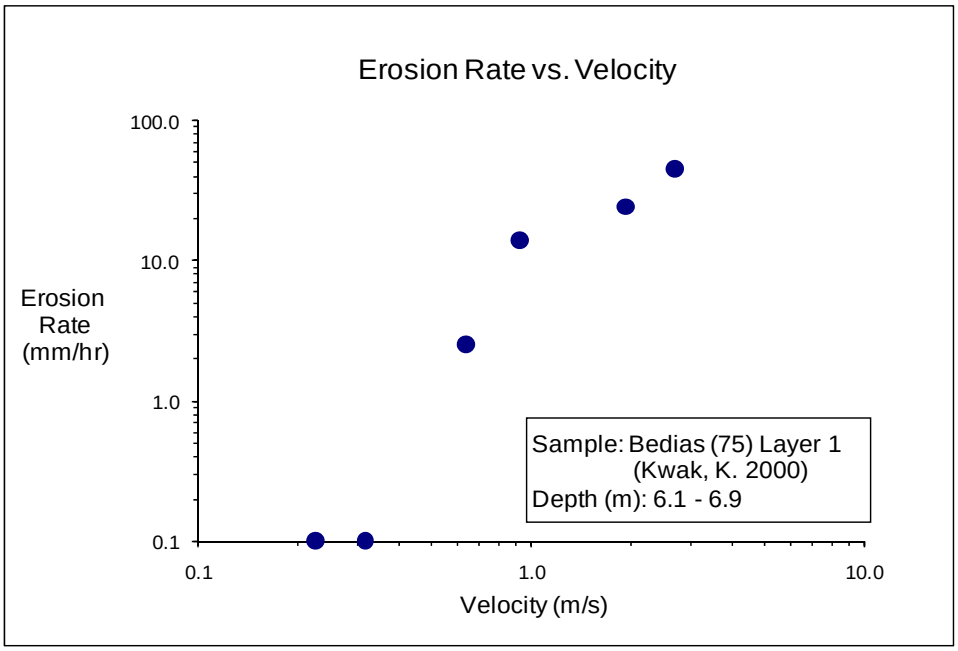

Figure D-21(b). EFA test results for soil sample Bedias (75) Layer 1 (Velocity).

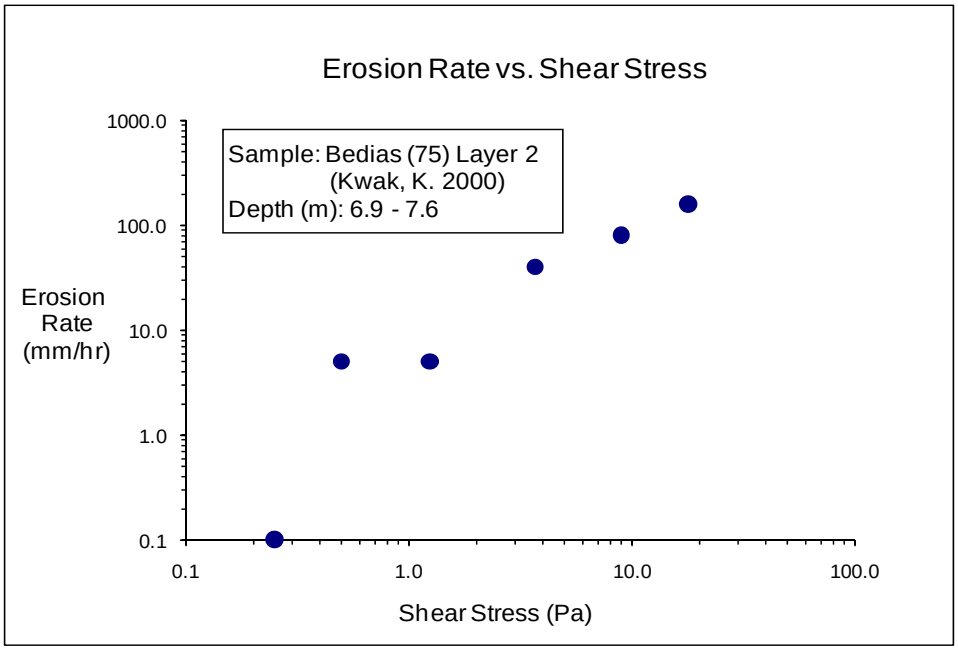

Figure D-22(a). EFA test results for soil sample Bedias (75) Layer 2 (Shear Stress).

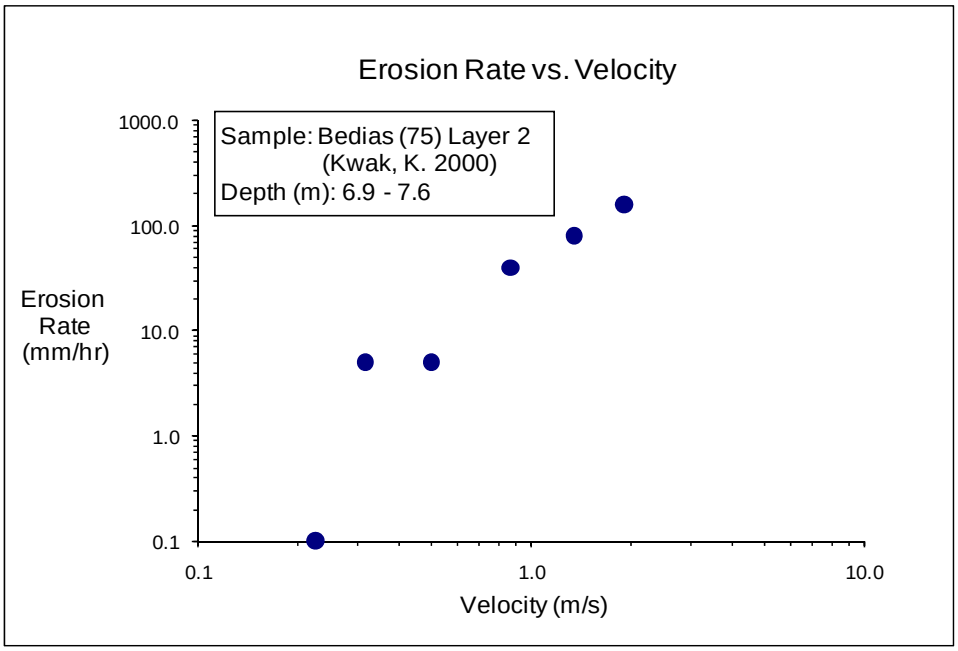

Figure D-22(b). EFA test results for soil sample Bedias (75) Layer 2 (Velocity).

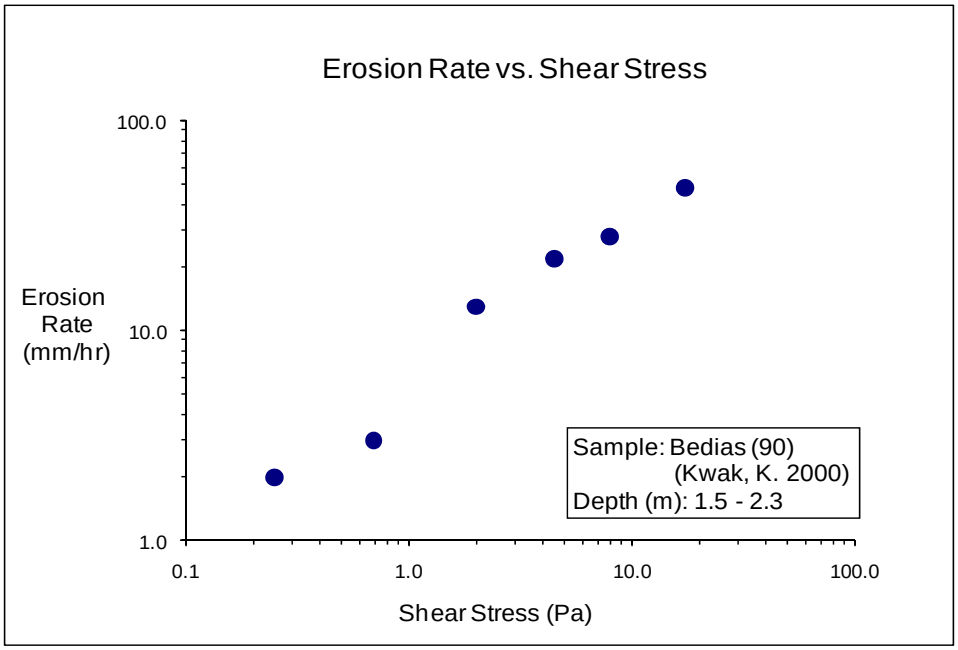

Figure D-23(a). EFA test results for soil sample Bedias (90) (Shear Stress).

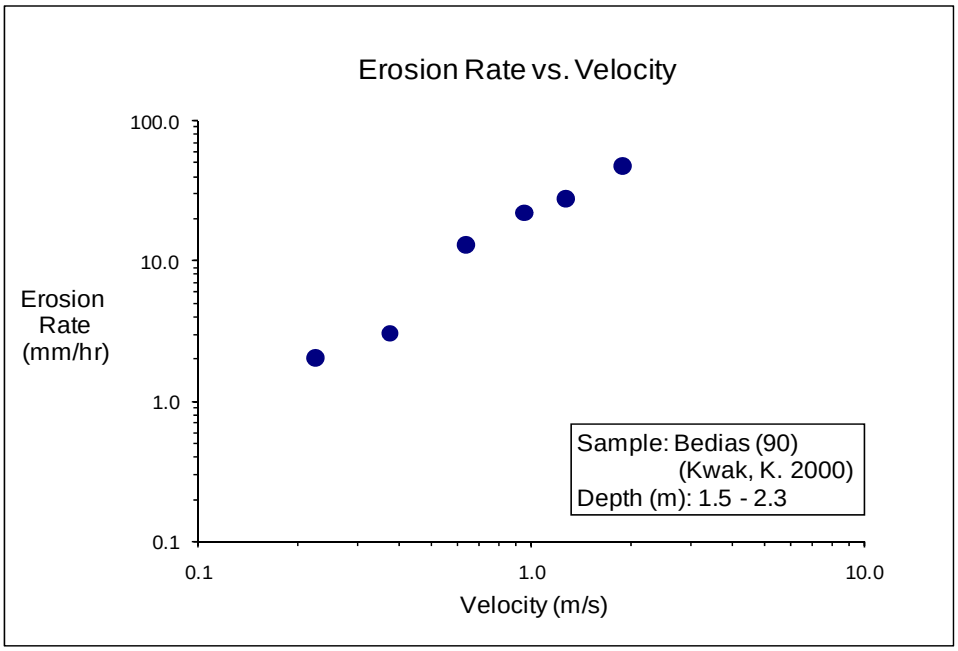

Figure D-23(b). EFA test results for soil sample Bedias (90) (Velocity).

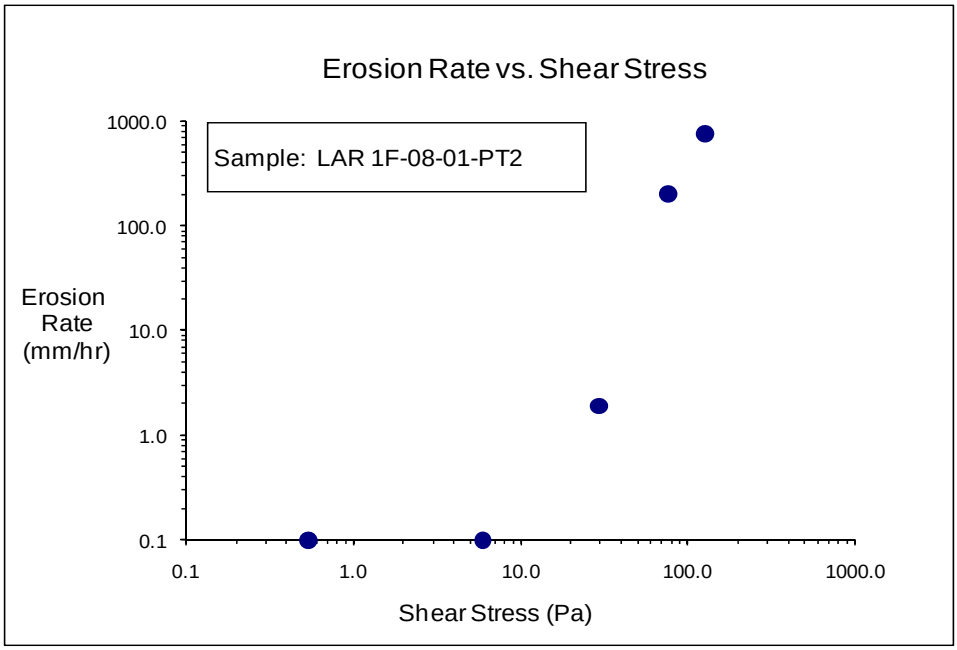

Figure D-24(a). EFA test results for soil sample LAR 1F-08-01-PT2 (Shear Stress).

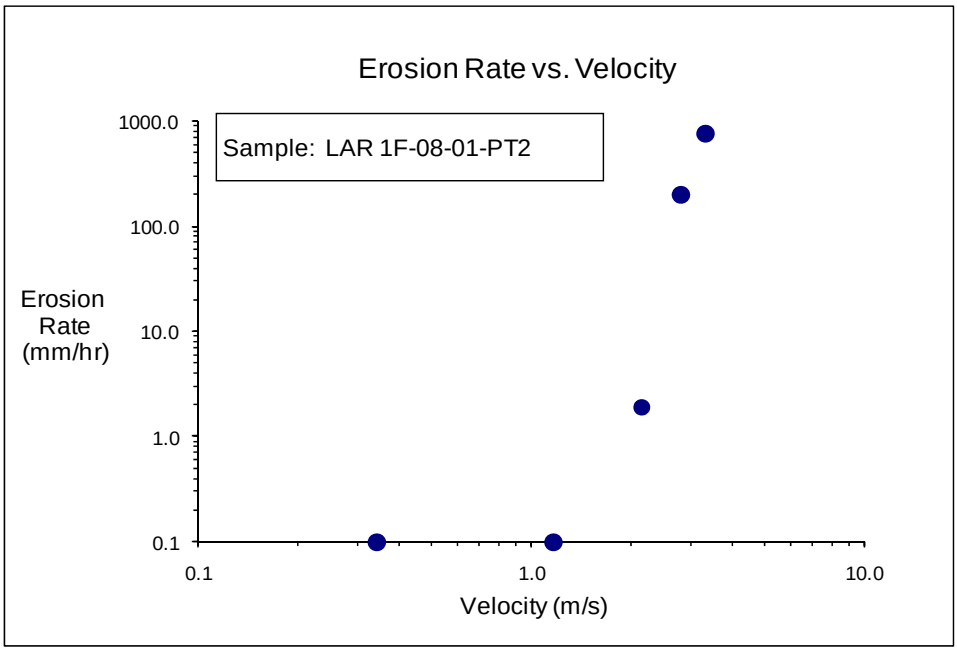

Figure D-24(b). EFA test results for soil sample LAR 1F-08-01-PT2 (Velocity).

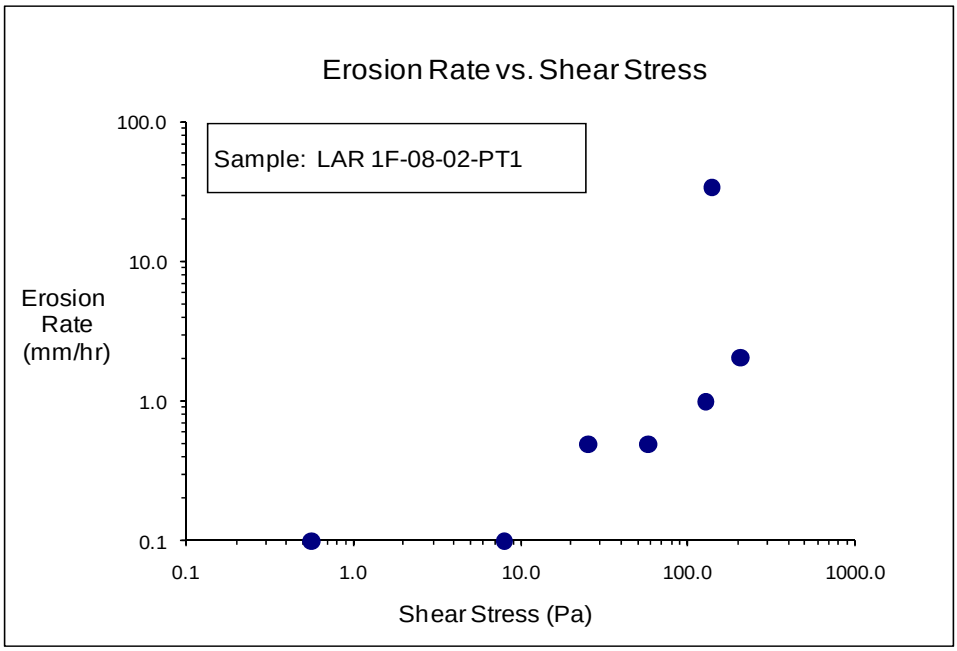

Figure D-25(a). EFA test results for soil sample LAR 1F-08-01-PT1 (Shear Stress).

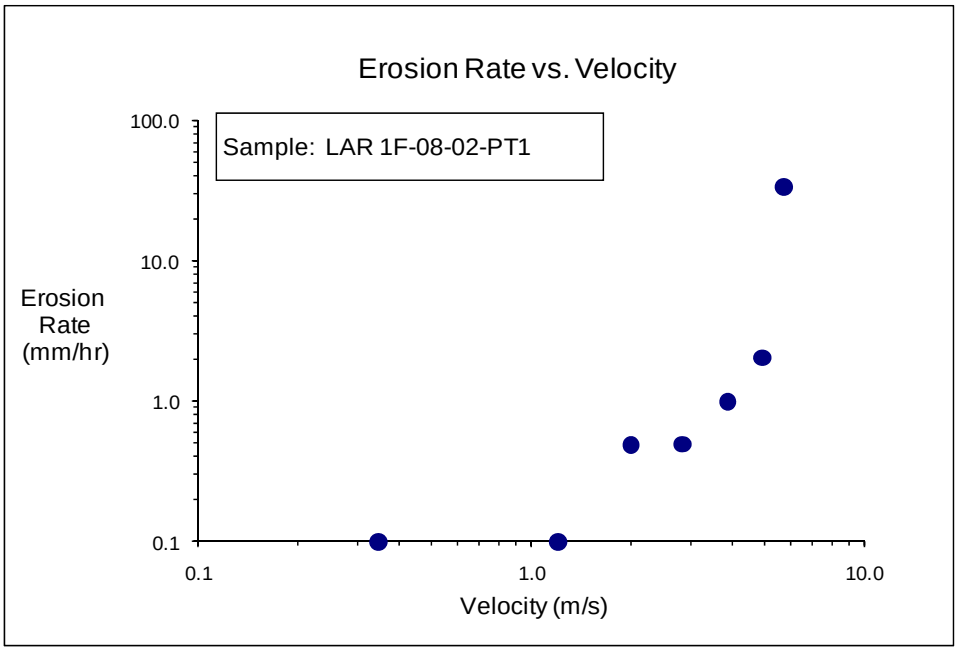

Figure D-25(b). EFA test results for soil sample LAR 1F-08-01-PT1 (Velocity).

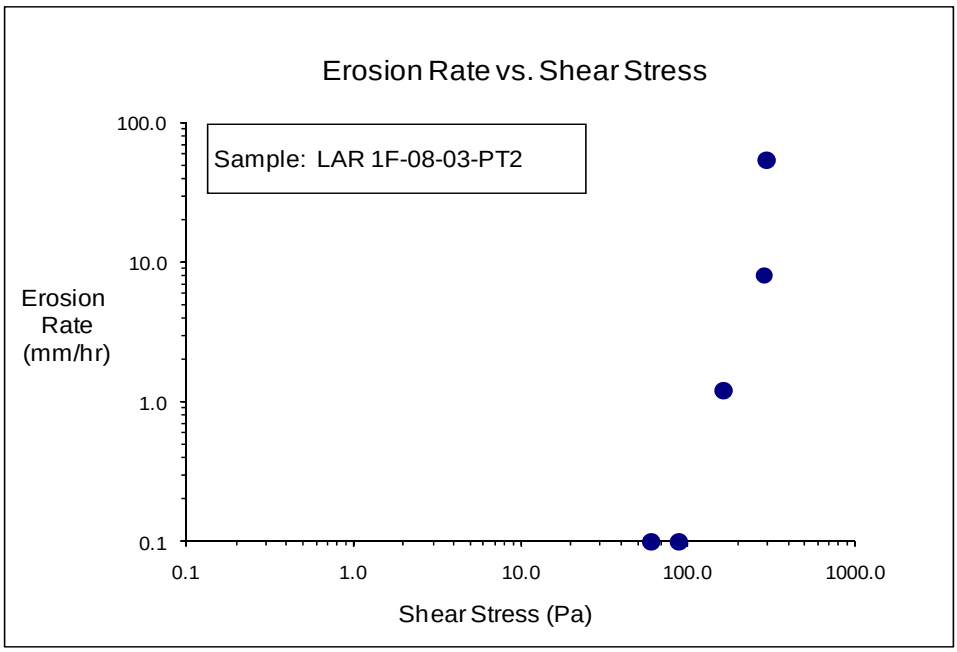

Figure D-26(a). EFA test results for soil sample LAR 1F-08-03-PT2 (Shear Stress).

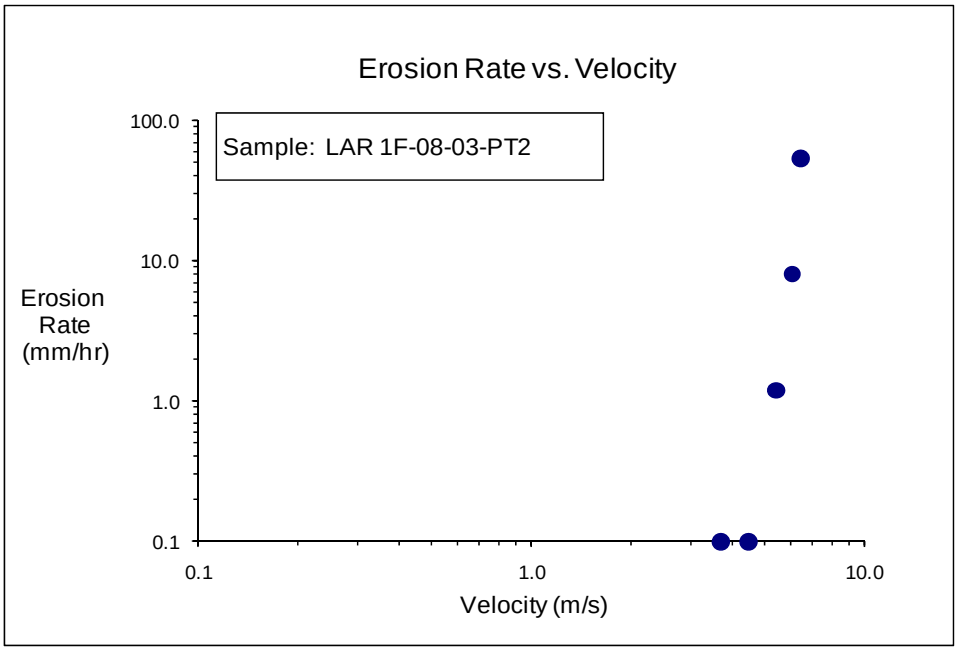

Figure D-26(b). EFA test results for soil sample LAR 1F-08-03-PT2 (Velocity).

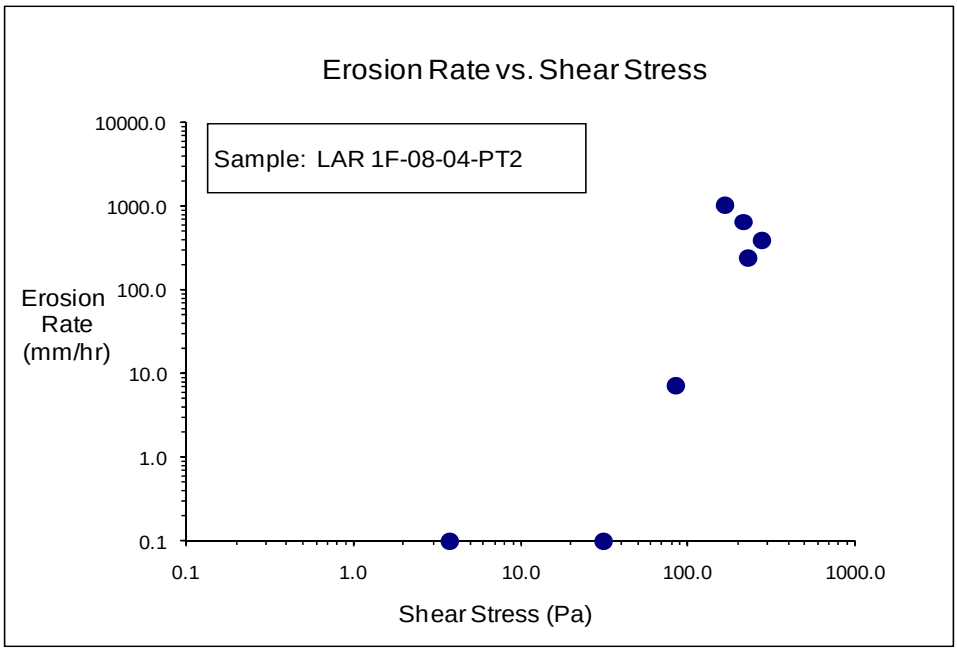

Figure D-27(a). EFA test results for soil sample LAR 1F-08-04-PT2 (Shear Stress).

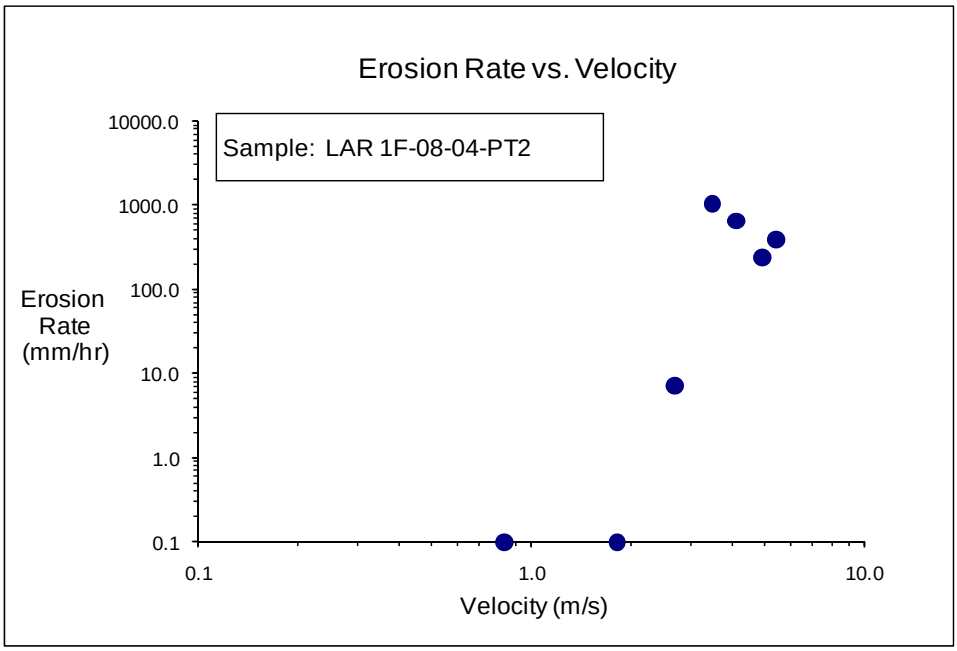

Figure D-27(b). EFA test results for soil sample LAR 1F-08-04-PT2 (Velocity).

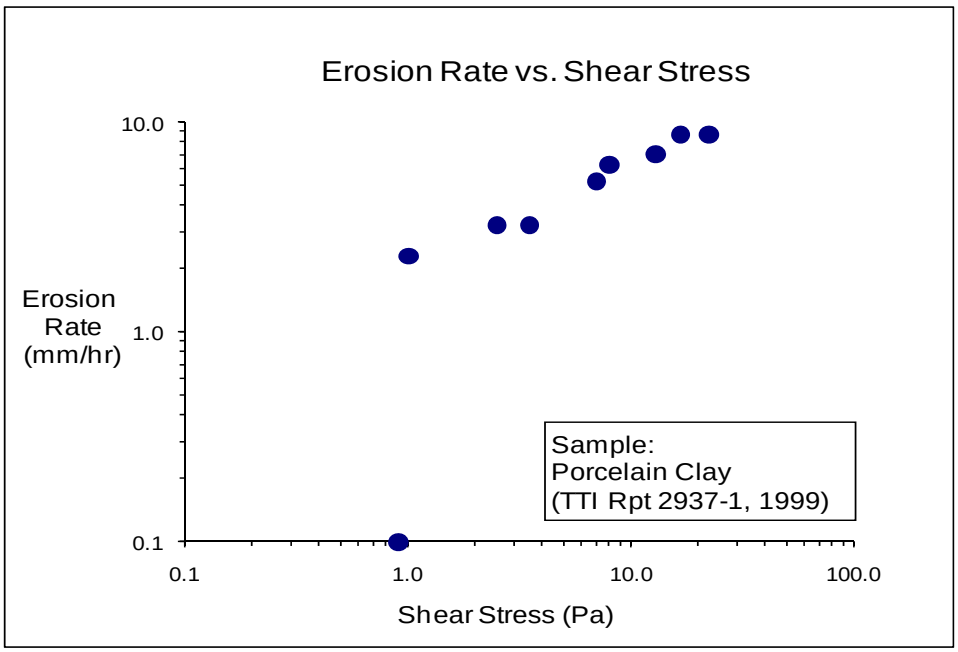

Figure D-28(a). EFA test results for soil sample Porcelain Clay (Shear Stress).

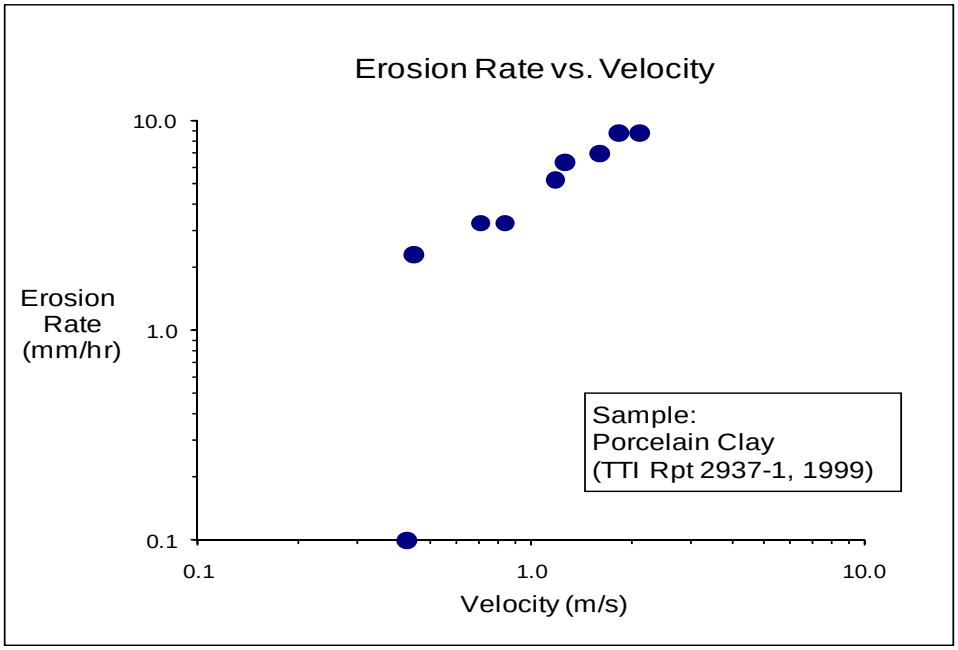

Figure D-28(b). EFA test results for soil sample Porcelain Clay (Velocity).

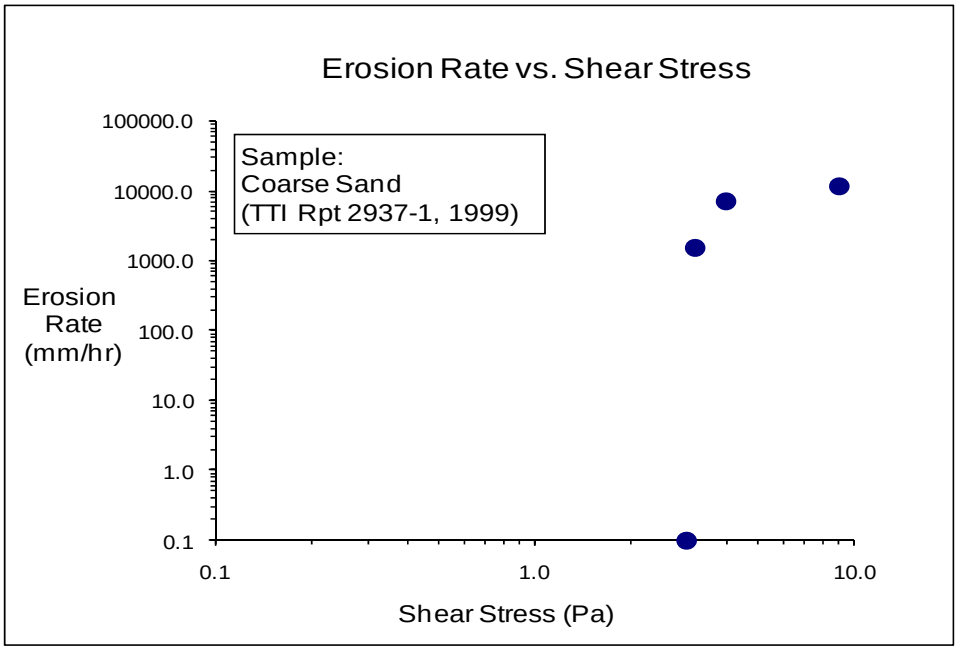

Figure D-29(a). EFA test results for soil sample Coarse Sand (Shear Stress).

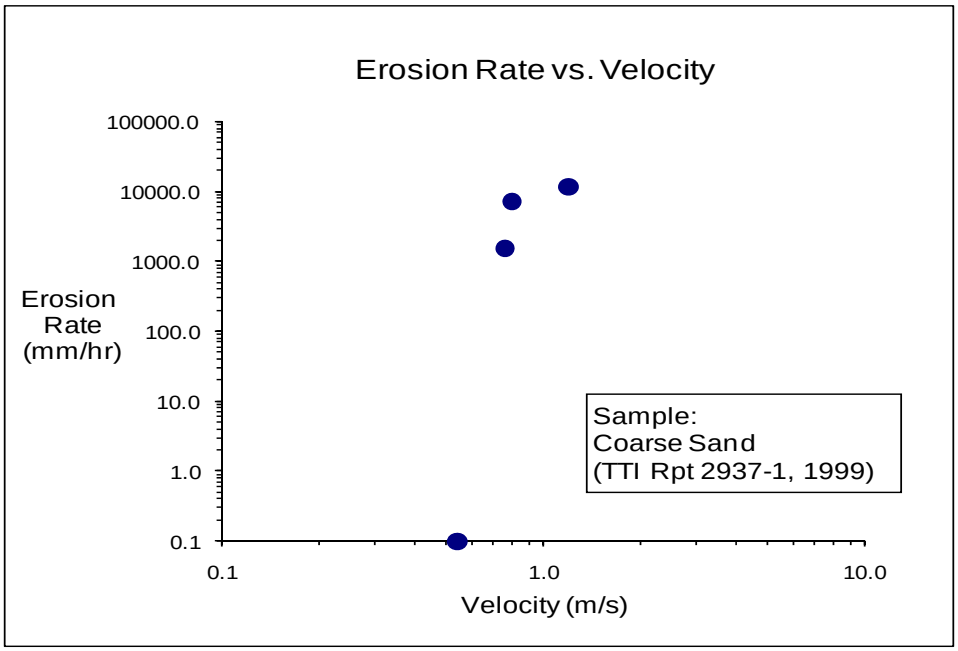

Figure D-29(b). EFA test results for soil sample Coarse Sand (Velocity).

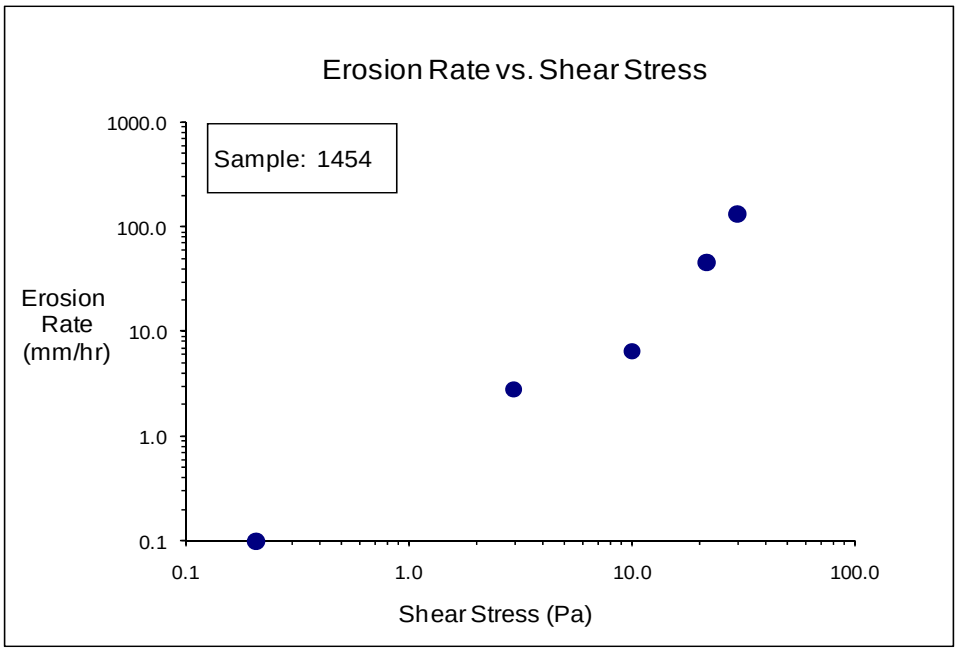

Figure D-30(a). EFA test results for soil sample 1454 (Shear Stress).

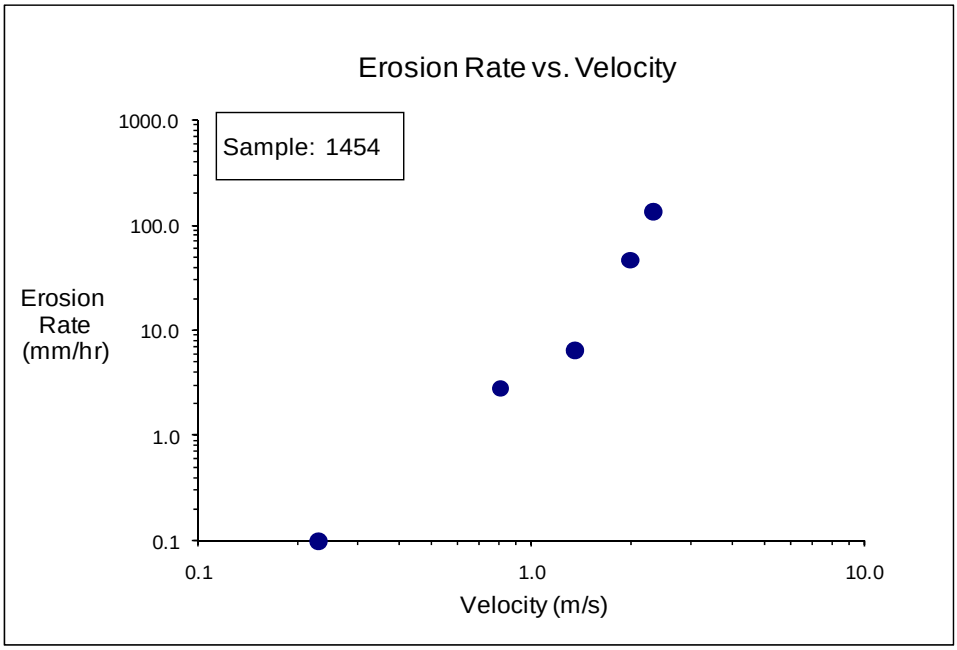

Figure D-30(b). EFA test results for soil sample 1454 (Velocity).

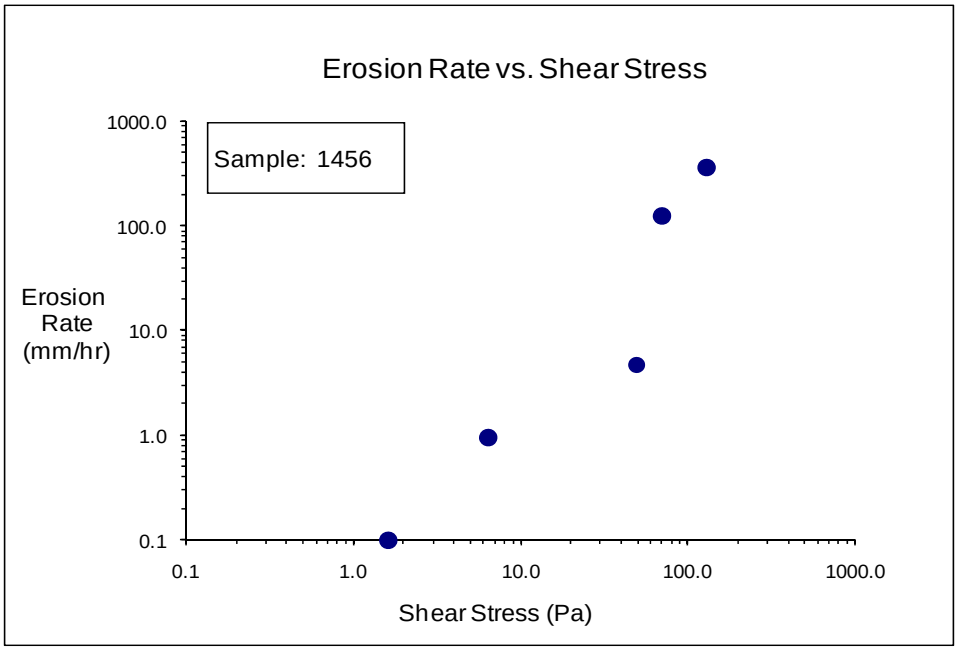

Figure D-31(a). EFA test results for soil sample 1456 (Shear Stress).

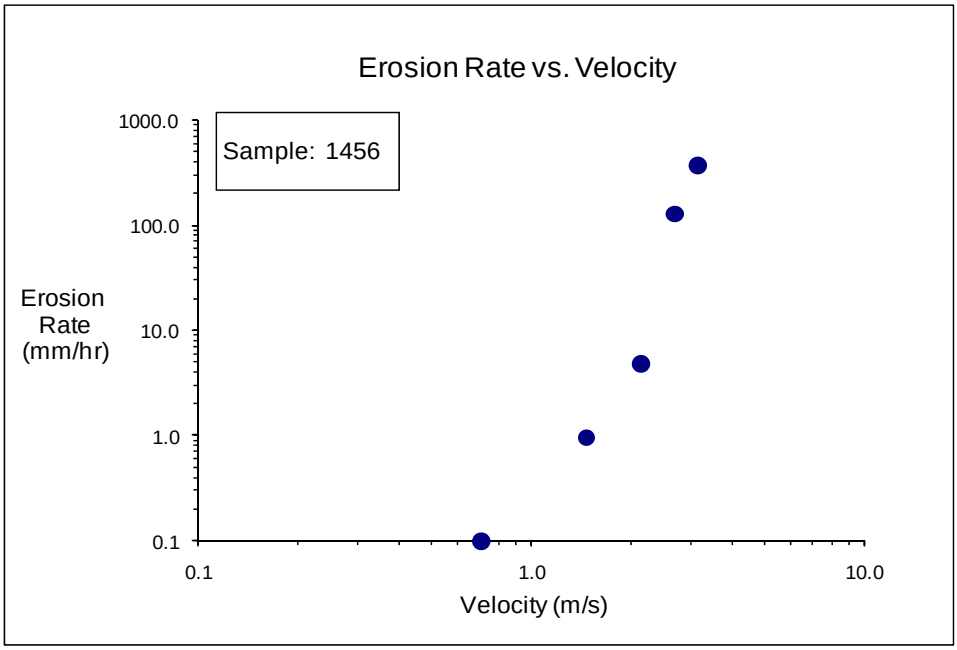

Figure D-31(b). EFA test results for soil sample 1456 (Velocity).

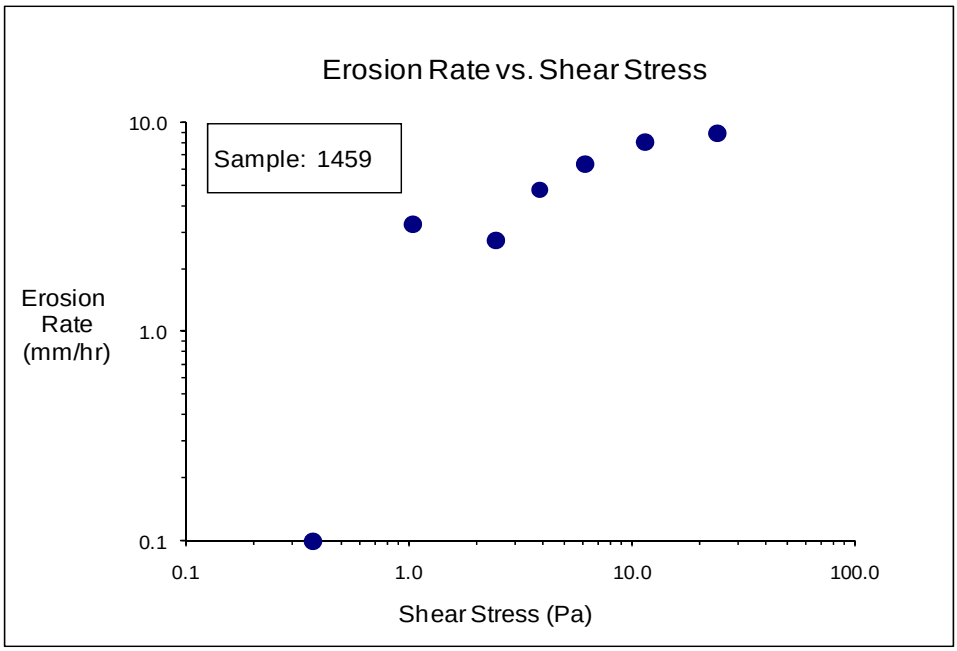

Figure D-32(a). EFA test results for soil sample 1459 (Shear Stress).

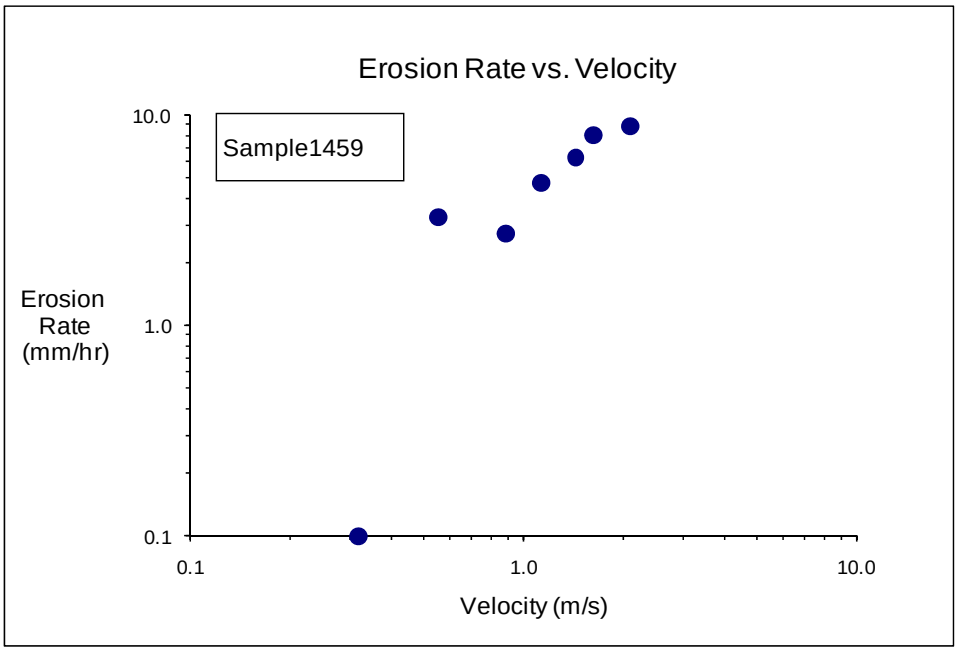

Figure D-32(b). EFA test results for soil sample 1459 (Velocity).

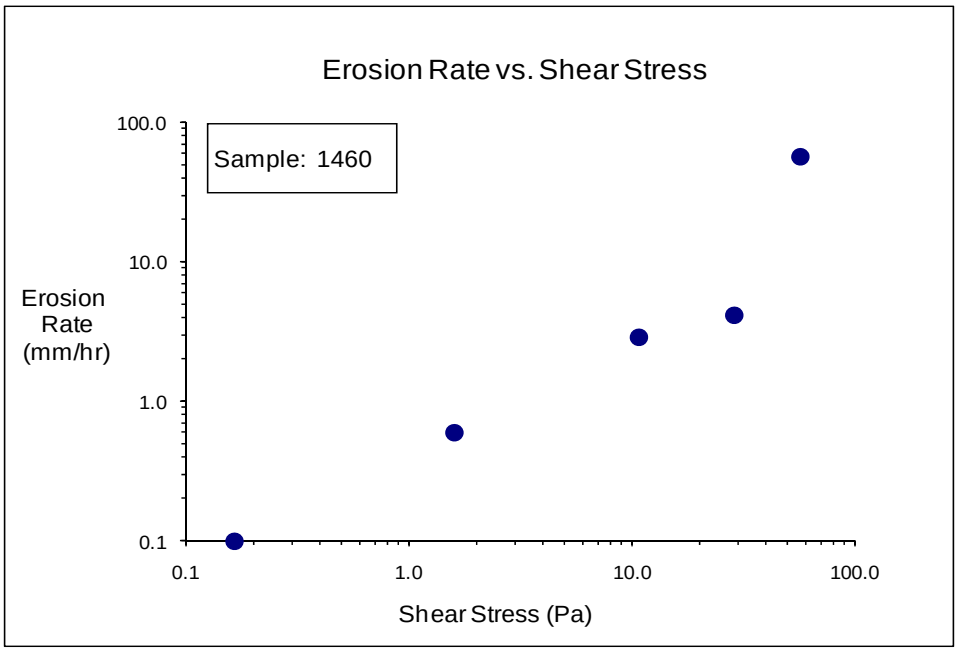

Figure D-33(a). EFA test results for soil sample 1460 (Shear Stress).

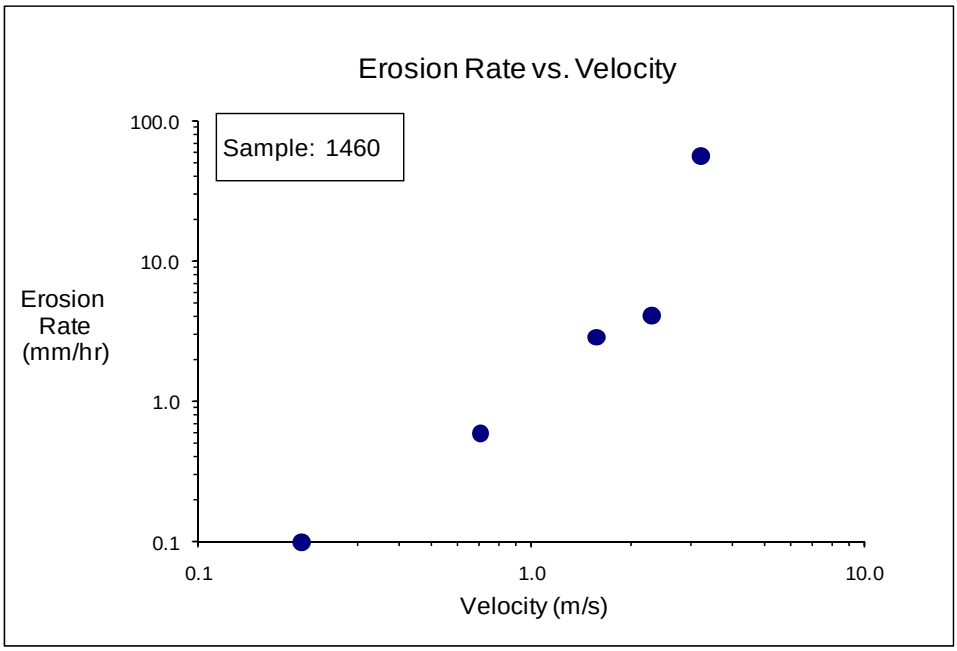

Figure D-33(b). EFA test results for soil sample 1460 (Velocity).

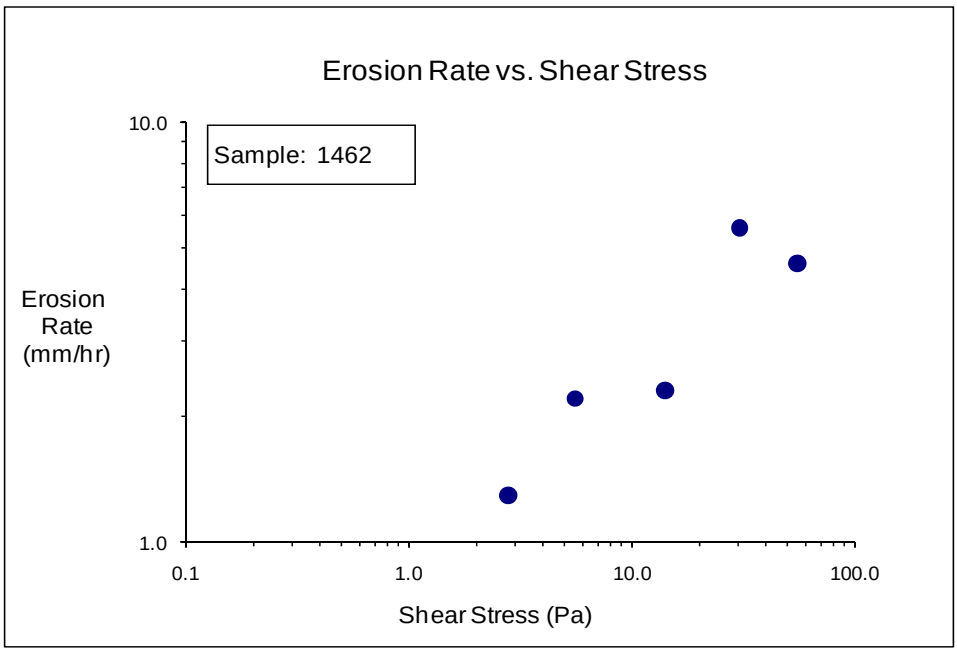

Figure D-34(a). EFA test results for soil sample 1462 (Shear Stress).

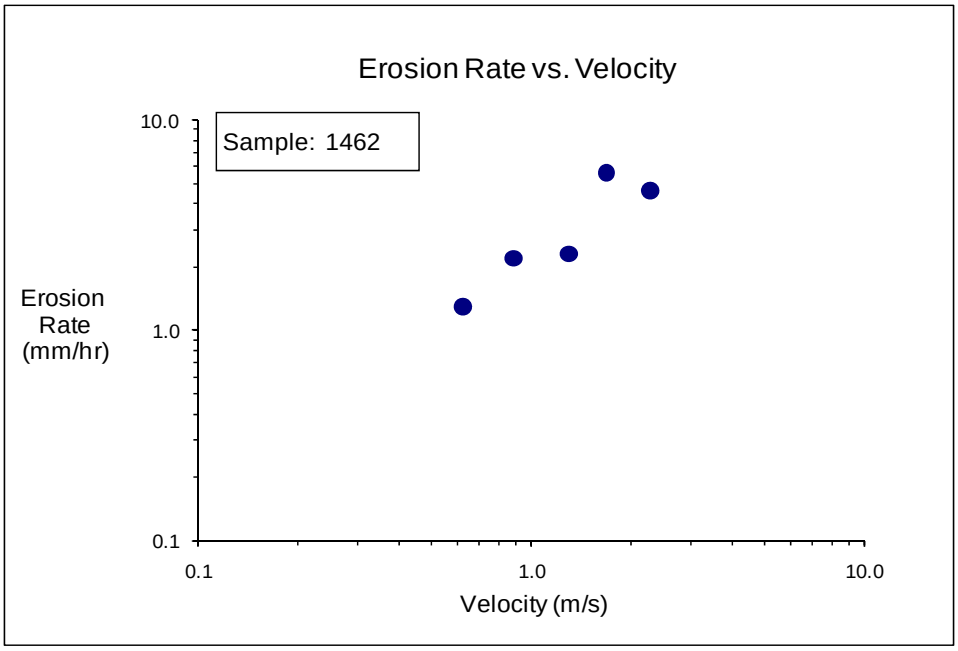

Figure D-34(b). EFA test results for soil sample 1462 (Velocity).

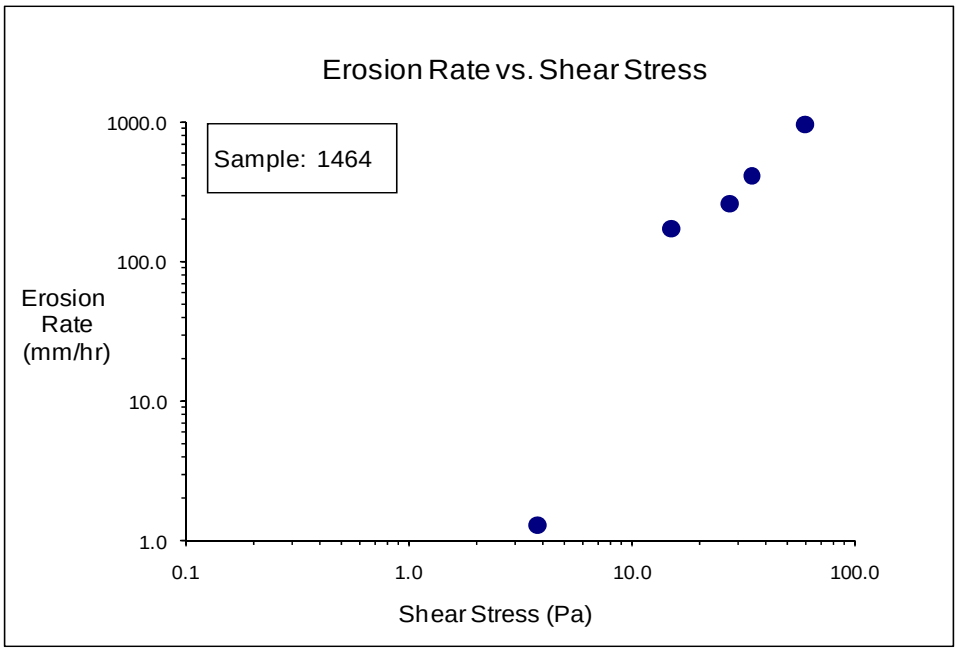

Figure D-35(a). EFA test results for soil sample 1464 (Shear Stress).

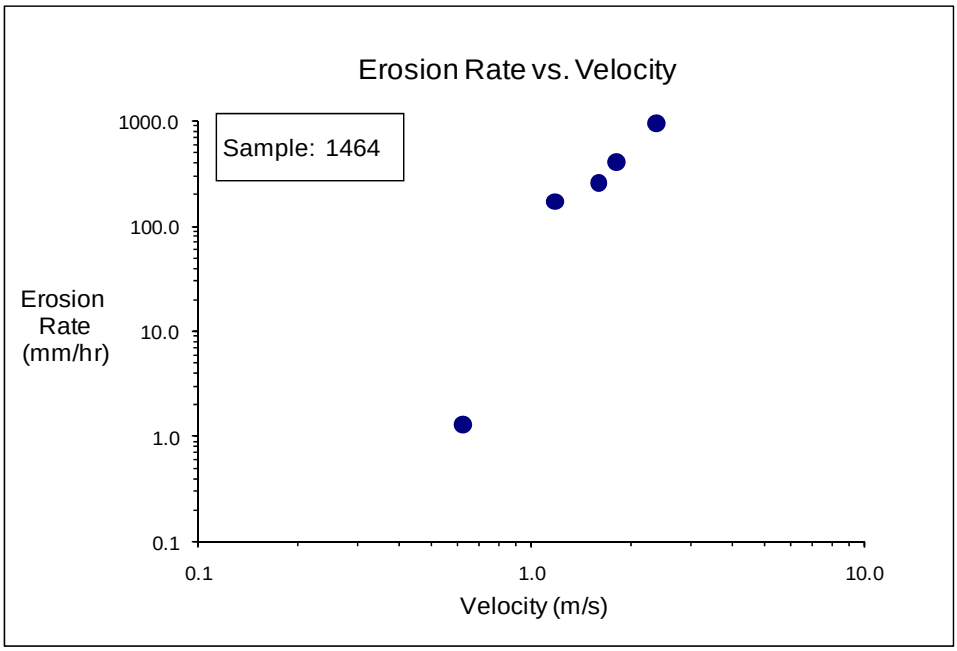

Figure D-35(b). EFA test results for soil sample 1464 (Velocity).

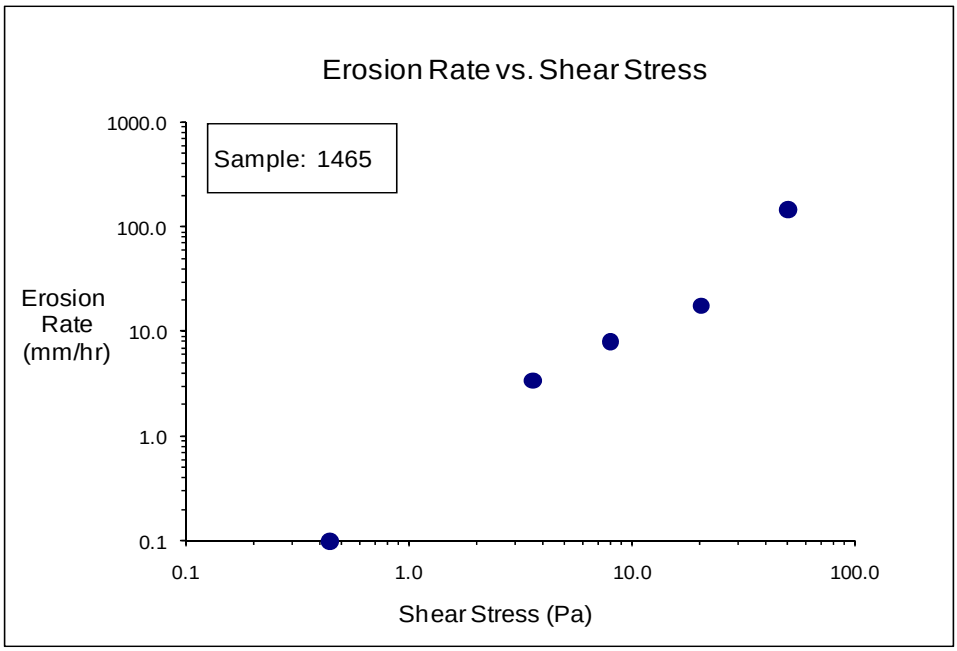

Figure D-36(a). EFA test results for soil sample 1456 (Shear Stress).

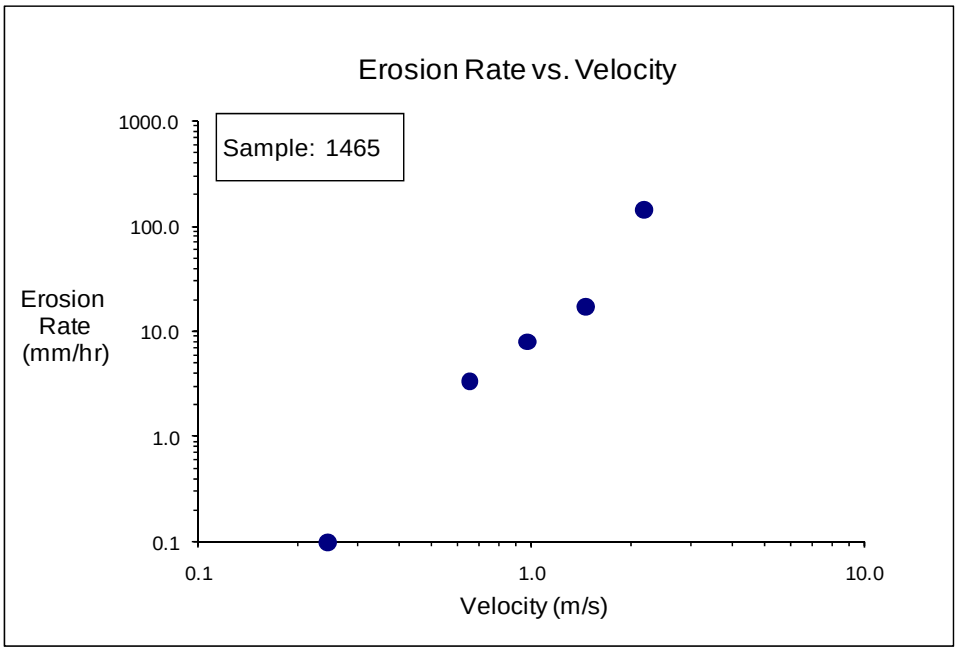

Figure D-36(b). EFA test results for soil sample 1456 (Velocity).

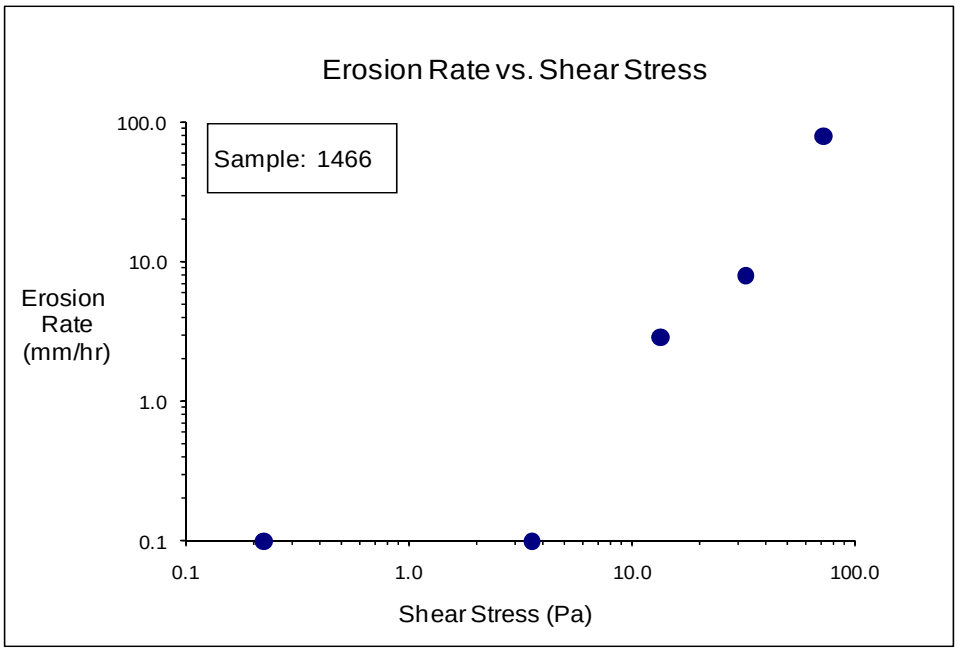

Figure D-37(a). EFA test results for soil sample 1466 (Shear Stress).

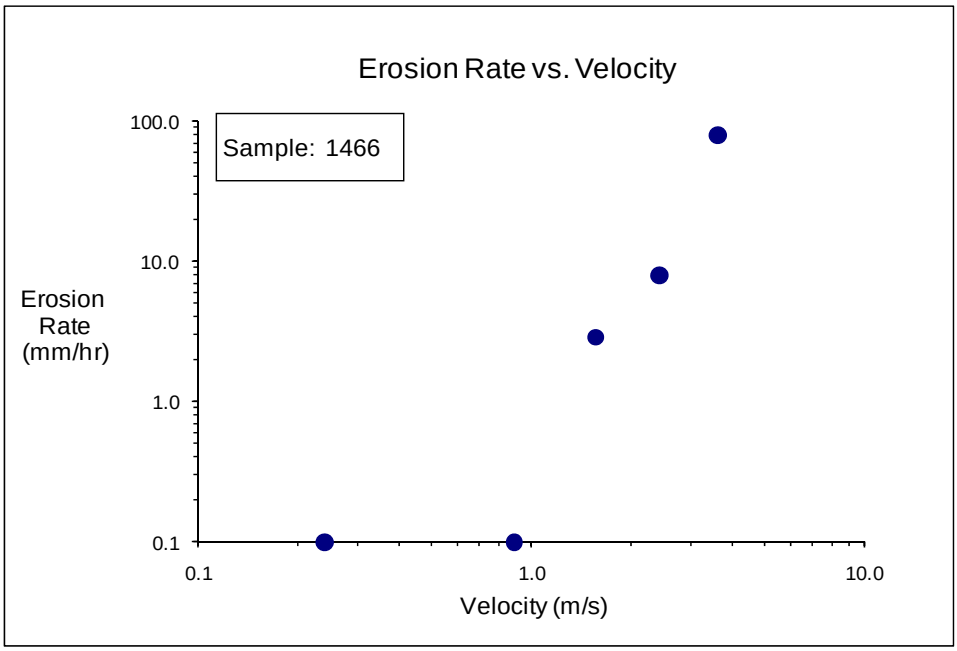

Figure D-37(b). EFA test results for soil sample 1466 (Velocity).

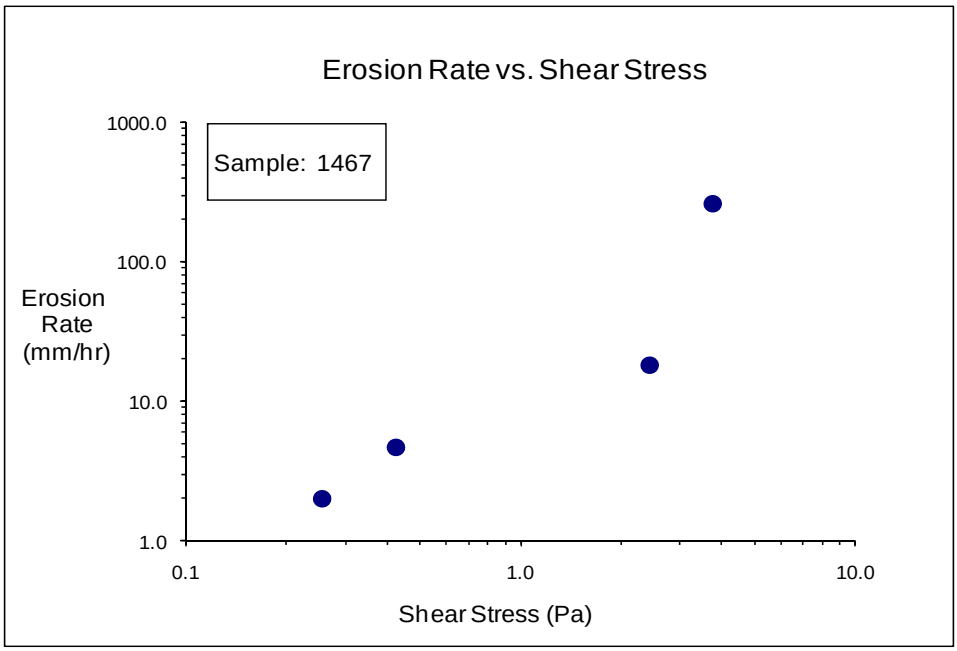

Figure D-38(a). EFA test results for soil sample 1467 (Shear Stress).

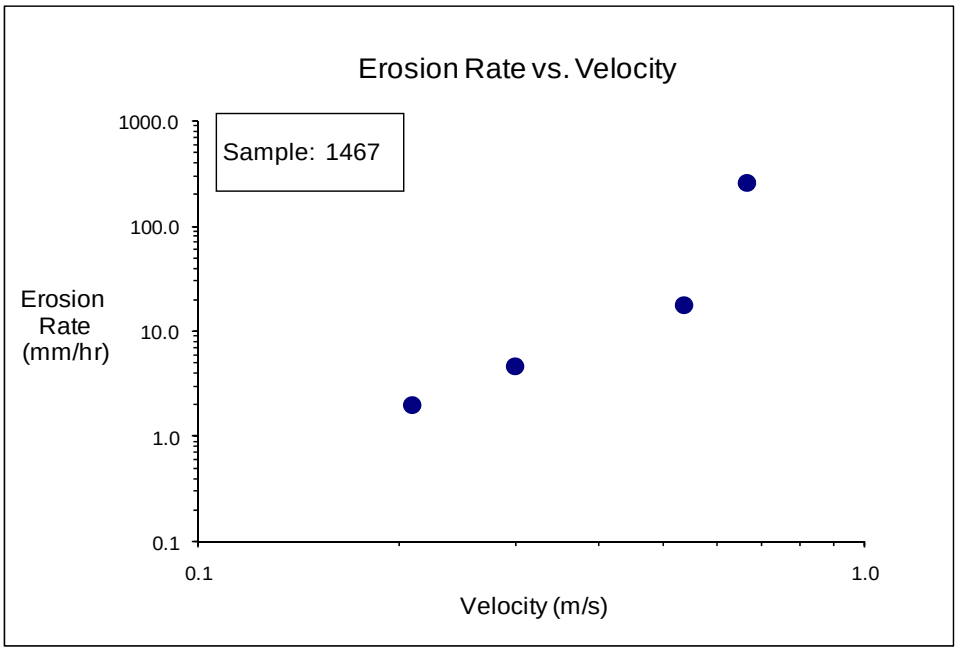

Figure D-38(b). EFA test results for soil sample 1467 (Velocity).

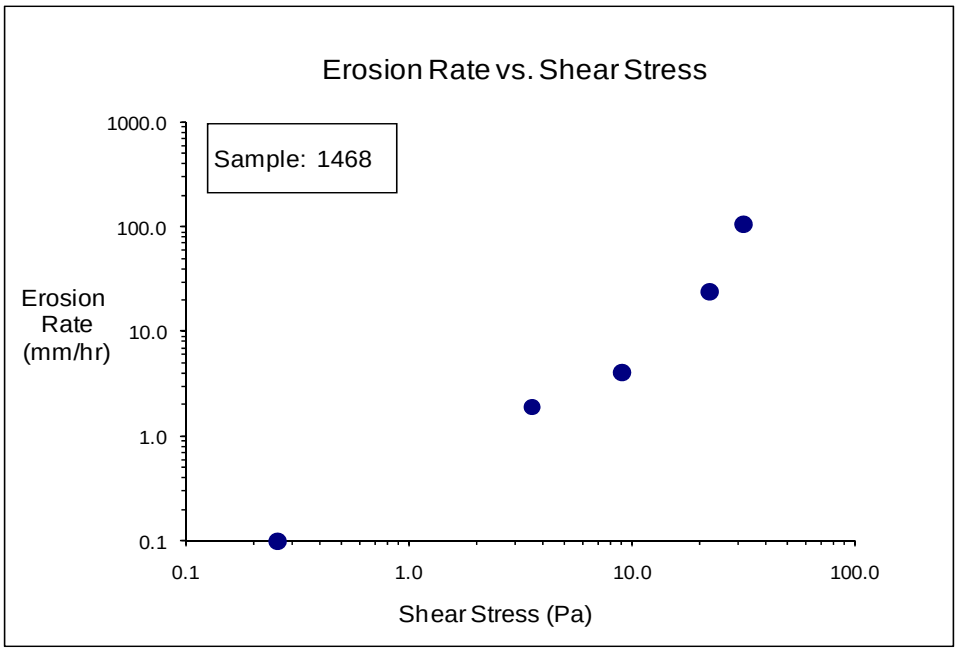

Figure D-39(a). EFA test results for soil sample 1468 (Shear Stress).

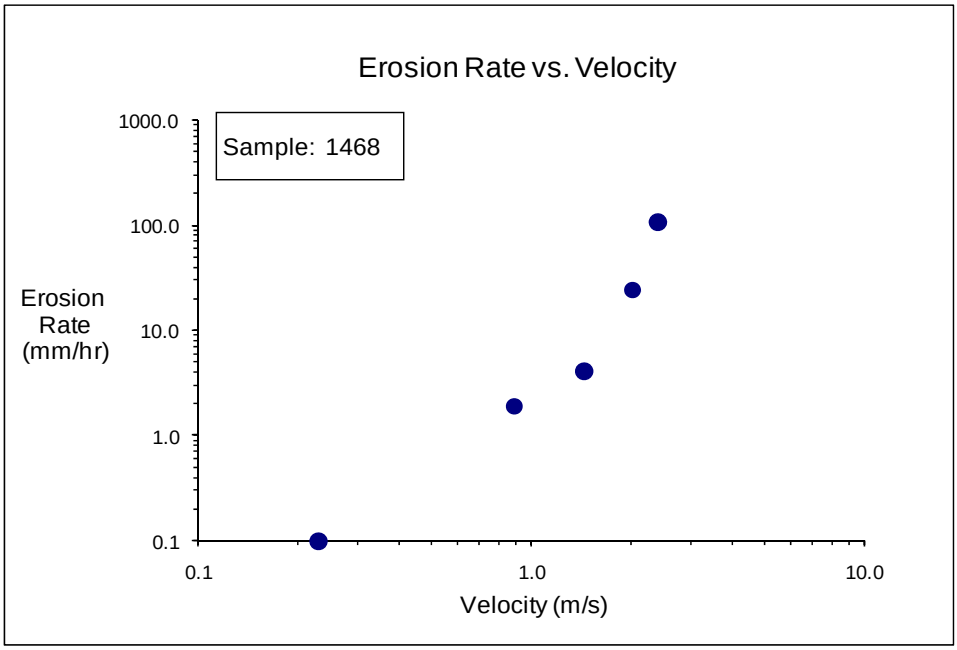

Figure D-39(b). EFA test results for soil sample 1468 (Velocity).

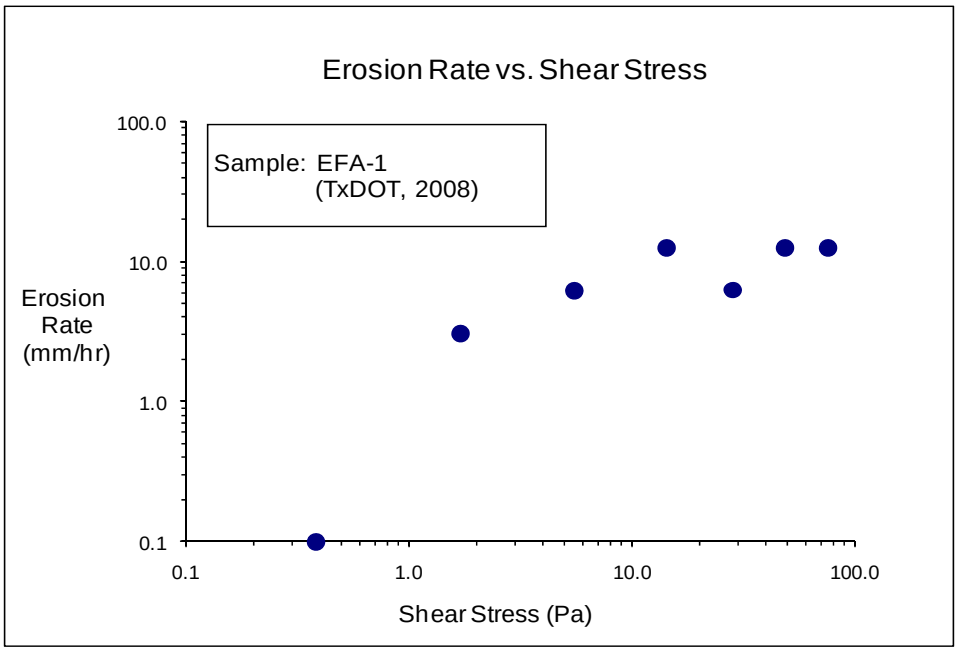

Figure D-40(a). EFA test results for soil sample EFA-1 (Shear Stress).

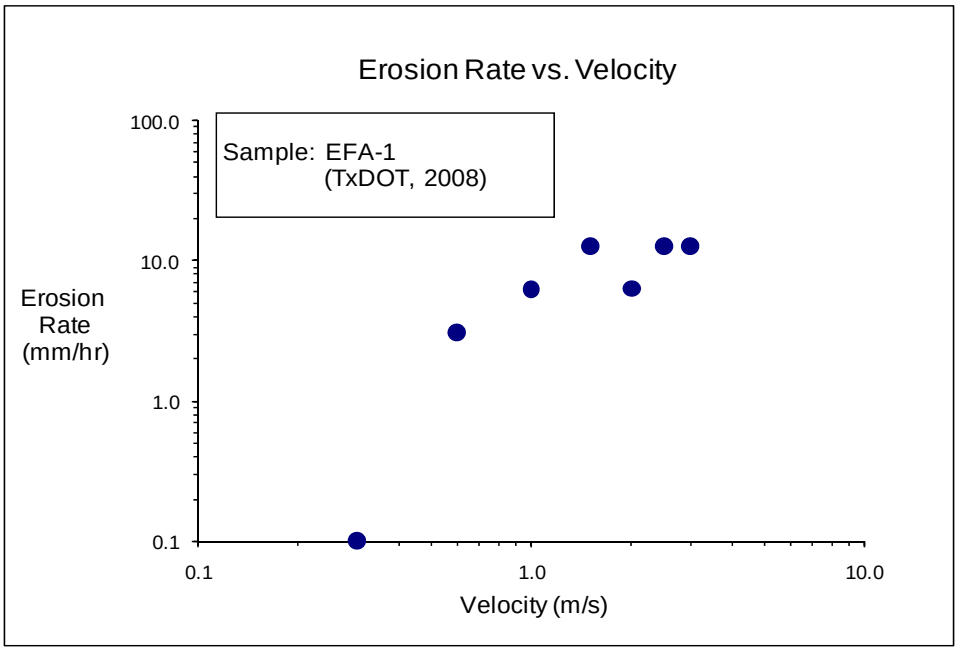

Figure D-40(b). EFA test results for soil sample EFA-1 (Velocity).

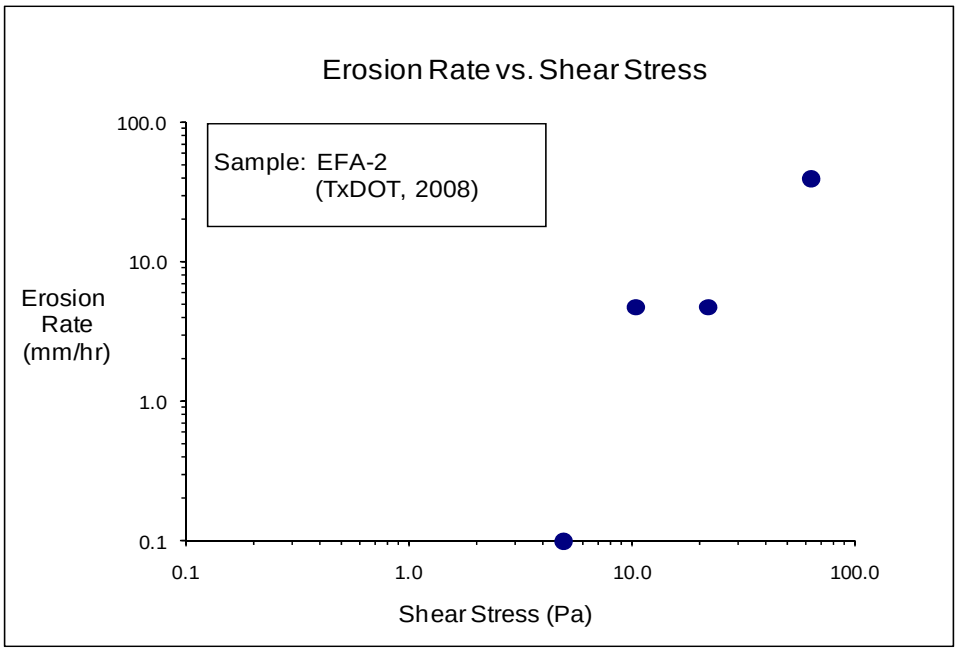

Figure D-41(a). EFA test results for soil sample EFA-2 (Shear Stress).

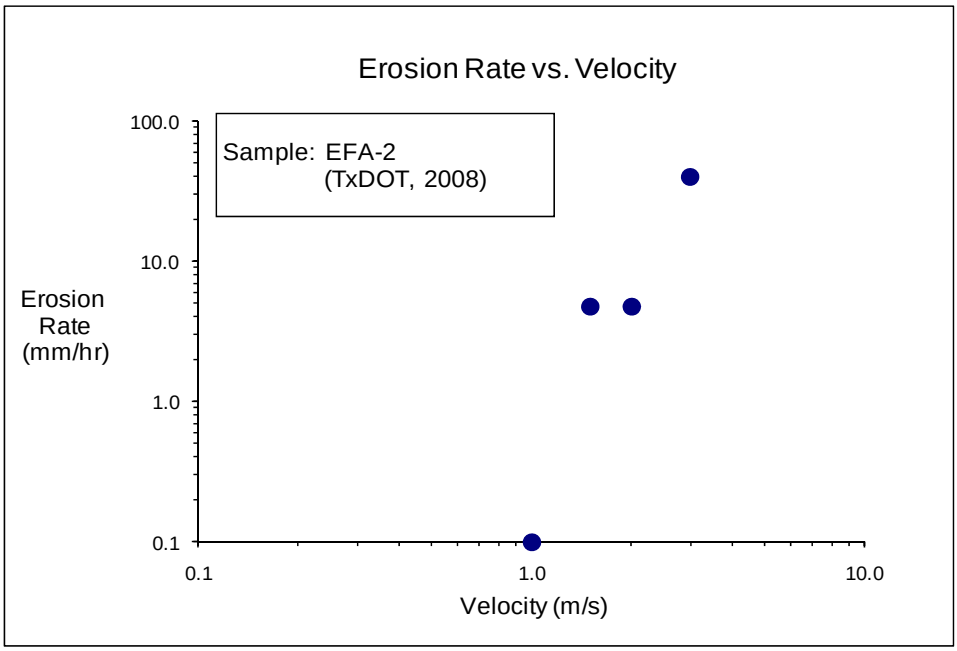

Figure D-41(b). EFA test results for soil sample EFA-2 (Velocity).

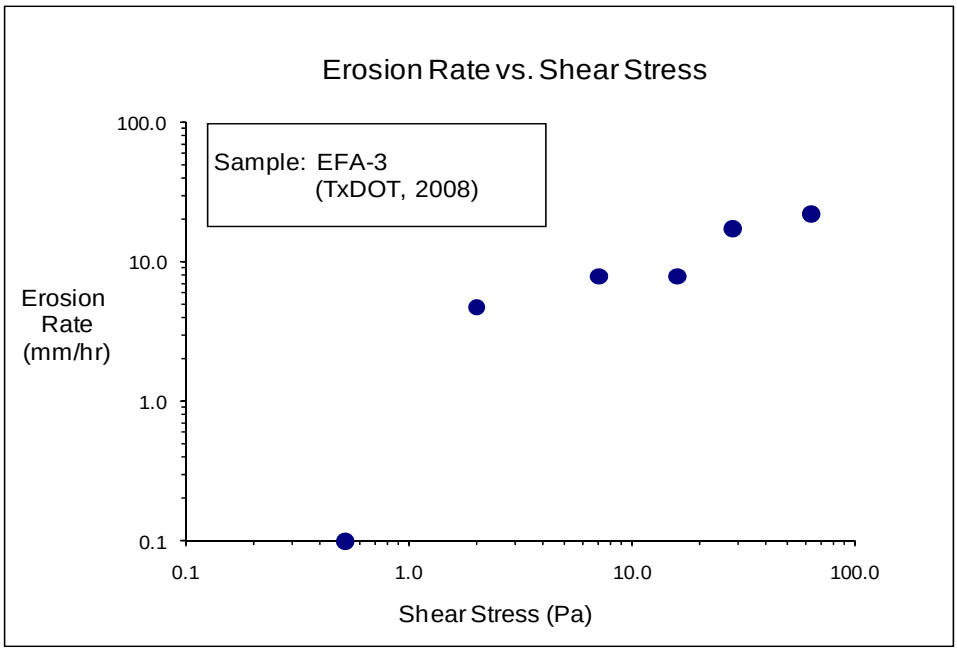

Figure D-42(a). EFA test results for soil sample EFA-3 (Shear Stress).

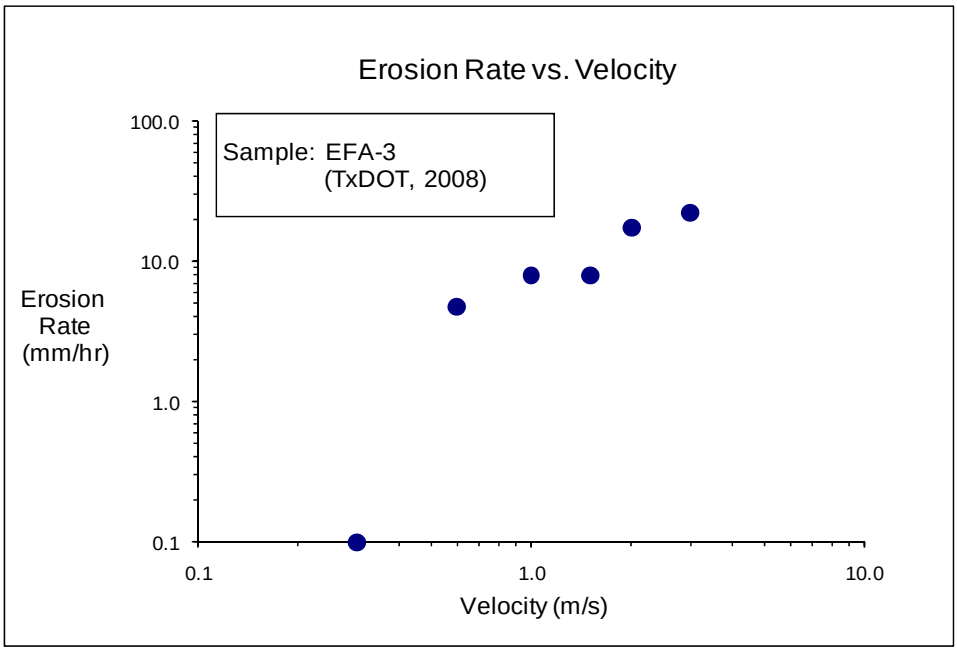

Figure D-42(b). EFA test results for soil sample EFA-3 (Velocity).

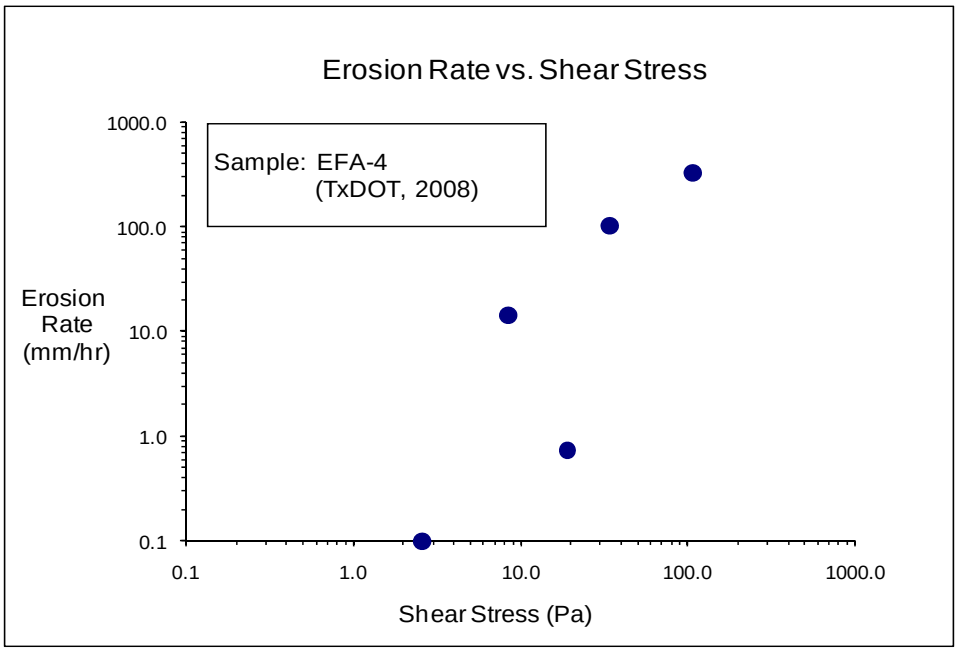

Figure D-43(a). EFA test results for soil sample EFA-4 (Shear Stress).

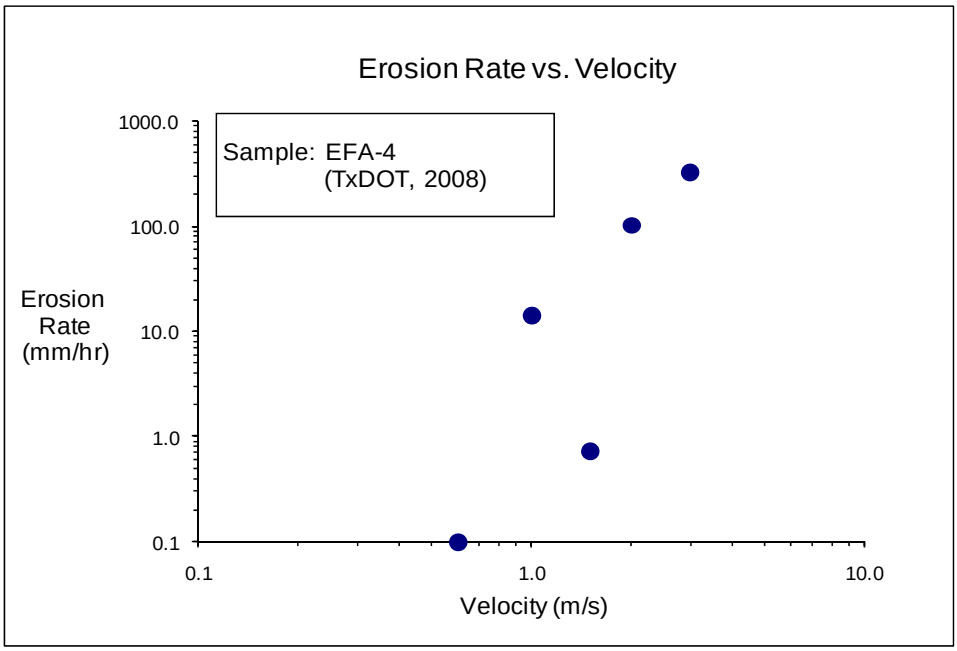

Figure D-43(b). EFA test results for soil sample EFA-4 (Velocity).

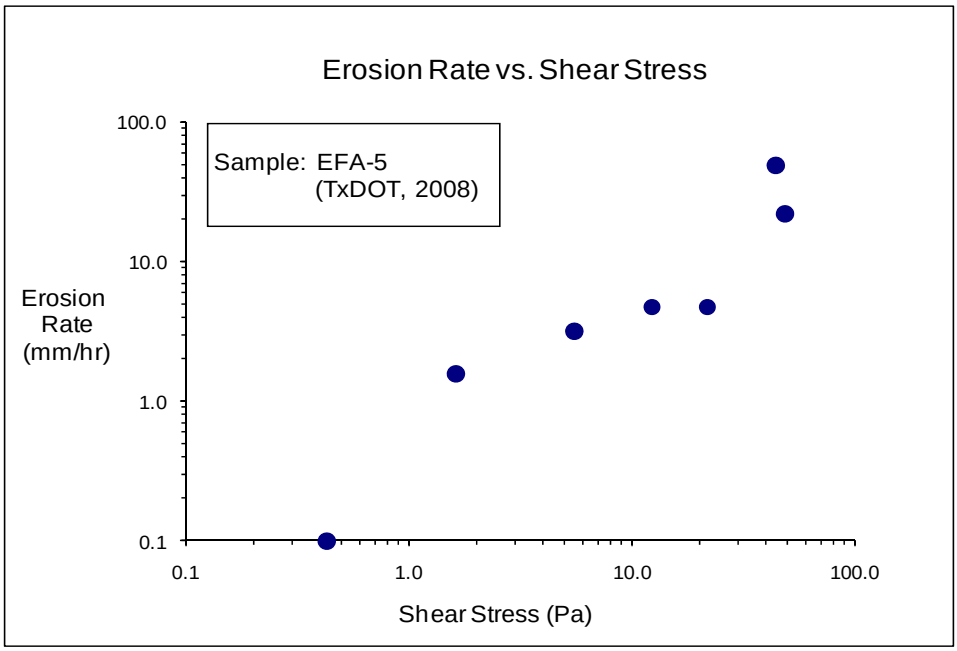

Figure D-44(a). EFA test results for soil sample EFA-5 (Shear Stress).

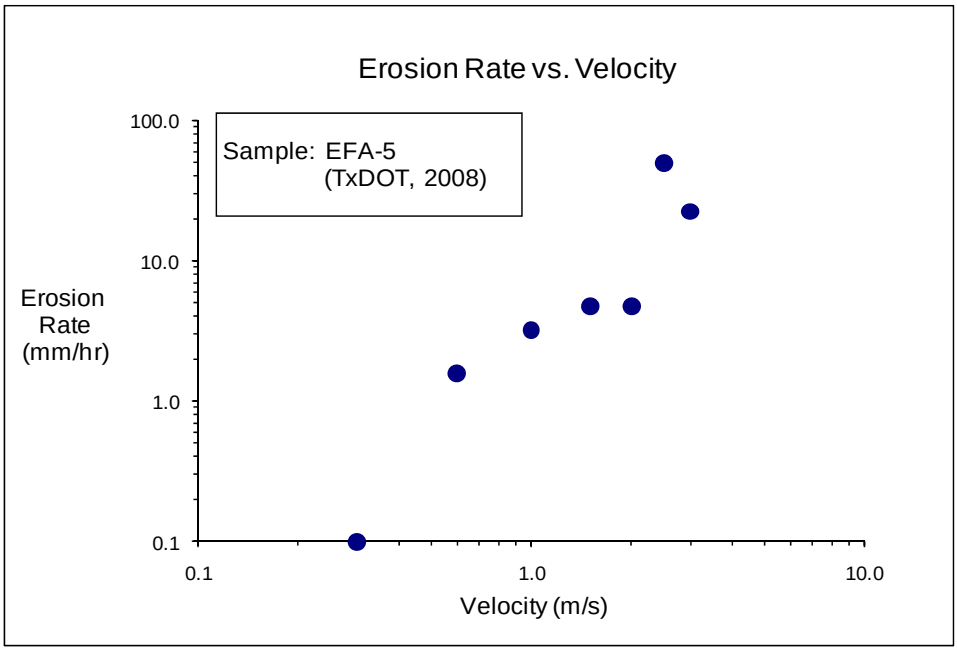

Figure D-44(b). EFA test results for soil sample EFA-5 (Velocity).

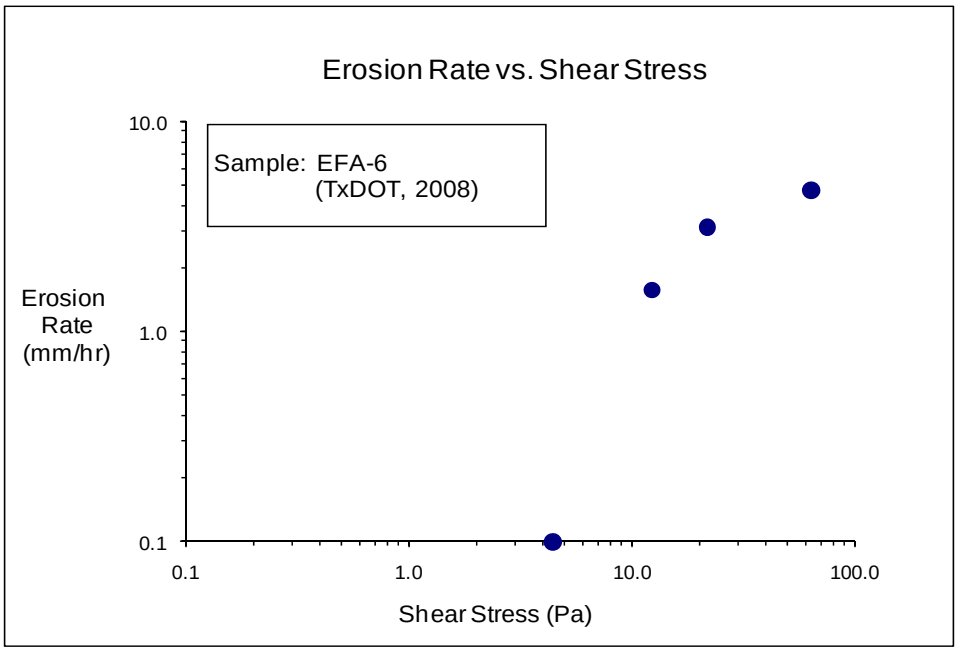

Figure D-45(a). EFA test results for soil sample EFA-6 (Shear Stress).

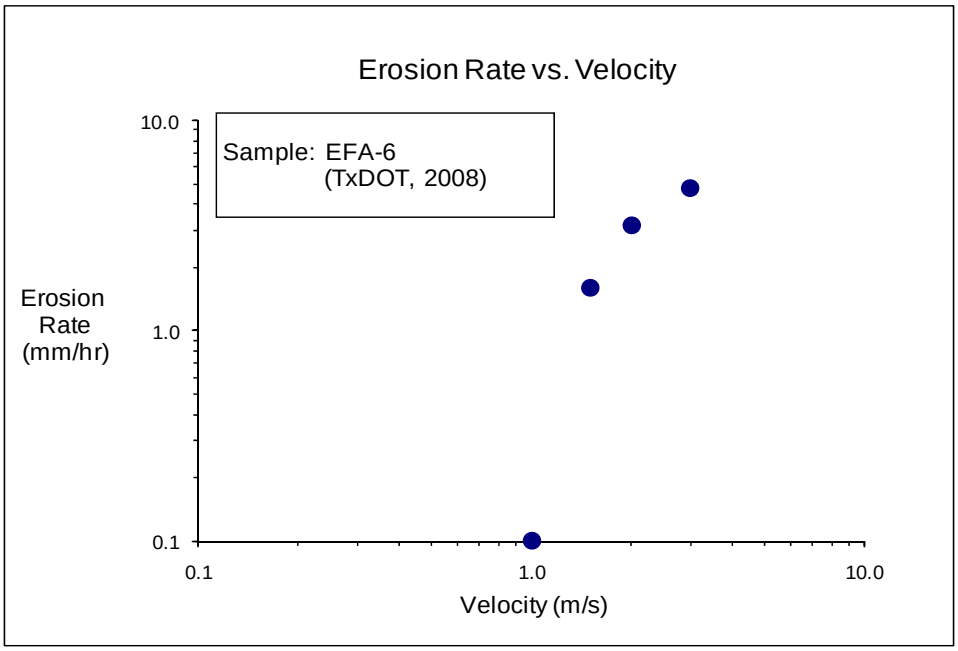

Figure D-45(b). EFA test results for soil sample EFA-6 (Velocity).

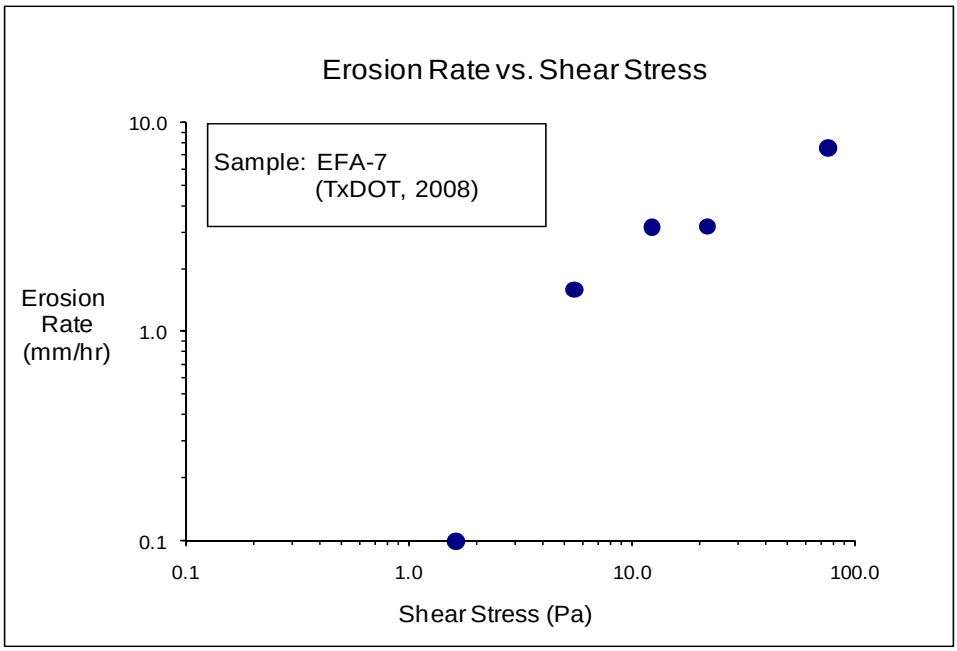

Figure D-46(a). EFA test results for soil sample EFA-7 (Shear Stress).

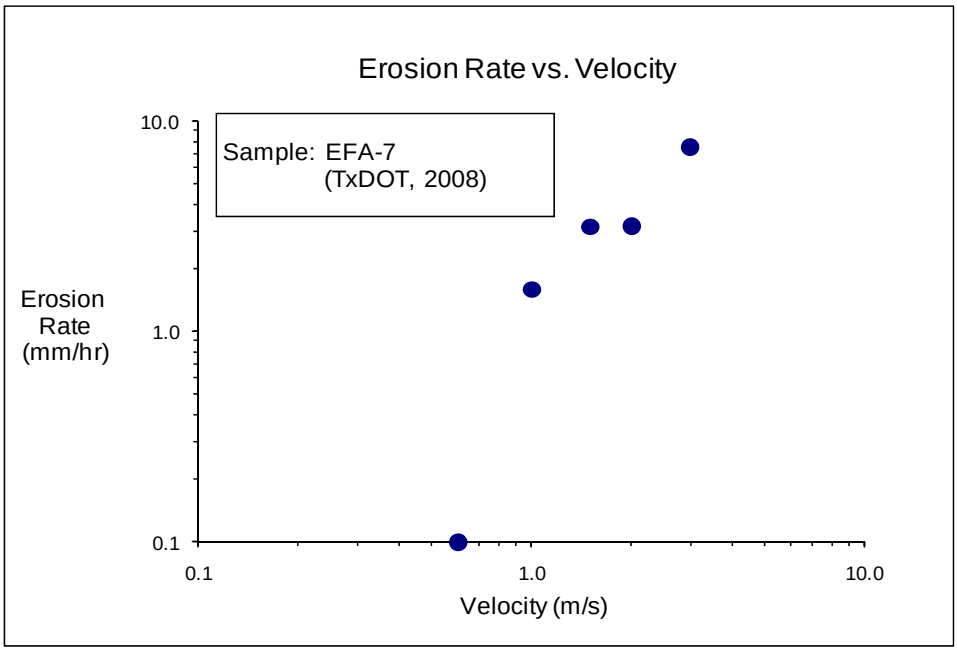

Figure D-46(b). EFA test results for soil sample EFA-7 (Velocity).

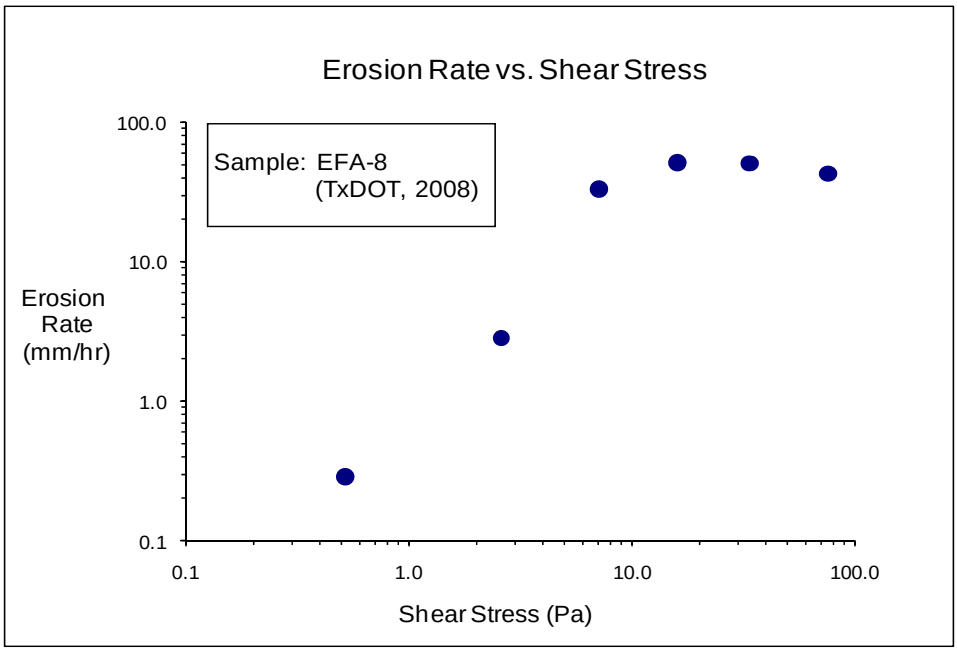

Figure D-47(a). EFA test results for soil sample EFA-8 (Shear Stress).

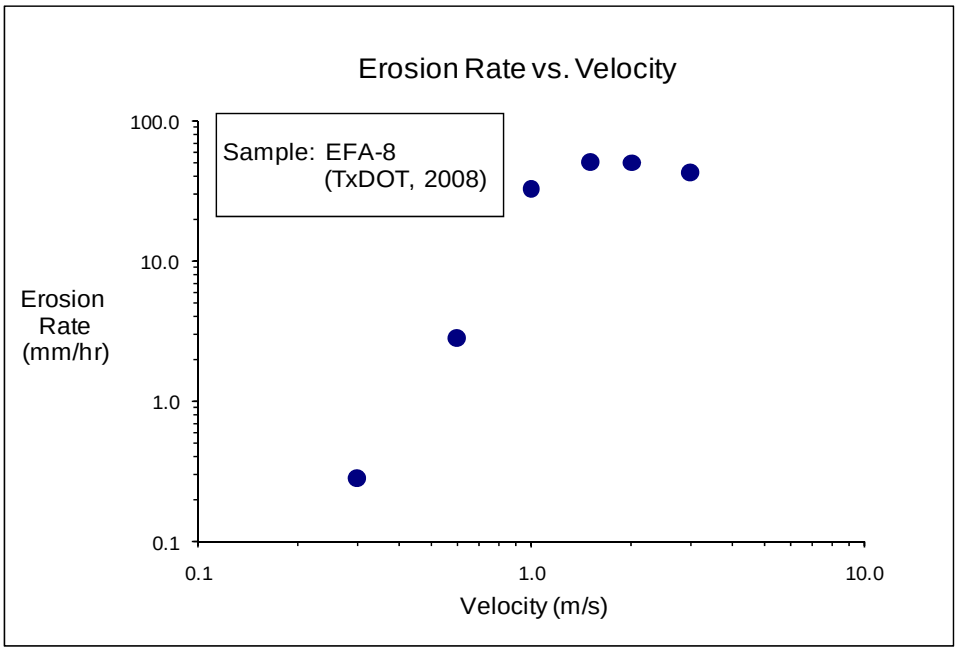

Figure D-47(b). EFA test results for soil sample EFA-8 (Velocity).

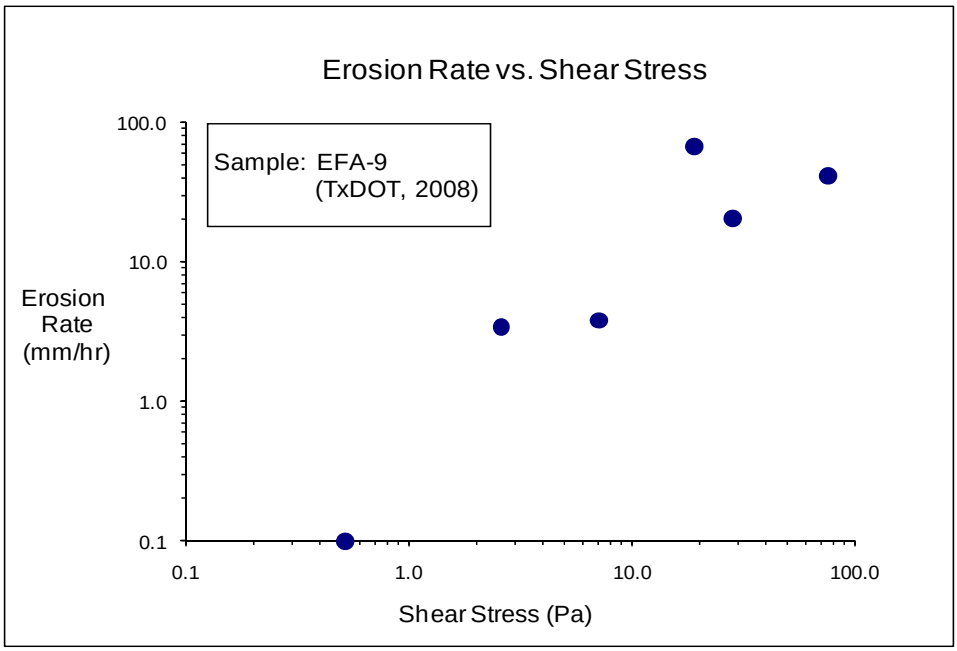

Figure D-48(a). EFA test results for soil sample EFA-9 (Shear Stress).

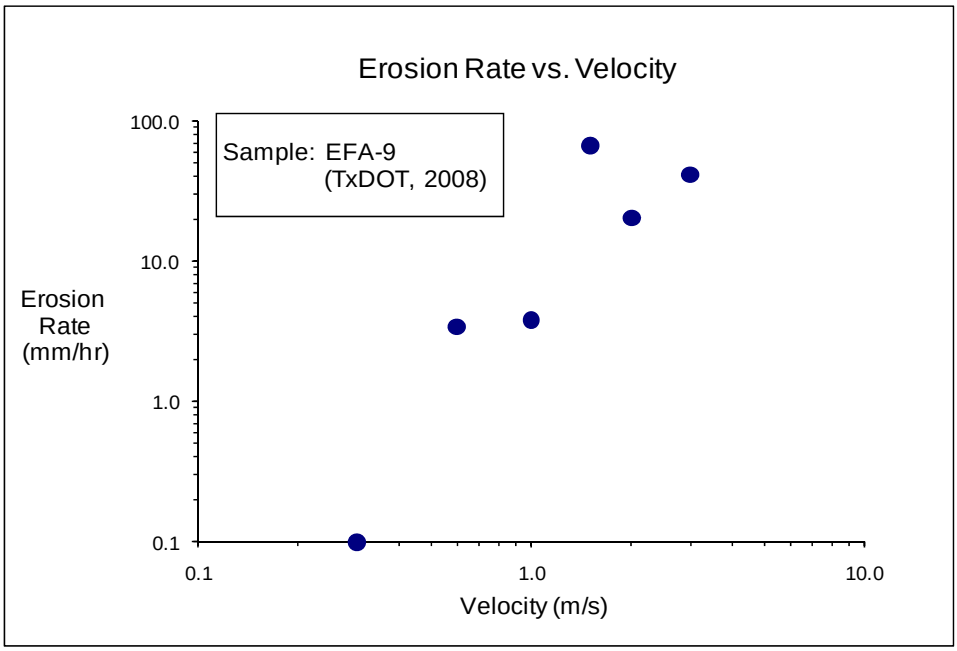

Figure D-48(b). EFA test results for soil sample EFA-9 (Velocity).

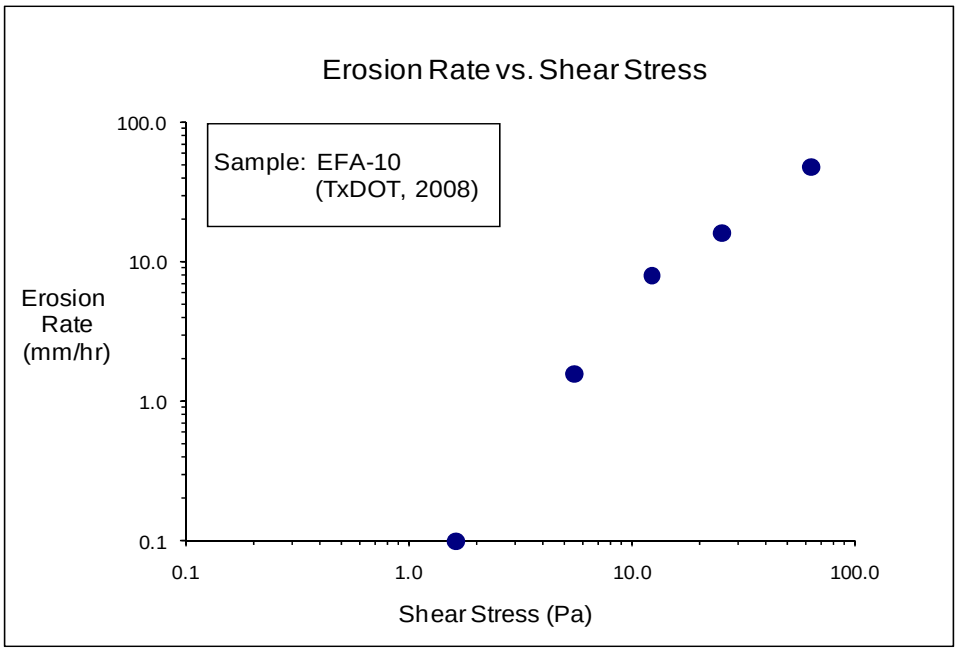

Figure D-49(a). EFA test results for soil sample EFA-10 (Shear Stress).

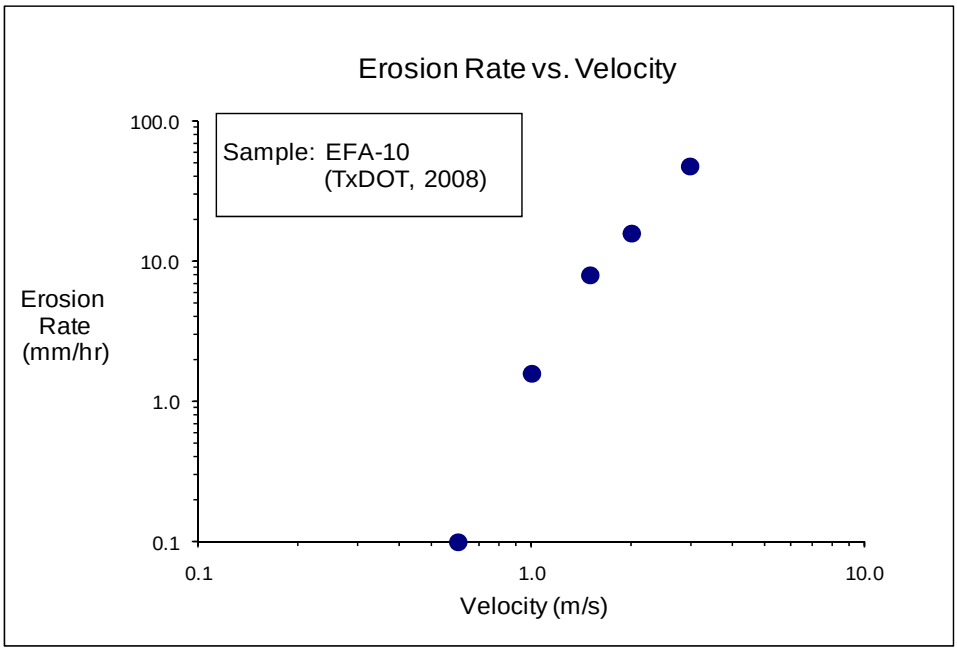

Figure D-49(b). EFA test results for soil sample EFA-10 (Velocity).

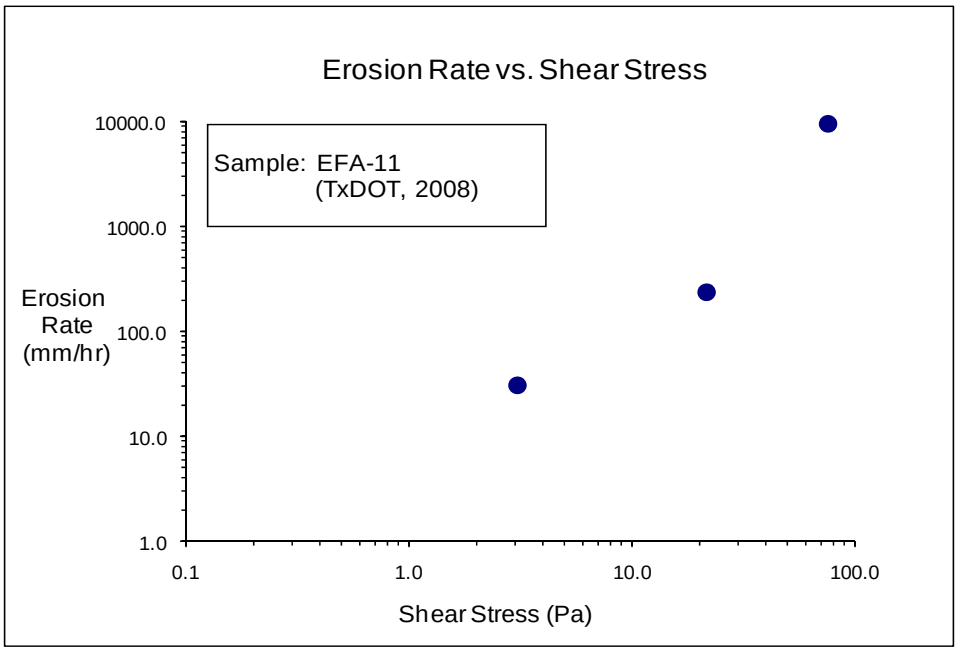

Figure D-50(a). EFA test results for soil sample EFA-11 (Shear Stress).

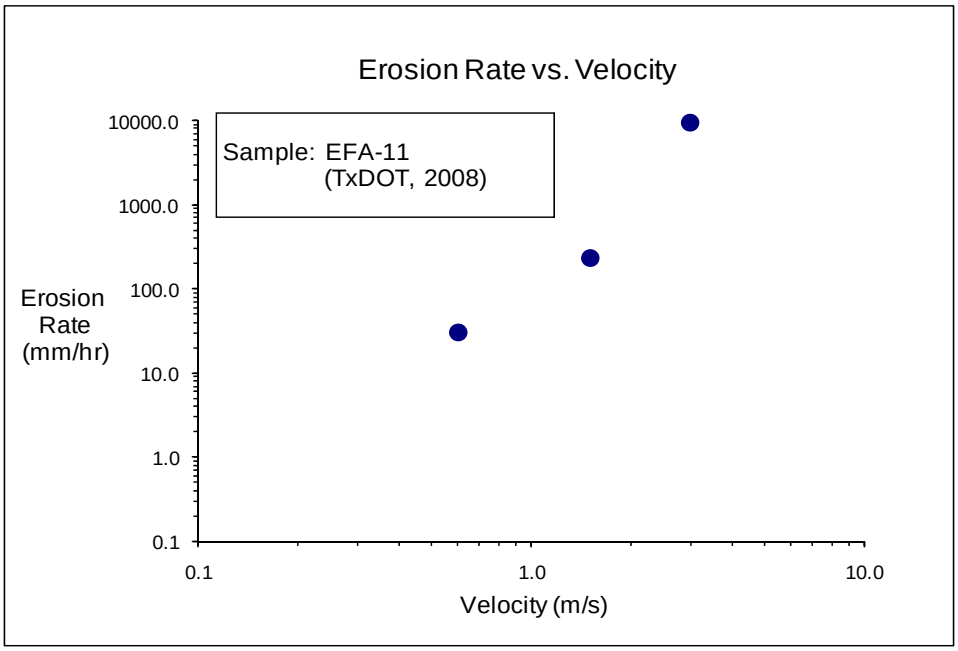

Figure D-50(b). EFA test results for soil sample EFA-11 (Velocity).

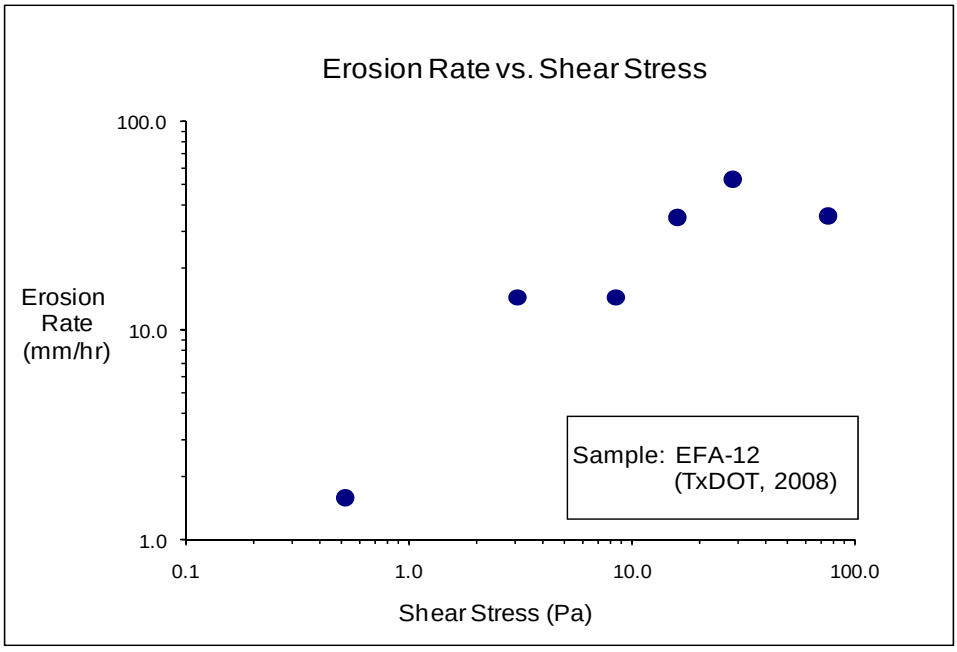

Figure D-51(a). EFA test results for soil sample EFA-12 (Shear Stress).

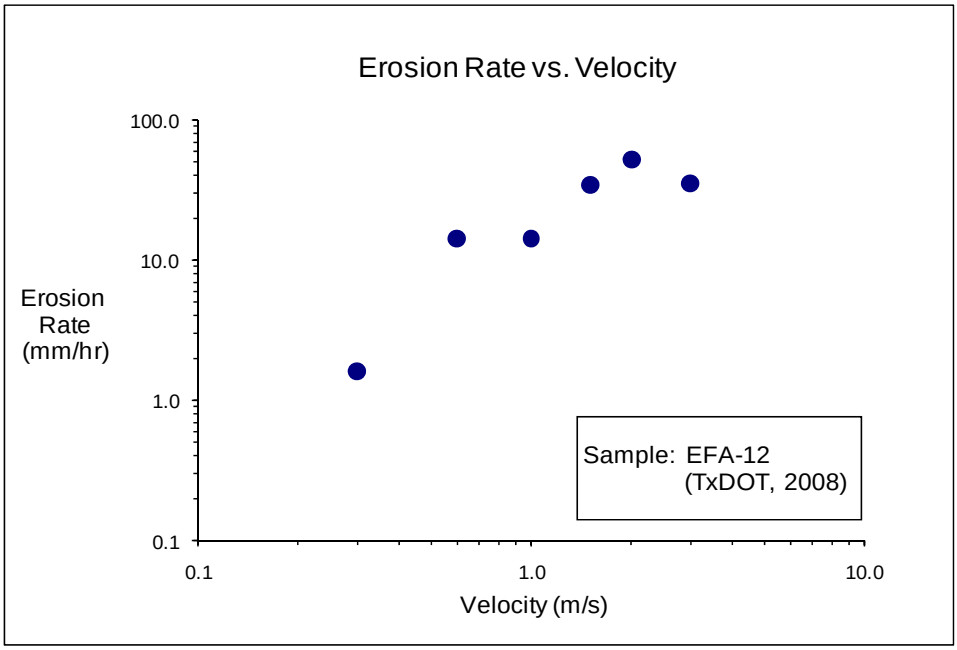

Figure D-51(b). EFA test results for soil sample EFA-12 (Velocity).

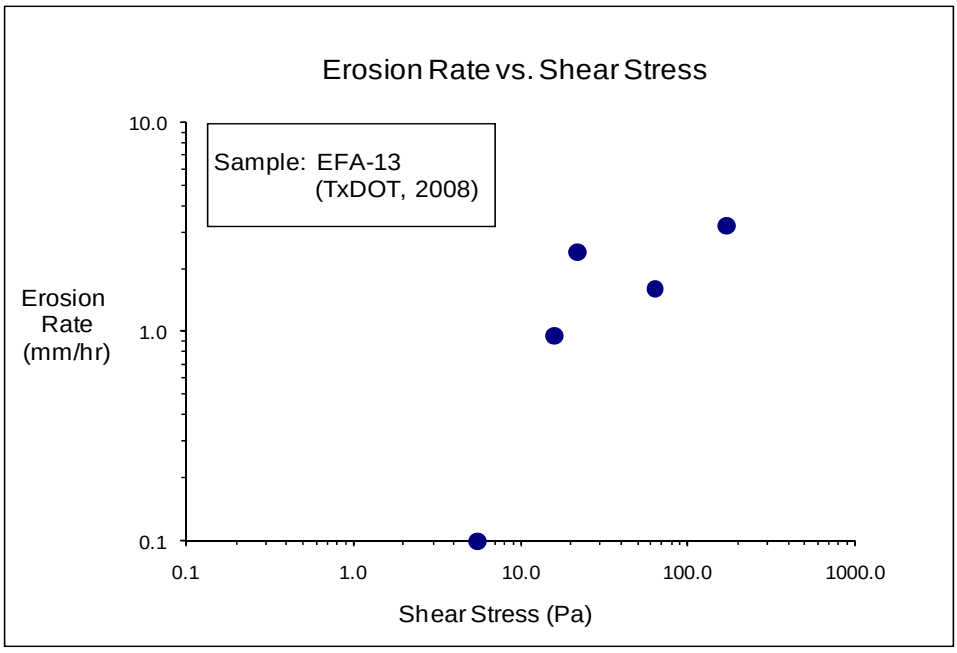

Figure D-52(a). EFA test results for soil sample EFA-13 (Shear Stress).

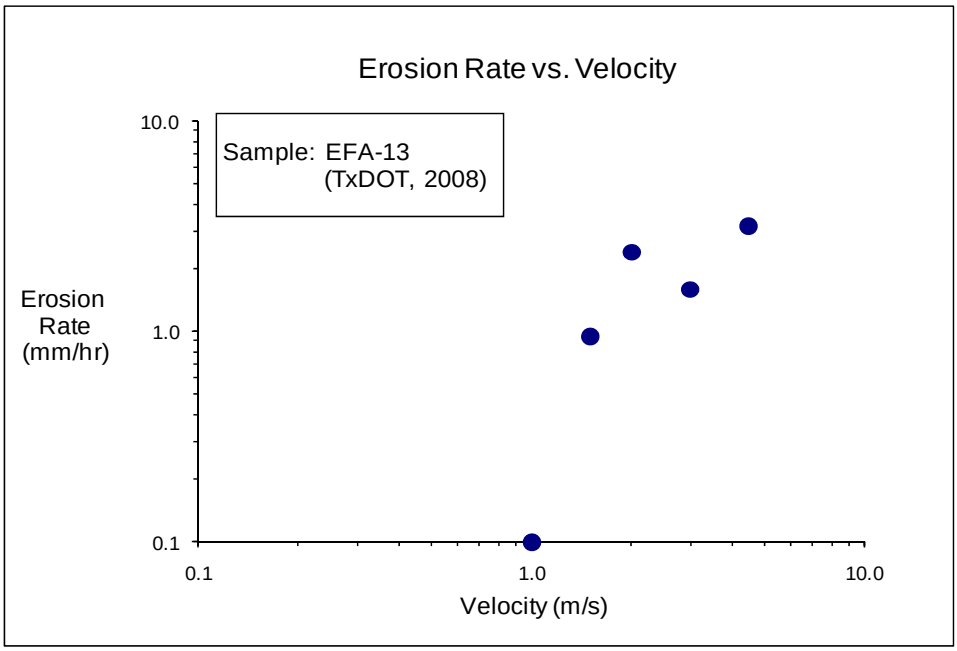

Figure D-52(b). EFA test results for soil sample EFA-13 (Velocity).

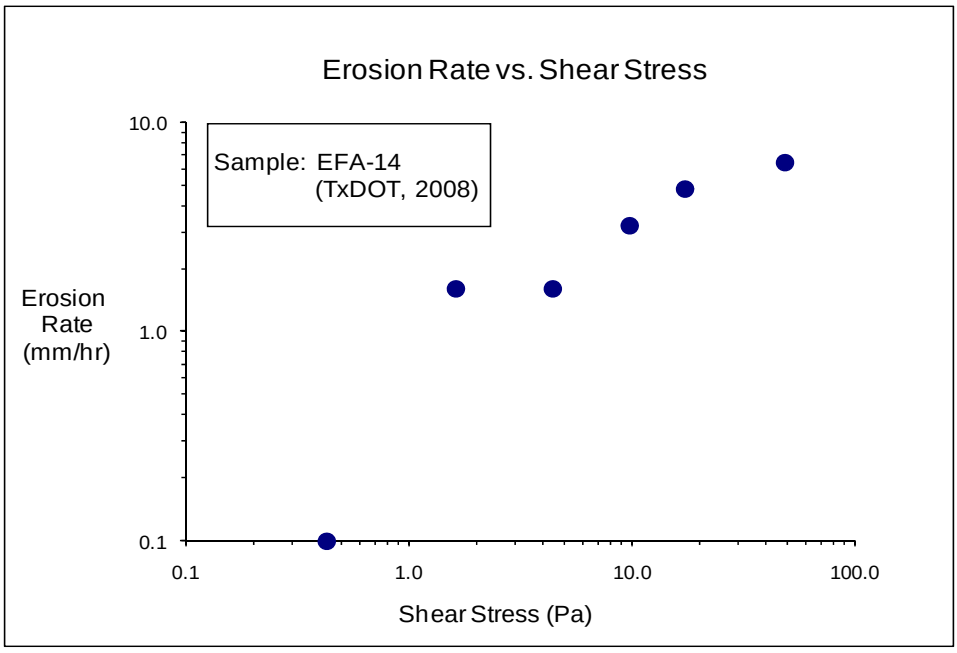

Figure D-53(a). EFA test results for soil sample EFA-14 (Shear Stress).

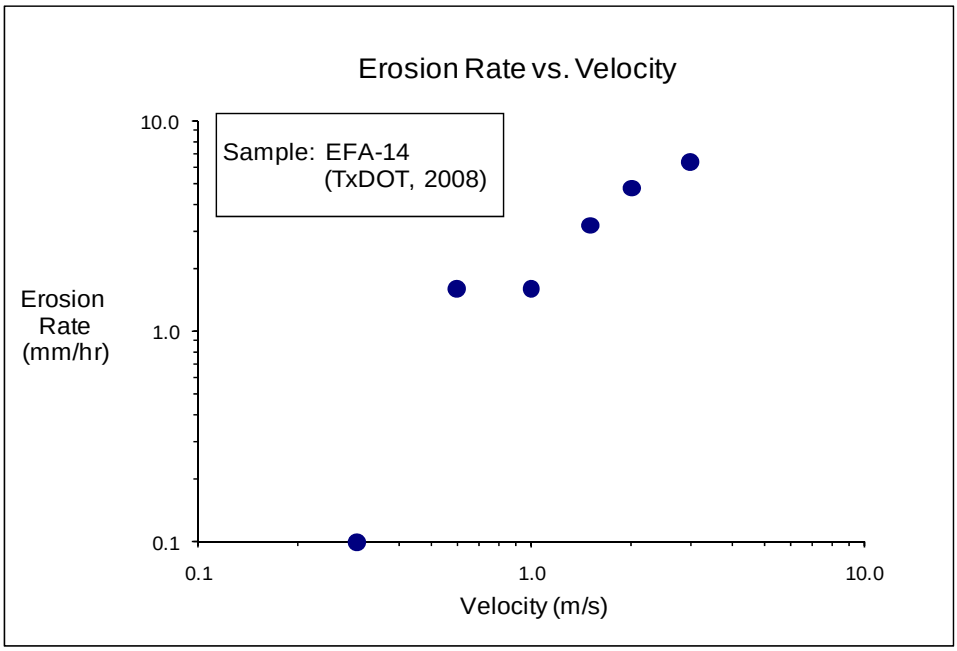

Figure D-53(b). EFA test results for soil sample EFA-14 (Velocity).

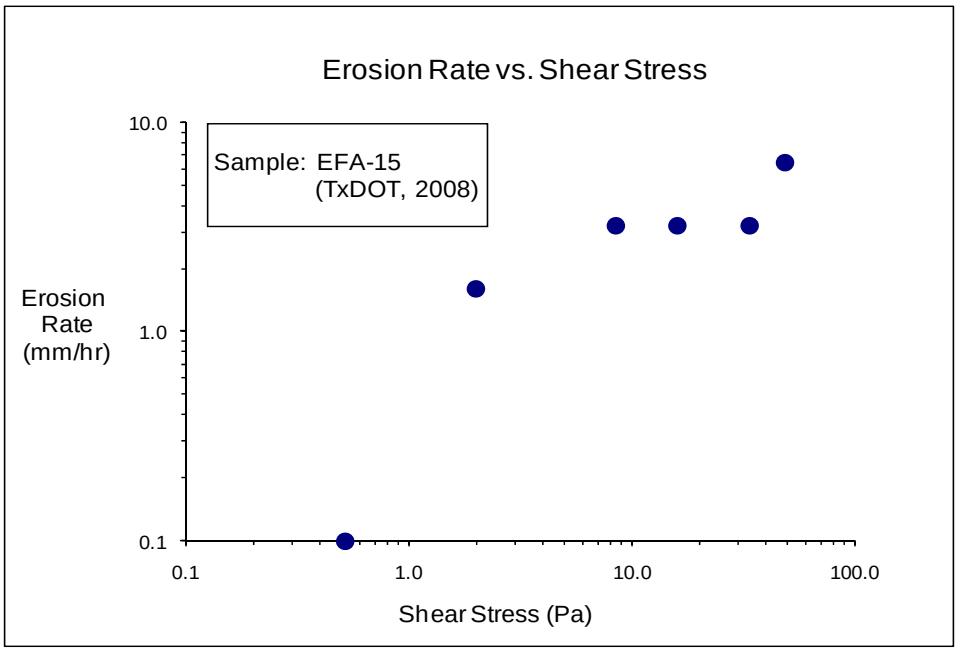

Figure D-54(a). EFA test results for soil sample EFA-15 (Shear Stress).

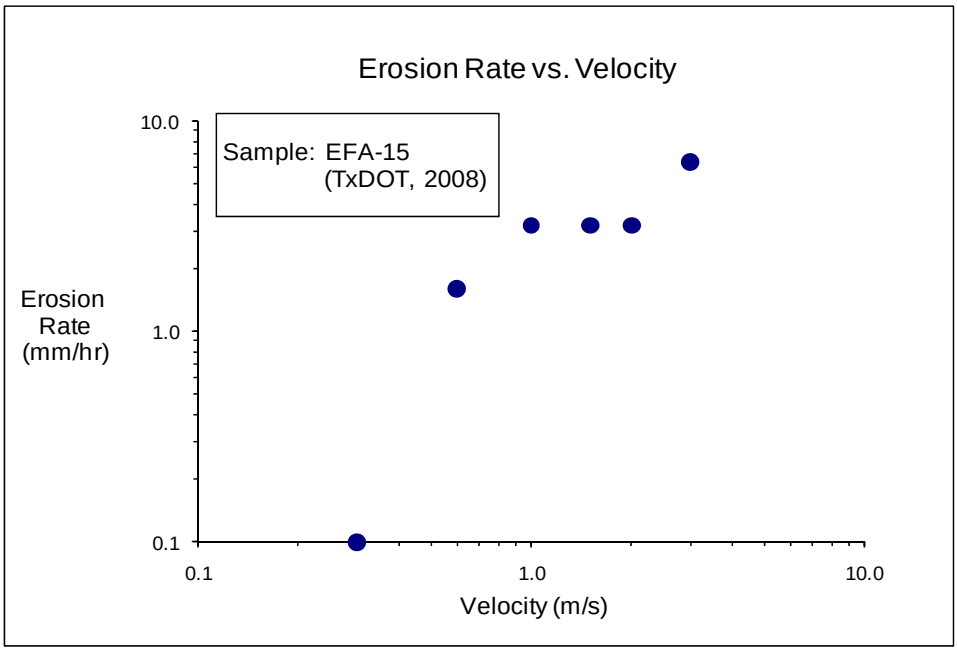

Figure D-54(b). EFA test results for soil sample EFA-15 (Velocity).

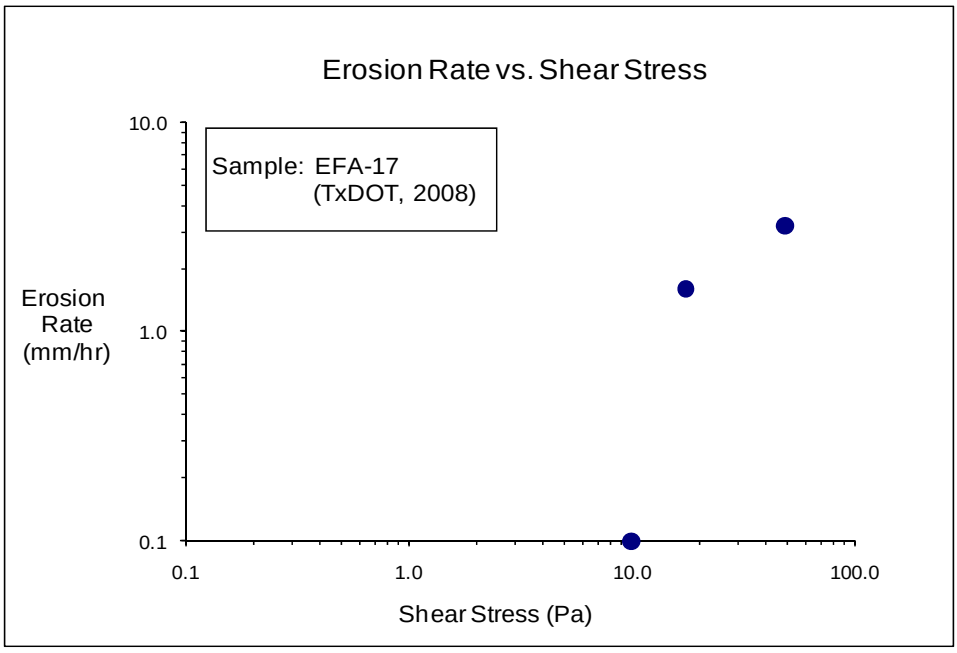

Figure D-55(a). EFA test results for soil sample EFA-17 (Shear Stress).

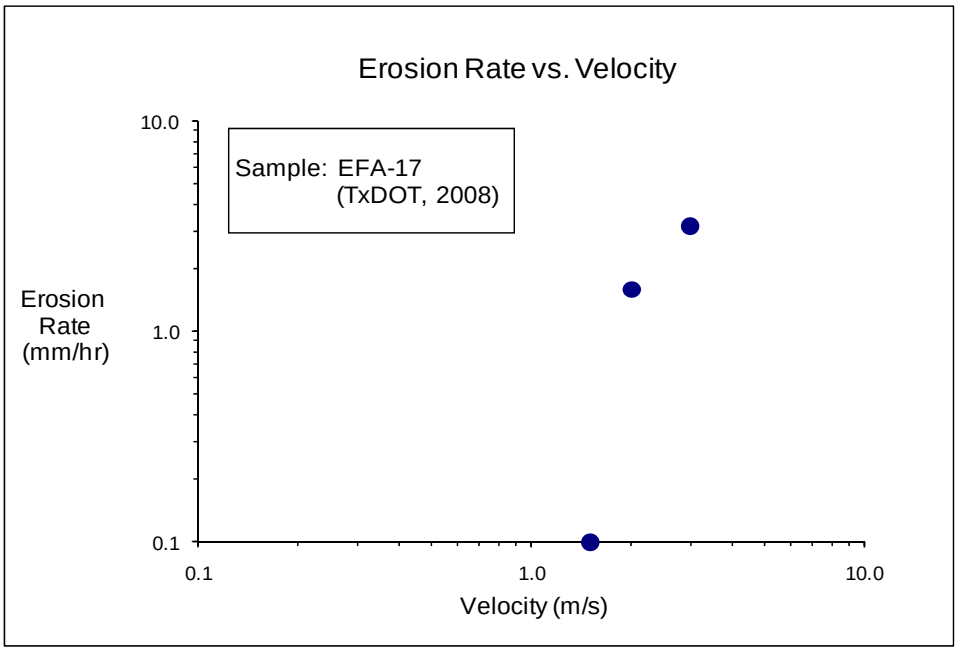

Figure D-55(b). EFA test results for soil sample EFA-17 (Velocity).

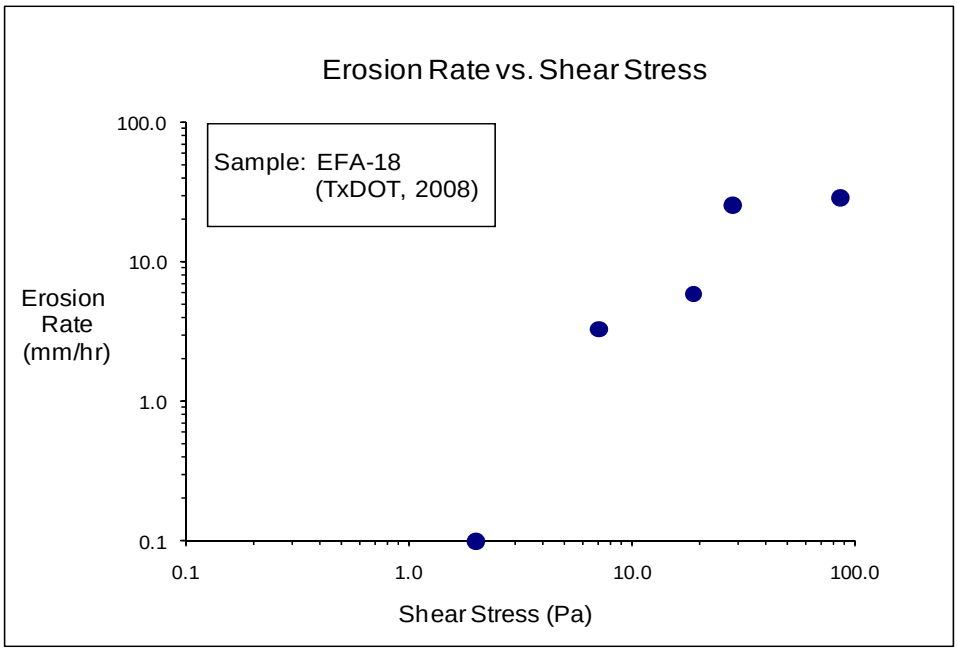

Figure D-56(a). EFA test results for soil sample EFA-18 (Shear Stress).

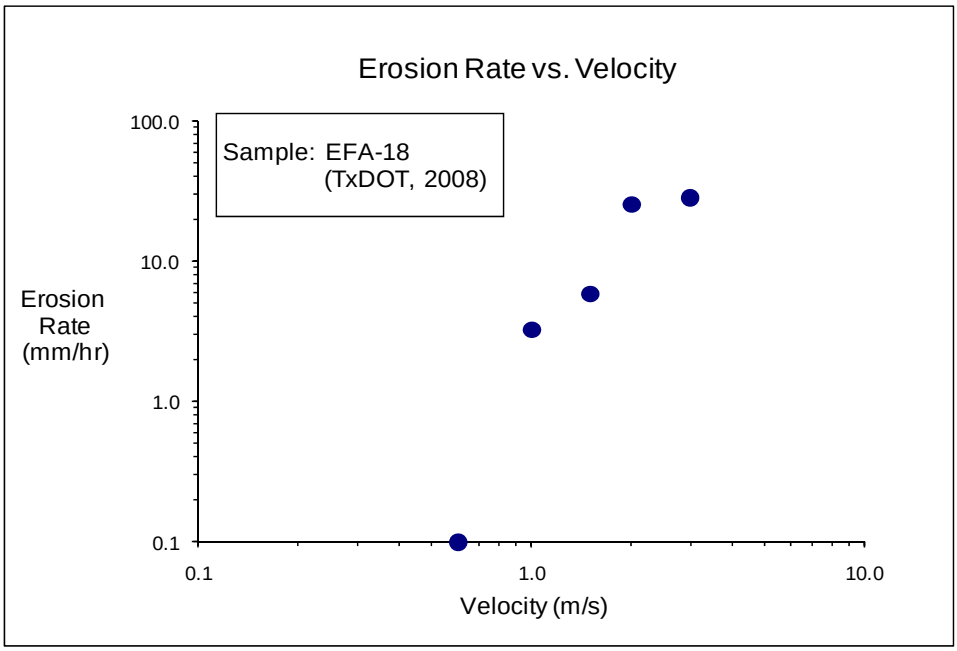

Figure D-56(b). EFA test results for soil sample EFA-18 (Velocity).

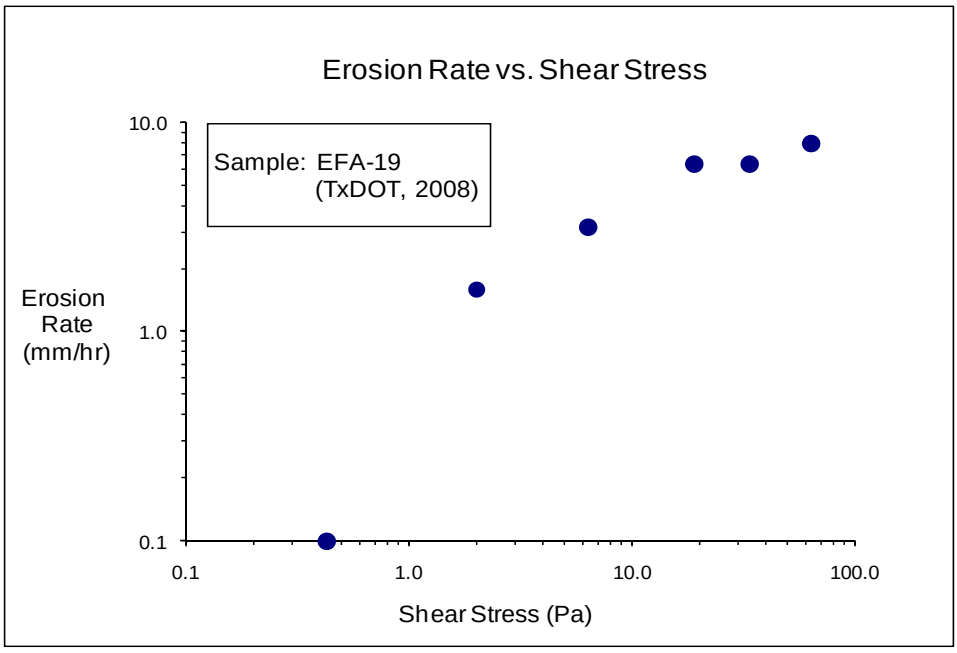

Figure D-57(a). EFA test results for soil sample EFA-19 (Shear Stress).

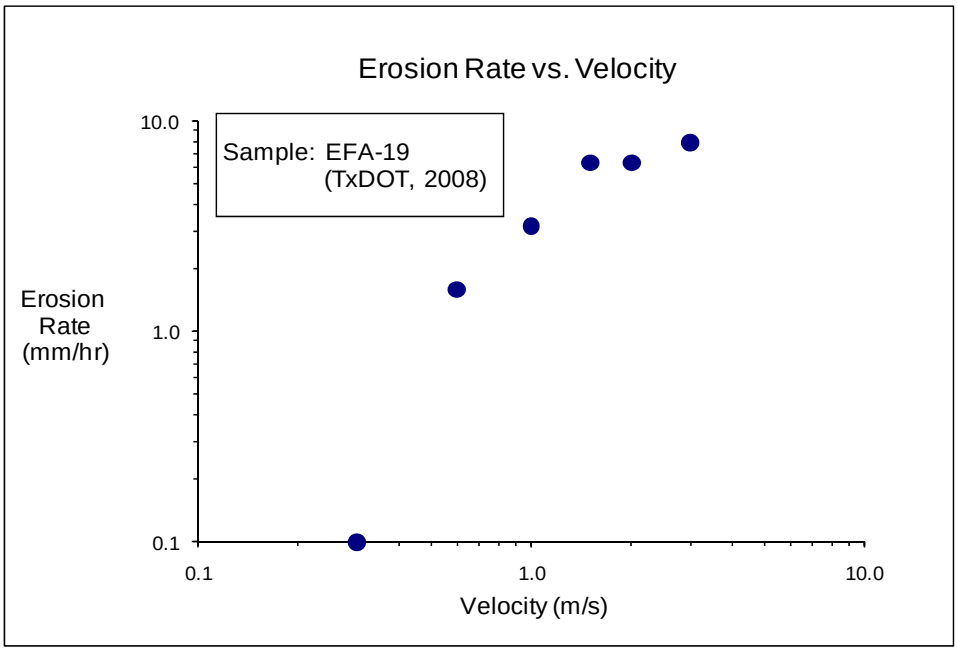

Figure D-57(b). EFA test results for soil sample EFA-19 (Velocity).

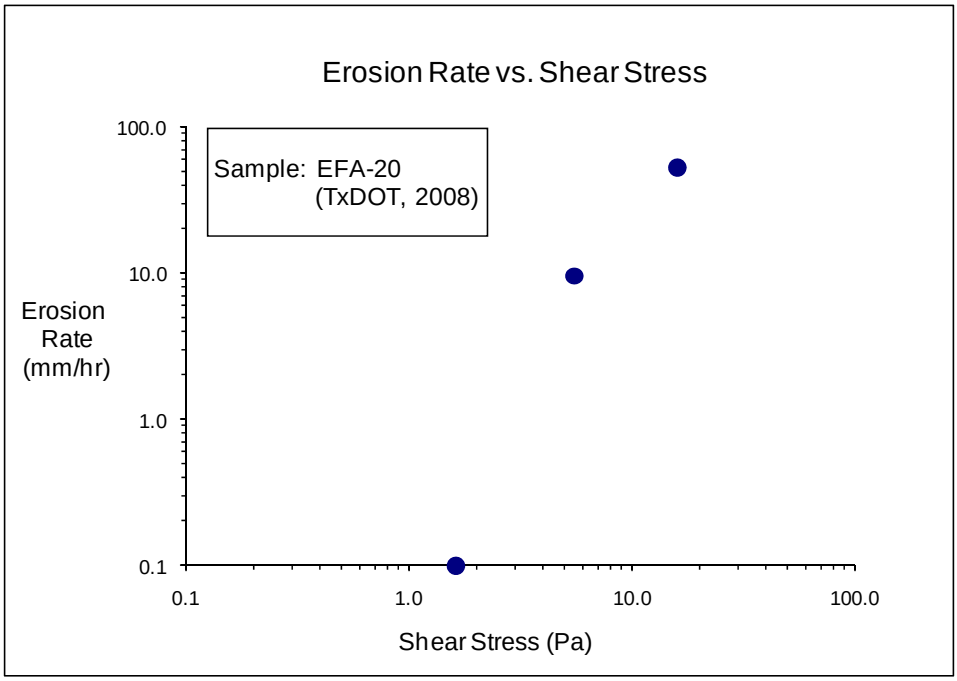

Figure D-58(a). EFA test results for soil sample EFA-20 (Shear Stress).

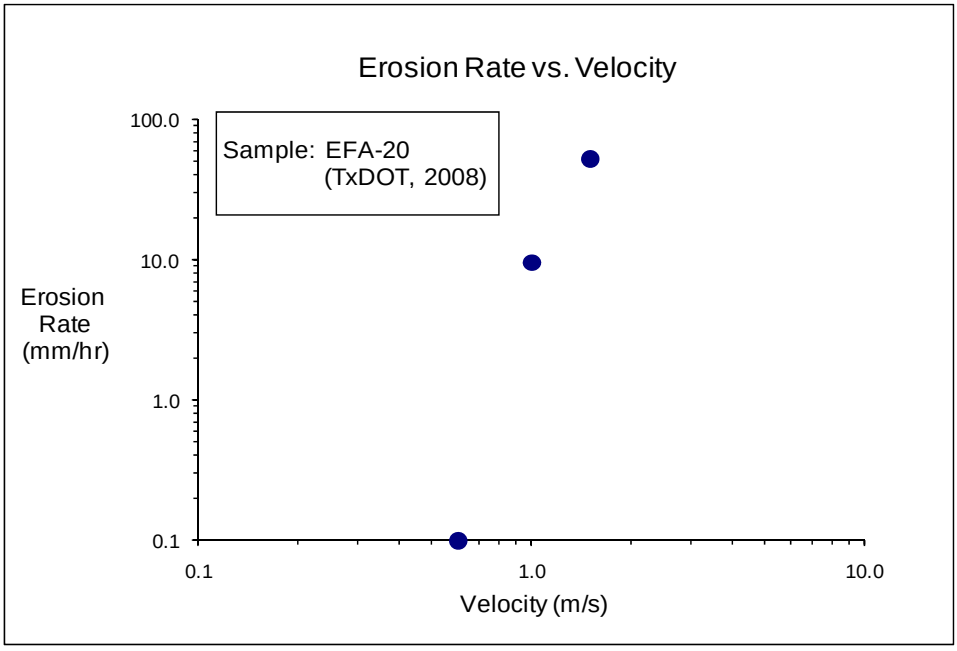

Figure D-58(b). EFA test results for soil sample EFA-20 (Velocity).

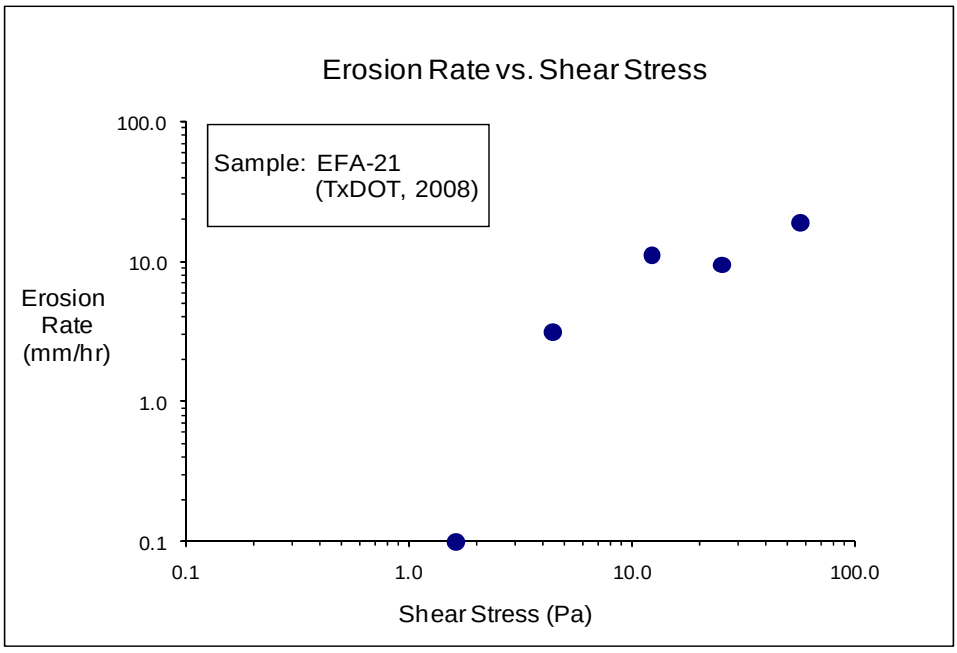

Figure D-59(a). EFA test results for soil sample EFA-21 (Shear Stress).

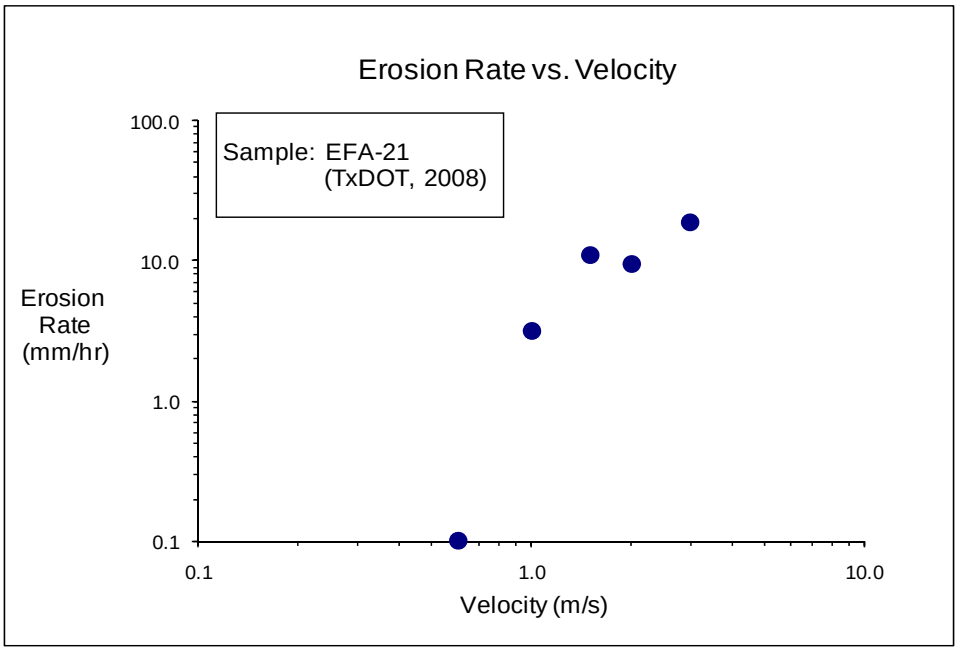

Figure D-59(b). EFA test results for soil sample EFA-21 (Velocity).

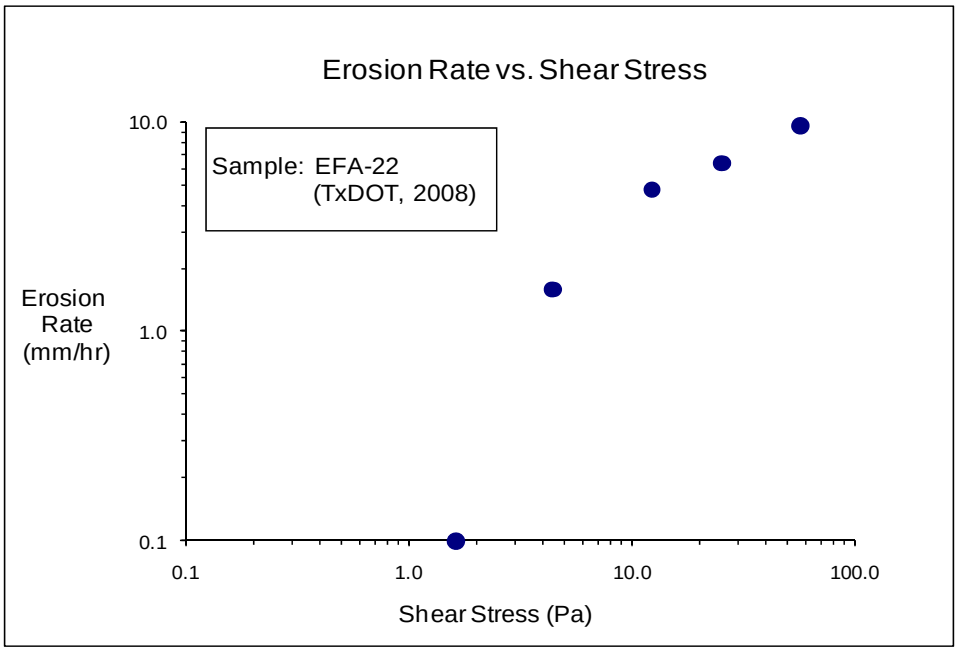

Figure D-60(a). EFA test results for soil sample EFA-22 (Shear Stress).

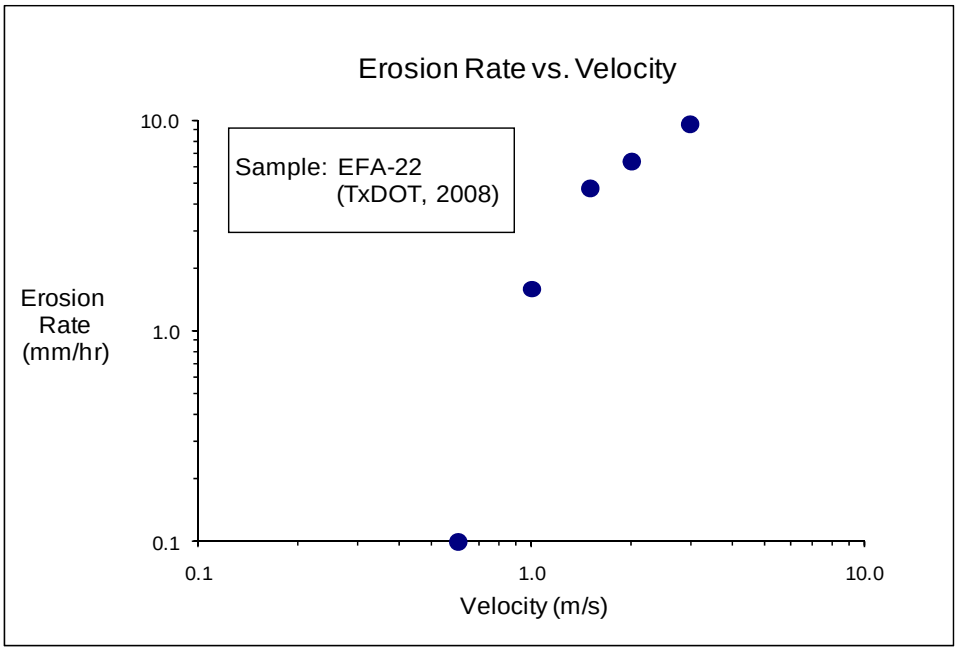

Figure D-60(b). EFA test results for soil sample EFA-22 (Velocity).

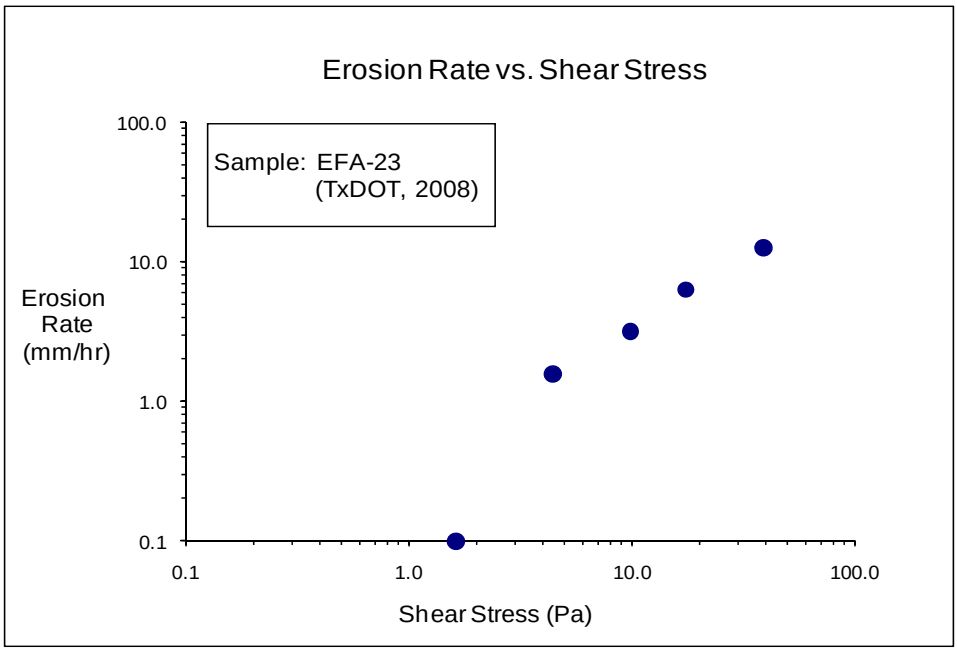

Figure D-61(a). EFA test results for soil sample EFA-23 (Shear Stress).

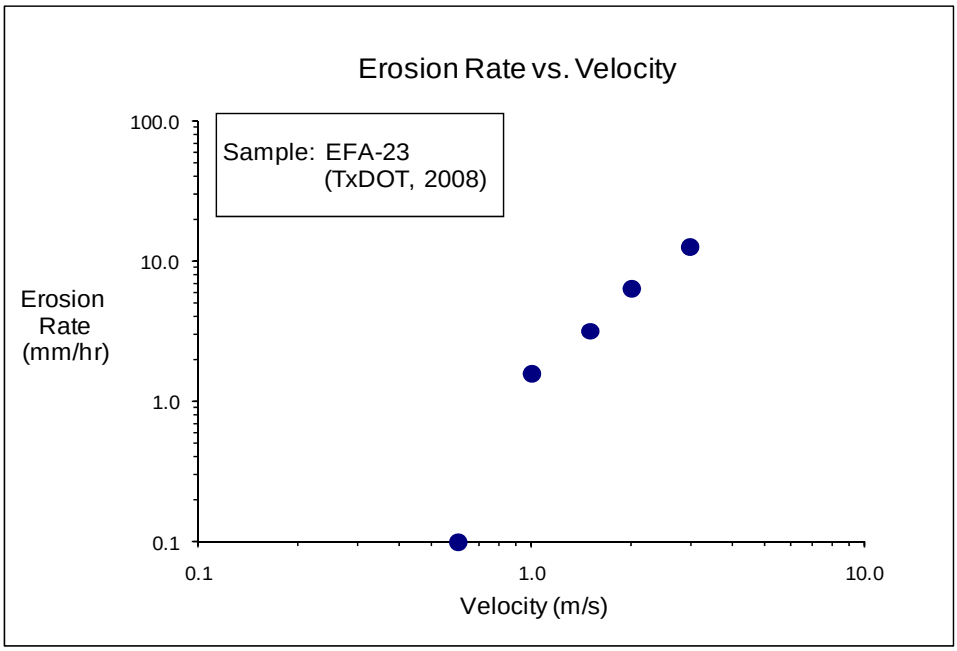

Figure D-61(b). EFA test results for soil sample EFA-23 (Velocity).

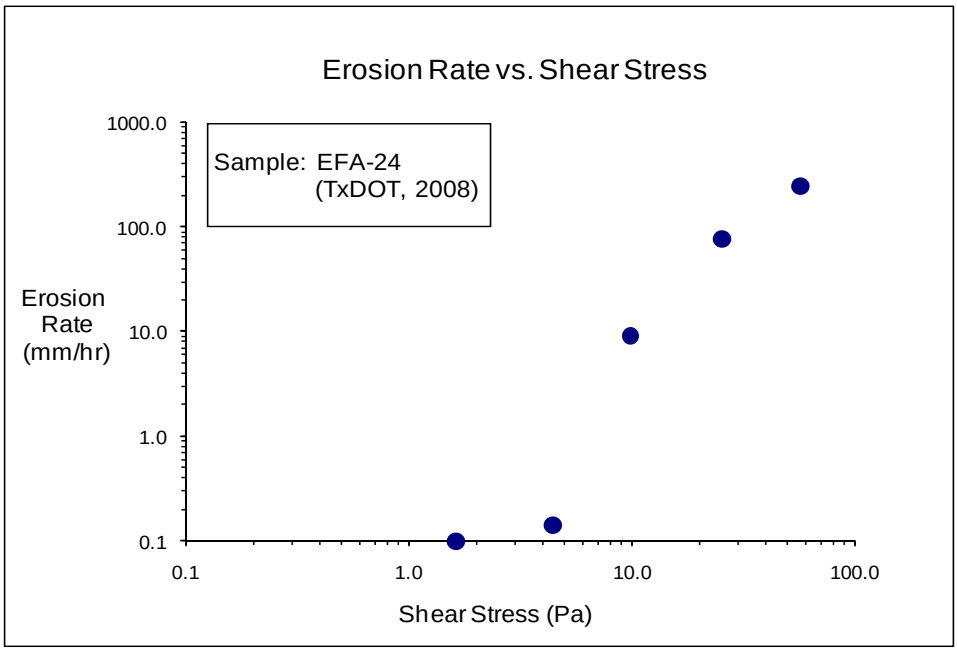

Figure D-62(a). EFA test results for soil sample EFA-24 (Shear Stress).

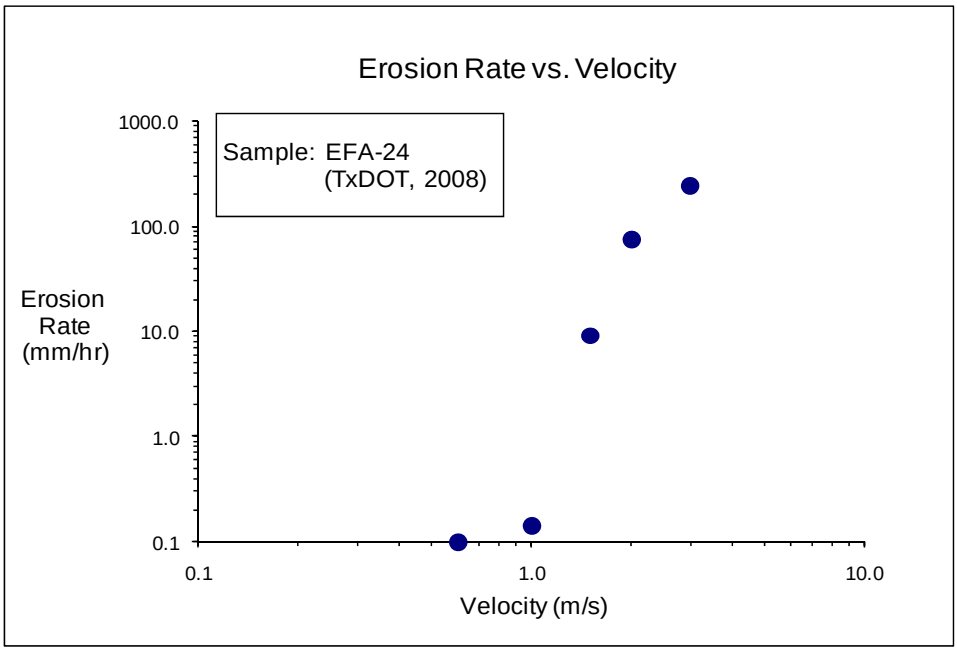

Figure D-62(b). EFA test results for soil sample EFA-24 (Velocity).

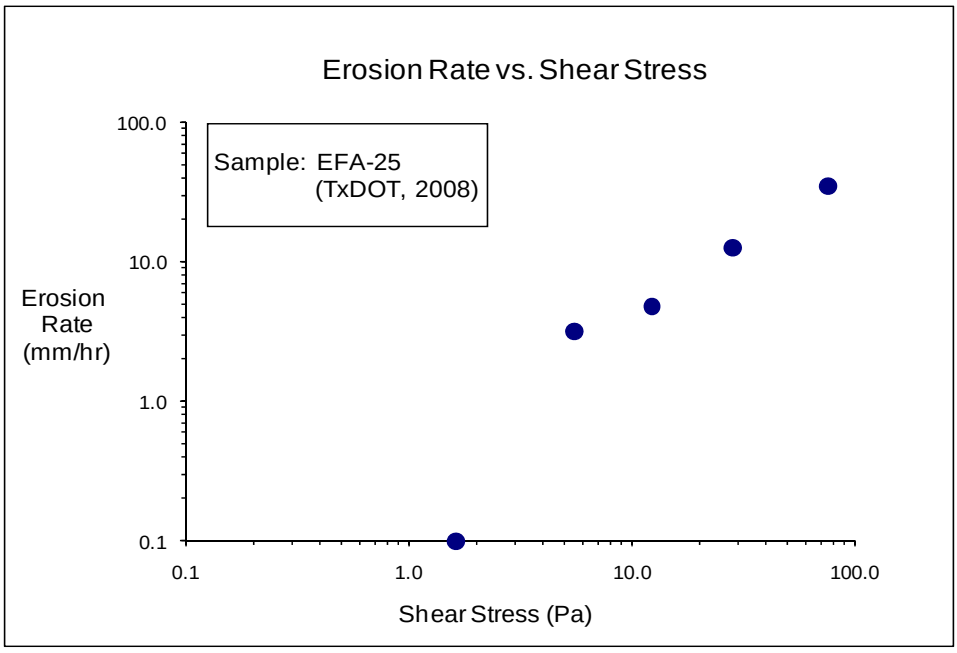

Figure D-63(a). EFA test results for soil sample EFA-25 (Shear Stress).

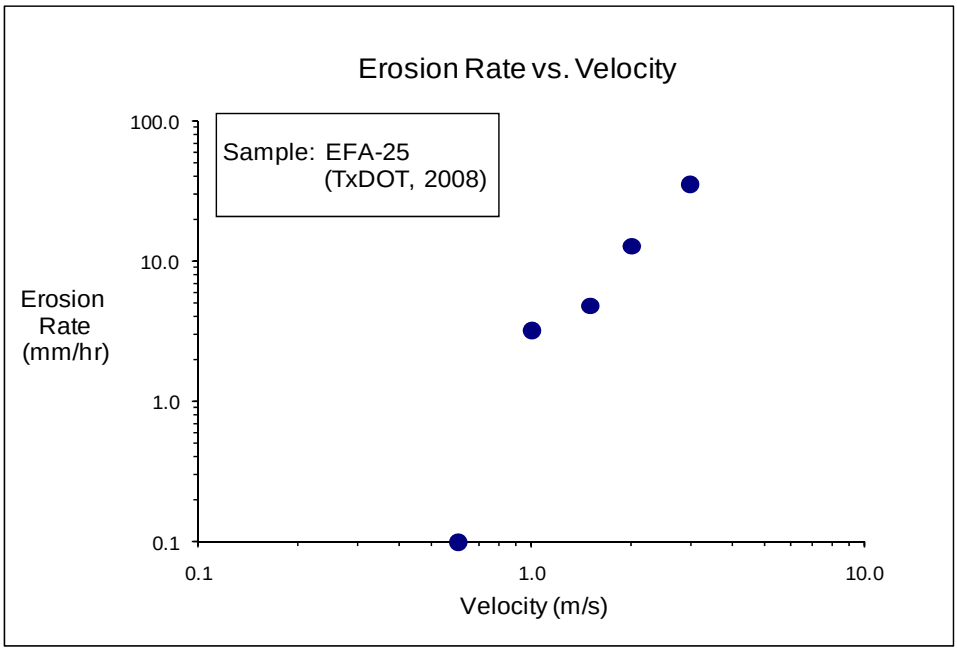

Figure D-63(b). EFA test results for soil sample EFA-25 (Velocity).

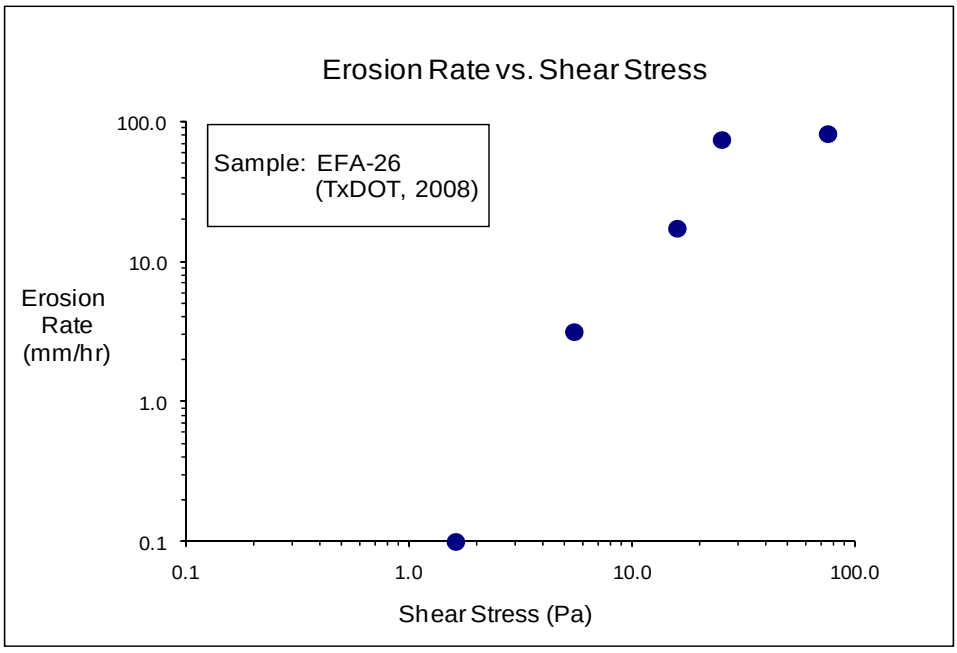

Figure D-64(a). EFA test results for soil sample EFA-26 (Shear Stress).

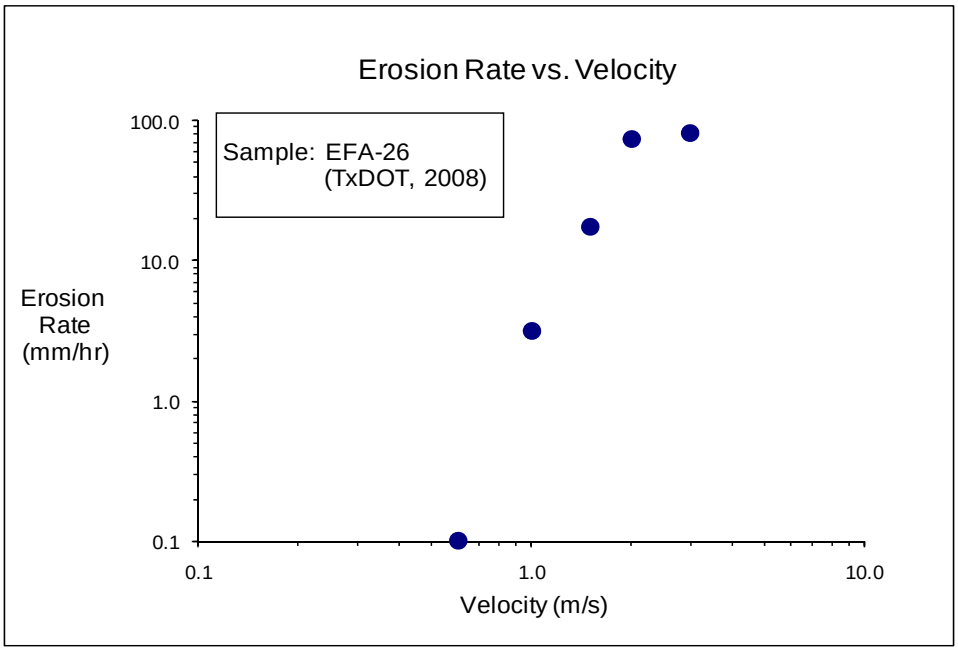

Figure D-64(b). EFA test results for soil sample EFA-26 (Velocity).

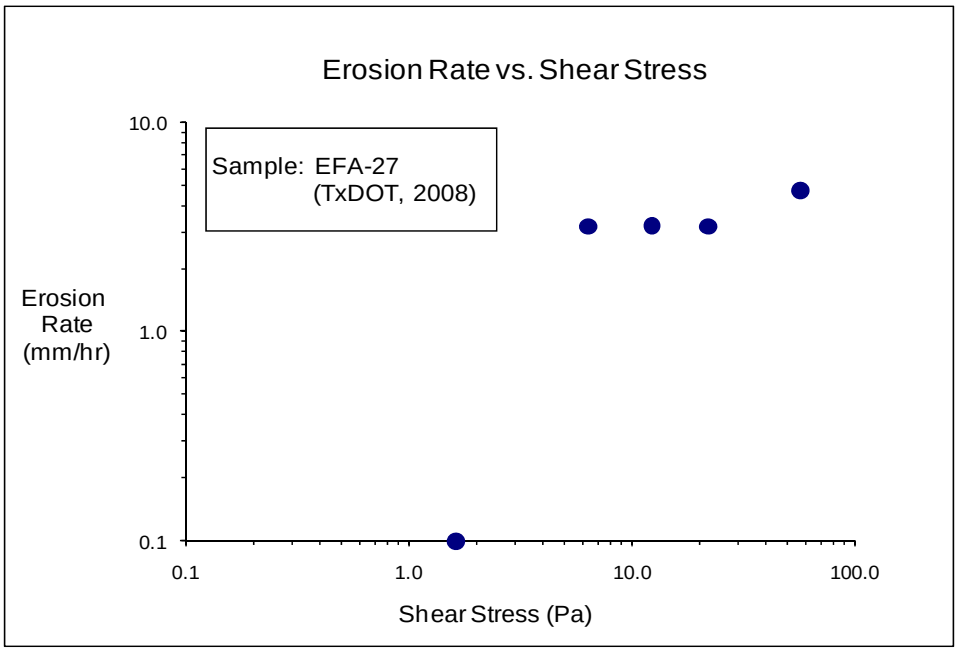

Figure D-65(a). EFA test results for soil sample EFA-27 (Shear Stress).

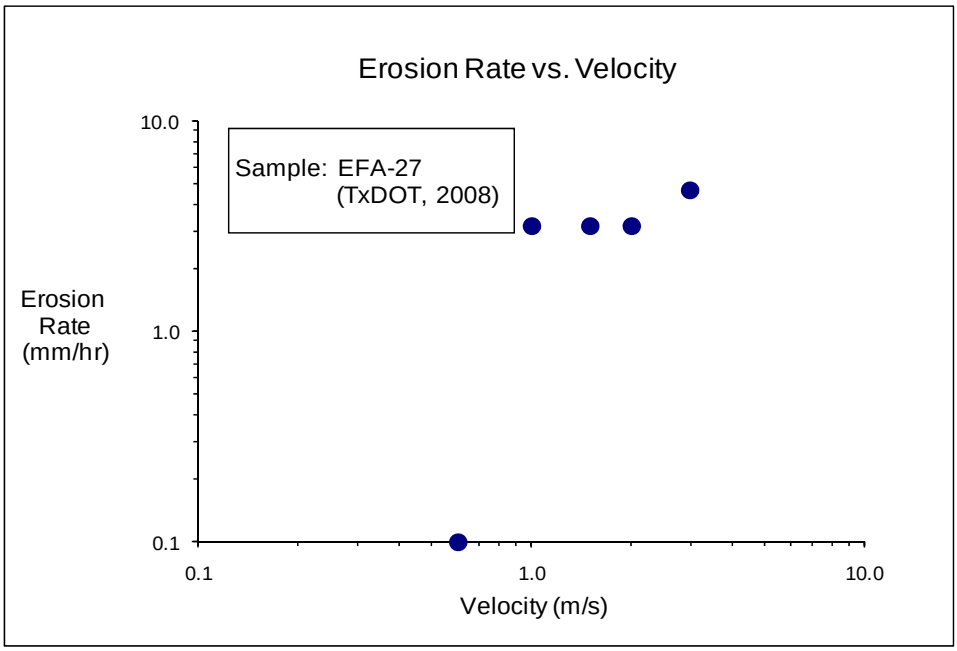

Figure D-65(b). EFA test results for soil sample EFA-27 (Velocity).

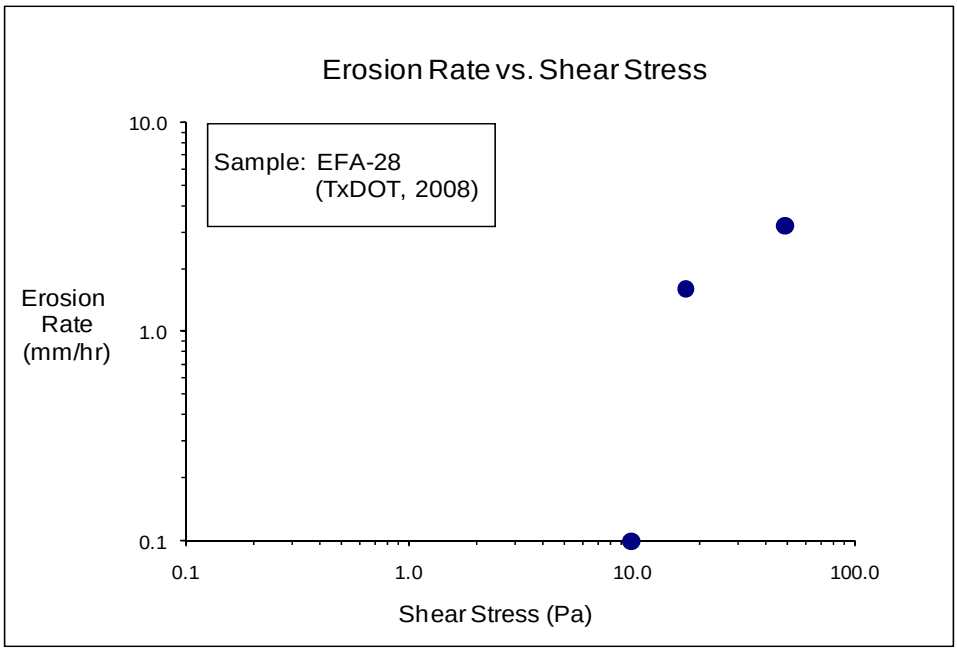

Figure D-66(a). EFA test results for soil sample EFA-28 (Shear Stress).

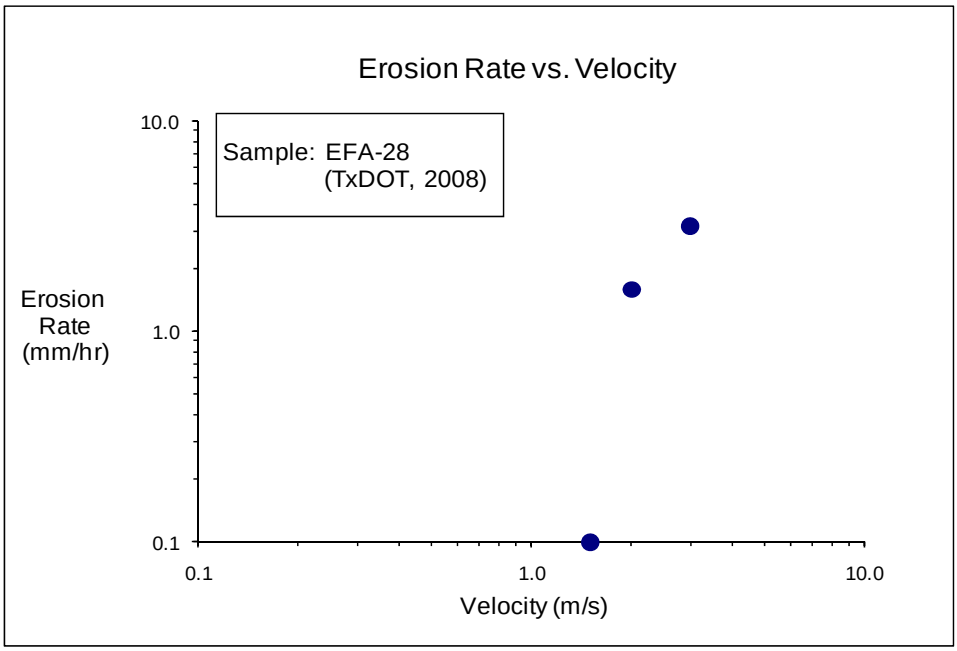

Figure D-66(b). EFA test results for soil sample EFA-28 (Velocity).

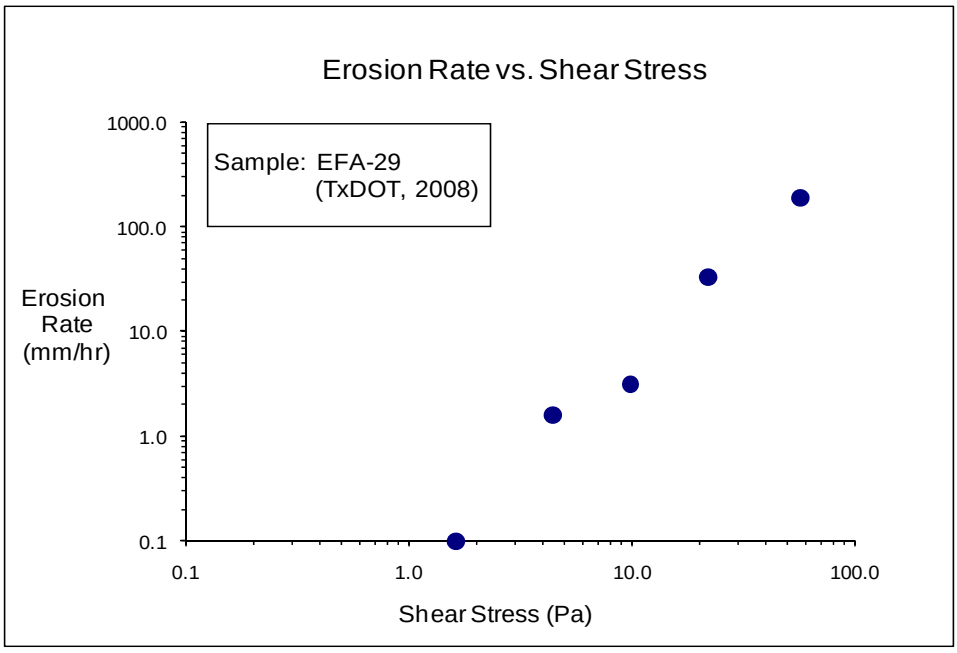

Figure D-67(a). EFA test results for soil sample EFA-29 (Shear Stress).

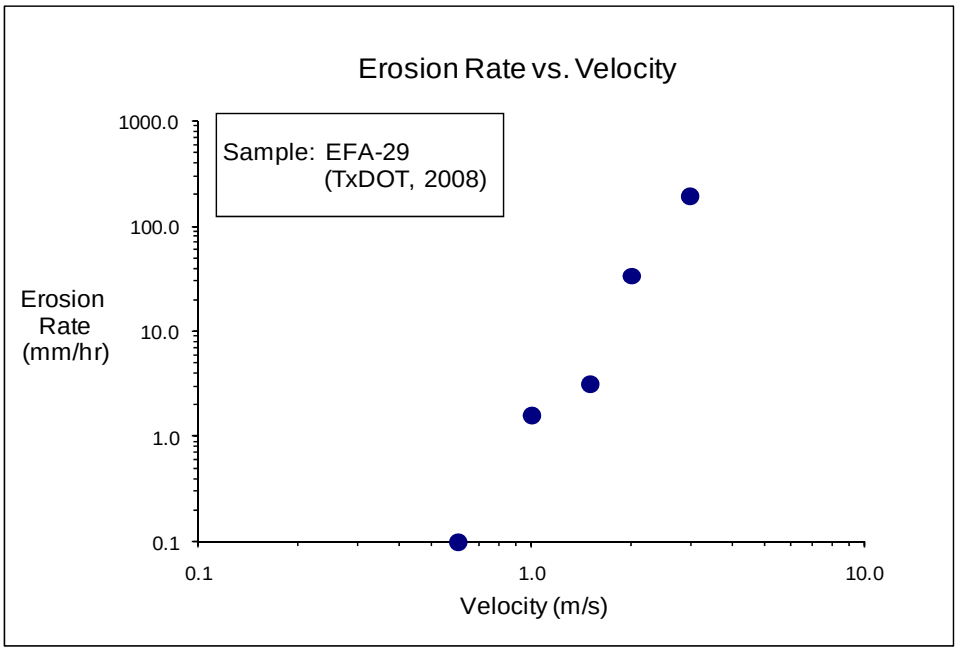

Figure D-67(b). EFA test results for soil sample EFA-29 (Velocity).

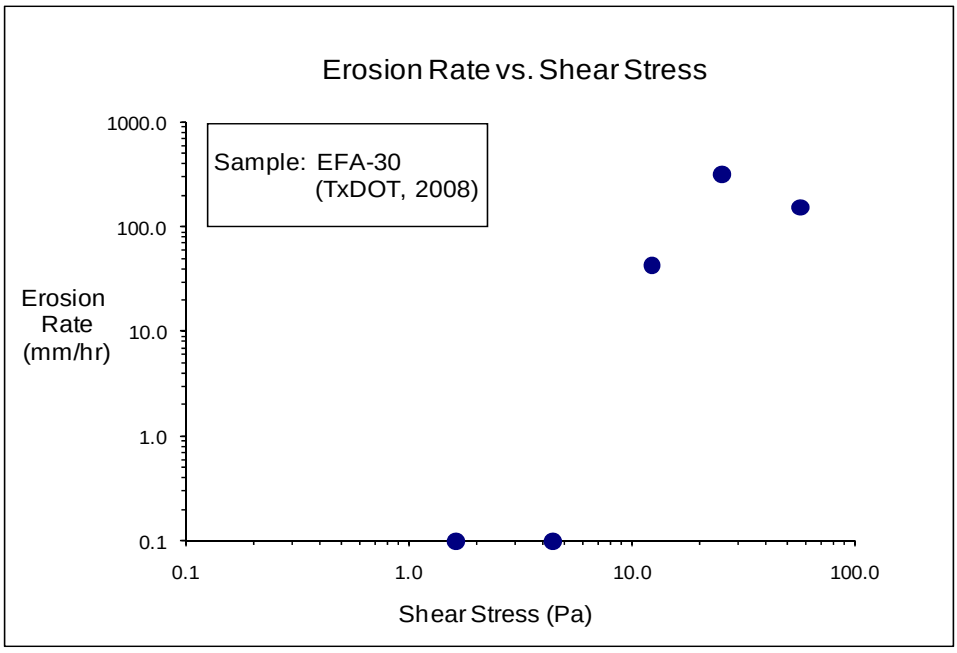

Figure D-68(a). EFA test results for soil sample EFA-30 (Shear Stress).

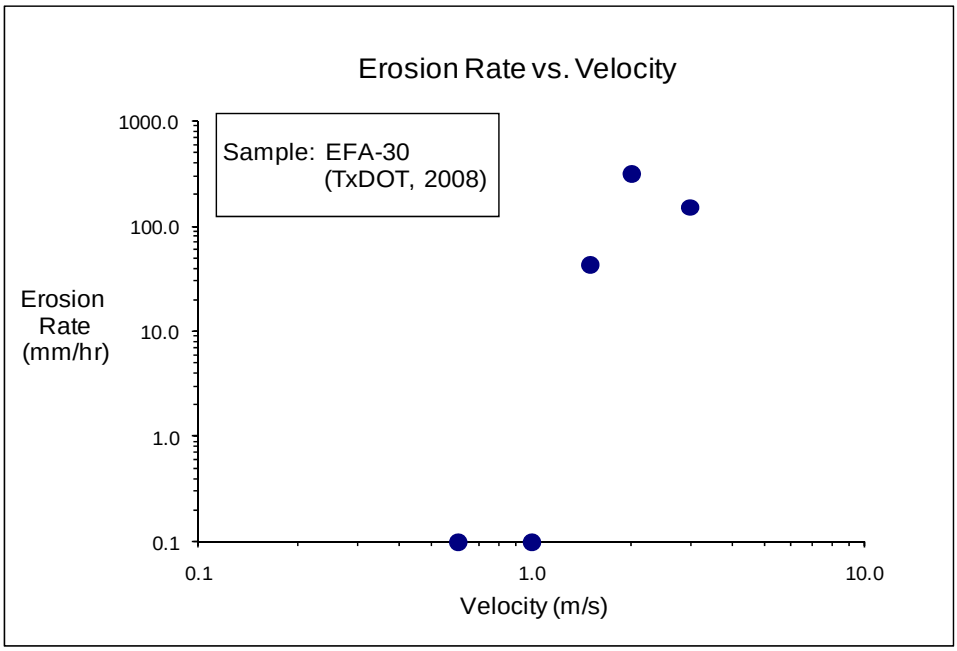

Figure D-68(b). EFA test results for soil sample EFA-30 (Velocity).

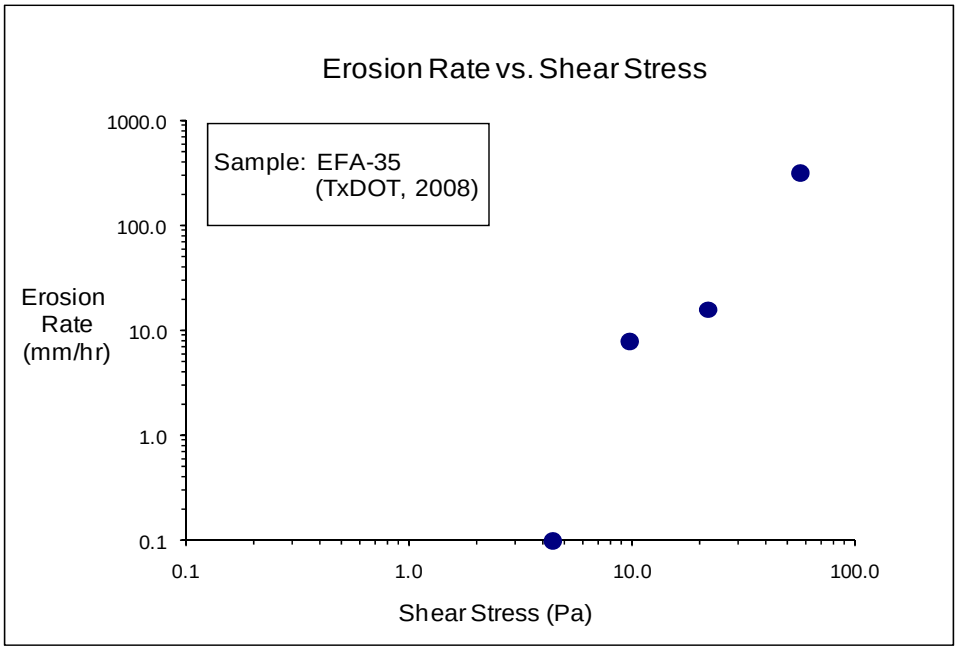

Figure D-69(a). EFA test results for soil sample EFA-35 (Shear Stress).

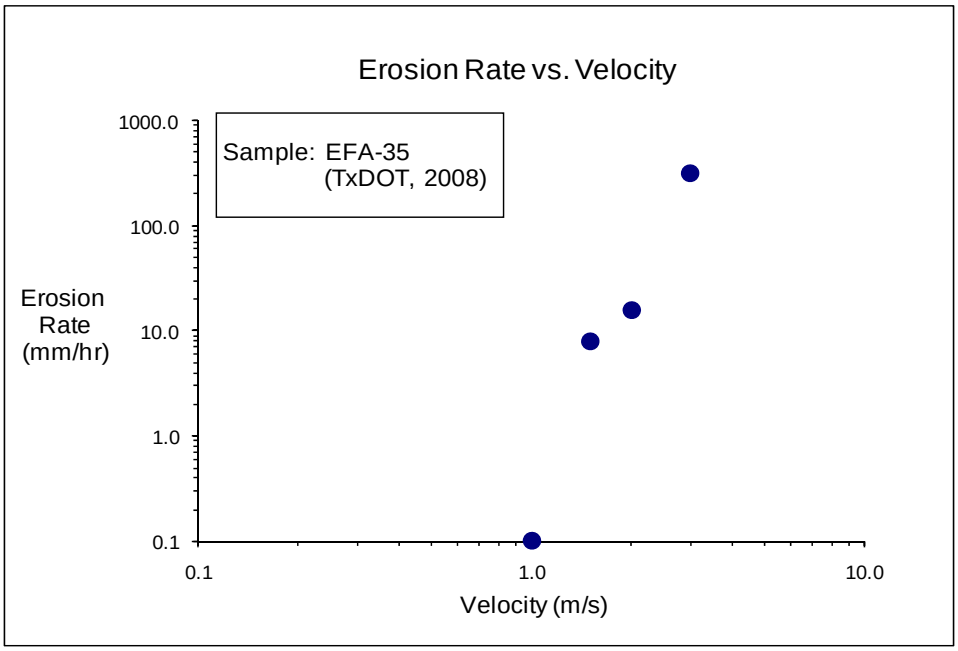

Figure D-69(b). EFA test results for soil sample EFA-35 (Velocity).

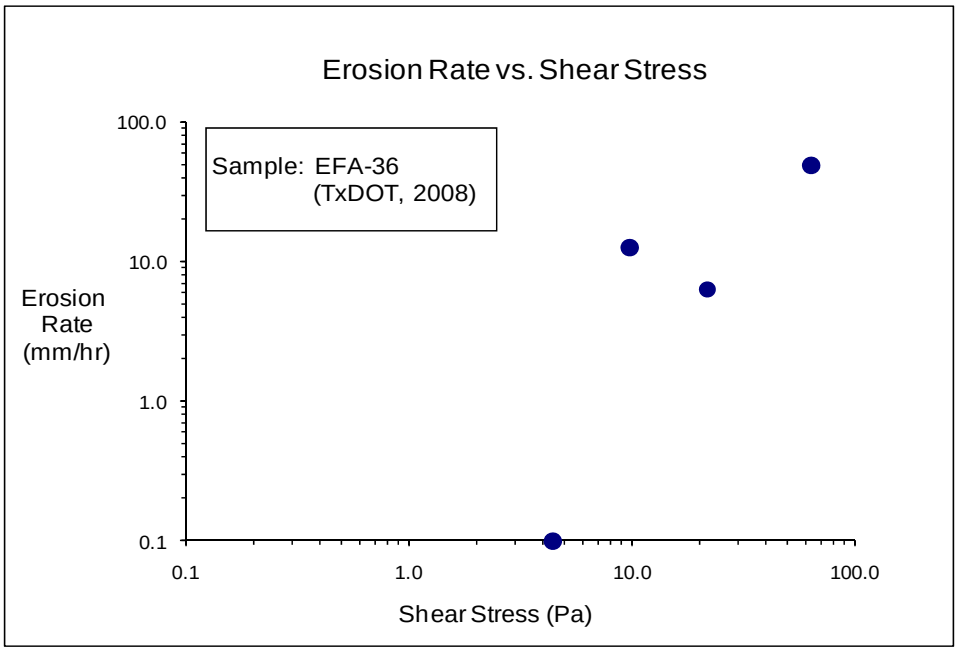

Figure D-70 (a). EFA test results for soil sample EFA-36 (Shear Stress).

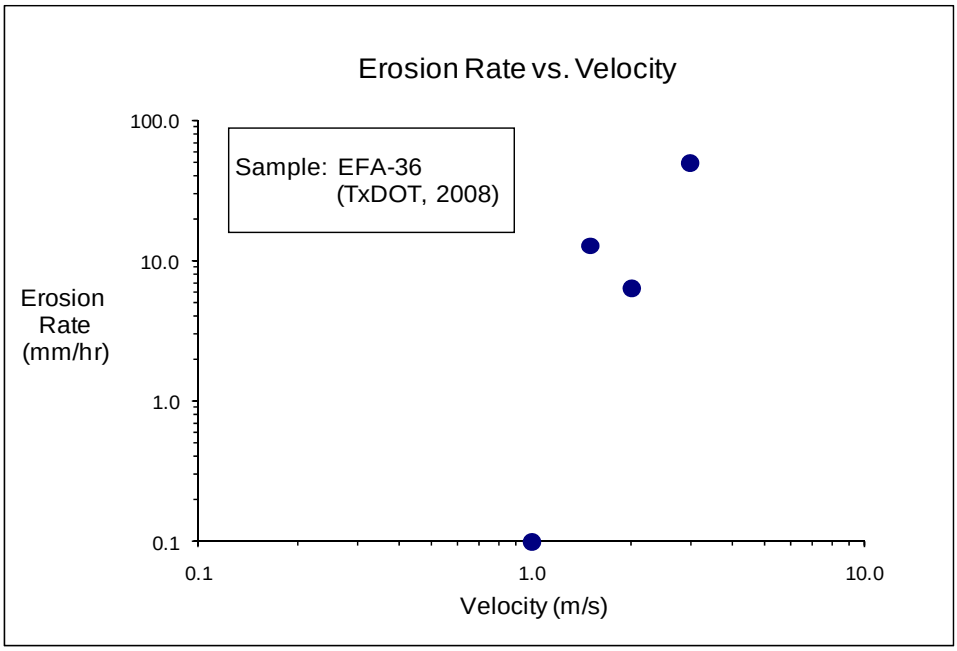

Figure D-70 (b). EFA test results for soil sample EFA-36 (Velocity).

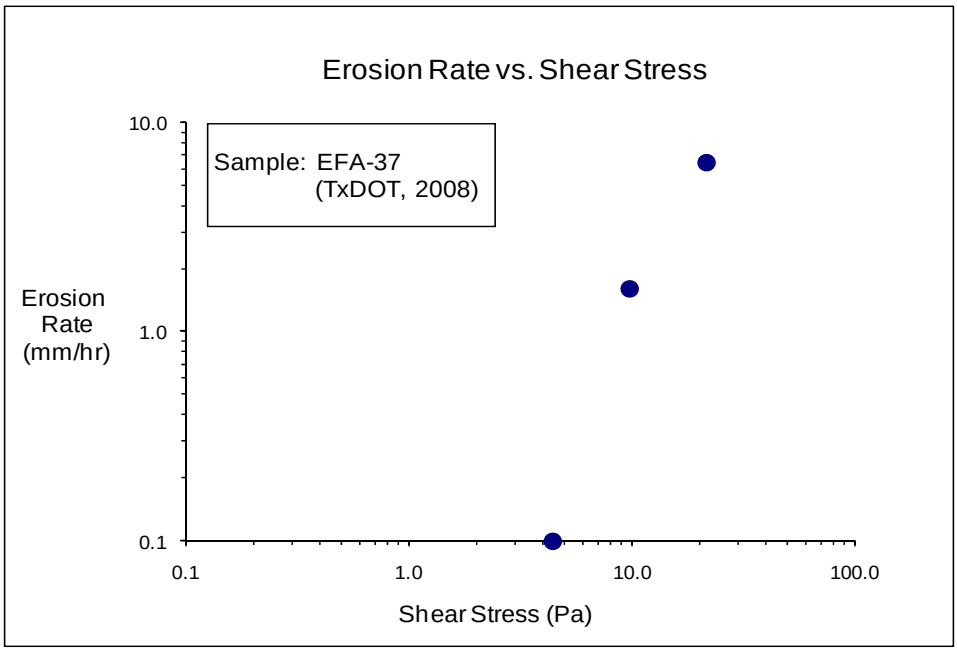

Figure D-71(a). EFA test results for soil sample EFA-37 (Shear Stress).

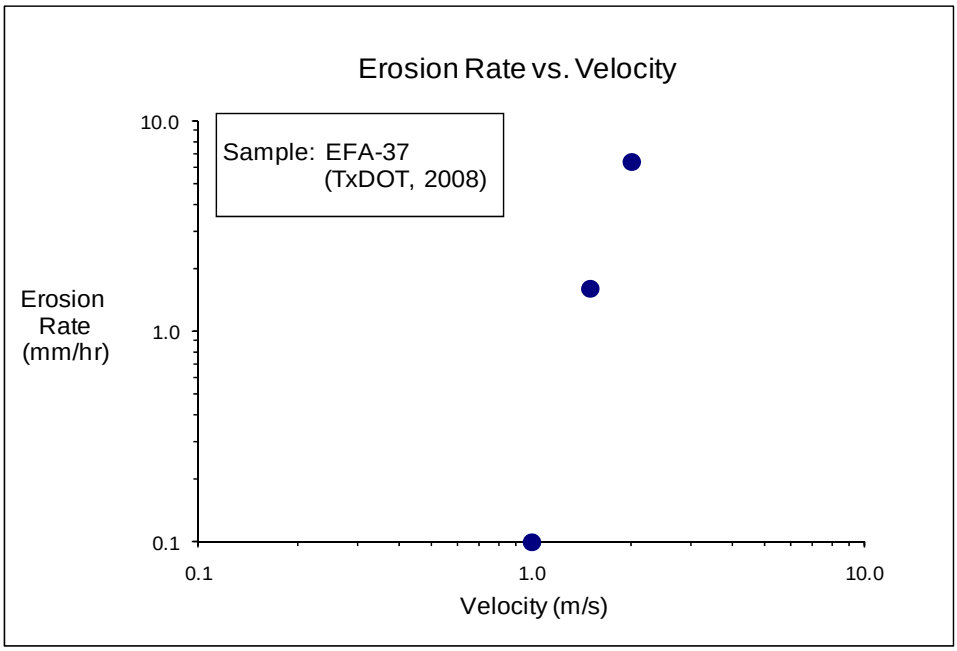

Figure D-71 (b). EFA test results for soil sample EFA-37 (Velocity).

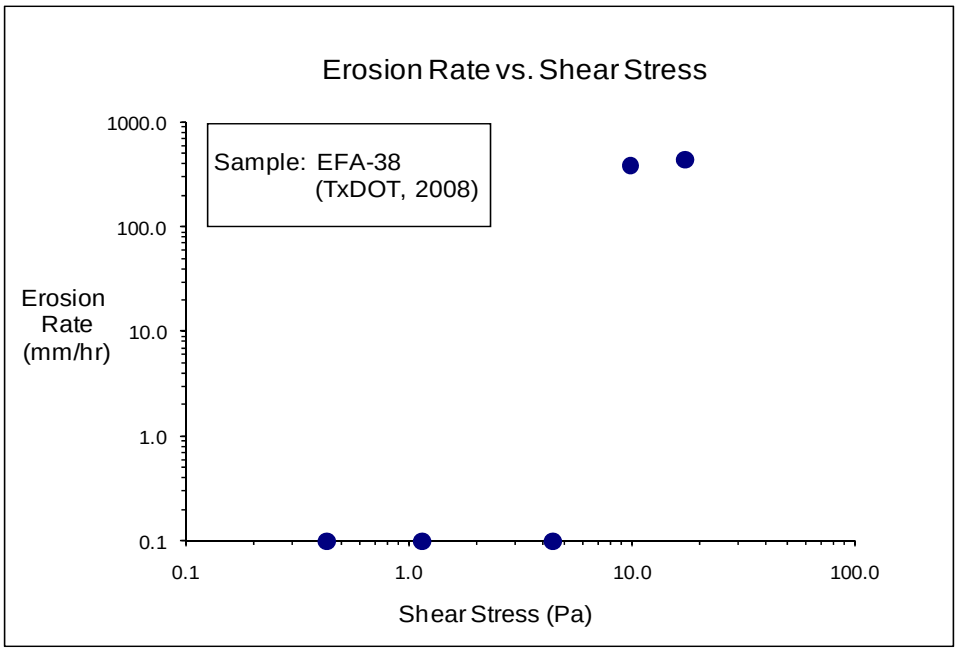

Figure D-72(a). EFA test results for soil sample EFA-38 (Shear Stress).

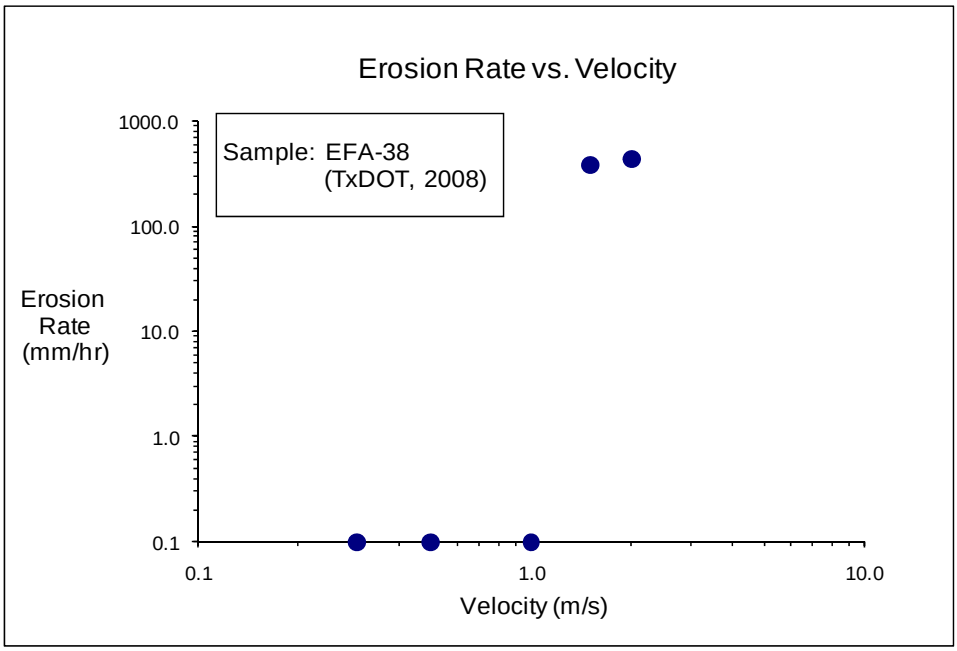

Figure D-72 (b). EFA test results for soil sample EFA-38 (Velocity).

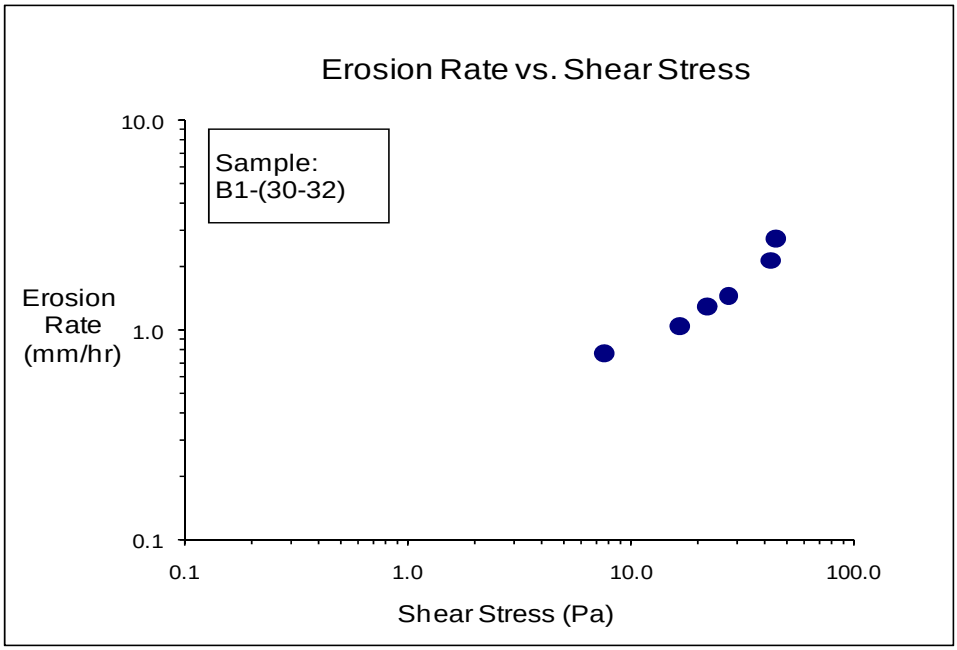

Figure D-73(a). EFA test results for soil sample B1-(30-32) (Shear Stress).

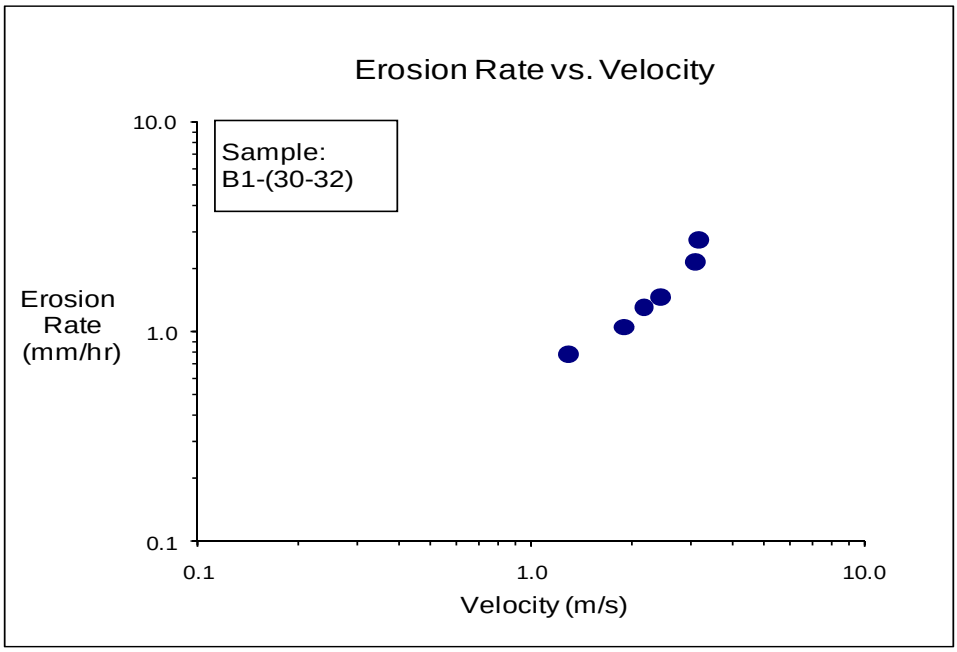

Figure D-73 (b). EFA test results for soil sample B1-(30-32) (Velocity).

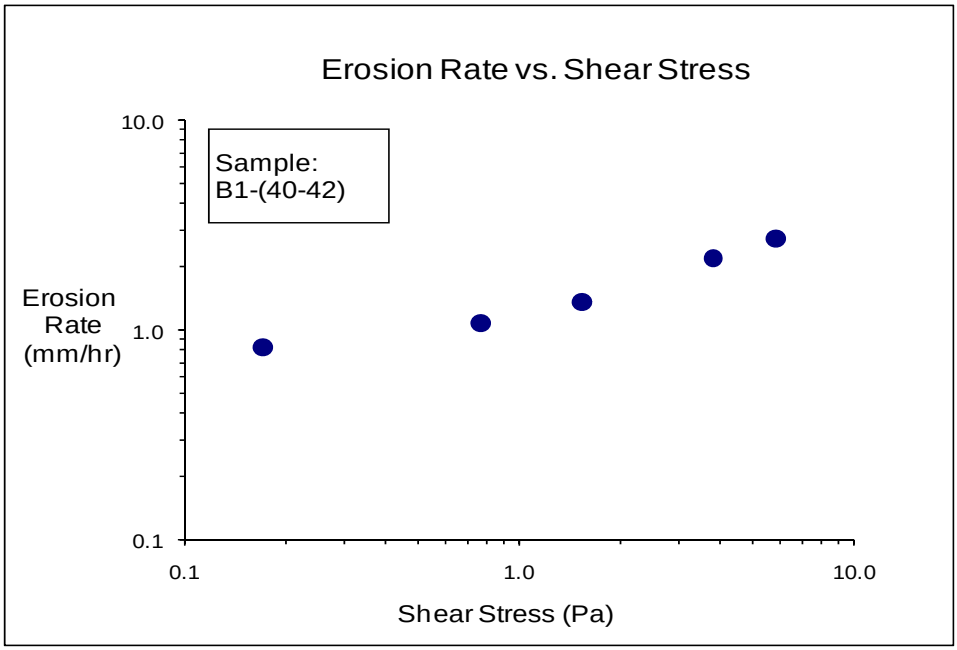

Figure D-74(a). EFA test results for soil sample B1-(40-42) (Shear Stress).

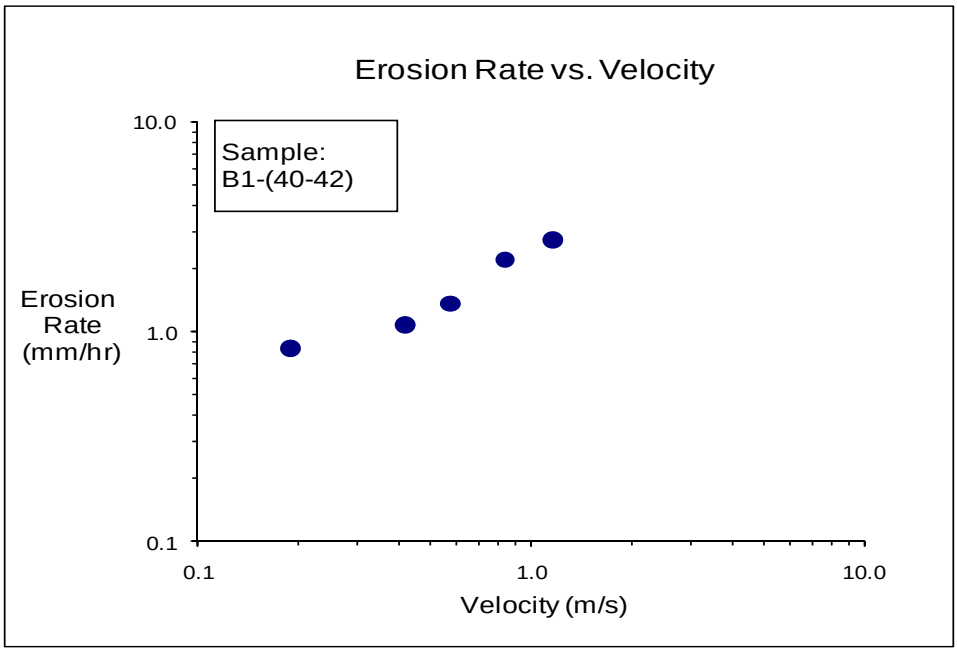

Figure D-74 (b). EFA test results for soil sample B1-(40-42) (Velocity).

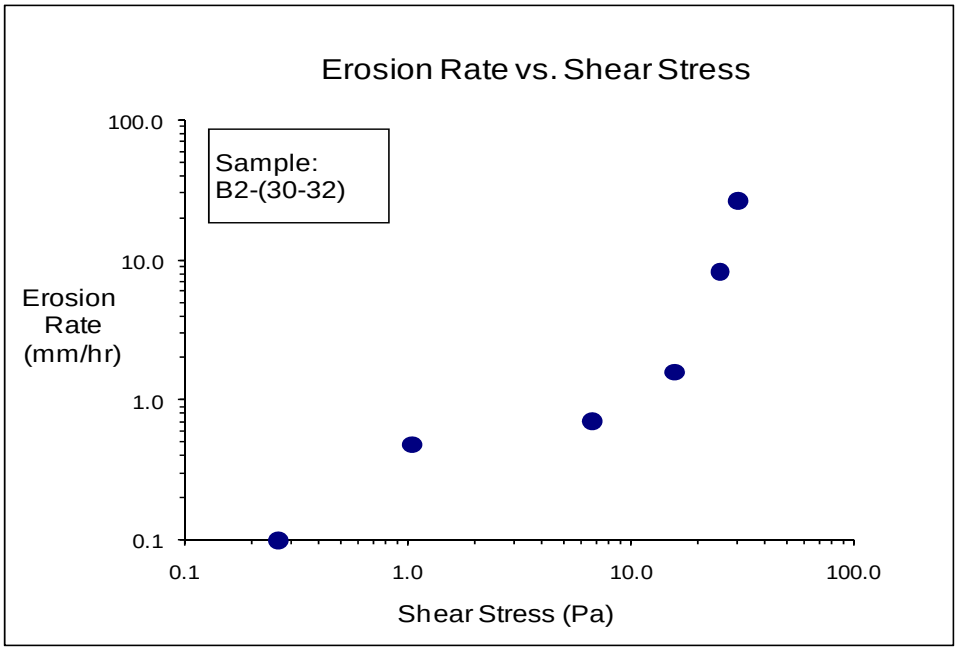

Figure D-75(a). EFA test results for soil sample B2-(30-32) (Shear Stress).

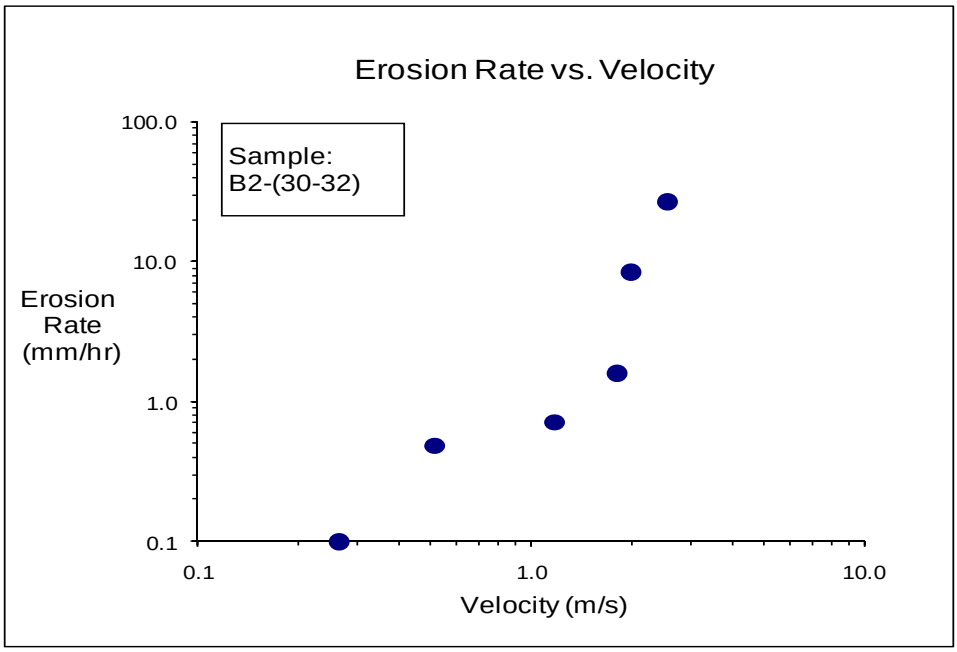

Figure D-75 (b). EFA test results for soil sample B2-(30-32) (Velocity).

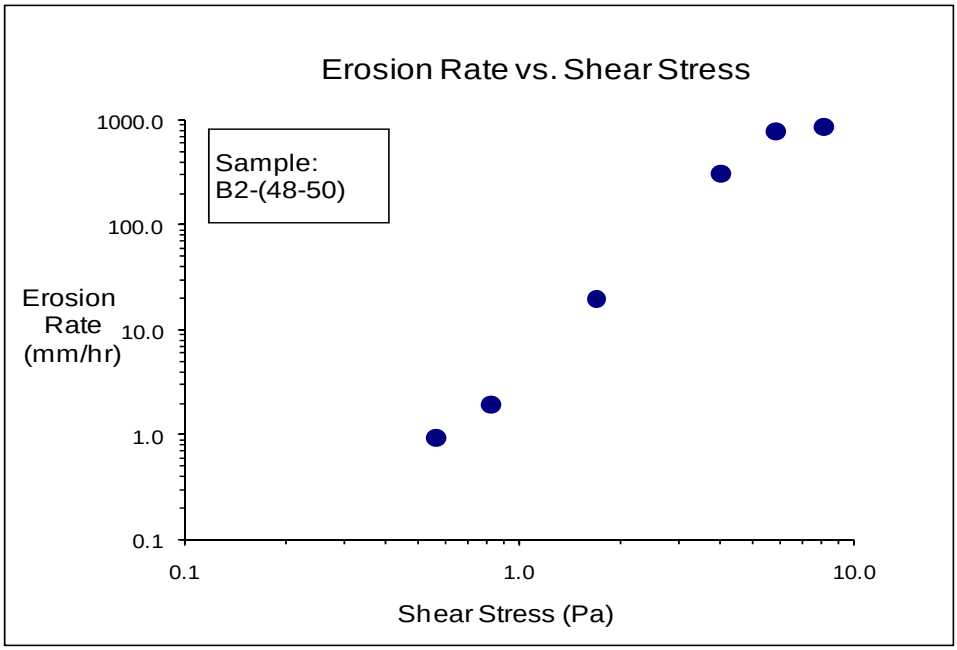

Figure D-76(a). EFA test results for soil sample B2-(48-50) (Shear Stress).

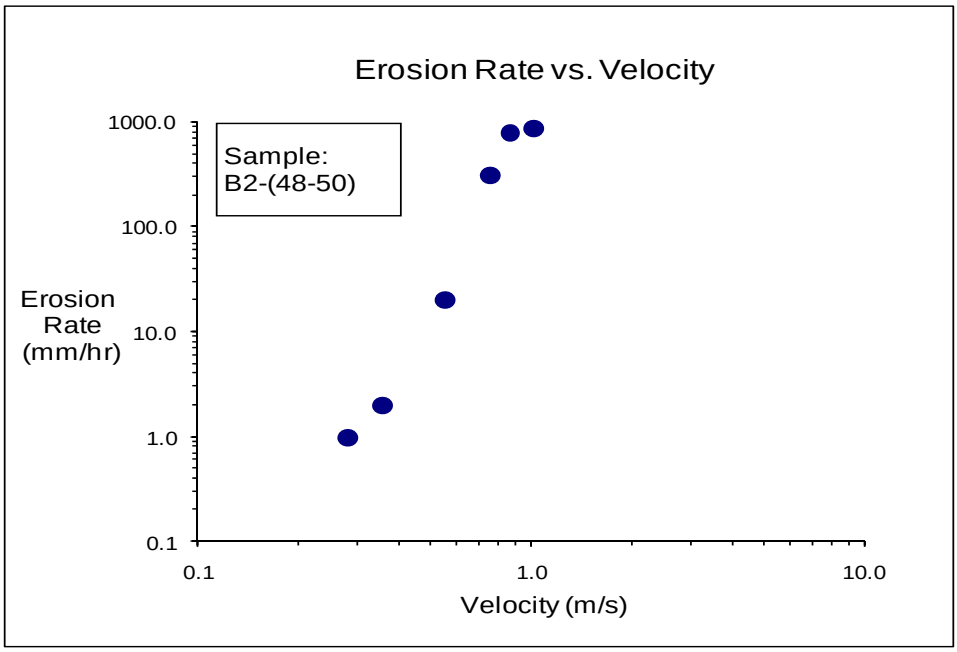

Figure D-76 (b). EFA test results for soil sample B2-(48-50) (Velocity).

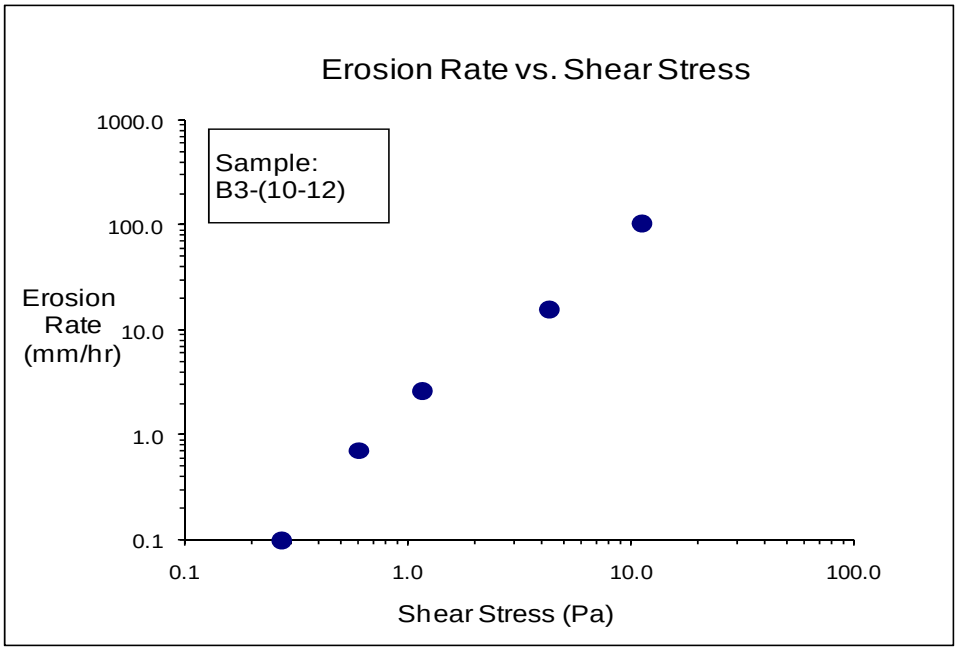

Figure D-77(a). EFA test results for soil sample B3-(10-12) (Shear Stress).

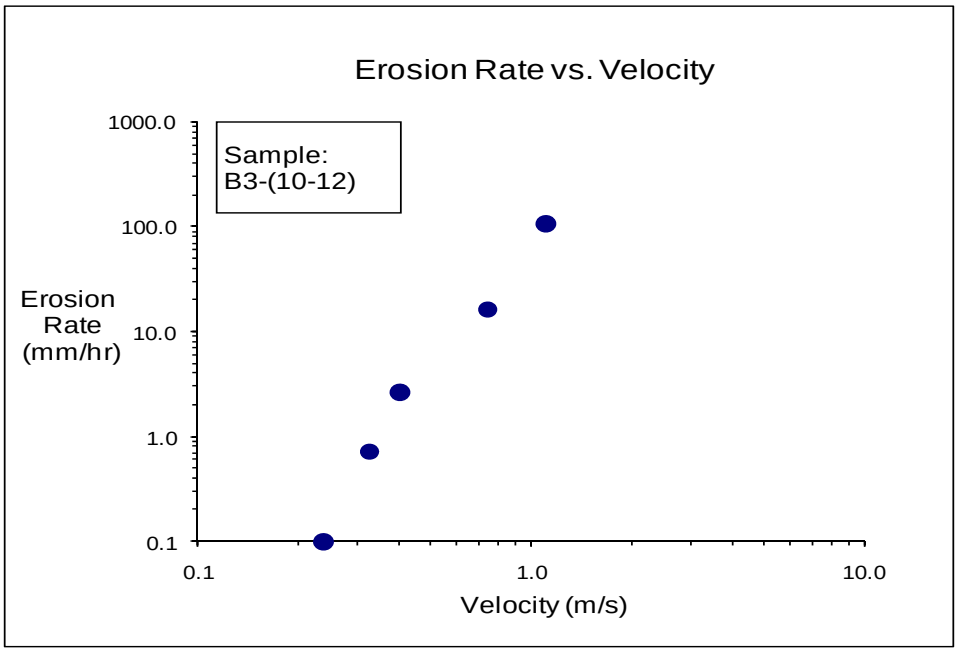

Figure D-77(b). EFA test results for soil sample B3-(10-12) (Velocity).

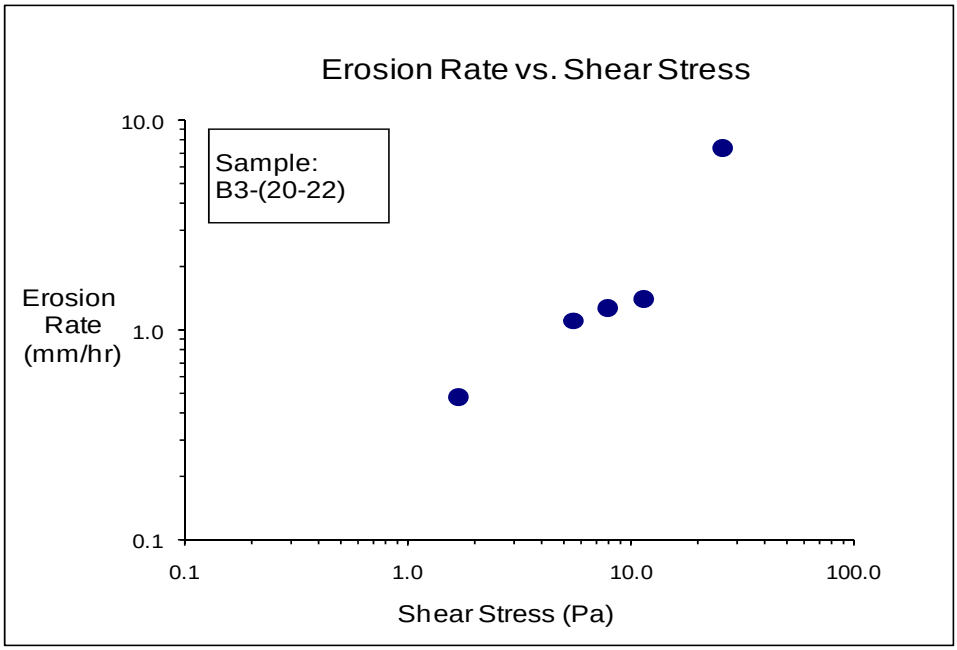

Figure D-78(a). EFA test results for soil sample B3-(20-22) (Shear Stress).

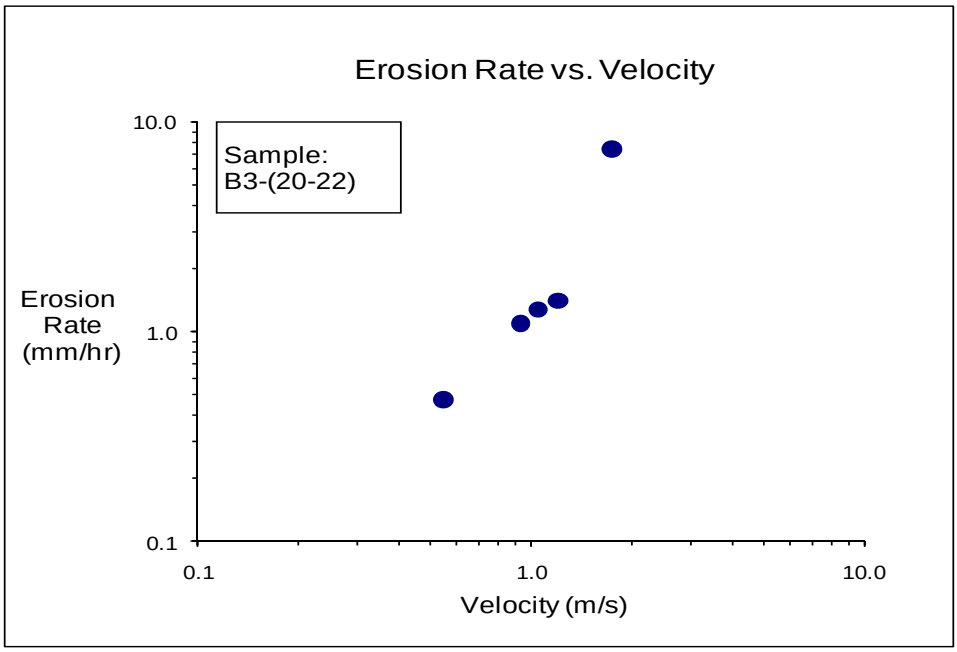

Figure D-78(b). EFA test results for soil sample B3-(20-22) (Velocity).

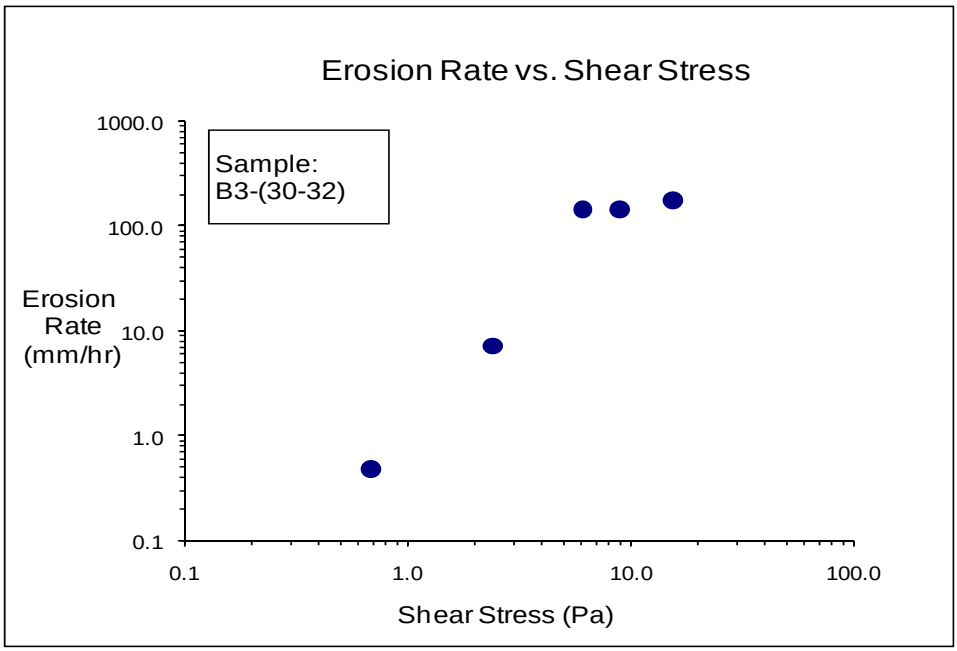

Figure D-79(a). EFA test results for soil sample B3-(30-32) (Shear Stress).

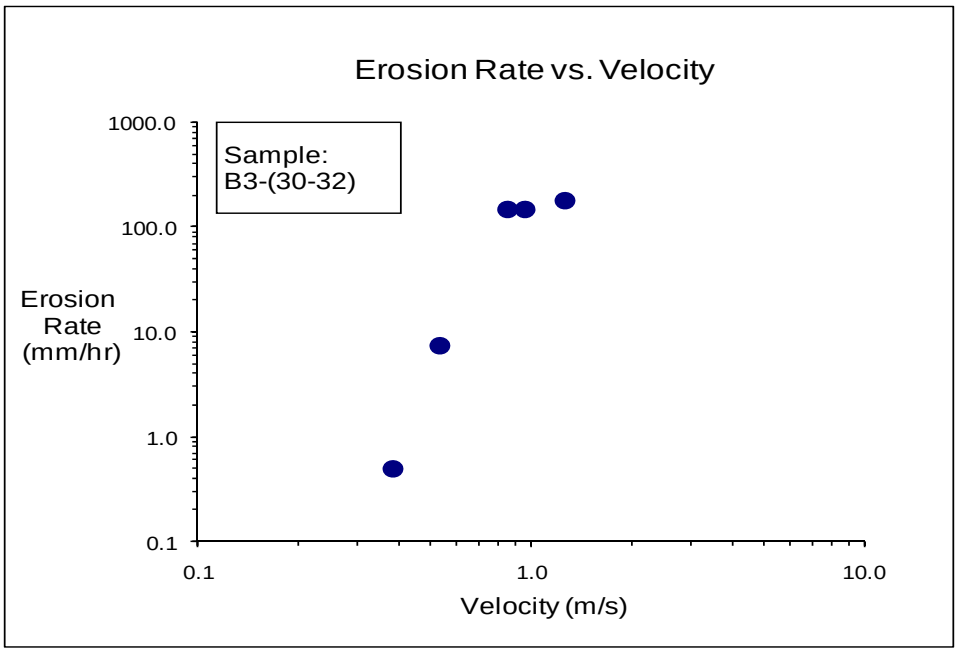

Figure D-79(b). EFA test results for soil sample B3-(30-32) (Velocity).

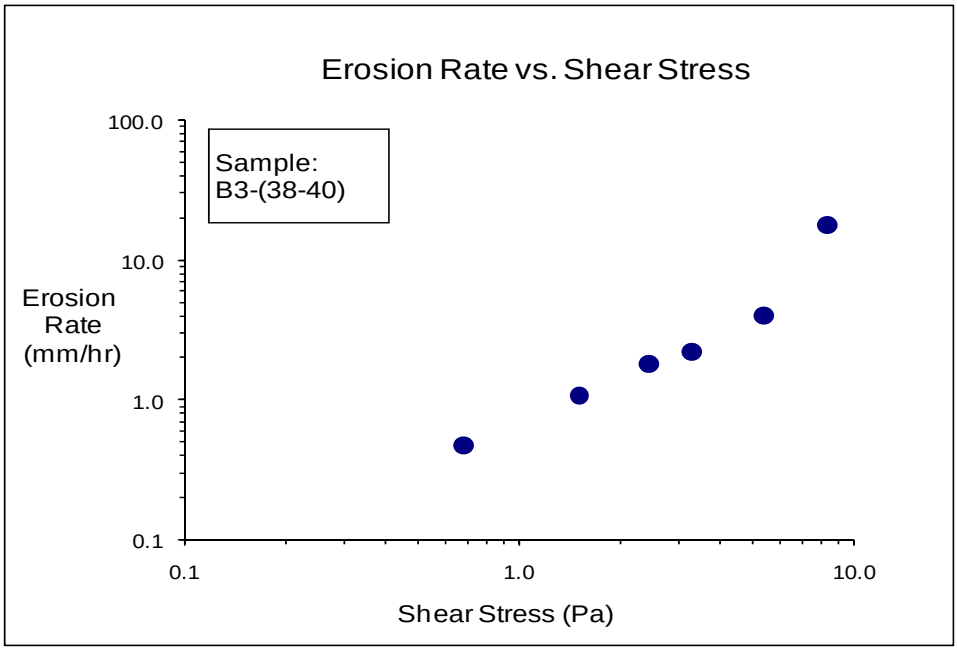

Figure D-80(a). EFA test results for soil sample B3-(38-40) (Shear Stress).

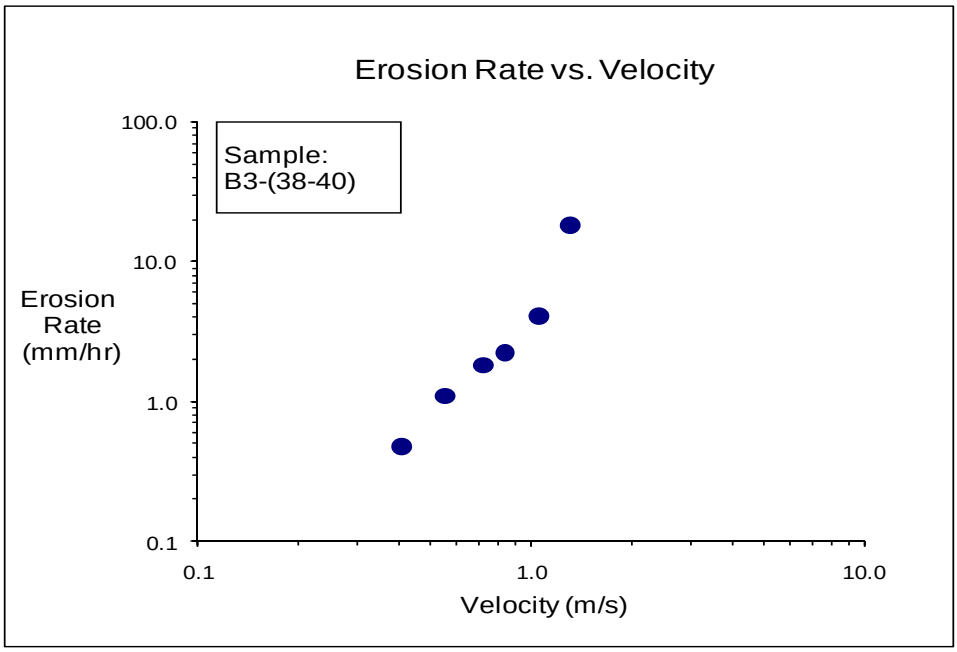

Figure D-80(b). EFA test results for soil sample B3-(38-40) (Velocity).

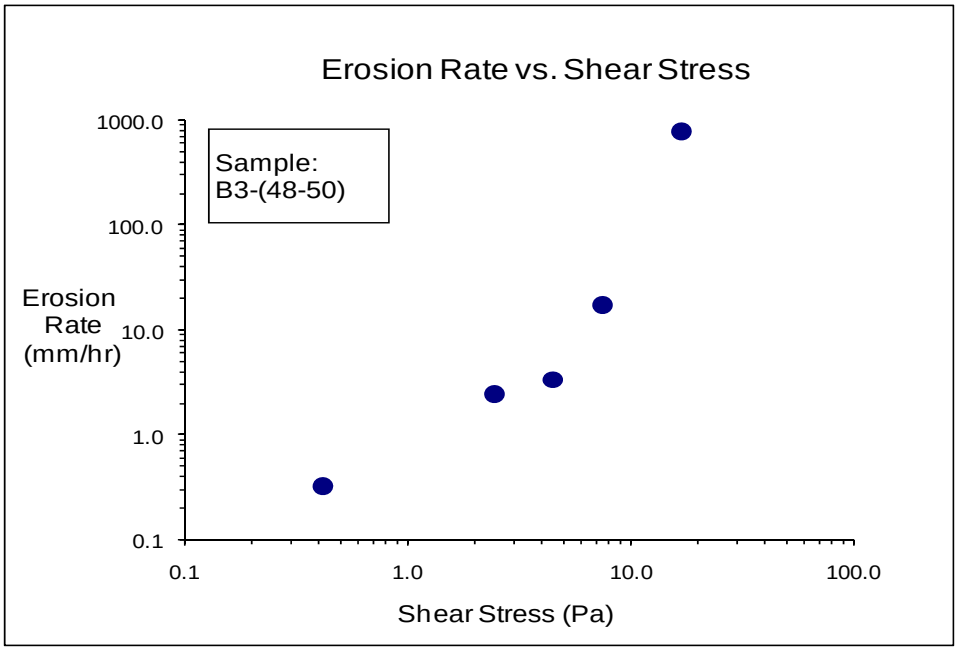

Figure D-81(a). EFA test results for soil sample B3-(48-50) (Shear Stress).

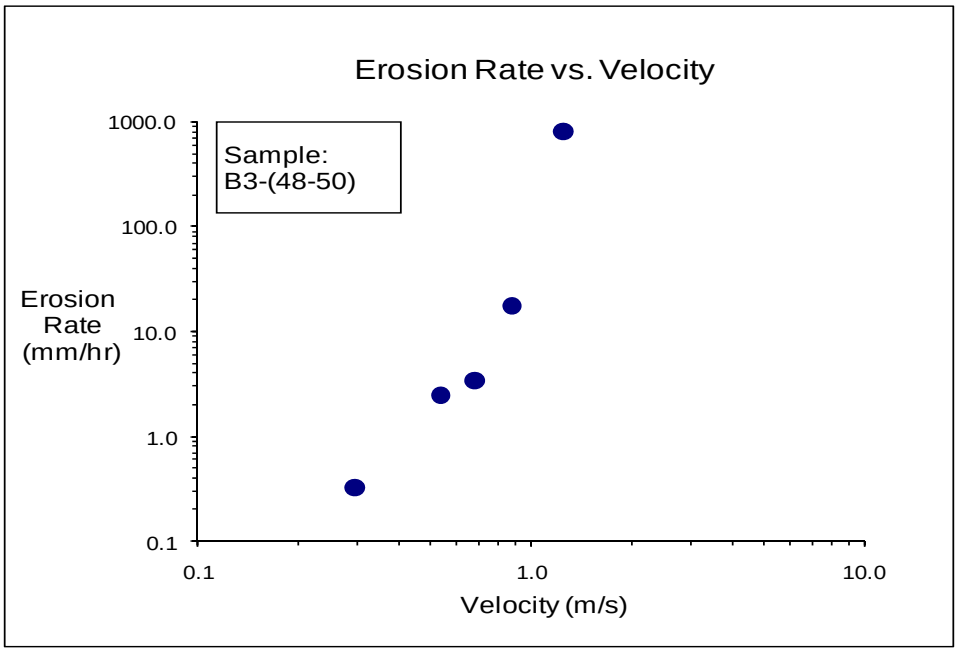

Figure D-81(b). EFA test results for soil sample B3-(48-50) (Velocity).

VITA

Anand V Govindasamy received his Bachelor of Engineering degree in civil engineering from Universiti Sains Malaysia, Pulau Pinang, Malaysia in 1999. He then went on to obtain his Master of Engineering degree in soil engineering from the Asian Institute of Technology, Bangkok, Thailand in 2001. From October 2001 to June 2005, he held positions in geotechnical engineering consulting in Singapore and Malaysia. In September 2005, he enrolled in the geotechnical engineering doctoral program at Texas A&M University where he was involved in bridge scour research. In 2006, he was a member of the Independent Levee Investigation Team organized by the University of California, Berkeley and the National Science Foundation to investigate the failure of the New Orleans levees during the Katrina Hurricane. He has also been an instructor for short courses in soil erosion organized by Texas A&M University in collaboration with the Geo-Institute of the American Society of Civil Engineers. His research interests are in bridge scour, soil erosion, risk analysis, and levee overtopping.

Name:	Anand V Govindasamy
Address:	Zachry Department of Civil Engineering
	Texas A&M University
	3136 TAMU, College Station, Texas 77843-3136
Phone:	(979) 845-7435
Education:	B.Eng. (Honors), Civil Engineering, Universiti Sains Malaysia, 1999
	M.Eng., Soil Engineering, Asian Institute of Technology, 2001